Using Superabsorbent Polymers in High Performance Concrete to mitigate Autogenous and Plastic Shrinkage while observing the Compressive Strength

by Nuraan Ebrahim

Thesis presented in fulfilment of the requirements of the degree of Master of Science (Research) in the Faculty of Engineering at the University of Stellenbosch

Supervisor: Prof. William Peter Boshoff

Co-supervisor: Dr. Riaan Combrinck

March 2017

بِسْمِ اللهِالرَّحْمَنِ الرَّحِيْمِ

In the Name of Allah

The Entirely Merciful

The Especially Merciful

Stellenbosch University https://scholar.sun.ac.za

Declaration

By submitting this thesis/dissertation electronically, I declare that the entirety of the work contain herein is my own, original work, that I am the sole owner thereof (save to the extent explicitly otherwise stated), that reproduction and publication thereof by Stellenbosch University will not infringe my third party rights and that I have not previously in its entirety or in part submitted it for obtaining my qualification.

Signature: ……

Date: ……March 2017……

Stellenbosch University https://scholar.sun.ac.za

Abstract

The use of high performance concrete (HPC) is relatively new in South Africa and guidelines on its production and use is lacking in the local construction industry. Conventional mix design methods are not suitable for HPC with low water to cement (w/c) ratios. A more sophisticated mix design approach is required. HPC with low w/c ratios tend to be sticky and have low workability. The high cement content also subjects the mix to early-age shrinkage and cracking. Conventional curing methods cannot be applied to low w/c ratio concretes to control shrinkage, due to its dense microstructure that inhibits the ingress of an external supply of curing water.

This study involved a material selection process to develop a mix that has high strength as well as high flowability of both pastes and concrete. Autogenous shrinkage was tested on pastes and plastic shrinkage was tested on concretes. Plastic shrinkage cracking was also measured. However, it was found that the test method used for plastic shrinkage cracking is not suitable for HPC with low w/c ratios.

Superabsorbent polymers (SAP), accompanied with additional water, was introduced as an internal curing agent. SAP was successful in reducing both autogenous and plastic shrinkage in all pastes and concretes, respectively. However, the presence of SAP and the extra water reduced the compressive strength in all pastes and concretes with the exception of one concrete mix variation. The variations in the mixes was the amount of internal curing water that was added to a given dosage of SAP. Previous literature reveals that the amount of internal curing water needed to saturate a SAP particle is often over estimated and leads to an effective increase in w/c ratio resulting in loss of strength. For this reason, the amount of internal curing water added was 50 and 75 % of the theoretical amount of water needed to saturate the SAP. Additionally, two different stone sizes, 6 and 9 mm, were also tested to observe the effect of larger aggregates on the desorption of SAP during mixing and setting.

The results of the tests showed that w/c ratio, stone size, SAP dosage and amount of internal curing water have a combined effect on the early-age shrinkage and compressive strength development of both pastes and concretes. The optimum amount of water needed to reduce early-age shrinkage while maintaining a reasonable strength is not unique to a given w/c, stone size or SAP dosage only, but is unique to each combination and requires an excessive amount of testing to provide a guideline to the use of SAP in HPC.

Stellenbosch University https://scholar.sun.ac.za

Opsomming

Die gebruik van hoë werkverrigting beton (HWB) is relatief nuut in Suid-Afrika en daar is nie genoegsame riglyne beskikbaar oor die produksie en die gebruik daarvan in die plaaslike konstruksiebedryf nie. ‘n Konvensionele mengselontwerp metode van lae water-en-sement (w/s) verhouding is nie geskik vir HWB. ‘n Meer gesofistikeerde mengselontwerp word vereis. HWB met 'n lae w/s verhouding is geneig om taai te wees en het 'n lae werkbaarheid. Die hoë sement inhoud veroorsaak dat die mengsel meer geneig is na vroeë ouderdom krimp en kraak. Konvensionele rehabliteringsmetodes kan nie toegepas word op 'n lae w/s verhouding met die doel om die krimping van die beton te beheer nie. Die rede hiervoor is dat die beton se digte mikrostruktuur die invloei van eksterne water verhoed.

Hierdie studie behels 'n keuringsproses om 'n mengsel wat 'n hoë sterkte asook 'n hoë vloeibaarheid van beide pastes en beton te ontwikkel. Outogene krimping is getoets op pastes en plastiese krimping is getoets op beton. Plastiese krimp krake is ook waargeneem. Daar is egter bevind dat die toetsmetode wat gebruik word vir plastiese krimp krake nie geskik is vir HWB met 'n lae w/s verhouding nie.

Super absorberend polymeer (SAP), vergesel met bykomende water, is ingestel as 'n interne genesingsagent. SAP was suksesvol in die vermindering van beide outogene en plastiese krimping in alle pastes en beton. Maar die teenwoordigheid van SAP en die ekstra water verminderd die druksterkte in alle pastes en beton met die uitsondering van een betonmengsel variasie. Die verskille in die mengsels was die hoeveelheid van interne genesing water wat op 'n gegewe dosis van SAP bygevoeg is. Vorige literatuur toon dat die hoeveelheid interne genesing water wat benodig is om 'n SAP deeltjie te absorbeer, dikwels oorgeskat word en lei tot 'n effektiewe verhoging in w/s verhouding wat weer lei tot die verlies van sy sterkte. Om hierdie rede is die hoeveelheid internegenesing water wat bygevoeg is, 50 en 75 % van die hoeveelheid water wat teoreties benodig is om die SAP te versadig. Daarbenewens was twee verskillende klip groottes, 6 en 9 mm, ook getoets om die uitwerking van ‘n groter aggregaat op die desorpsie van SAP waar te neem tydens die vermenging en instelling van die beton.

Die uitslae van die toetse het getoon dat ‘n w/s verhouding, klip grootte, SAP dosis en hoeveelheid interne genesing water 'n gekombineerde effek op die vroeë ouderdom krimping en druksterkte ontwikkeling van beide pastes en beton tot gevolg het.

Stellenbosch University https://scholar.sun.ac.za

Die optimale hoeveelheid water wat benodig word om vroeë ouderdom krimping te verminder, terwyl 'n redelike sterkte gehandhaaf word, is nie uniek aan 'n gegewe w/s verhouding, klip grootte of net SAP dosis nie,maar is uniek aan elke kombinasie en verdere toetse word vereis om voorsiening te maak vir die ontwikkeling van ‘n riglyn vir die gebruik van SAP in HWB in Suid-Afrika.

- *Vertaal deur Ardela van Niekerk*

Stellenbosch University https://scholar.sun.ac.za

Acknowledgements

The road has been long and windy, but could not be completed without acknowledging that All Thanks and Praise is due to Almighty God. After giving thanks for His countless Favours and never ending Guidance, I would like to thank the following people:

- My parents, for always making me believe I can achieve anything I want, even from the time I wanted to be a packer at Pick ‘n Pay.

- My supervisor, Professor Billy Boshoff, for his leadership and advice throughout this study. Thank you for giving me the opportunity to study under you and learn more about concrete, both locally and abroad.

- My co-supervisor, Doctor Riaan Combrinck, for his advice and assistance. Your optimistic motivation and encouragement through the toughest moments is greatly appreciated.

- The lab staff at the University of Stellenbosch, Charlton Ramat, Peter Cupido, Luhan Jacobs, Oom Johan van der Merwe and Dion Viljoen for their kind assistance in all my years in the lab.

- All the extra sets of muscles that lifted my moulds in the late hours of the night.

- Carlo Coenraad from Rothco/Blaser Swisslube for the supply and setup of the dial gauges for the autogenous shrinkage test setup at the University of Stellenbosch. Your tremendous effort and patients to get the equipment set up and running smoothly at such a frustrating time is unmatched.

- Guillaume Jeanson at SNF Floerger for supplying the University of Stellenbosch with superabsorbent polymers in support of our research in internally cured concrete.

- BASF chemicals for supplying the superplasticiser in support of my research.

- PPC for supplying the University of Stellenbosch with cement for all our research and lastly, but mostly, for the funding which was granted in support of completing my Master’s degree.

Stellenbosch University https://scholar.sun.ac.za

Contents

Stellenbosch University https://scholar.sun.ac.za

Stellenbosch University https://scholar.sun.ac.za

Stellenbosch University https://scholar.sun.ac.za

Stellenbosch University https://scholar.sun.ac.za

List of Figures

Stellenbosch University https://scholar.sun.ac.za

Stellenbosch University https://scholar.sun.ac.za

Stellenbosch University https://scholar.sun.ac.za

Stellenbosch University https://scholar.sun.ac.za

Stellenbosch University https://scholar.sun.ac.za

Stellenbosch University https://scholar.sun.ac.za

List of Tables

Chapter 1

Introduction

The use of high performance concrete (HPC) and ultra-high performance concrete (UHPC) is becoming more popular in South Africa as a prospect to design intricate concrete members of structures carrying substantial loads. This is attractive to Structural Engineers and more so, Architects since design limits on member shapes and slenderness ratios can be stretched. It is possible to obtain concrete with an ultimate compressive strength of up to 200 MPa with modern day building materials. However, with these sophisticated concrete mix designs, special attention needs to be given to the change in micro structure of HPC and UHPC compared to that of normal strength concrete (NSC) in its fresh and hardened state and the transition in between.

HPC can be defined as a concrete that possesses properties that surpass the limitations of conventional concrete. These properties can result in improvements during the construction process, as well as mechanical and/or non-mechanical improvements of the as-built structure. Typically, HPC contains large amounts of cement and/or supplementary cementitious material (SCM) such as silica fume, fly ash and corex slag as well as chemical admixtures such as water-reducing agents, viscosity modifying agents and shrinkage reducing admixtures. This increase in cement content and/or SCM's and chemical admixtures introduce parallel changes to the chemical interactions, which occur during hydration, as well as the microscopic dynamics between the solid particles in the concrete matrix. Not only does this call for alternative mix design considerations, but there are also concerns of early-age shrinkage and cracking in HPC due to its large amounts of cementitious material.

This study observes the extent of early-age volume change on HPC with low water to cement (w/c ratio) ratios by considering autogenous shrinkage using the corrugated tube method in accordance with ASTM C1579-06 as well as plastic shrinkage using the test method described by Slowik et al. (2008). Furthermore, the use of super absorbent polymers (SAP) is introduced to these cement-rich mixes as a means to mitigate the shrinkage through internal curing. Although internal curing is known to help regulate the internal relative humidity of cement-rich mixes, which combats the early-age shrinkage, the additional water may lead to a significant decrease in compressive strength.

The problem statement is defined in the following section along with the objectives and methodology used to gain insight regarding the use of SAP and internal curing water to mitigate early-age shrinkage without compromising the compressive strength of HPC.

1.1 Problem Statement

Low w/c ratio concretes are typically sticky mixes that are difficult to work with in the fresh state and also have a short time frame during which they can be successfully placed. Low w/c ratio concretes are also known to be prone to self-desiccation. Self-desiccation is a result of a drop in internal relative humidity in the capillary pores between the solid particles of the hardened concrete skeleton as hydration takes place. This process is more significant in concretes that are made up of a large portion of fine materials and a limited amount of water (Tazawa, 1998). In other words, self-desiccation is more significant in HPC. Self-desiccation is the mechanism that is responsible for autogenous shrinkage and thus, in the production of HPC, special attention needs to be given to the extent of autogenous shrinkage and the risk of autogenous shrinkage cracking if HPC is to be a viable solution for specialised construction processes and intricate structures.

With the increased interest in HPC, more focus is being put on the measurement of autogenous shrinkage. For this study, a test setup for measuring autogenous shrinkage is required in order to formulate an empirical solution for the mitigation of autogenous shrinkage and the detrimental effects that it may have if precaution is not taken. There are a number of test variations for the measurement of autogenous shrinkage. The most widely used test method is the corrugated tube method, which is becoming the standard test method of autogenous shrinkage amongst many research institutions. This method is beneficial because measurements can start immediately after casting. However, some difficulty is introduced when placing sticky mixes. The main concern for proper implementation of this method is to use a concrete that has good flowability and workability to minimise voids in the corrugated moulds. Compoundedly, the mix should have an appropriate window of workability to complete the filling of the tubes. Obtaining these fresh properties of HPC with low w/c ratio is particularly challenging. For this reason, careful material selection needs to be considered to obtain the high strength requirements while maintaining flowability and workability and ensuring economical production of the concrete.

Jensen and Hansen (2001) introduced the use of super absorbent polymers (SAP) to manage self-desiccation by controlling the internal relative humidity of low w/c ratio concretes to mitigate autogenous shrinkage. SAP particles are able to absorb large amounts of water.

Employing these polymers along with extra water provides internal curing which is successful in controlling the internal relative humidity in the fine pore structure of HPC.

To date, there has been many publications which portray a trend that while the addition of SAP in HPC successfully mitigates the autogenous shrinkage; it is at the cost of its compressive strength. Tange et al. (2012) concluded that the reduction of compression strength of HPC with SAP is not so much due to the addition of SAP, but the over estimation of internal curing water.

This vacillating problem statement is illustrated in ASh – Autogenous shrinkage

SAP – Superabsorbent polymers

ICW – Internal curing water

Figure 1.1 where a) producing a concrete with high strength means that the concrete is vulnerable to autogenous shrinkage which is undesirable, b) adding SAP along with internal curing water is effective in mitigating autogenous shrinkage, but at the cost of compressive strength which is undesirable because the concrete is no longer classified as having a high strength and c) finding a medium between adequate reduction of autogenous shrinkage by employing SAP and internal curing water, but at a lower saturation level to restore some of the strength loss.

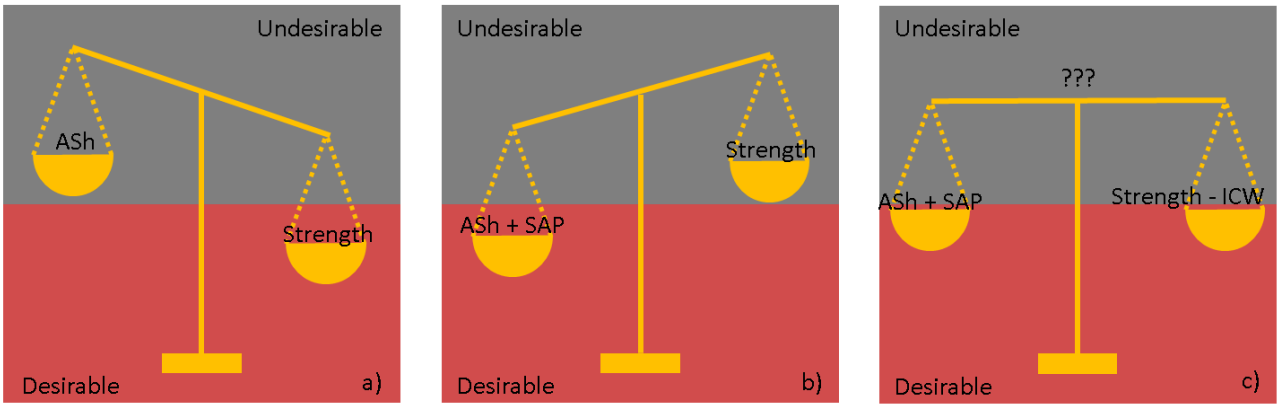

ASh – Autogenous shrinkage
SAP – Superabsorbent polymers
ICW – Internal curing water

Figure 1.1: Problem statement a) Increasing the strength increases the autogenous shrinkage b) adding saturated SAP to mitigate autogenous shrinkage decreases the strength, c) reducing the amount of internal curing water may restore some of the strength loss, but may not be as effective in mitigating autogenous shrinkage

This leaves the goal of obtaining maximum autogenous shrinkage reduction with minimal strength reduction.

1.2 Objectives

The objective of this study is to provide insight regarding the use of SAP in HPC in South Africa to mitigate early-age shrinkage and cracking while observing the effect of internal curing water on the compressive strength. This objective is achieved in three parts:

- Setup the corrugated tube test method to measure the autogenous shrinkage of low w/c ratio pastes according to ASTM C1579-06.
- Develop a self-compacting concrete (SCC) with high strength, as well as a paste with excellent flowability in the fresh state to allow the observation of autogenous shrinkage using the corrugated tube method.
- Determine the optimum amount of internal curing water to add to HPC containing SAP that does not compromise the compressive strength extensively.

1.3 Methodology

The above objectives are achieved using the following methodology:

- Setup the corrugated tube test method
    - Source equipment and parts according to the specifications in ASTM C1579-06
- Develop a SCC with high strength
    - Develop a low w/c ratio concrete at two different w/c ratios below 0.35 to achieve a concrete with high strength.
    - Select appropriate mix proportions and superplasticiser dosage to achieve a SCC
- Determine the optimum amount of internal curing water
    - Observe the effect of altering the amount internal curing water on the compressive strength of concrete and pastes mixes.
    - Observe the effect of altering the amount of internal curing water on the plastic shrinkage of concrete and the autogenous shrinkage of the corresponding paste.
    - Observe the effect of stone size on the strength and plastic shrinkage of HPC containing SAP.
    - Compare the trends between plastic shrinkage of concrete and autogenous shrinkage of pastes to observe the role of fine and coarse aggregate in HPC containing SAP.
    - Provide a guideline for further research to be able to quantify appropriate dosages of both SAP and internal curing water that can successfully mitigate early-age shrinkage of HPC without compromising its strength.

1.4 Report Layout

The layout of this report is as follows:

- Chapter 2 reviews previous literature on the topic to complete a background study to gain an understanding of the relevance of the topic and available information on the components of HPC, SAP and mechanisms of early-age shrinkage.
- Chapter 3 presents preliminary work that was carried out after the background study in order to develop the required mix design suitable for this study.
- Chapter 4 looks at the experimental framework and discusses the test program and test set up used to measure autogenous and plastic shrinkage.
- Chapter 5 presents the results obtained from the test methods described in Chapter 4.
  Chapter 6 discusses the trends observed in the results of the previous chapter to draw some conclusions of the influence of SAP and internal curing water on HPC, as well as presents some recommendations for future studies on related topic

Chapter 2

Background Study

This chapter provides a review of literature regarding the production of high performance concrete (HPC) as well as the related concerns of early-age shrinkage and cracking including the mechanisms responsible. In an attempt to mitigate this early-age shrinkage and reduce the early-age crack risk, the use of superabsorbent polymers (SAP) for internal curing as well as the effect on the compression strength is considered.

2.1 High Performance Concrete

The use of HPC is relatively new in South Africa and with increasing focus and research being put on the use thereof; it is slowly creating a shift in the design and construction approach of more modern and specialised structures. Conventional mix design methods are not suitable for HPC with low water to cement (w/c ratio) ratios and low workability. This section looks at the definition of HPC, its applications and the challenges in producing two types of HPC namely; high strength concrete (HSC) and self-compacting concrete (SCC).

2.1.1 Definition

HPC is a recent and on-going development in the concrete material industry. Its development is augmented by the rising popularity of structures made up of intricately shaped elements such as long, slender, curved columns and beams which require exceptional performance in either or both its fresh and hardened state. A broad definition of HPC as given by the Strategic Highway Research Program (1991) is any concrete that possess properties that surpass the limitations of conventional concrete. According to Shah and Ahmad (1994) these properties can fall in to one of three categories, construction process improvements, mechanical improvements and non-mechanical improvements. These categories along with types of HPC are shown in Figure 2.1

.

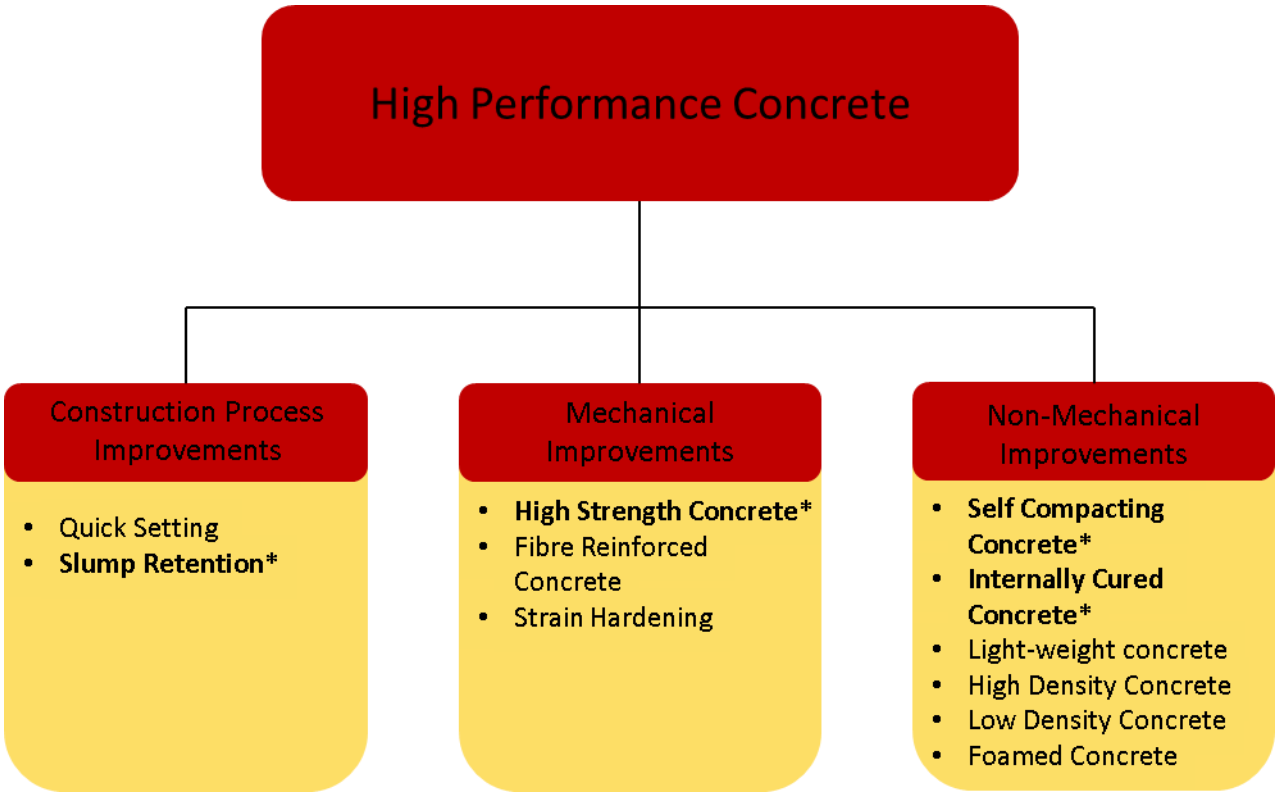

Figure 2.1: Types of High Performance Concrete

** The desired performance properties of this study*

According to the American National Institute of Science and Technology (NIST) and American Concrete Institute (ACI) in 1900, HPC is a homogenous concrete made of high quality raw materials that allow easy casting, without segregation, yielding stable mechanical properties, high early strength, stiffness and durability. In 1992, Malier from France, stated that HPC is characterised by good workability, high strength, sufficient early-age strength and is economical in terms of engineering and durability.

In Xincheng's book on *"Super-High-Strength High Performance Concrete"*, he states that HPC cannot merely be described as a concrete that has high strength or properties such as durability. This leaves a wide range for quantifying HPC, rather HPC should possess all of the following (Xincheng, 2013):

1. Good flowability and adhesion that has no segregation during placing.
2. HPC must have a high compressive strength.
3. Hardened concrete should not undergo extensive deformation like shrinkage and creep.
4. High durability.

In contrast to point two as stated previously, some argue that HPC need not have a high strength and that a normal strength concrete (NSC) with other performance improvements such as workability or durability can still be classified as a HPC (Owens, 2009). The terms HSC and HPC are commonly used interchangeably, some researchers argue that high-performance should be defined according to the specialised requirements of the specific application (Owens, 2009) and not entirely on the compressive strength.

In this study HPC refers to a concrete having a compressive strength higher than 60 MPa while possessing good flowability, no segregation, a decent workability retention period and a final setting time not longer than 8 hours, all of which is discussed in greater detail in Chapter 3. HSC in turn refers to a concrete that has a compressive strength higher than 60 MPa but does not possess all of the aforementioned properties.

In recent years it has become convenient to classify concrete according to its strength. This is particularly useful for design purposes as member strength and ultimately the strength of a structure is largely dependent on the strength performances of the concrete itself.

Moreover, the transition from NSC to HSC and further to ultra-high strength concrete (UHSC) is empirically related to an increase in cement content. This increase in cement content introduces parallel changes to the chemical interactions during hydration and the microscopic dynamics between the particles of a concrete matrix. For this reason, HSC cannot be designed the same as NSC. Different and careful consideration needs be given to aspects such as the material selection and mix constituent ratios, keeping in mind the specialised performance properties required for the specific application.

2.1.2 Applications

Typical structures that need high-performance properties are long slender bridges, high-rise buildings and piers. These specialised kinds of projects are commonly found in countries such as Korea and Japan. In South Africa, there is a tendency to stick to the more conventional building materials and construction methods. The use of HPC is relatively new in South Africa and with increasing focus and research being put on the use thereof; it is slowly creating a shift in the design and construction approach of more modern and specialised structures. Reservations in South Africa on the use of concrete with high compressive strengths is also that our design codes only account for concrete having and ultimate compressive strength of 50 MPa. However, the European design code is being adopted in South Africa, which makes provision for concretes of up to 105 MPa.

Another reservation is that the initial cost of producing HPC is higher than that of NSC owing to the high cement content and the use of superplasticisers. However, it should be noted that the use of HPC reduces the total life cycle cost of a structure because it allows for smaller member sizes, less reinforcement and also cuts maintenance cost due to the improved durability.

2.1.3 Typical Constitutes of High Performance Concrete

High compression strengths can only be attained by a low w/c ratio. This considerable increase in cement content presents some challenges to the fresh mix. Firstly, large amount of cement increases the price of concrete. Substituting a portion of cement with supplementary cementitious material (SCM) can reduce the material costs of producing HPC, but it is not the sole reason for including them in a HPC concrete mix. When used correctly, SCM's can also improve the fresh and hardened performance of concrete (Uchikawa et al., 1992). Secondly, in concretes with low w/c ratios, cement particles are not dispersed evenly which leads to sticky mixes with little or no flowability. Water-reducing admixtures are therefore employed to increase the workability and flowability without increasing the water content. HPC cannot be produced without the use of SCM's and water-reducing admixtures as discussed in the following sections.

2.1.3.1 Supplementary Cementitious Materials

SCM's are also known as mineral admixtures or extenders as they extend the production of calcium silicate hydrates (C-S-H) in the presence of water and calcium hydroxide (lime), a by-product from the hydration of Portland cement.

Substituting a portion of cement with SCM can reduce the material costs of producing HSC, but this is not the sole reason for their addition to HSC. Historically, SCM's were introduced to concrete as a means to reduce the amount of Portland cement consumed, which reduces the environmental impact due to lower cement production as well as preserve our resources. Furthermore, SCM's can improve the fresh and hardened performance of concrete (Uchikawa et al., 1992). This includes improved rheology, durability and high strengths while economic and environmental advantages are also being achieved.

In early research SCM's such as fly ash and silica fume were considered as fine aggregates which improved strength and durability due to its' fine packing ability (Aïtcin, 1998). However, fly ash and silica fume are in fact pozzolans, which produce a supplement formation of C-S-H to cement by reacting with calcium hydroxide and water.

In recent years, the term w/c ratio for HSC has become questionable for two reasons; modern day cements may contain small amounts of limestone and/or silica filler, so the cement is not 100 % pure Portland cement. In addition, it is quite common to make use of SCM's in a HSC mix (Aïtcin, 1998). For these reasons, the term water to binder (w/b ratio) ratio is commonly used, with the binder referring to the cement content along with any SCM's. The two most widely used SCM's, are fly ash and silica fume which will be discussed in to following sections.

Fly Ash

Fly ash is the fine particles that are collected during coal burning in furnaces by electrostatic precipitation or bag filters ((Aïtcin, 1998) and (Owens, 2009)). The particles are divided into fine and coarse fractions and the fine portion, particles passing the 45 µm sieve, are used as a mineral admixture in concrete (Owens, 2009). There are different classes of fly ash depending on the type of coal used. Class C and Class F fly ashes are commercially used in concrete. Class F fly ash is mainly made up of siliceous and aluminous compounds and Class C fly ash is mainly made up of calcium (Strategic Highway Research Program, 1991). Due to their mineral make up, Class C fly ash are cementitious when used on its own as well as pozzolanic in the presence of cement while Class F fly ash only behaves pozzolanically in the presence of cement.

Silica Fume

Condensed silica fume, commonly referred to as just silica fume or micro silica, is a by-product from the production of silicon metals and alloys. (Owens, 2009). As a result, silica fume has a high SiO_2 content of up 90 % depending on the metal or alloy being produced (Aïtcin, 1998). This high SiO_2 content greatly contributes to its high pozzolanic reactivity.

Silica fume is more expensive than cement, however if used correctly it can still be cost effective due to high pozzolanic reactivity and therefore increase concrete strength (Strategic Highway Research Program, 1991).

2.1.3.2 Water-reducing Admixtures

Several advancements in concrete technology have been made over the last few decades that allow specific performance attributes of a mix to be altered in either or both its' fresh and hardened state. One such advancement is the addition of chemical admixtures to the mix. According to ASTM C 125 (2000), chemical admixtures are defined as materials that are not water, cementitious, aggregates or fibres, which are added to concrete or mortar during the mixing process.

There is a wide range of admixture types, which can be characterised by their chemical composition and are grouped as surface-active chemicals, soluble salts, polymers or insoluble minerals. Each of these four groups of admixtures react with the water-cement system of a concrete mix through different mechanisms and are responsible for different performance improvements which include workability, setting time, acceleration or retardation (Mehta et al., 1993).. Surface-active chemicals, also called surfactants, in particular are chemical admixtures that are useful for air entrainment and water reduction. Water-reducing admixtures (WRA) are of concern in the production of HSC and HPC. In fact, it is impossible to produce a HSC and HPC without the use of water-reducing admixtures.

In concretes with low w/b ratios, cement particles are not dispersed evenly which leads to sticky mixes with little or no flowability. The lack of dispersion is due to two main reasons, the first being the high surface tension that is developed in the mix water. The mix water has a high ionic strength resulting from the dissolution of alkali, sulphates, clinker and gypsum. The attractive Van Der Waal forces exceed repulsive forces and thus the cement grains attract each other (Li, 2011). The second cause for flocculation is the positive and negative forces of the edges and corners of cement particles which further attract one another and cause the cement particles to form clusters and flocculate (Mehta et al., 1993). Surfactants are effective in breaking up these flocculations when their polar chains are absorbed at the edges of cement particles. The polar end of the surfactant chains is then extended towards the water, making the cement particles hydrophilic. This interaction between surfactant and water-cement system also lowers the surface tension in the water and successful dispersion of cement particles in limited amounts of water can be obtained. Subsequently, lower water contents can produce a concrete with higher strength and durability while maintaining a certain workability (Li, 2011). Converse to this, water-reducing admixtures may be used to increase the workability and flowability without increasing the water content and thus maintaining the strength and is said to "plasticize" the concrete in this regard. WRA are therefore commonly known as plasticisers and can reduce the water demand of concrete between 5 and 10 % (Li, 2011).

High-range water reducing agents (HRWRA) can reduce the water requirement between 15 and 40 % and are known as superplasticisers (Li, 2011). The superplasticiser is the game changer and is the key ingredient to producing a workable HSC. The type and dosage of superplasticiser can change the chemical interactions to different degrees. For the most part, superplasticiser is used by trial and error. This is because the use thereof in concrete is relatively new and unknown.

On a macroscopic level, superplasticiser makes concrete more flowable, but understanding the interaction of superplasticiser on a microscopic level is required to predict the efficiency thereof, especially since the use of superplasticisers can easily increase the unit cost of concrete.

Careful consideration should be taken when deciding on the dosage of superplasticiser in a HPC. Large dosages of superplasticiser can bring about excellent flowability in terms of the slump flow measurement, but this flowability may be at the expense of cohesion, setting time, workability and its retention. The most common consequence of a concrete that is overdosed with superplasticiser is either segregation or even stickiness, which should both be avoided. A mix can have a very high slump flow within the first 20 minutes of casting, but become very sticky, very quickly if it is overdosed with superplasticiser.

The dosage at which a mix starts to segregate gives an indication of the maximum dosage of superplasticiser that is effective in a particular mix with a given w/b ratio. This dosage is known as the saturation point of a superplasticiser for that particular mix. The saturation point can also be described as the dosage at which there is no more significant improvement to the flowability with increasing superplasticiser dosage. The dosage of superplasticiser is closely related to the amount of binder, as the mobility of the binder particles is directly influence by the chemical admixture.

2.1.4 High Strength Concrete

A concrete is considered as HSC when its compressive strength exceeds that of conventional concrete. Conventional concrete is also referred to as normal NSC and typical values for its compressive strength are between 20 and 40 MPa.

The relationship between compressive strength and w/c ratio for HSC is not as defined as it is for NSC. A w/c ratio less than 0.4 is essential for obtaining a concrete with compressive strength greater than 50 MPa. The typical w/c ratio range for HSC is between 0.2 and 0.4, however the compressive strength becomes less dependent on the w/c ratio as it decreases. SCM's become quite handy, water-reducing agents become necessary and a look at the particle size distribution becomes nifty. The following sections consider the classification of HSC, the principles used to develop HSC and some practical guidelines for its production.

2.1.4.1 Classification of High Strength Concrete

A concrete is considered as HSC when its compressive strength exceeds that of conventional concrete. Conventional concrete, or NSC however, is relative.

Its strength category depends on the period of time as well as location (Shah & Ahmad, 1994). Location is a critical factor because some countries have more expertise in research and the production of HSC. Another contribution to the location factor is the disposal of local materials. The combination of these two factors influence the typical strength of NSC that is used in design and construction in a particular place at a particular time.

In Europe concrete is considered as HSC when its strength reaches 60 MPa, while in America, the limit is 40 MPa (Owens, 2009). In South Africa, a concrete with compressive strength of more than 50 MPa is classified as HSC. Moving from HSC to ultra UHSC brings about the same discussion on the compressive strength that distinguish the two. In Europe, UHSC is defined as a concrete having a compressive strength of 150 MPa or more and in America, it is 120 MPa. In this study, HSC is considered as a concrete having a compressive strength between 60 and 100 MPa, while concrete with a compression strength exceeding 100 MPa is considered as UHSC.

It is also useful to classify HSC and UHSC in intervals or classes as done by Aïtcin (1998) over a range of 50 - 175 MPa in 25 MPa increments. Aïtcin (1998) suggests that different considerations during material selection are relevant from class to class. For example, it may not be necessary to make use of silica fume in Class I and II HSC, but from Class III upwards it is essential. These classes are illustrated in Figure 2.2. It should be noted that these classes are not particularly universal and may differ from place to place according to the local experience and typical applications of concrete in that country.

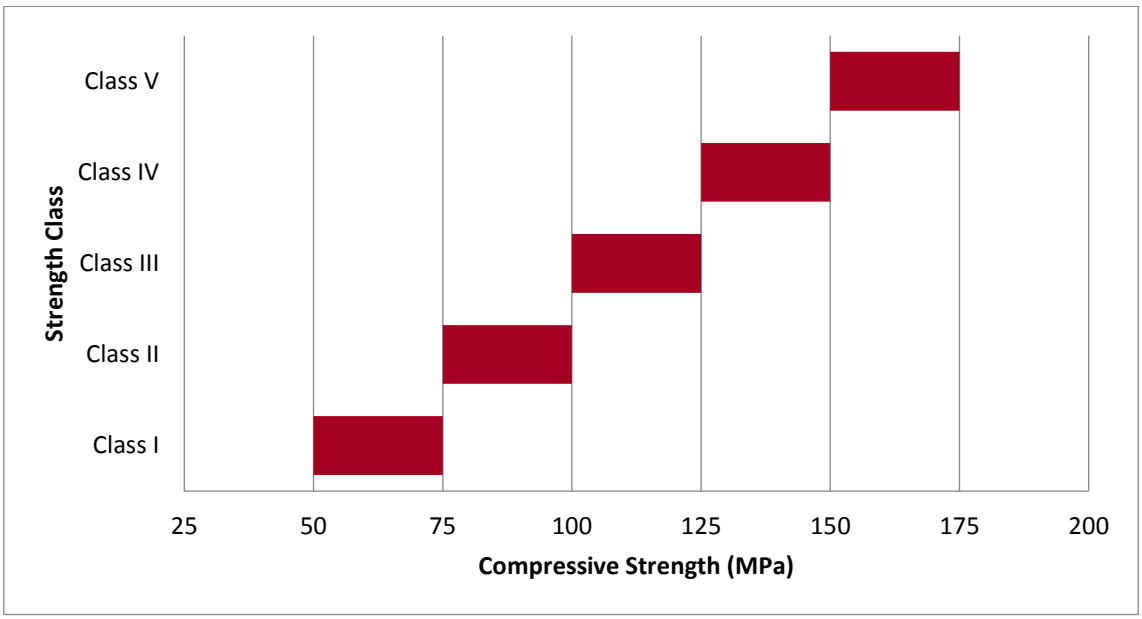

Figure 2.2: High Strength Concrete Strength Classification (data extracted from (Aïtcin, 1998))

When considering the application of HSC, it becomes necessary to look at other fresh and hardened properties beyond the compressive strength. A concrete that has a very high compressive strength, but is stiff and not workable has limited application. Therefore, understanding the principles of HSC are important for material considerations when producing HSC, as discussed next.

2.1.4.2 Principles of High Strength Concrete

From the time water is added to the dry ingredients of a HSC, the clock starts ticking for all the chemical reactions and microstructure developments between the particles. Close attention needs to be paid to the performance of a HSC in its fresh state to control the ease of placement and compaction, since HSC tends to be more sticky than NSC (Aïtcin, 1998). Regulating the fresh properties of HSC can also augment its hardened properties. Performance properties that make HSC a HPC include; workability, slump loss, setting time and early-age deformation. A closer look at the driving forces of these properties follows.

Low w/c ratio

In both NSC and HSC, the w/c ratio is the basic factor that influences the compressive strength of a concrete (Xincheng, 2013). The simple explanation for the increase in strength with decrease in w/c ratio is that the crystalline structures of hydrated cement are packed more closely in a concrete with a low w/c ratio since the cement content is higher. This is illustrated in Figure 2.3.

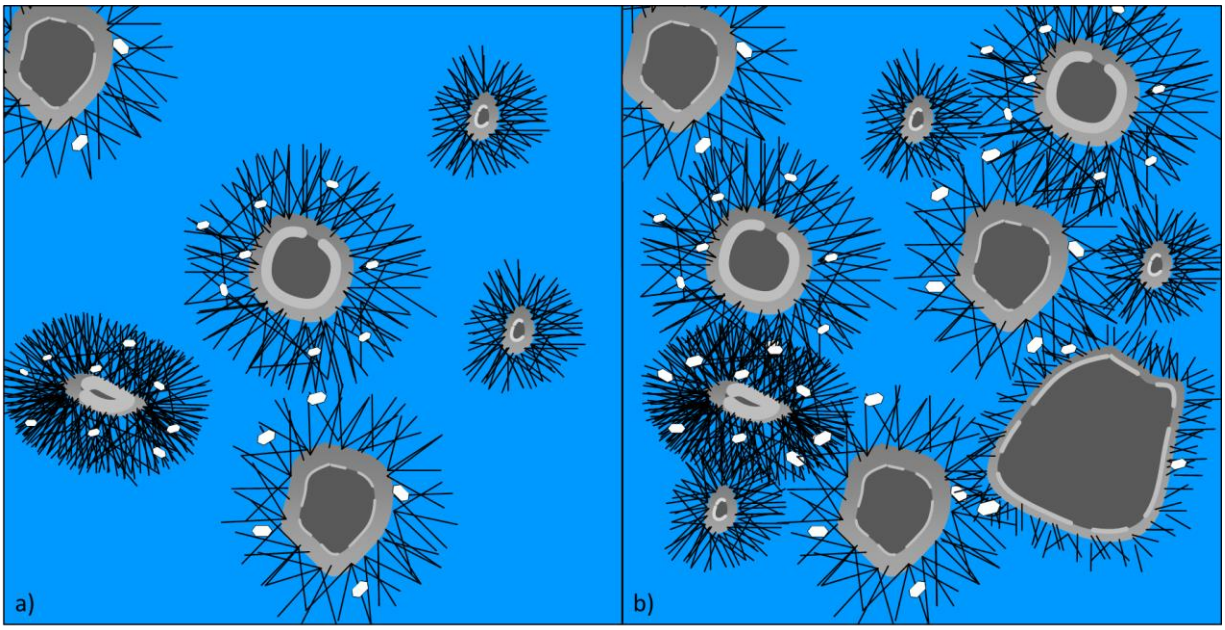

Figure 2. 3: Microstructure of cement paste with a) a high w/c ratio and b) a low w/c ratio

The relationship between compressive strength and w/c ratio for HSC, is not as well defined as it is for NSC. Figure 2.4 illustrates the relationship between the w/c ratio of concrete and its compressive strength. It can be seen that a w/c ratio less than 0.4 is essential for obtaining a concrete with compressive strength greater than 50 MPa. The typical w/c ratio range for HSC (50 - 100 MPa) is 0.2 to 0.4. However, choosing a w/c ratio within this range is not guaranteed to yield a particular strength. The figure also illustrates how the compressive strength becomes less dependent on the w/c ratio as it decreases.

As a guideline, the cement content required in a mix to produce a HSC is in the range of 380 to 500 kg/m^3. For NSC the range is between 250 and 350 kg/m^3 and for UHSC it is between 580 and 1000 kg/m^3 (Owens, 2009). This high cement content calls for attention to other factors.

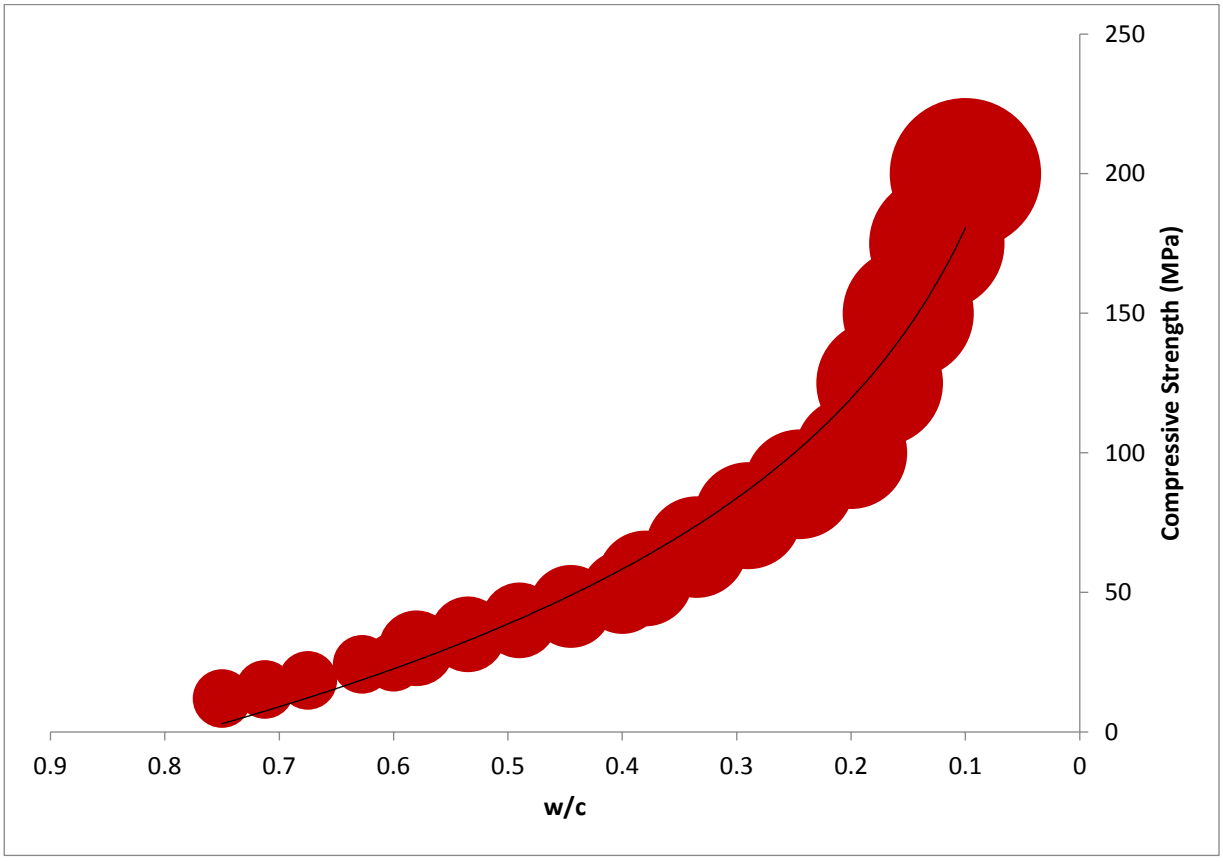

Figure 2.4: Relationship between w/c ratio and compressive strength (data extracted from (Owens, 2009))

The water content of HSC is very low compared to NSC and has two functions; a physical function that aids rheological properties and a chemical function, which is the hydration of cement (Aïtcin, 1998). The hydration process is discussed in the next section.

Cement Hydration

Portland cement hydration is a chemical and physical process, that is complex and still not fully understood. To date, the only insight to Portland cement hydration is the investigation of how the compounds found in cement react individually (Li, 2011). Of course, this is not the case in actuality, but it does provide sufficient understanding of cement hydration and even how to control this process using mineral and chemical admixtures as discussed in Section 2.1.3, to some extent. The first and most influential of the compounds for strength development found in Portland cement are the calcium silicates; C_3S and C_2S. The reactions of these silicates with water are as follows:

$$2C_3S + 11H \rightarrow C_3S_2H_8 + 3CH \quad \text{Eq. 1}$$

$$2C_2S + 9H \rightarrow C_3S_2H_8 + CH \quad \text{Eq. 2}$$

These silicates hydrate to form calcium silicate hydrates (C-S-H), which attributes concrete its strength formation and also CH, calcium hydroxide (Li, 2011).

Once water is added, the cement matrix is in suspension (Shah & Ahmad, 1994). This is shown in Figure 2.5a. Within minutes the C-S-H, also commonly referred as hydration products, start to form on the surface of the cement grains and as time goes on, the hydration products form a crust around the cement particle. The C-S-H comprises about 60 % of the structural component of a cement paste and CH about 25 % (Mehta et al., 1993). As the hydrates grow around the cement particle, the crystals amalgamate and form bridges that changes the concrete from a suspension to a continuous solid (Shah & Ahmad, 1994). C-S-H is the biggest contributor to the strength development of hardened concrete because of its amount and small size (Li, 2011). CH increases the pH of concrete and assists in corrosion protection, but its content should be kept to a minimum as too much may lead to leaching, carbonation or alkali-aggregate reaction (Li, 2011). These products keep growing and essentially, they slow down the hydration as it prevents water from reaching the unhydrated part of the cement particle. This is quite common in NSC with w/c ratio greater than 0.4. According to Shah & Ahmad (1994), hydration in NSC does not really stop; hydration just becomes increasingly slower, but still continues and is warranted by anhydrous cores that may be found in very old concrete. In HPC with w/c ratio less than 0.4, it is more likely that there is not enough water available for complete hydration of cement particles.

Although this is not particularly ideal, in terms of the inhibition of the production of C-S-H, these unhydrated cement particles may act as a fine filler and in fact contribute to improving the strength and impermeability of the concrete (Owens, 2009).

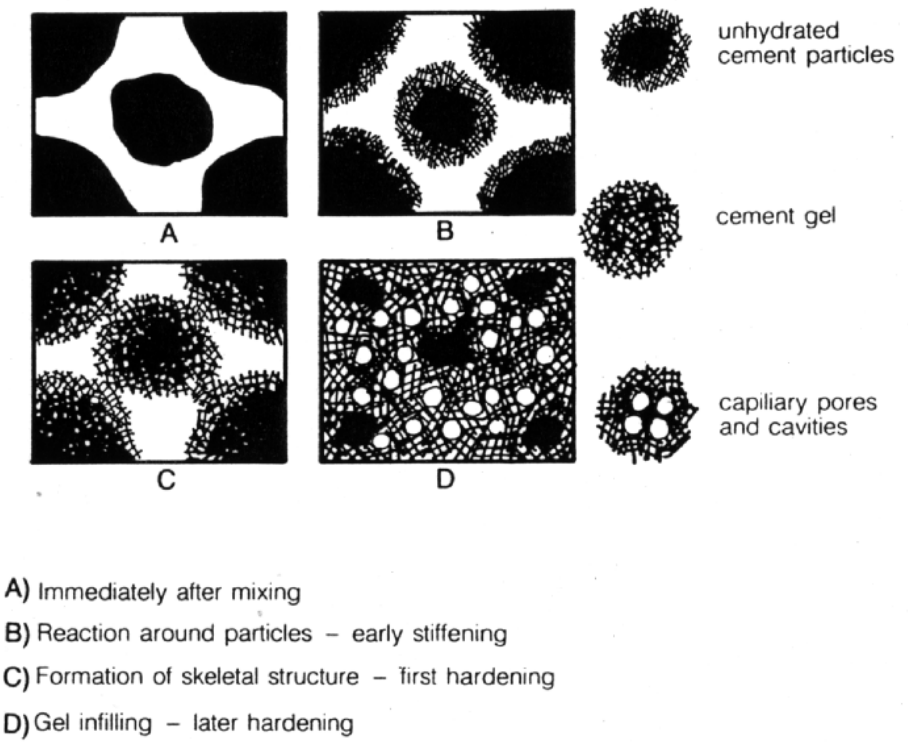

Figure 2.5: Cement hydration process (Li, 2011)

The other two important compounds are the two aluminates; C_3A and C_4AF. The aluminates hydrate at a much faster rate than the silicates and are largely responsible for the stiffening and setting of concrete (Mehta et al., 1993). The reaction of the aluminates is as follows:

$$C_3A + 3(CSH_2) + 26H \rightarrow C_6A_3H_{32} \quad \text{Eq. 3}$$

$$C_4AF + 3(CSH_2) + 21H \rightarrow C_6(A,F)S_3H_{32} + (F,A)H_3 \quad \text{Eq 4}$$

C_3A reacts with water in the presence of large quantities of gypsum and forms $C_6A_3H_{32}$, which is more commonly referred to as ettringite. Ettringite is a needle-shaped crystal which is quite expansive and is aggressive in its growth. These characteristics can be either beneficial or detrimental to the strength gain of concrete. If ettringite forms before hardening, it can contribute to the early-age strength gain by providing reinforcement of C-S-H as they grow.

However, if ettringite forms after hardening, due to its' aggressive nature, it can break down the surrounding network of C-S-H products already formed to make space for its own crystals to grow. This is undesirable as it causes cracks and volume instability (Li, 2011). The reaction of C_4AF in Equation 4 is similar to the reaction of C_3A but occurs at a slower rate.

The reaction of C_3S and C_3A is the fastest and contributes to most of the early heat of hydration (Aïtcin, 1998). C_3S contributes to the early strength gain. C_3A does not contribute to strength gain but it can lead to flash setting in the presence of water. The gypsum in Portland cement helps to retard this fast reaction of C_3A allowing the concrete to remain workable long enough for placing (Li, 2011). For the production of low w/c concretes, a cement with a low C_3S and C_3A content is desirable as it will have a slower heat of hydration development. Cements with low C_3S and C_3A also requires a smaller dosage of superplasticiser for a required slump and is able to maintain a longer slump retention (Aïtcin, 1998) and (Jayasree & Gettu, 2008).

Slump Loss

Slump loss can be defined as the loss of workability of concrete or loss of the consistency of the slump over a period of time in its fresh state (Li, 2011). The period where slump retention is of concern is right after mixing, until the time needed to place and consolidate the concrete. This is usually between one and two hours. Longer slump retention periods may be required for concrete that is batched off-site to account for the traveling time as well as placement and compaction. Retaining the slump of a concrete is important because when a concrete becomes difficult to place, various problems can occur; extra strain is put on the mixers, concrete can stick to the sides and blades of the mixer, difficulty in placing and pumping arise, labour and time increases, productivity and quality of work decrease and most crucial of all, strength and durability is lost due to poor compaction and finishing.

While slump loss occurs in both normal and HPC, rapid slump loss is more likely to occur in HPC. Slump loss is the result of the stiffening of a concrete mix as the cement hydrates over time. One would expect that a HPC would have longer slump retention than NSC because of its longer setting time due to increased amounts of superplasticiser, but slump loss is in fact a bigger concern in HPC than it is in NSC. This is because of the delicate relationship between cement and superplasticiser, of which both are added at large dosages. The slump loss of a concrete mix with a given cement-superplasticiser combination can therefor give an indication of the compatibility of that combination.

The slump of concrete gradually reduces over time as free water is lost due to three main reasons; water being absorbed by dry aggregates or formwork, loss of water due to evaporation and the cement hydration process (Owens, 2009).

In HPC, slump loss is further increased by high concrete temperatures in these cement-rich mixes, which have an excessive heat of hydration. Concrete temperatures may further be intensified by dry ingredients, which have a high ambient temperature, which is quite common with aggregates that are stored outside in the sun for on-site batched concrete (Mehta et al., 1993).

There are ways to manage and reduce the risk of rapid slump loss. The first and most effective precaution would be selecting a suitable cement-superplasticiser combination. However, the most common precaution in practise, particularly for off-site batched concrete, is producing a mix with a high initial slump to accommodate for the slump loss by the time the concrete is ready to be placed, or adding extra water and remixing just before placing (also known as retempering). Both batching at a higher slump and retempering could result in other problems. The higher the initial slump, the higher the rate of slump loss (Previte, 1977). While retempering can be advantageous in regaining the slump, it can also be detrimental to the strength of concrete since the w/c ratio is effectively increased. A study by West (1990) showed that retempering can in fact be a viable solution to recover slump loss without significantly reducing strength when careful consideration is given to the amount of extra water to be added (West, 1990). This careful consideration takes in to account the amount of free water that is lost due to absorption and evaporation. A corresponding amount of retempering water is considered safe to add for sufficient slump regain while maintaining sufficient strength.

Figure 2.6 shows examples of compatible and incompatible cement-superplasticiser combinations. The solid line represents a compatible combination where the slump remains constant for 120 min. A practical slump retention time is between 60 – 90 min, but would differ according to the particular application. The dashed and dotted lines are examples of incompatible mixes. The dashed line maintains the initial slump for about 30 min, but after that it drastically reduces. The dotted line does not maintain the initial slump at all and decreases constantly. These two combinations would not be able to be used in practise. The slump flow axis is presented as dimensionless as it represents an arbitrary slump for the specific mix under consideration from time zero.

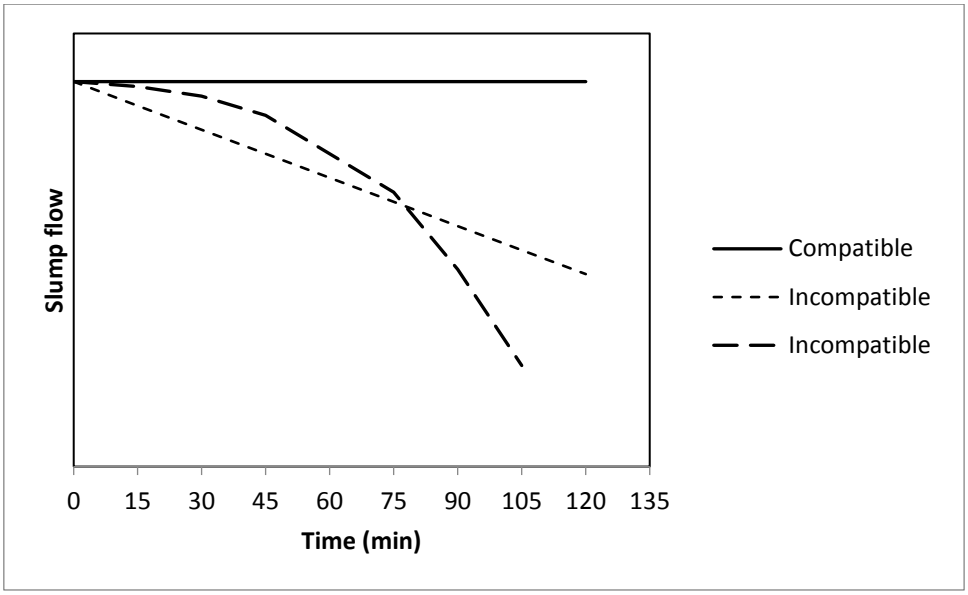

Figure 2.6: Slump loss of a compatible and incompatible cement-superplasticiser combination

A more cognisant approach to reduce slump loss is the selection of a compatible cement-superplasticiser combination and also the use of SCM's. SCM's are typically always used in HPC. They are effective in two ways; they provide supplementary C-S-H through pozzolanic activity and also their fineness improves the packing density, which provides a dense microstructure leading to a better mechanical and durable performance.

Interfacial Transition Zone

It is well known that concrete is strong in compression, but comparatively weak in tension for both normal and HPC. The interfacial transition zone (ITZ) provides some insight to how and why this is the case. The ITZ is also known as the aggregate-paste interface and is subsequently the space adjacent to the aggregate surface and the bulk paste as illustrated in Figure 2.7 (Li, 2011). Although the structure of the elements in this space are the same as that found in the bulk hydrated cement paste, their microstructure and properties are not the same (Mehta et al., 1993). The space surrounding the coarse aggregate has a higher w/b ratio because of the water that lines the aggregate or bleed water that may be trapped underneath. When cement is present in an excess of water, large crystalline hydration products form instead of C-S-H, which provide the strength (Aïtcin, 1998). As a result, this ITZ with high w/b ratio is very porous and weak compared to the bulk paste. This is the case in NSC with w/b ratio > 0.4 where high compressive strengths cannot be reached because there is limited stress transfer from the paste to the aggregate (Aïtcin, 1998).

To understand and improve of strength of HPC, the interactions in the ITZ are key. The first thing to recognise is that concrete is a non-homogeneous material, composed of three parts; the hydrated cement-paste, aggregate and the space between them called the ITZ. The compressive strength of a concrete is governed by the weakest link of these three parts. To obtain a concrete with high strength, the weakest link of the three phases, illustrated in Figure 2.8, need to be strengthened. In NSC, the weakest link is typically found to be the bulk cement paste or the ITZ (Aïtcin, 1998). The use of large amounts of fine materials like cement and mineral admixtures, such as silica fume in particular, result in a denser microstructure of both the bulk cement paste and the ITZ (Owens, 2009). The ITZ of a low w/b ratio concrete is consequently less porous and much stronger than that of conventional concrete. Looking at Figure 2.7 it can be seen that the ITZ of low w/b ratio concrete in b) has more C-S-H products closely packed to one another, the width of the ITZ is narrower than the ITZ in a) and also less porous.

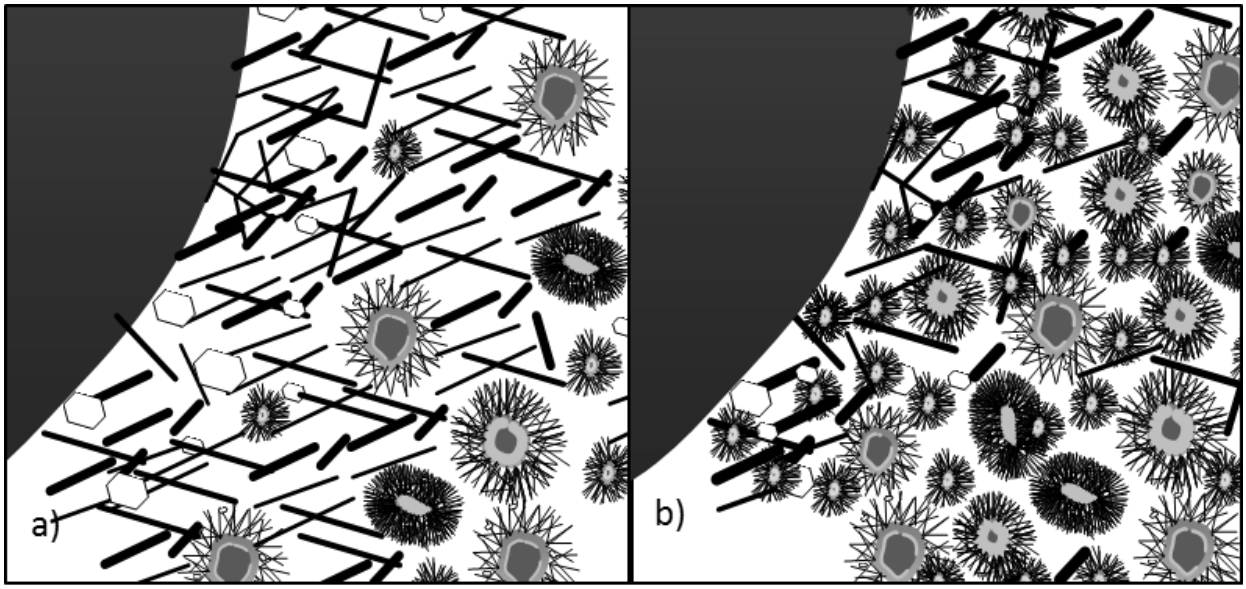

Figure 2.7: ITZ of a) high w/c ratio and b) low w/c ratio

Goldman and Bentur (1993) suggested that the use of silica fume in HPC improves the strength of the bulk cement paste and ITZ because of its fine filling abilities rather than its pozzolanic activity. The dense microstructure in the ITZ of HPC also reduces the risk of cracking because it is harder for micro-tensile cracks to propagate and coalesce (Aïtcin, 1998). In addition to the increased compression strength due to the improved ITZ, the tensile strength is also increased in this regard, albeit not that much (Mehta et al., 1993).

Decreased particle size thus leads to the improved strength of the bulk cement paste and the ITZ because it reduces porosity and inhomogeneity in the matrix (Nielsen, 1993). Mortars and pastes have more homogeneous matrices than concretes containing coarse aggregates and consequently they will be less permeable and stronger than the corresponding concrete (Mehta et al., 1993)..

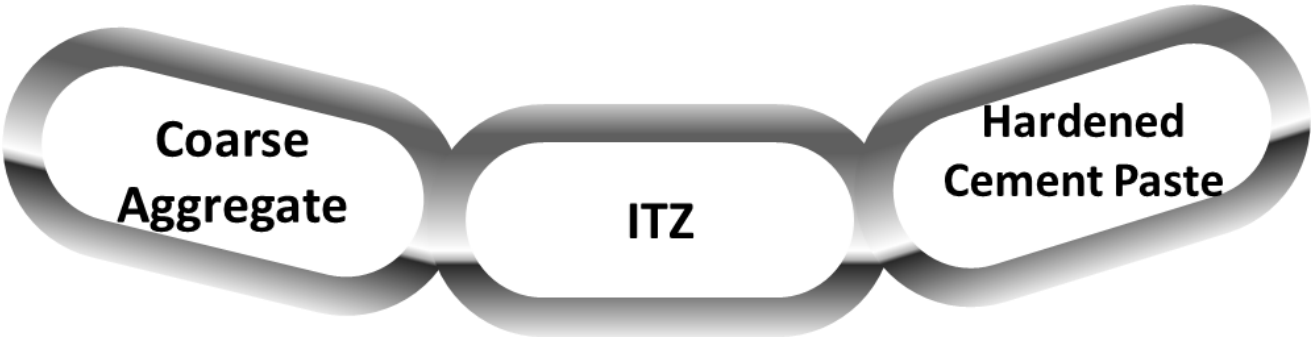

Figure 2.8: Three phases of concrete: hardened cement paste, interfacial transition zone and aggregate

Considering that the aggregate is commonly the weakest link of HPC, decreasing the w/b ratio beyond a certain value will not result in a stronger concrete, since the compressive strength will be governed by the strength of the aggregate (Aïtcin, 2003). Obtaining a hardened cement paste and ITZ that is equal to or slightly stronger than the specific aggregate used in a mix is thus the maximum obtainable strength. Seeking a higher compressive strength would require the use of a stronger aggregate. Improving the strength of the hardened cement paste and ITZ beyond the aggregate, could improve other properties such as impermeability and durability if desired (Aïtcin, 2003).

2.1.4.3 How to Achieve a High Strength Concrete

Producing a HSC is more a material selection process as opposed to a mix design process as in the case of NSC. The material selection focuses on selecting combinations of materials that are compatible with one another and result in excellent fresh and hardened properties, most desirably high strength, durability and consistency (Neville, 1995). In HSC and more so HPC, the properties of the individual constitutes are principally more important than in NSC. The materials used, including the fine and coarse aggregate, have to be good quality. Selecting the best available materials is the first step in achieving a HSC.

Conventional mix design methods are not suitable for low w/b ratio concrete with low workability (Owens, 2009). The workability of HPC is controlled by the use of superplasticisers, which changes the fundamentals on which conventional methods are based. The use of SCM's also introduce certain complexities to the conventional concrete system.

The addition of superplasticiser and SCM's suddenly turn the simple concrete technology, as we know it, in to a complex system of chemical interactions. This presents difficulties in developing a universal, theoretical mix design method for HSC.

The production of HSC is thus more an art, than it is a science (Aïtcin, 1998) and it cannot be achieved without a series of trial mixes. The next step would be to find the right combination of cement and/or SCM with superplasticiser. Their interaction is characteristically a chemical reaction; this is why not all superplasticisers are equally compatible for all types of cementitious material even though each component may be of the highest equality.

Efforts have been made to stream line the process and present some guideline. There are a number of computer programs that have been developed for material selection and mix proportioning of HSC based on the required fresh and hardened properties.

One such expert system is called the *HPCMIX* as designed by Islam et. al. (2005) and is summarised in Figure 2.9. The procedure is based on the passing or failure of three criteria: strength, workability and durability (Islam et al., 2005). Each of the requirements in the three categories is specified and each time a mix is produced; it is checked if the requirements are met. If not, the program gives explanations and recommendations for the next trial mix until all the requirements are met. This is typically how a HSC is produced, a set of requirements are specified and if they are not met, adjustments have to be made and the mix is iterated until a satisfactory mix is achieved.

Some practical guidelines taken from the information mentioned in this chapter is as follows:

- w/c ratio < 0.4 for a compressive strength greater than 50 MPa.
- Select an appropriate cement/superplasticiser combination
- Introduce SCM according to desired fresh and hardened properties
- Reduce water content and increase workability with the use of superplasticisers
- Do not overdose the mix with superplasticisers, this will cause rapid slump loss
- Reduce water requirement by eliminating as much fines from the aggregate as possible

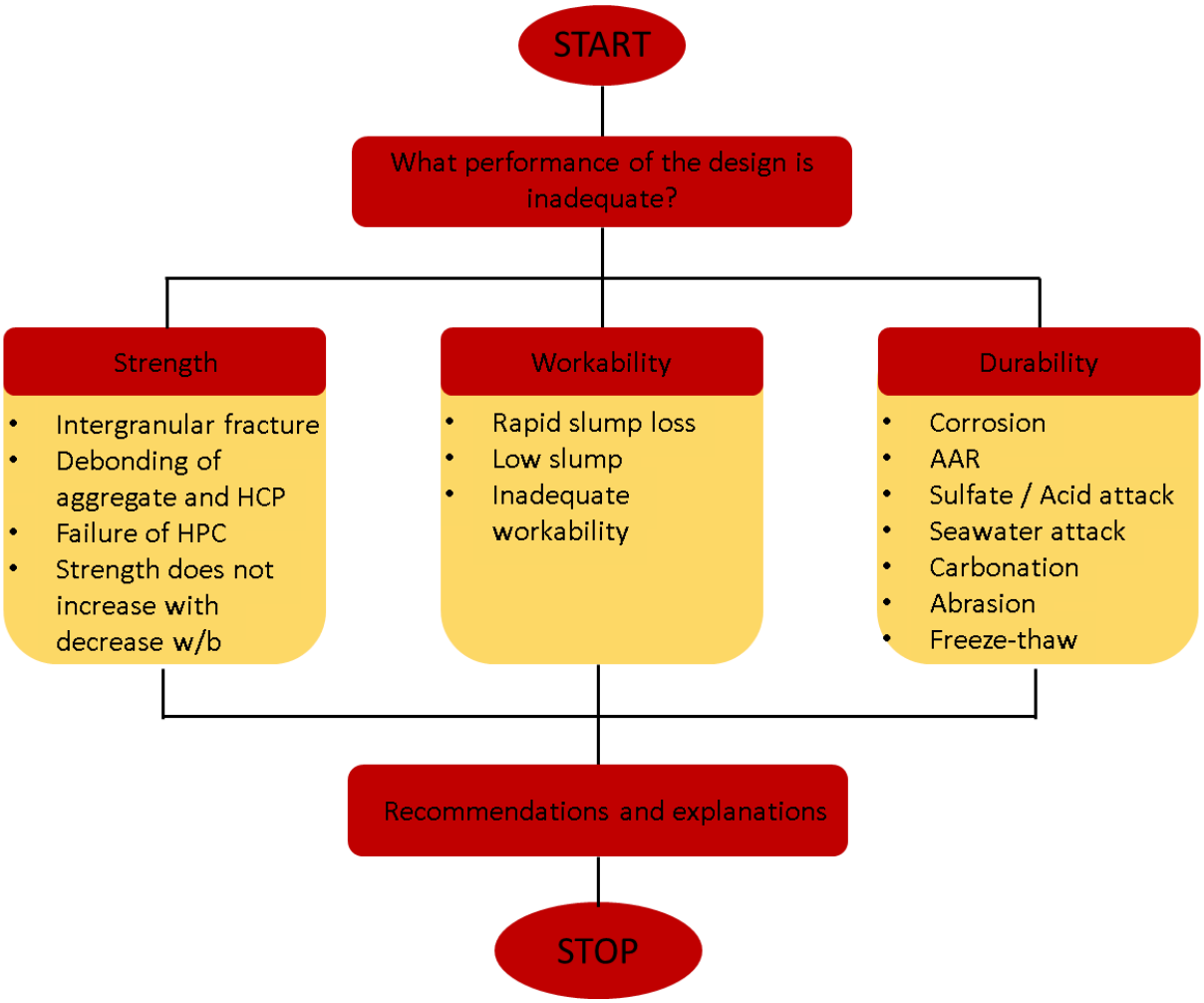

Figure 2.9: Mix performance adjustment of HSC adapted from (Islam et al. 2005)

2.1.5 Self-Compacting Concrete

Self-compacting concrete (SCC) is also known as self-consolidating, self-levelling, high-fluidity or rheoplastic concrete and it is just that. It is a concrete that is able to compact, consolidate and level itself due to its high fluidity and possesses excellent rheologic properties in its plastic state. Combining the definition given by Mehta et al. (1993), (Owens, 2009) and (Li, 2011), SCC is a flowing concrete that can be cast into place and consolidates in any shape of formwork and between reinforcing bars under its own weight, without the need for external or internal vibration, while maintaining homogeneity without any segregation and does not result in surface defects such as honeycombs or bug holes. This section considers the classification of SCC, the principles used to develop SCC and some practical guidelines for its production.

2.1.5.1 Classification of Self-Compacting Concrete

High flowability is the most important criterion that needs to be met to classify concrete as self-compacting and then a few auxiliary tests that confirm if the concrete mix is in fact deemed acceptable to uphold high performance properties when casting in the field. Such a mix can be obtained in two ways; dictating unconventional mix proportions to have a high powder content which ensures a homogeneous flow, or the use of a viscous modifying agent (VMA) without the need for a high cementitious content (Mehta et al., 1993). SCC is typically classified into two categories which is defined on the basis of the two mix proportioning approaches described above; powder-type SCC and VMA-type SCC (Bonen & Shah, 2005).

Powder-type SCC is achieved by merely improving mix proportioning of conventional ingredients so as to increase the fines content (Li, 2011). Figure 2.10 shows a schematic representation of the typical proportions of conventional ingredients used in concrete to produce a SCC and NSC in a) and b) respectively.

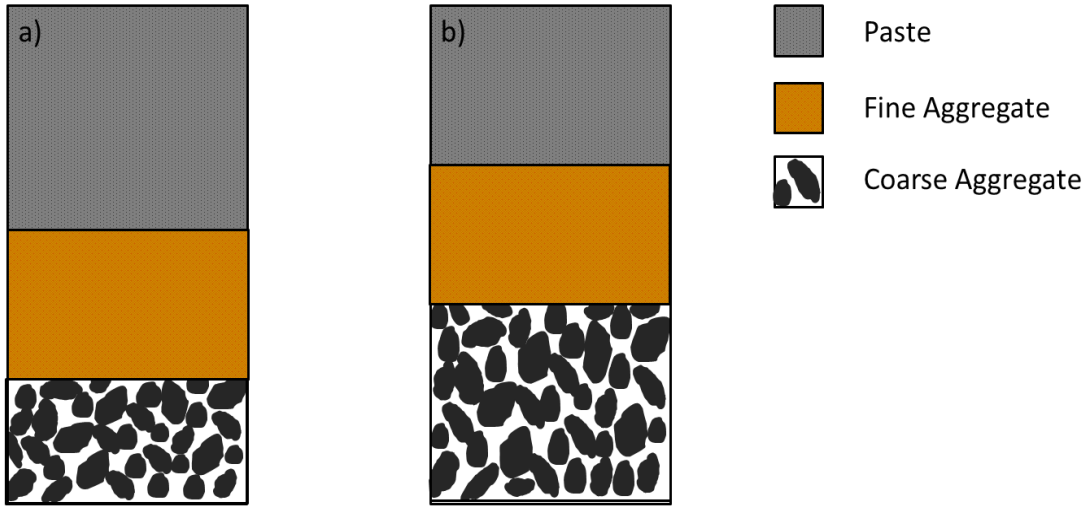

Figure 2.10: Schematic representation of mix proportions for a) self-compacting concrete and b) normal concrete

If for a given total volume, the amount of water is kept the same, the increased binder content in SCC, consequently lowers the w/b ratio. The use of a superplasticiser is therefore crucial to achieve a mix with high flowability (Okamura & Ouchi, 2003). The increased fines content introduces concerns toward high early-age shrinkage and an increase in superplasticiser may lead to segregation. Both increased binder and superplasticiser contents increases material cost. The alternative to the powder-type SCC, the VMA-type SCC, is not as rich in cementitious material and can thus reduce the risk of early-age shrinkage and provide resistance to segregation.

Although VMA's can successfully provide enough viscosity to resist segregation, it should be noted that the powder-type SCC was specifically designed to be more durable due to the high fines content (Bonen & Shah, 2005) in addition to its excellent flowability. Good thought would have to be put in to deciding which of the two proportioning methods to develop SCC would be most appropriate and economically viable for the specific application. Figure 2.11 shows the difference in typical proportions of conventional ingredients, as adapted from (Li, 2011), of a) NSC, b) VMA-type SCC and c) powder-type SCC.

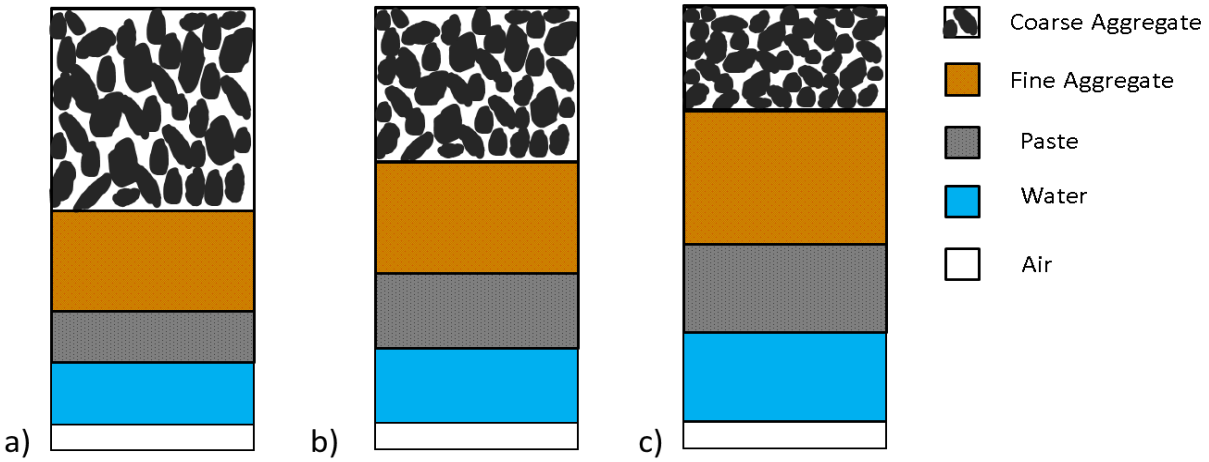

Figure 2.11: Typical mix proportions of a) NSC, b) VMA-type SCC and c) powder-type SCC (information extracted from (Li, 2011))

More information on the effects of different types of VMA's can be found in an overview study by Khayat (1998).

The classification of SCC in terms of its fresh state performance is not strictly defined. Regulatory bodies such as ERFNSC and the Japan society of Civil Engineers have categorised SCC into classes according to their slump flow and slump flow times. However, these classes cannot always be used universally. Instead, the fresh state requirements of a SCC are dictated according to its application. The fresh state performance required of a SCC for a foundation is much different to the performances required for a long slender column for example (Bonen & Shah, 2005).

In addition, the lack of a universal performance standard is also due to the advancement in research and application of SCC in countries such as Japan and North America, which are continually developing, faster than the specifications set by regulatory bodies. In South Africa, SCC is not researched and used as widely as in Japan and North America, so focus is not being put on the exclusive definition of these performance classes.

In 2005, *"The European Guidelines for Self-Compacting Concrete"* was published by ERFNSC at the time to provide useful information on the production of SCC to increase the acceptance and use of SCC in Europe.

The ERFNSC includes the classification of SCC according to its slump flow in their guideline which is summarised in Figure 2.12a, with the minimum flow being 550 mm. Figure 2.12b shows slump flow class intervals as defined by Walraven (2003) which requires a minimum slump flow of 470 mm before a concrete is classified as SCC.

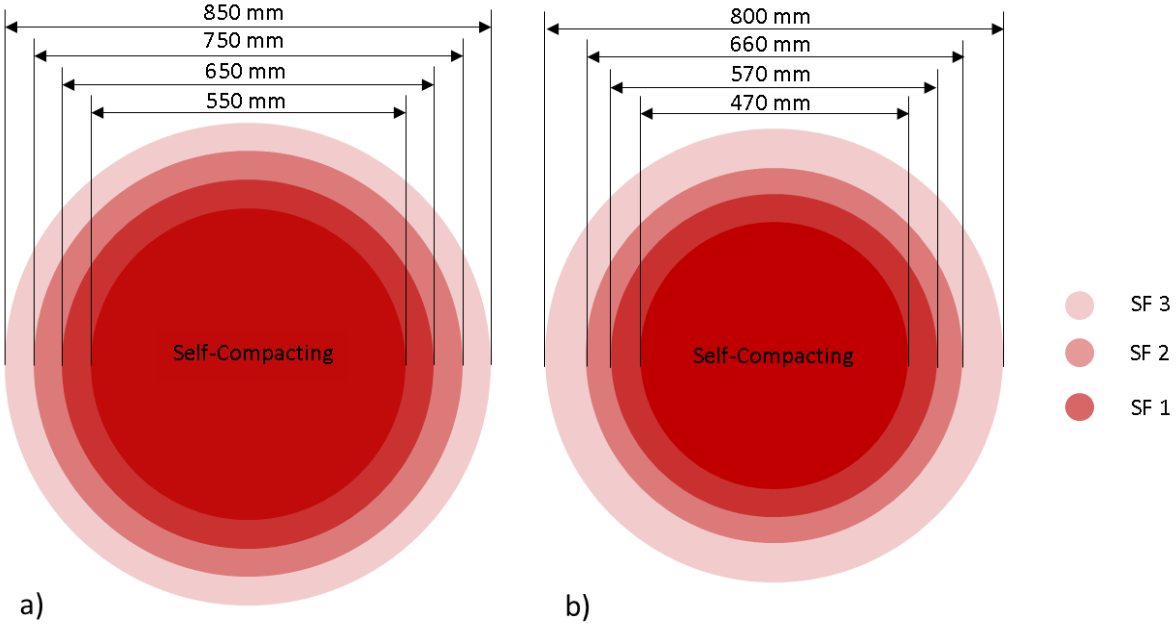

Figure 2.12: SCC slump flow classes according to a) EFNARC and b) (Walraven, 2003)

There are a number of tests used to evaluate the fresh performance of SCC. The slump flow gives an indication of the ability of the concrete to flow and level itself under its own weight. The slump flow is also used to verify the consistency of different batches of the same concrete mix (Bonen & Shah, 2005) during research as well as during production and placing on site. Other performance properties such as passibility, fillability and segregation resistance can be observed through tests like the J-ring test, V-funnel test and the sieve segregation tests.

Observing these properties are beyond the scope of this literature study, but a summary of these properties and the tests used to observe them are summarised in Appendix A.1.

2.1.5.2 Principles of Self-Compacting Concrete

Self-compacting concrete is characterised by its ability to deform and fill any space while remaining stable during both casting and transportation (Mehta et al., 1993). This deformability and fillability is governed by rheological properties such as the yield stress and plastic viscosity of the material (Skarendahl & Petersson, 2000). The target rheological properties for SCC are low yield stress and moderate viscosity (Khayat, 1998 and Bonen & Shah, 2005). The yield stress is related to the friction action between the coarse aggregate and other solid particles while the viscosity is related to the shear resistance of the paste and mortar.

Although the physical testing of rheology is beyond the scope of this study, the principles thereof and how to obtain a low yield stress and moderate viscosity are considered to gain an understanding of the mechanisms involved.

The paste and the mortar are perhaps the key components to consider since they are the vehicle that drive the coarse aggregate to flow cohesively within the material and more crucially, around reinforcing and other obstacles in the formwork. These two components, the coarse aggregate and the mortar, are considered in the following sections. The particle size distribution (PSD) of the two components are also considered and how their proportions can be optimised to produce a SCC with low yield stress and moderate viscosity.

Low Yield Stress and Coarse Aggregates

To come to grips with the principles of SCC, it is convenient to consider the Bingham and Newtonian models that describe the rheological behaviour of suspensions. The models are shown in Figure 2.13. The Bingham model commonly represents NSC that requires a minimum shear stress, or yield stress which is denoted by τ_0, before there is any shear strain, i.e. before the concrete starts to flow. This yield stress is applied to conventional concrete through internal or external vibration, which provides the material with the energy required to induce flow and fill the spaces in a formwork. However, the Newtonian model represents a material that does not require applied energy to induce flow and this is the model that mix designers try to achieve when developing a SCC. For this reason, vibration is not required for consolidation of SCC. Water closely represents a Newtonian fluid and of cause SCC is not a true Newtonian fluid, but the principle is to proportion the concrete so that is has a very low yield stress (Skarendahl & Petersson, 2000 and Owens, 2009).

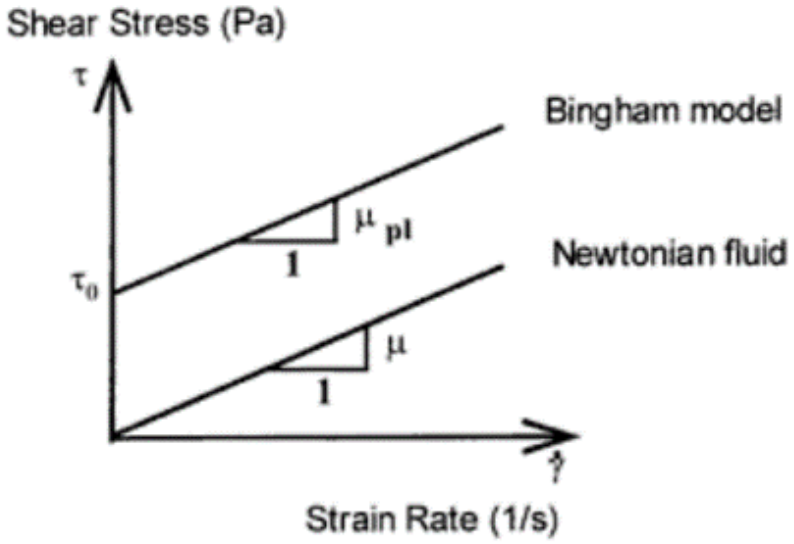

Figure 2.13: Principles of the Bingham and Newtonian models for the rheological behaviour of suspensions (Skarendahl & Petersson, 2000)

The yield stress is a result of inter-particle friction between the coarse aggregates, fine aggregates and all other cementitious material particles which build up internal stresses as they collide with one another while trying to flow (Skarendahl & Petersson, 2000 and Okamura & Ouchi, 2003).

The first and most effective approach to lower the yield stress of a SCC is to limit the coarse aggregate content, as their energy consumption is the highest (Okamura & Ouchi, 2003). Besides controlling the volume of coarse aggregate in SCC, the maximum size thereof should also be limited to ensure the stability of these high flowing mixtures (Mehta et al., 1993). The content and maximum size of coarse aggregate is particularly of concern in terms of the interaction between the concrete and reinforcing bars, since structures that require SCC are typically made up of densely reinforced elements. Along with the maximum aggregate size, the grading of the coarse aggregate also needs to be considered for reinforcing that has a minimum spacing that is not much bigger than the maximum coarse aggregate size itself (Okamura & Ouchi, 2003). The actual shape of the aggregate is not of significant concern according to Matsuo et al. (1994), the self-compatibility of concrete is more dependent on the ratio between coarse aggregate and total solids by volume (Okamura & Ouchi, 2003). According to De Scchutter et al. (2008) as well, the grading of the coarse aggregate is a more of concern in SCC than the size and shape when considering the required powder content to achieve sufficient stability for SCC.

Figure 2.14 shows the difference in distribution of coarse aggregates in a) conventional concrete and b) SCC with at a smaller volume.

From the figure, it can be seen that the frequency of collision between the coarse aggregates would be reduced in the SCC, which subsequently reduces the solid-solid friction (Li, 2011). This is effective in lowering the yield stress of SCC by increasing the inter-particle distance between the coarse aggregates.

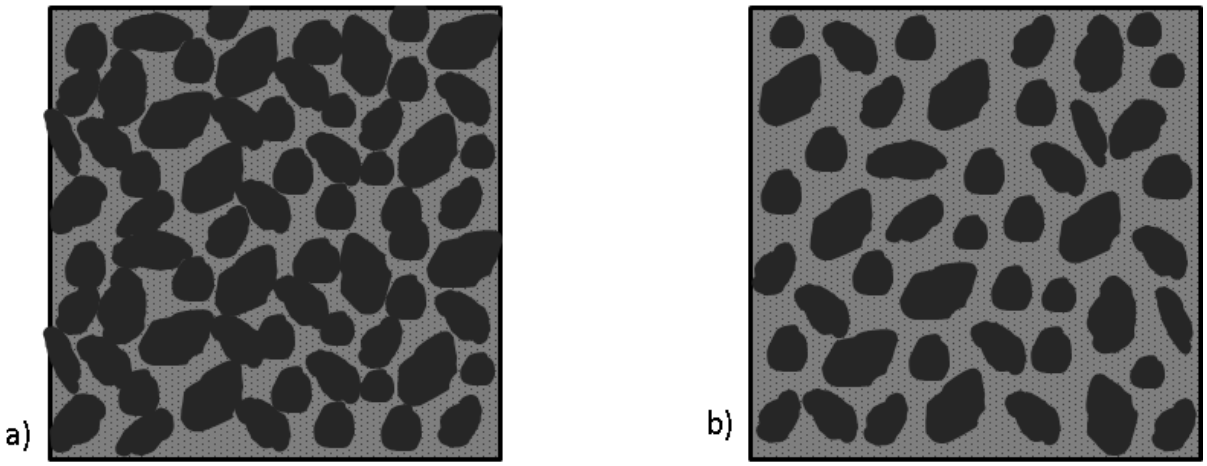

.

Figure 2.14: Coarse aggregate distribution in a) conventional concrete b) self-compacting concrete

Considering the other particles in the mix, fine aggregate and cementitious material, it is not as simple to increase the inter-particle distance by reducing their contents to lower the yield stress. This would mean that the water content should be increased which increases the risk of segregation, which has a detrimental effect on the concrete strength and durability.

Instead, the inter-particle distance is enhanced by making use of superplasticisers to effectively disperse these fine particles (Skarendahl & Petersson, 2000).

Moderate Viscosity and Flowability

The use of high dosages of superplasticiser and low w/b ratio respectively employs high flowability and moderate viscosity. These two approaches are complimentary. High superplasticiser dosages increase flowability by efficiently dispersing the fine particles in the mix (Skarendahl & Petersson, 2000). Too much superplasticiser, however, increases the risk of bleeding, segregation and settlement, which ultimately has a detrimental effect on the ITZ between the mortar and coarse aggregate as well as on the reinforcement interface (Mehta et al., 1993). A low w/b ratio means that the mix has a high fine content, which in turn provides resistance to segregation. A medium between these two allows a moderate viscosity to be achieved which is not only effective in inhibiting segregation, but also reduces localised internal stresses caused by collision of coarse aggregates (Okamura & Ouchi, 2003).

Thus, the reduced free water and increased fines content improves the cohesiveness and viscosity of the mix (Felekoğlu et al., 2007).

Viscosity is defined as the resistance a fluid has towards flowing. This sounds like a counterintuitive characteristic to desire for a high flowing mix. However, a moderate viscosity is the sweet balance between high flowability and high cohesiveness that is required of a SCC to flow homogeneously while preventing segregation.

This is important because typical applications of SCC are made up of densely reinforced elements, which provide more sites for material separation, or segregation, on the interface between reinforcement and the concrete as well as the coarse aggregate and the rest of the mortar (Mehta et al., 1993). Referring to the suspension models shown in Figure 2.15, once the yield stress of the mix is overcome, there is an increasing shear stress with an increasing strain rate which represents the plastic viscosity (μ) (Billberg, 1999).

Okamura and Ouchi (2003) explains that the mortar of a SCC plays two roles in its flow characteristics; it acts as a fluid in the fresh state, but it can also act as a solid particle between the coarse aggregates as the material flows. With the mortar acting as a fluid, it lubricates the coarse aggregates so to speak and allows the coarse aggregates to gently shear passed one another and around reinforcing while the material is flowing. When the mortar is sandwiched between two coarse aggregates as shown in Figure 2.15, it acts as a solid and there is a pressure transfer from the coarse aggregate to the mortar, subjecting the mortar to normal stresses and allowing the material to deform and flow under its own weight.

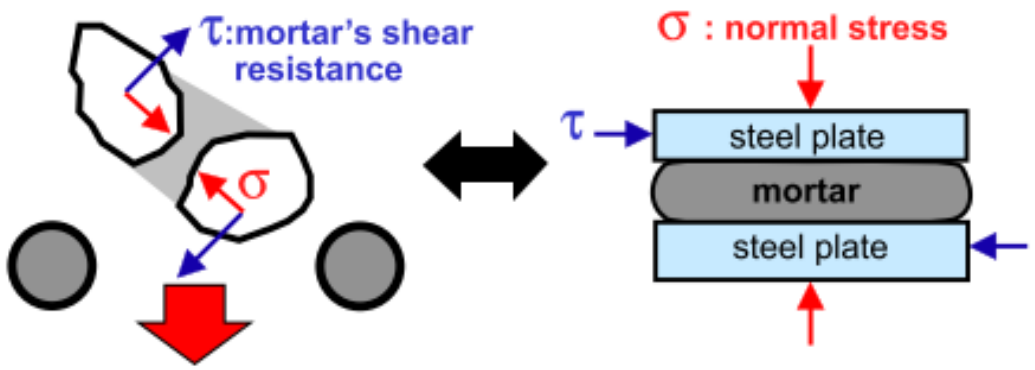

Figure 2.15: Mortar subject to normal stresses (Okamura & Ouchi, 2003)

The viscosity of SCC can also be controlled by the use of VMA's without an increase in fine aggregate and cementitious materials (Li, 2011). VMA's are commonly used in combination with superplasticisers; the superplasticiser can completely reduce the yield stress and the VMA is employed to provide resistance to segregation and cohesion (Owens, 2009). There are various types of VMA's. More information on the effects of different types of VMA's are presented by Khayat (1998), which will not be discussed here.

Particle Size Optimization

While high dosages of superplasticiser to make concrete flow, and a high content of cementitious material to provide the viscosity needed to resist segregation could produce a SCC, this is not necessarily the best approach. By giving careful consideration to the materials and their proportions used in SCC, the particle size distribution (PSD) can be optimised to reduce the ecological and economic impact that consuming large amounts of cement and superplasticiser have (AbdElrahman & Hillemeier, 2014). Furthermore, an increase in fine particles increases the risk of early-age shrinkage and cracking which is not desirable.

Besides the ecological and economic advantages of this approach, it also provides practical advantages. The mix design process of SCC is an experimental one, which undoubtedly requires a number of trial mixes. By making use of idealised grading curves, the amount of time and material needed to reprise a desired SCC can be reduced. Fuller and Thompson (1907) presented work on the influence that the grading of aggregates has on the particle packing density of concrete. A higher packing density means that there is less voids in a particular concrete mix, thus improving factors such as strength and durability.

As presented in the work of Matsuo et al. (1994) and De Scchutter et al. (2008), the grading of coarse aggregate is more influential on the flowability and fillability of SCC. The grading of all solid particles in a concrete are in fact important to consider. Figure 2.16 shows Fuller's parabola for the ideal grading of aggregates for optimum packing density and the Ideal Fuller curve for the ideal grading of aggregates and fine particles.

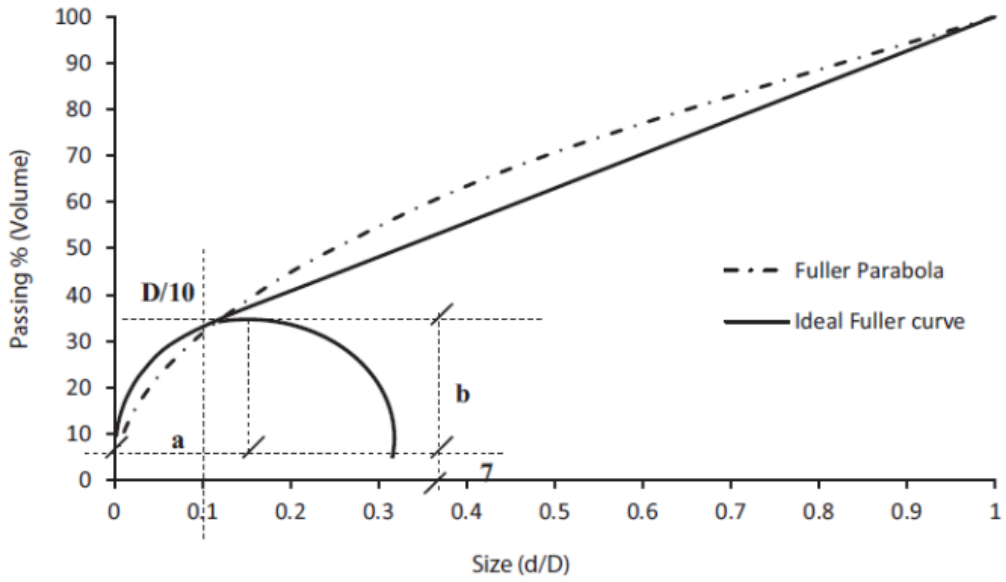

Figure 2.16: Fuller parabola and ideal Fuller curve for aggregates (AbdElrahman & Hillemeier, 2014)

Since the work of Fuller and Thompson, there has been a lot of development with regards to aggregate grading and particle packing. The curves in Figure 2.16 are more suited for concretes that are largely made up of particle sizes greater than 500 µm, as in the case with conventional concrete, and not so much for HPC and SCC (Brouwers & Radix, 2005).

Equations 5 and 6 were developed from Fuller's work by Powers (1969) and Funk & Dinger (1994) respectively with q, the gradation ratio, being equal to a number between 0 and 1 (Brouwers & Radix, 2005). Equation 5 with q = 0.5 closely resembles Fuller's parabola for conventional concrete (Wang et al., 2014). The work of Andreasen & Andersen (1930) suggests that the optimum gradation ratio for SCC is 0.37 which takes account of particles that are smaller than 500 µm and also the decrease in void content because of this finer particle packing (Brouwers & Radix, 2005 and Wang et al., 2014). Equation 6 was later developed to take in to account the actual size of the smallest particle.

$$P = \left(\frac{d}{Dmax}\right)^q \quad \text{Eq. 5}$$

$$P = \frac{d^q - Dmin^q}{Dmax^q - Dmin^q} \quad \text{Eq. 6}$$

where P is the percentage of material passing through a sieve with diameter d and D_{max} is the size of the largest particle, D_{min} is the size of the smallest particle and q is a gradation ratio.

Figure 2.17 shows a comparison between four different PSD curves, two representing ideal curves, one for NSC and one for SCC and the other two curves representing the PSD of two SCC mixes designed by Su et al. (2001) and Su & Miao (2003). This comparison was carried out by Brouwers & Radix (2005). The methodology of the mixes designed by (Su et al., 2001) and (Su & Miao, 2003) is to firstly consider the packing of the fine and coarse aggregate and then consider the paste as filling the voids between the aggregates. Their approach is aimed at developing a SCC that contains the least necessary amount of paste, which is made up of the most expensive constitutes; cement and superplasticiser, to produce the strongest and most durable SCC mix possible.

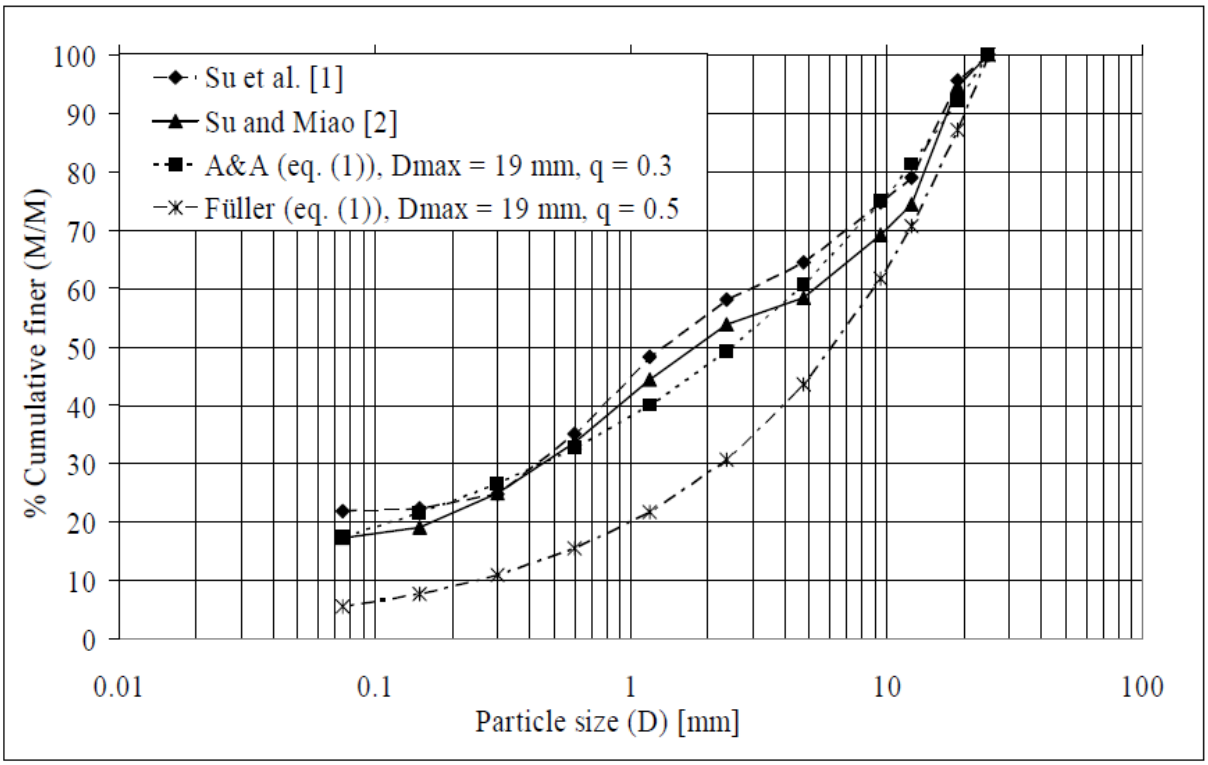

Figure 2.17: Comparison of different ideal optimisation curves for aggregates with a maximum size of 16 mm (Brouwers & Radix 2005)

Brouwers and Radix (2005) also presented a comparison between three different mixes with three different ideal PSD curves. Their work put emphasis on selecting the appropriate *q* value that represents the ideal curve for SCC and HSC in particular. The mix that performed the best contained a larger portion of very fine particles in the fine aggregate, which was a combination of 0 to 1 mm and 0 to 4 mm fine aggregate. The other two mixes contained fine aggregate with a smaller portion of very fine particles; one with fine aggregate 0 to 4 mm and the other two a combination of 0 to 2 mm and 0 to 4 mm.

The mix containing fine aggregate in the range of 0 to 1 mm interestingly also required the least amount of superplasticiser to obtain the same or better fresh performance properties. This shows that finer particles indeed play a role in optimising the particle packing and thereby improving the stability and flowability of SCC. This is shown in Figure 2.18. From the figure, it can be seen that the three mixes more closely represent the ideal curves that have a smaller *q* value.

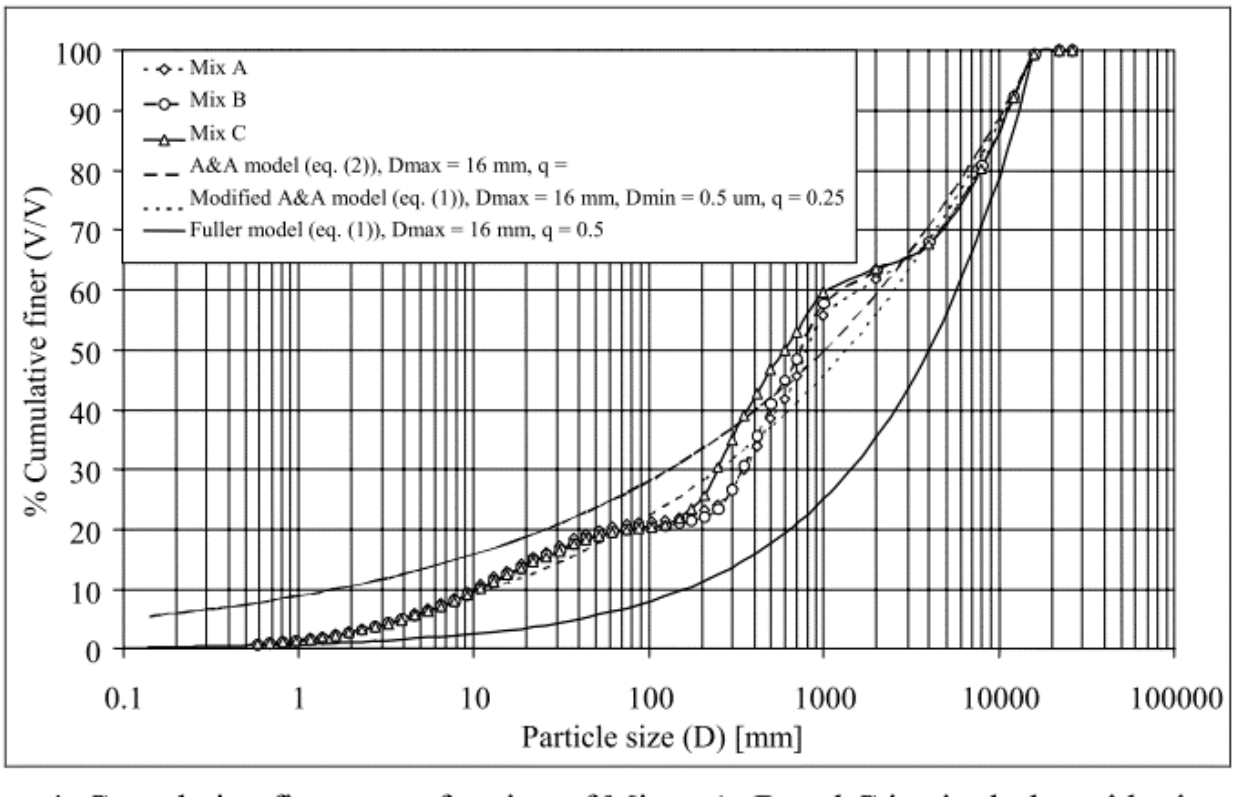

Figure 2.18: Comparison between three different mixes with three different ideal PSD curves(Brouwers & Radix 2005)

While (Andreasen & Andersen, 1930) suggests a gradation value of $q = 0.37$, (Hunger, 2010) suggests a *q* value between 0.21 and 0.25. On the other hand (Wang et al. 2014) suggests a *q* value between 0.23 and 0.29 between the extremes of a low q value, which produces a very cohesive mix and a high q value, which represents a mix more prone to segregation.

2.1.5.3 How to Achieve a Self-Compacting Concrete

The mix design process of SCC is an experimental one and undoubtedly requires a number of trial mixes since conventional mix procedures cannot be followed (Owens, 2009). The just of producing a powder-type SCC is summarised in three steps as suggested by Okamura and Ouchi (2003); limit coarse aggregate, reduce w/b ratio and make use of a superplasticiser.

The superplasticiser allows high flowability while the low w/b ratio provides segregation resistance and limiting the coarse aggregate is beneficial to both high flowability and segregation resistance. This play-off between high flowability and segregation resistance to produce a SCC is diagrammatically shown in Figure 2.19.

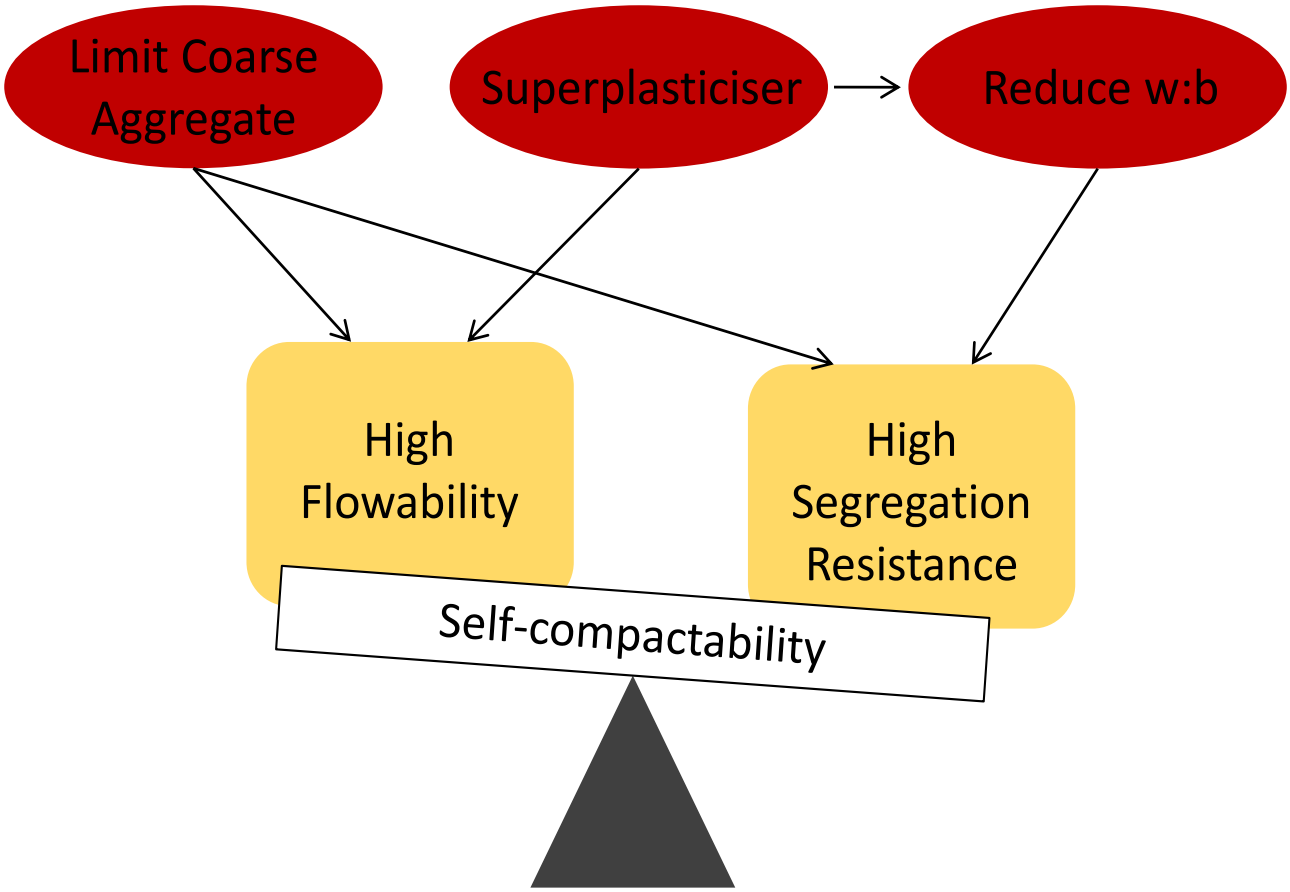

Figure 2.19: Approach to achieve a powder-type SCC

Pioneering work on the development of SCC by Okamura, Ouchi and Ozawa provides a mix design method that is known as *"The General Method"*. The concept of *"The General Method"* is to produce a mortar with good flowability and viscosity and then add the coarse aggregates to it to produce a SCC (Owens, 2009). The mix constitutes used in SCC are conventional materials used in conventional concrete, but the exceptional flow characteristics are a result of unconventional mix proportions. Table 2.1 summarises different limitations set on mix proportioning by various researchers that have been developed over time.

Table 2.1: Comparing mix proportion guidelines for SCC

	Su et.al.	Okamura	RTC 174 - SCC	EFNARC
Coarse Aggregate	28 – 36 %	50 % (dry rod, eq. to 35 %)	30 – 34 %	27 – 36 %
Fine Aggregate	29.5 – 38.76 %			48 – 55 %
Total Aggregate	59 – 68 %			
Sand : Mortar	54 – 60 %	40 %	40 – 50 %	
Mortar				
Paste	32 – 41 %		34 – 40 %	30 – 38%
Water			15.5 – 17.5 %	15 – 20 %
Max coarse aggregate	20 mm			

In contrast to *The General Method*, Su et al. (2001) developed a method where the aggregates were considered first, in terms of shape and grading. The paste is then added to fill the voids between the aggregates. This approach is aimed at limiting the amount of paste needed to require certain fresh state properties while keeping the material cost as low as possible (Brouwers & Radix, 2005). Limiting the paste content of a SCC is also advantageous as it reduces the effects of early-age shrinkage and cracking that are associated with cement-rich mixes.

2.2 Early-Age Shrinkage and Cracking

Early-age shrinkage refers to the volume change that a concrete body experiences right after casting. There are different types of early-age shrinkages, which occur at overlapping intervals and are a consequence of different mechanisms and sometimes a combination of mechanisms, that take place as soon as water is added to a mix. The different types of shrinkage are also defined as such due to specific testing conditions and time frames used by researchers. Four types of early-age shrinkage are briefly discussed as follows:

Plastic shrinkage is the shrinkage that develops due to evaporation from the time that water is added to concrete up until final set.

Autogenous shrinkage starts after final set and continues for as long as there is a volume change under sealed, isothermal conditions. (Also referred to as chemical shrinkage or self-desiccation shrinkage)

Drying shrinkage is a result of the loss of water due to evaporation after the concrete has already hardened (Aïtcin, 1998).

Thermal shrinkage is due to the decrease in temperature (Aïtcin, 1998).

The factors responsible for early-age shrinkage are interdependent and occur concurrently in a fresh concrete body. This makes it difficult to explicitly differentiate which mechanism is directly responsible for which shrinkage type or even in which direction. These volume changes become a concern when they develop internal stresses big enough to lead to micro and macro cracking.

In this study, plastic shrinkage and autogenous shrinkage are discussed in more detail in the following sections. Plastic shrinkage and autogenous shrinkage were measured in this study, as these are the two types of shrinkage that have the most profound influence on HPC with low w/b ratio and a high fine content. Furthermore, early-age cracking is also discussed to gain a more fundamental understanding.

2.2.1 Plastic Shrinkage

A concrete mix is referred to as fresh concrete while it is in a workable, or plastic state, before it starts to harden. Plastic shrinkage is thus the volume change that a concrete body experiences while it is in this fresh state i.e. from the time of water addition up until final set. A number of chemical and mechanical processes occur between the particles during this time.

These processes occur on a microscopic level, but are of significance to engineers as it may influence the long-term behaviour of the concrete member.

Since concrete members are undoubtedly exposed to environmental conditions once they are casted, the fresh concrete is subject to evaporation. The effect of this loss of water from the surface of the concrete body is a reduction in volume, mainly in the horizontal direction termed as plastic shrinkage.

A volume reduction in the vertical direction is also experienced and is known as plastic settlement. Capillary Pressure is the main driving force of plastic shrinkage and plastic shrinkage cracking. Settlement and capillary pressure along with the effects of different environmental conditions on the evaporation rate of free concrete water are discussed in the following sections.

2.2.1.1 Settlement

The solid particles in a concrete mix; cement, sand and stone, all have different sizes and densities (Addis 1998). The heavier particles tend to settle downward and the water wants to migrate to the top because of gravity while the concrete is in a plastic state (Domone & Illston, 2010). .

Plastic settlement is the term given for the vertical volume change of concrete caused by the downward movement of solid particles in a fresh concrete mix. This happens on a microscopic level, but it is worthwhile to note because when this volume change is retrained, it leads to early-age cracking. The restraint could be provided by external obstacles in the formwork such as reinforcement or coarse aggregates, which provides a form of internal restraint. In NSC, bleeding and settlement go hand in hand. As the solid particles collapse in to one another, free water is pushed up as bleed water and when this bleed water is evaporated, the vertical dimension is effectively reduced. In HPC however, there is not much available free water for bleeding and consequently a smaller settlement is expected. The particles are already tightly packed so there is not much space for further compaction or pathways for water to travel upward (Wittmann, 1976).

2.2.1.2 Capillary Pressure Build-up

Plastic shrinkage is sometimes referred to as capillary shrinkage as pressure build-up in the capillary pores is the primary cause of shrinkage in the horizontal direction. Figure 2.20 shows the typical trend of capillary pressure build-up in a cementitious system as the water in the pore system decreases. In NSC, the loss of water from the surface of the concrete is due to the evaporation of bleed water.

In HSC, bleeding is typically not observed so the onset and rate of capillary pressure build-up is amplified as mix water is evaporated from the surface of the concrete body.

As the water in the pore system is reduced due to evaporation, water tries to bridge adjacent particles and forms menisci that causes a negative pressure on the water in the capillary system (Wittmann, 1976 and Slowik et al., 2008). This is illustrated in Figure 2.21. As long as this takes place during the plastic state while the concrete is exposed to ambient conditions, it is considered to be plastic shrinkage. When the hydration in a sealed system, no evaporation, causes pressure build-up in the capillary pores, it is termed as autogenous shrinkage. Autogenous shrinkage is discussed in Section 2.2.2.

From Figure 2.20, it can also be seen that the rate of pressure build-up is very slow initially and then rapidly increases until a maximum point where the pressure drops suddenly. This pressure drop is known as air entry and is said to be the start of strain localisation leading to early-age cracking (Slowik et al., 2008).

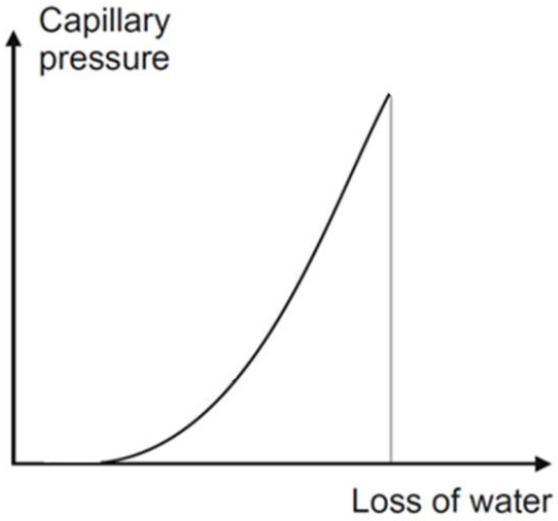

Figure 2.20: Typical capillary build-up trend adapted from (Slowik et al. 2009)

In the plastic state, all particles are moving with small vibrations relative to each other. There are small attractive forces between the particles, which attract them to each other so the distances between the particles are reduced (Wittmann, 1976). In HPC, with many small particles, the sum of these forces are considerably higher than NSC, so the HPC system results in a more compact system which relates as plastic shrinkage.

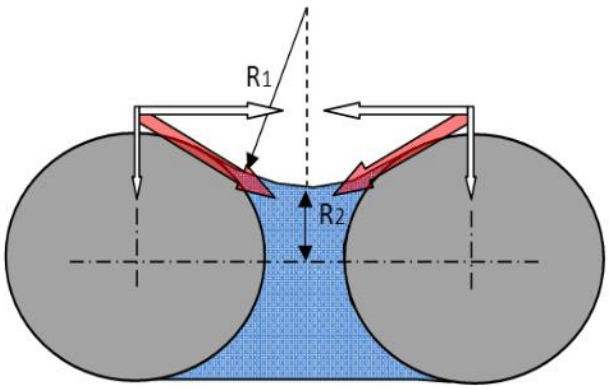

Figure 2.21: Meniscus forming in capillary pore (Combrinck 2011)

Equation 7 is the Gauss-Laplace formula of capillary pressure with γ representing the surface tension (Slowik et al., 2008). The equation shows that the capillary pressure is indirectly proportional to the radii of the menisci showing that a larger capillary pressure is expected for cementitious systems that are made up of smaller particles. HPC with low w/b ratio and fine SCM's, particularly silica fume, results in a fine pore structure. The menisci radii between these fine particles thus lead to high capillary pressures and cause the concrete body to experience higher early-age shrinkage and cracking (Craeye et al., 2011). The capillary pressure is further increased when the evaporation rate, the rate at which water is removed from the surface of concrete, is higher than the rate of bleeding (Wittmann 1976). This is often the case as HPC has negligible bleeding.

$$p = -\gamma \left(\frac{1}{R_1} + \frac{1}{R_2}\right) \quad \text{Eq. 7}$$

It should be noted that the tension forces causing the capillary pressure has a horizontal and vertical component. This means that there is a horizontal and vertical contraction of particles due to the capillary pressure forces. Since the tension forces that cause the capillary pressure is so high in HPC, the vertical component could be substantial enough to contribute to plastic settlement.

2.2.1.3 Evaporation Rate

Since concrete members are undoubtedly exposed to environmental conditions once they are casted, the fresh concrete is subject to evaporation. Casting concrete in areas that experience ambient conditions with high temperatures, high wind speeds and low relative humidity raise concerns for high evaporation rates of water from the surface of the concrete body. South Africa is one such region. When casting HPC in South Africa, especially slabs or bridge decks, environmental conditions of the specific location and time of year need to be considered to determine the evaporation rate.

The *National Ready Mixed Concrete Association/ National Sand and Gravel Association* (NRMCA/NSGA) of America developed a nomograph, shown in Appendix B.1, to estimate the evaporation rate of bleed water from the surface of fresh concrete (ACI 305R-91). Uno (1998), then developed a simple, single-operation formula to calculate the evaporation rate which relates to this nomograph as given in Equation 8.

$$E = 5\,([T_c - 18]^{2.5} - r[T_a + 18]^{2.5})\,(V + 4)\,10^{-6} \quad \text{Eq. 8}$$

Where E *= Evaporation rate (kg/m^2/h)*

T_c *= Temperature of concrete (°C)*

T_a *= Temperature of air (°C)*

r *= relative humidity (%/100)*

V *= wind velocity (km/h)*

According to the Australian Pre-Mixed Concrete Association (1995), an evaporation rate of 1 kg/m^2/h is likely to cause plastic shrinkage cracking in a concrete structure and casting precautions are to be taken when evaporation rates reach 0.5 kg/m^2/h.

2.2.2 Autogenous Shrinkage

Autogenous shrinkage is the external volume change experienced by a concrete body under sealed, isothermal, unrestrained conditions (Reinhardt et al. 2012). Autogenous shrinkage is a phenomenon that is experienced in cement-rich concrete with low w/b ratio.

As the cement hydrates, water from the capillary pores is used up with causes a decrease in internal relative humidity.

The hydration of concrete mixes rich in cementitious material possess two inherent characteristics that are responsible for its early-age deformation and internal stress development; the chemical shrinkage of the cement paste and its exothermic nature (Bentur 2003).

More focus is put on the investigation of autogenous shrinkage as its effects are more detrimental towards early-age cracking.

2.2.2.1 Chemical Shrinkage vs Autogenous Shrinkage

The cause of early-age shrinkage in concrete can be described by the observation of Le Chatelier in 1900. He observed that the density of C-S-H products formed during hydration is higher than that of its reactants, cement and water. With the mass of the reactants that yield the C-S-H products remaining constant before and after hydration, as the law of conservation of mass dictates; the volume that the C-S-H products occupy is less than that of its contributing reactants (Mechtcherine & Dudziak, 2012). This is known as chemical shrinkage, an internal, microscopic volume change (Reinhardt et al. 2012).

Autogenous shrinkage on the other hand is defined as the external, macroscopic volume change of a concrete body under sealed, isothermal conditions and was first observed by Lyman (1934). While the concrete is in its plastic state, the chemical and autogenous shrinkage are equal. This is because the cement paste collapses in to itself, as the volume decreases, while it is still in its fluid state. As the concrete begins to harden however, internal vapour or water filled spaces are found between the shrunken C-S-H particles (Sant et al. 2009). This is where chemical shrinkage deviates from autogenous shrinkage and is believed by most researchers to be the point where autogenous shrinkage measurements should start.

Chemical and autogenous shrinkage is also commonly known as absolute and apparent volume change respectively (Jensen & Hansen, 2001a). Le Chatellier's paper on the hardening of cement pastes in 1900 made a clear distinction between an apparent and absolute volume change and he attributed it to self-desiccation, which is discussed in the next section.

Furthermore, according to Sant (2005), the point of deviation between chemical and autogenous shrinkage can be identified as the point of setting as in Figure 2.22. This point is known to be the time zero, where autogenous shrinkage starts.

Increasing focus has been put on distinguishing between the two in the last 20 to 30 years because of the inclination towards understanding and producing HPC and UHPC. More focus is put on the investigation of autogenous shrinkage as its effects are more detrimental towards early-age cracking. At the time of autogenous shrinkage, the solid skeleton of the pore structure is sensitive to stresses when the concrete body is subject to internal or external restraint. Chemical shrinkage on the other hand occurs while the concrete is in its plastic state so there is little or no threat against stress build-up due to restraints (Mechtcherine & Dudziak, 2012).

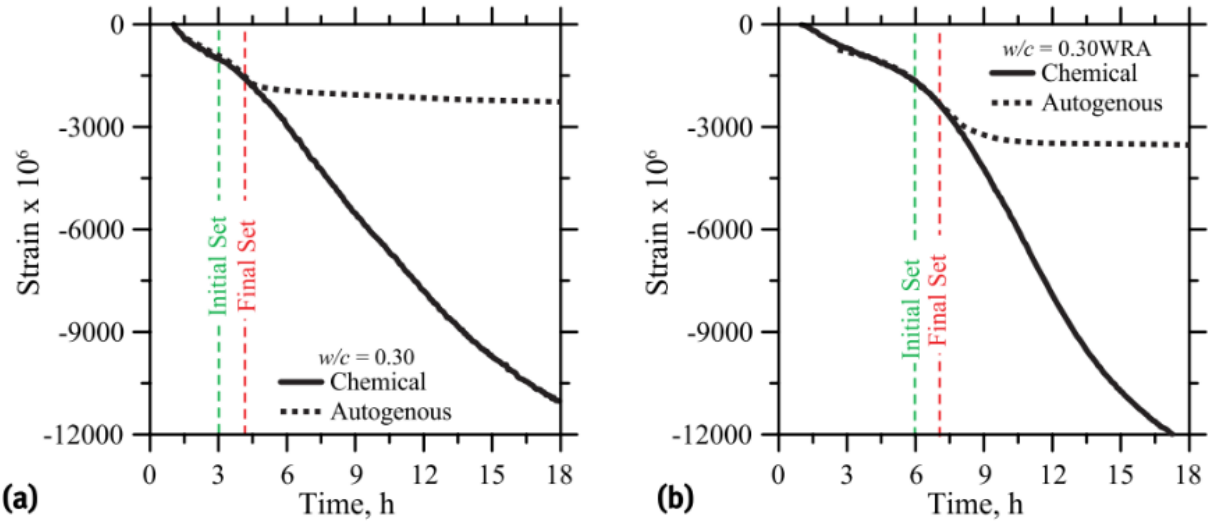

Figure 2.22: The deviation of the chemical and autogenous shrinkage used to identify solidification: (a) plain cement mixture (w/c ratio = 0.30); and (b) mixture containing a polycarboxylate-based high-range water-reducing admixture (w/c ratio = 0.30WRA). (Sant et al. 2005)

2.2.2.2 Self-desiccation

Once a solid skeleton is formed, there is no more apparent volume change and small water filled spaces remain between the solid particles. As hydration continues, water is used up from these pores, essentially drying them out (Shah & Ahmad, 1994). In low w/b ratio concretes, the scarcity of water causes a rapid decrease in the internal relative humidity in the pore structure as water is used up for hydration. This is commonly referred to as self-desiccation; the decrease in internal relative humidity in the pore structure of a sealed, isothermal cementitious system due to hydration (Reinhardt et al. 2012).

In NSC, water from the capillary pore network is also used for hydration, but the internal relative humidity is maintained close to 100 % as long as the pores are replenished from external sources of water (Aïtcin, 1998). This is why external curing is effective in NSC and why self-desiccation is not profound in NSC.

However, in HPC with low w/b ratio, external water cannot reach the drying pores due to its dense matrix. When the pore water is used up for hydration, the menisci radii between adjacent particles keep decreasing which increases the tension in the pore water and on the surface (Mechtcherine & Dudziak, 2012).

The solid skeleton then counteracts the development of these tensile stresses by contracting towards each other, resulting in the external volume change known as autogenous shrinkage.

Similar to the capillary pressure build-up that causes plastic shrinkage as described in Section 2.2.1.2. Considering evaporation to be the external loss of water from a concrete body, self-desiccation can be considered as the internal loss of water due to hydration. Just as evaporation has the effect of increasing the capillary pressure in the pores of a concrete body resulting in a volume change due to the loss of water, so does self-desiccation.

It should be noted that autogenous shrinkage of low w/b ratio concrete is also experienced fundamentally in non-sealed and non-isothermal conditions. To simplify research, autogenous shrinkage is always observed in sealed, isothermal conditions because effects of the ingress of other particles and variation in temperature would superimpose the extent of autogenous shrinkage due to self-desiccation (Jensen & Hansen, 2001a). This allows the effects of self-desiccation to be observed and more importantly, controlled, by considering the w/b ratio, cement composition, effect of silica fume, fineness of cementitious material, volume of aggregate and temperature. The amount, type and fineness of cementitious material is important to consider as they dictate the rate and temperature of hydration, which directly relates to the rate and extent of self-desiccation.

For example, cements that contain a high C_3A content exhibit rapid hardening and will also experience a higher autogenous shrinkage, developing at a faster rate (Craeye et al., 2011). The use of slow hydrating cements is thus a prospect for reducing the development of chemical and autogenous shrinkage.

2.2.2.3 Determining Time Zero

All research performed on autogenous shrinkage of concrete and cement pastes confront the issue of defining time zero. The first issue is defining the internal mechanism that indicates the onset of autogenous shrinkage and then the second and perhaps more challenging issue is using a suitable test method to quantitatively determine that point. Studies have been done to relate the solidification of a cement paste to the rate of hydration heat, but Sant (et al. n.d.) suggests that solidification should rather be related to the formation of a solid structure in the cement paste. Other researches are in agreement with this conjecture.

There are a number of methods available which can be divided into three groups as follows: (Sant et al., n.d.)

- **Techniques sensitive to volume change**
  - Deviation between chemical and autogenous shrinkage – as discussed in Section 2.2.2.1.
  - Acoustic emission measurement – detects vapour-filled spaces, which indicate the beginning of setting.
- **Techniques sensitive to stress resistance and development**
  - Vicat test – needle penetration test
  - Rheological measurements – relates deformation under an applied shear stress to the development of a solid structure in the material
  - Ring test – relates the development of a solid network to the ability of the material to generate a stress.
- **Techniques sensitive to structure development**
  - Ultra-Sonic testing – Assesses the time it takes a high-frequency pulse to propagate through a cementitious sample. As hydration increases, the velocity of the ultra-sonic pulse increases.
  - CEMHYD3D – Provides virtual information on hydration development
  - Electrical response - A method of determining set time using the modified parallel law to model the electrical response of cementitious materials

Adding to the fact that setting time tests merely give an indication of the final set of the actual concrete body, it should be noted that autogenous shrinkage and setting time are not usually carried out on the same specimen. The autogenous shrinkage and setting time specimens could have different hydration developments owing to difference in sample size, ambient conditions and casting procedures (Darquennes et al., 2011)). Ideally, setting time and autogenous shrinkage should be carried out on the same sample. Darquennes et al. (2011) suggests observing time zero according to the evolution of the shrinkage rate. Finding an appropriate method to define time zero is a topic that still requires research (Mechtcherine & Dudziak, 2012). While most researchers agree that autogenous shrinkage starts at the time of final set, Sören Eppers (2010) argues that autogenous shrinkage begins before the transition of the cement-based material from fluid to solid is complete.

Other test methods have also been used to define time zero such as; temperature development and hydraulic pressure variation.

More recently, a non-contact electrical resistivity method (ERM) has been used by (Li, et al. 2007). This method involves analysing critical points on a curve representing the electrical resistivity of a concrete over time, as it hardens (Li, 2011). This method is attractive because it is less labour intensive, it can be observed on a small concrete sample in addition to initial and final set, information of the strength development over that time can also observed. This has been helpful in studies to determine the optimum superplasticiser dosage by considering the effects of setting time and strength development simultaneously. Such studies have been carried out by various researchers (Li & Li, 2003, Xiao et al., 2007, Li et al., 2007, Wei & Xiao, 2013).

Irrespective of the technique used to define time zero, uncertainties remain especially since most changes in the autogenous behaviour occurs around the final set. However, the Vicat needle penetration test is the most widely used and accepted method to determine the final set which can be used as time zero.

2.2.2.4 Testing Autogenous Shrinkage

With an increased interest in producing HPC, more focus is being put on the measurement of autogenous shrinkage. For this study, the development of a test setup for measuring autogenous shrinkage is required in order to formulate an empirical solution for the mitigation of autogenous shrinkage and the detrimental effects that it may have if precaution is not taken. Autogenous volume change can be measured linearly or volumetrically. This section compares different test variations for the measurement of autogenous shrinkage, highlighting some challenges and the developments that were introduced to address these challenges.

Membrane Method Protocol

This method involves a sample of fresh cement paste enclosed in a polyurethane membrane, which is submerged in a paraffin bath and suspended from a scale. This is a volumetric strain technique and the shrinkage is measured by the change in water level in the bath. Paraffin is used instead of water which would absorb in to the sample and consequently show an increased drop in the water level which does not represent the true autogenous shrinkage of the sample (Lura & Jensen, 2006). The paraffin bath is surrounded by water to maintain isothermal conditions.

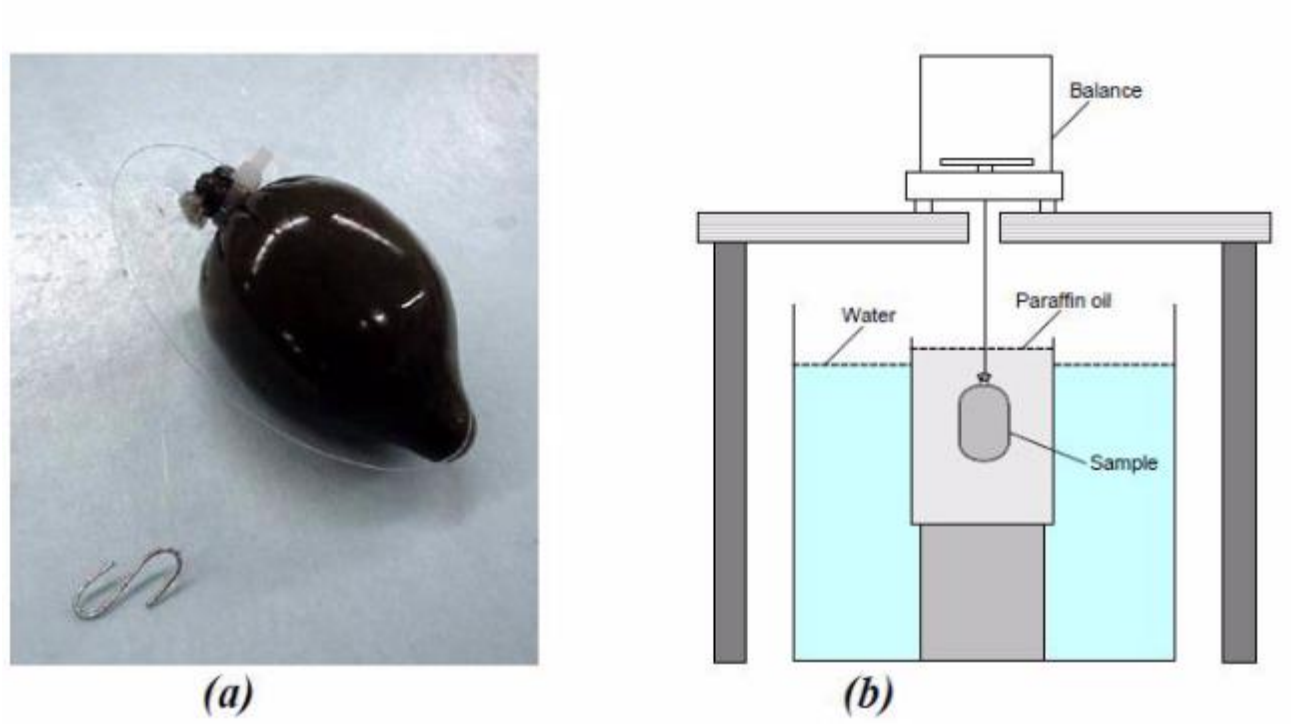

Figure 2.23: An illustration of the procedure to measure autogenous shrinkage a) a photo of the autogenous test specimen and b) an illustration of the buoyancy method for measuring autogenous shrinkage (Sant et al, n.d)

The specimen shown in Figure 2.23 is a 100 to 150 g cement paste sample enclosed in a polyurethane condom membrane. The biggest disadvantage of this method is that the typical rubber membrane doesn't allow constant contact between the membrane and the paste (Sant et al., 2005).

According to Sant et al. (2005), the lack of contact may be due to bleeding or entrapped air in the sample. The specimen setup should be insensitive to bleeding, since bleeding will give a false indication of the shrinkage.

German Standard

One type of linear measurement is the use of prismatic specimens according the German Standard DIN 52450. The specimens have dimensions of 160 x 40 x 40 mm and are cast with an anchorage pin on either end as shown in Figure 2.24. One anchorage pin ensures contact between the specimen and the bottom of the frame and the other contact between the specimen and displacement transducer, which measures the autogenous deformation.

These specimens are demoulded after 1 day and then sealed with a self-gluing aluminium foil to prevent evaporation which would constitute as drying shrinkage (Mechtcherine & Dudziak, 2012).

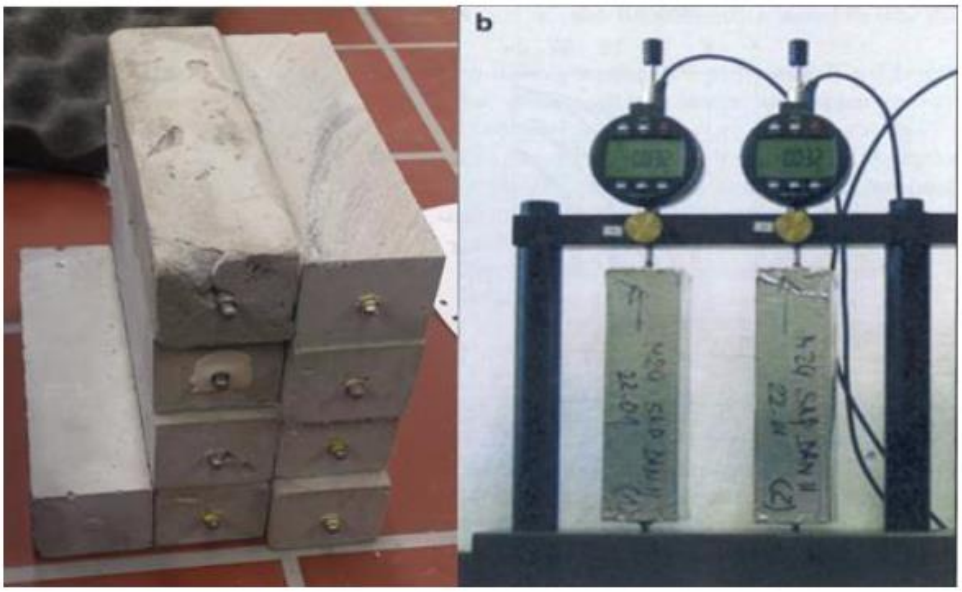

Figure 2.24: German standard DIN 52450 autogenous shrinkage test method a) rectangular specimens and b) specimens attached to length measuring gauge

Experiments were carried out by Mechtcherine and Dudziak (2012) and results of this method were compared with that of the corrugated tube method which is described in the next section. The curves in Figure 2.25 show that there is a pronounced difference in the autogenous shrinkage readings and it is owing to the delayed start of autogenous shrinkage measurements of the prismatic samples as most of the autogenous shrinkage takes place soon after final set which is typically 10 to 12 hours.

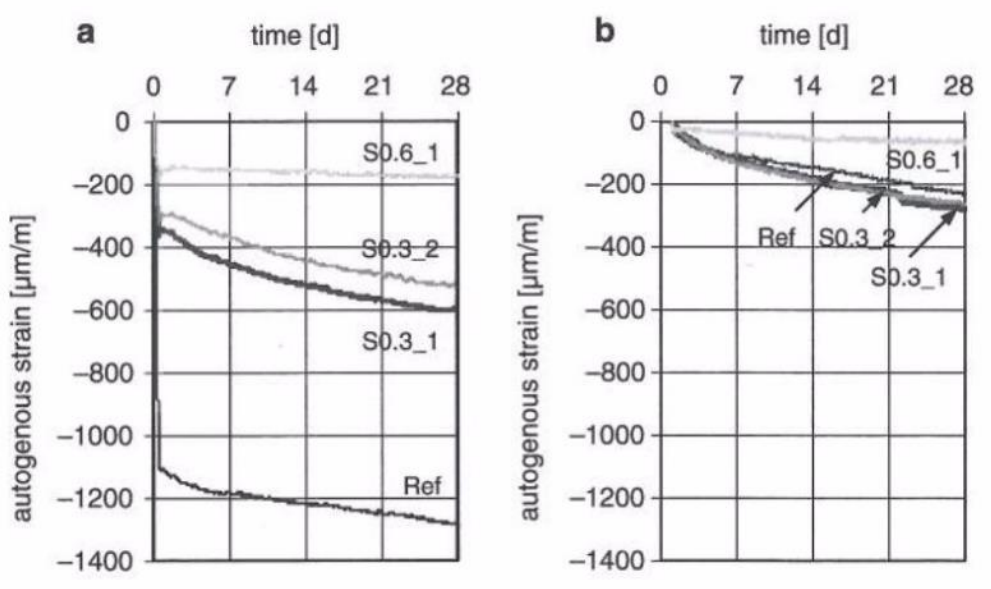

Figure 2.25: Autogenous shrinkage strains measured using (a) corrugated moulds from setting time (b) demoulded prisms from the age of 1 day (Mechtcherine & Dudziak, 2012)

Corrugated Tube Method

The first horizontal dilatometer was developed in 1988 and has since been improved and further developed (Tian & Jensen, 2008). In 1995, Jensen and Hansen developed a method to measure the linear volume change of cement pastes to address the disadvantages of volumetric methods as mentioned in the previous sections. This method involves encapsulating the cement paste in corrugated moulds as shown in Figure 2.26. According to (Jensen, 1995), the corrugated moulds are suitable to measure the shrinkage of cement paste because the moulds are rigid tubes with low friction which has insignificant restraint on the hardened cement paste. The shrinkage is measured with the use of a displacement transducer, which has a spring tip that tracks the displacement of the tubes at one end. Typically, these tubes are placed at a slant to allow the displacement to accumulate at the top end.

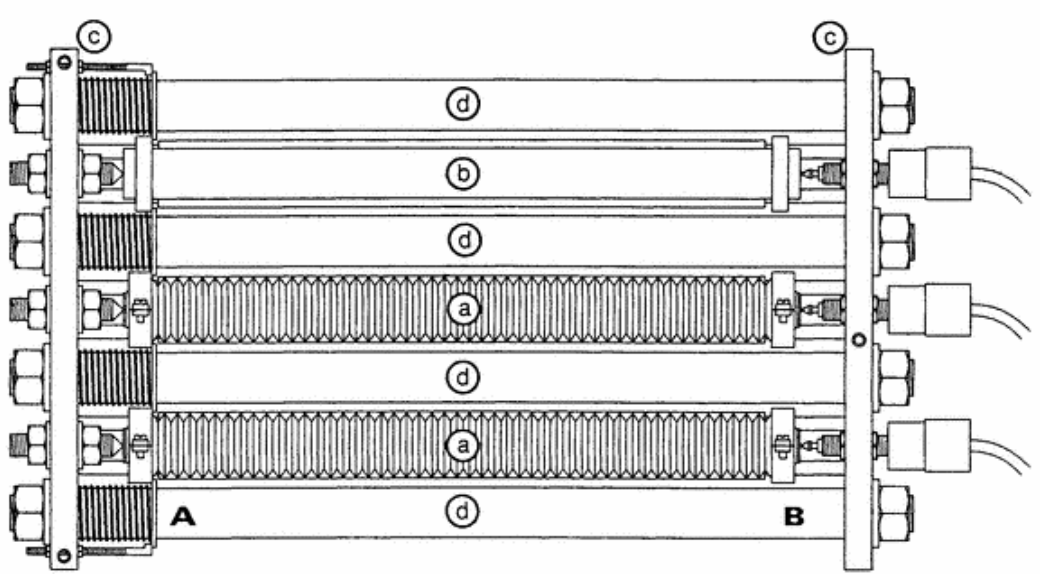

Figure 2.26: Dilatometer frame with two test specimens a and an invar reference specimen b (Jensen, 1995)

The tubes are filled immediately after mixing and placed in the dilatometer bench. The readings may start from this point, but autogenous shrinkage is only considered from the point of final set by definition. Determining the point of final set is also open to interpretation as discussed in Section 2.2.2.3, but the general method used is with the Vicat apparatus. Jensen (1995) also mentions that there is a risk of the tubes having some restraint shortly after final set but this risk may be reduced by lubricating the tubes.

There are a few restrictions with the use of this method. The effect of material properties, tube size, effect of bleeding and direction of measurement as well as entrapped air are discussed next.

Material Properties – The material used in these samples are referred to as concrete by Tian & Jensen (2008) but it should be noted that the maximum aggregate size was only 2 mm and is therefore referred to as mortar in this report.

It should also be noted that in Figure 2.27 to Figure 2.31, where there is differences in the autogenous shrinkage readings, one of the curves have been translated to obtain a point of superposition from where the curves are identical. Also, note that this point of superposition was just after final set for all tests presented by Tian and Jensen (2008).

Tube Size – Experiments were carried out on a big and small tube, both made of LDPE plastic as shown in Figure 2.27a, to observe the ratio between the volume and length change of each tube. From Figure 2.27c, it can be seen that the ratio is less than one, but there is a defined linear relationship between the volume strain and length strain for both the big and small tube.

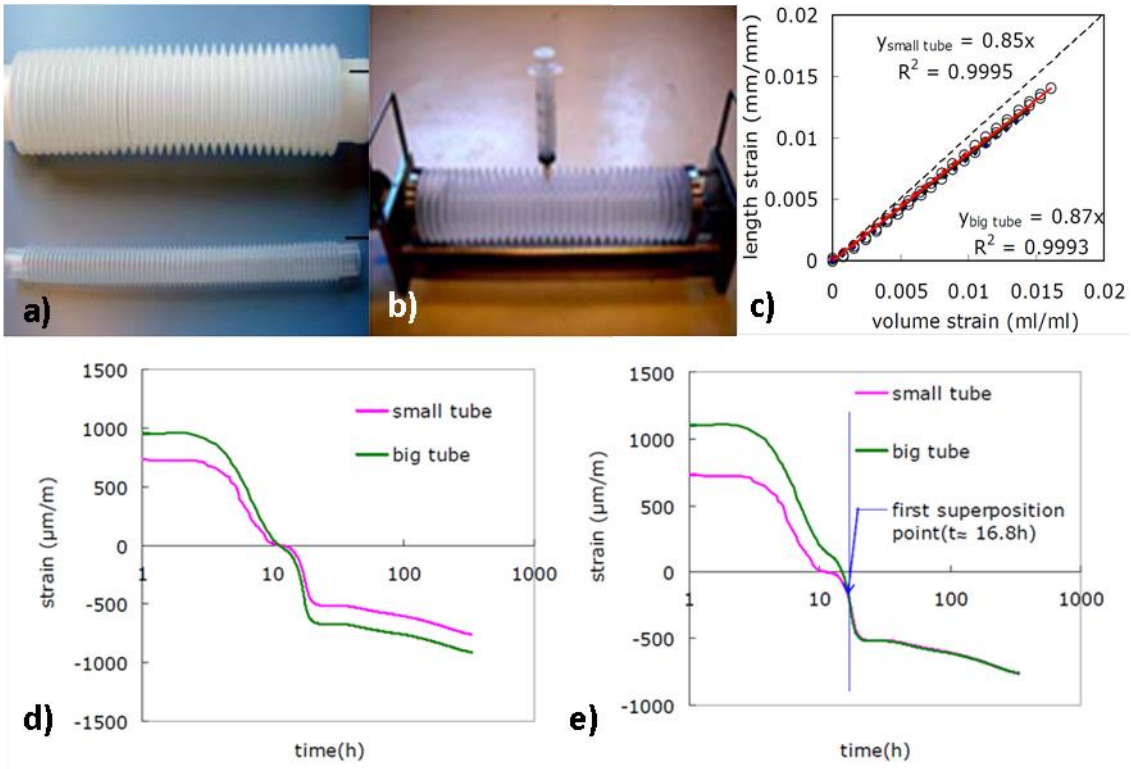

Figure 2.27: a) Big and small corrugated tubes, b) Setup to compare volume change vs. length change, c) Ratio between length and volume change, d) Effect of mould size on autogenous shrinkage, e) From first superposition (Tian & Jensen, 2008).

The experiments concluded that although the size of the tube should not influence the amount of autogenous shrinkage, the bigger tube showed 20% more strain at the age of two weeks. However, this difference mostly occurred before setting and is attributed to a delayed equilibrium in temperature from the centre of the specimen to the surrounding temperature in the bigger cross section.

Furthermore, it was observed that after final set, the developing rate of autogenous shrinkage of the big and small tubes where identical which is illustrated in Figure 2.27e.

Another explanation given by Tian and Jensen (2008) for the difference in autogenous shrinkage is the "wall effect" of the corrugated tubes; the packing adjacent to the tube is different to the centre of the two tubes.

Mould Elasticity – The elasticity of three polyethylene moulds with different densities; low, medium and high density (LDPE, MDPE and HDPE) were tested by applying varying compression forces and measuring the displacement experienced. As expected, the lower the density, the higher the displacement. The relationship is illustrated in Figure 2.28c.

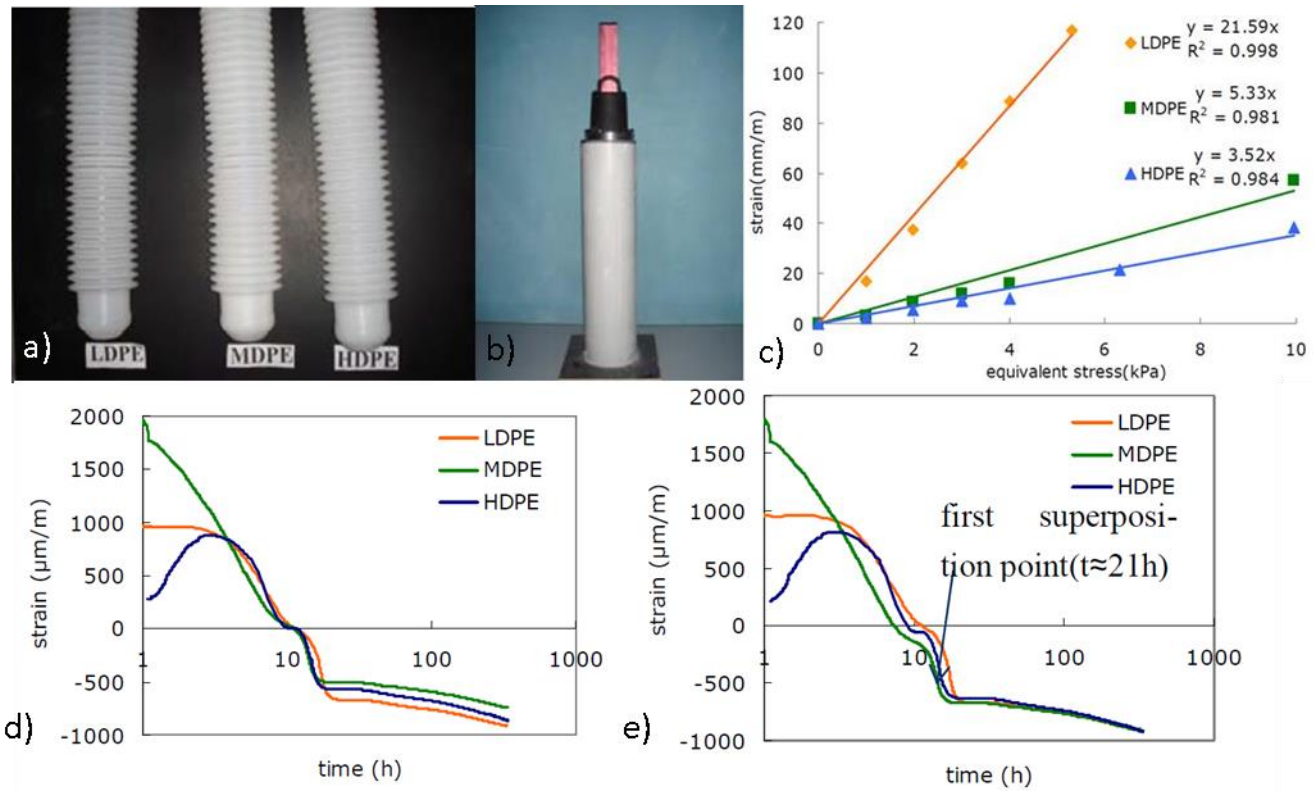

Figure 2.28: a) Three moulds of different density, b) Setup for measuring elasticity of tubes, c) Elastic behaviour of the three kinds of tubes, d) Effect of tube stiffness on autogenous shrinkage, e) From first superposition (Tian & Jensen, 2008).

The autogenous shrinkage results shown in Figure 2.28 illustrate the same trend as Figure 2.27, where there is a pronounced deviation in autogenous shrinkage in tubes with different densities before final set. However, after final set, the development of autogenous shrinkage is the same in all three moulds.

These results suggest that after final set, the density of the moulds do not influence the readings of autogenous shrinkage of the mortar.

Entrapped Air – To see the effect of air on the measured autogenous shrinkage, two tubes were filled with mortar, one completely filled and the other only 2/3 as shown in Figure 2.29a.

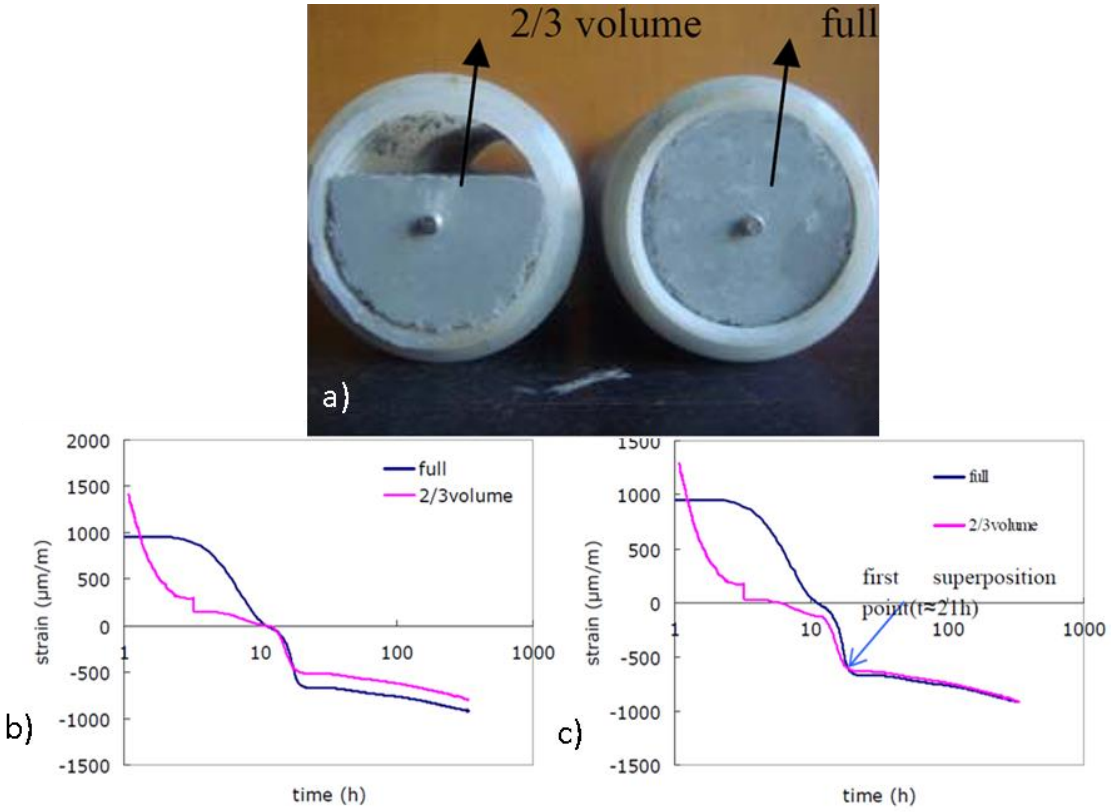

Figure 2.29: Cross section of specimen, b) Effect of air on autogenous shrinkage c) From first superposition

The results in Figure 2.29b show that the autogenous shrinkage measured of the tube filled with 2/3 after two weeks was about 13% lower than the tube that was completely filled. Again, these graphs show that after final set, the autogenous shrinkage development is almost identical. Suggesting once more that the effect of air is insignificant after final set. Tian and Jensen (2008) also mention that at early-ages, the 2/3 filled tube reports less shrinkage because the shrinkage force of the mortar is distributed across the entire cross section of the tube, which reflects a lower autogenous shrinkage reading.

Measuring Direction and Bleeding – To observe the effect of bleeding when measuring the autogenous shrinkage in either the horizontal or vertical direction, experiments were carried out with a non-bleeding mix and two bleeding mixes with different bleeding ratios.

Figure 2.30a shows the autogenous shrinkage of a non-bleeding mortar in tubes tested in both the vertical and horizontal direction. From the figure, it can be seen that the autogenous shrinkage is identical after final set in both directions without manipulating the curves.

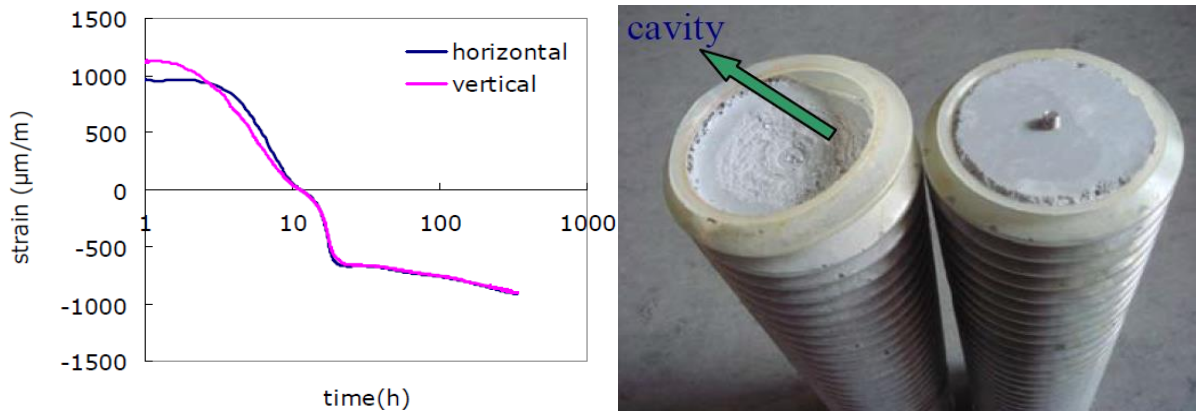

Figure 2.30: a) Effect of measuring direction on autogenous strain measurement of non-bleeding mortar b) Effect of direction on specimen

Although the measured autogenous shrinkage did not show a pronounced difference, the anchorage screw of the vertically tested mould seemed to have sunken in to the mortar as a result of settlement during the plastic stage. Figure 2.30b shows a 10 mm cavity between the specimen surface and enclosure. The mould on the right in Figure 2.30b was tested horizontally with the anchorage screw remaining in position. Tian and Jensen (2008) hold that this had no influence on the autogenous shrinkage measurements.

High Bleeding mixes however showed pronounced differences when measured in the different directions. Two bleeding mixes with different bleeding ratios were tested. Horizontal readings showed an autogenous expanding trend, while vertical readings showed autogenous shrinkage trends as showed Figure 2.31d and e. Figure 2.31a shows the bleed line in the tube a few hours after casting. Figure 2.31b and c shows how the mortar settled. The same settlement was observed in the vertically measured tube but with a deeper cavity of 25 mm as shown in Figure 2.32. The figures show that the anchorage screw in the horizontally tested tube is still intact while the anchorage screw in the vertically tested tube has detached completely.

From Figure 2.31Figure 2.32 it can be concluded that the direction of measurement influences the autogenous shrinkage readings and is especially significant in mixes with high bleeding. Tian and Jensen (2008) developed two theoretical models to study the effect of measurement direction.

The setup is show in Figure 2.33, and from it they concluded that the horizontally measured tube showed expansion because of the reabsorption of bleed water into the pores. This reabsorption of bleed water happens in the vertically measured tube as well but to a lesser extent because of the smaller surface area exposed to the bleed water. Furthermore, they concluded that bleeding increases vertical settlement of a cement-based material body and swelling in the horizontal direction.

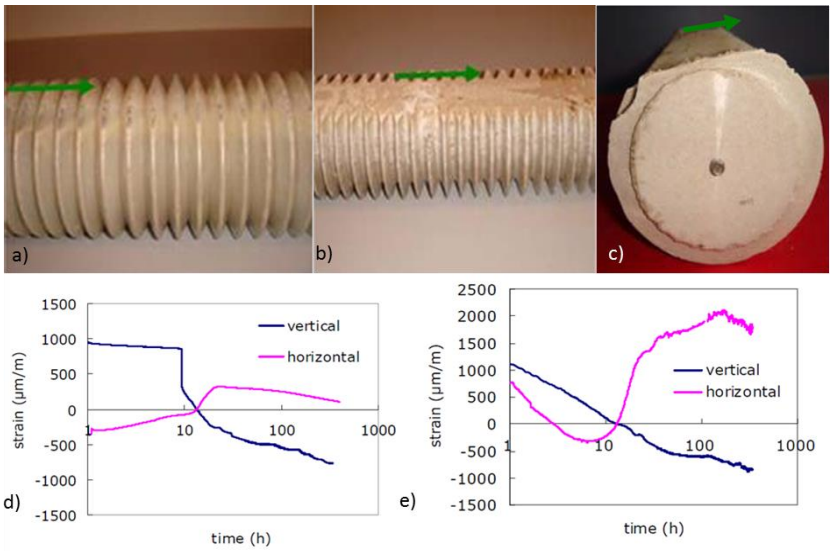

Figure 2.31: Details of the concrete in the tube for horizontal bleeding specimen a) Bleeding line, b) Surface defect, c) Perfect embedment of the anchorage screw, d) Autogenous shrinkage of bleed Mix 1 and e) Autogenous shrinkage of bleed Mix 2

Figure 2.32: Investigation of the bleeding concrete by vertical measurement

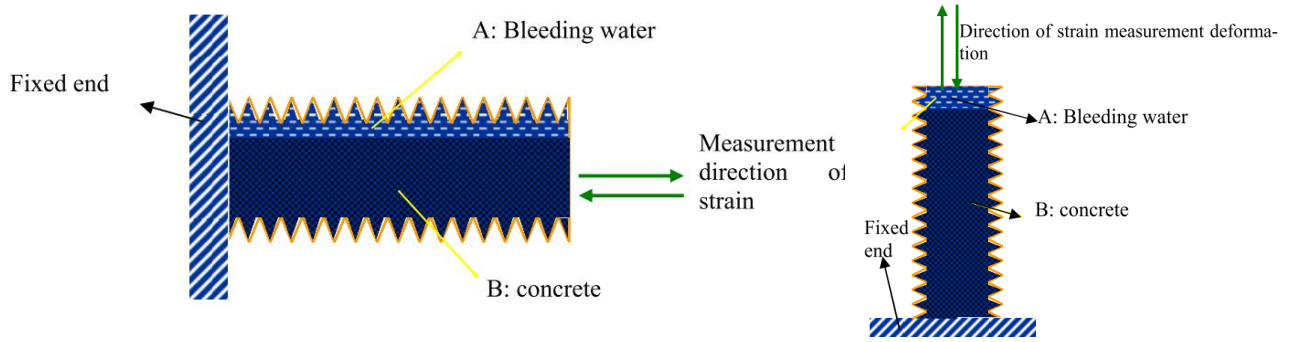

Figure 2.33: a) Parallel connection model for the horizontal measurement of the bleeding specimen b) Series model for vertical bleeding specimen

The corrugated tube method is about to become the standard method for measuring the autogenous shrinkage of cement paste and mortar under quasi-isothermal conditions (Sören Eppers, 2010).

Difficulties arise when using this method when testing sticky mixes. The use of an applicator gun was proposed by Sören Eppers (2010) to facilitate the ease and accuracy of filling tubes. Another alternative is performing autogenous shrinkage tests on a cone shaped mould. Comparative experiments were carried out to observe the validity of each of the alternatives and are reported in the following sections.

Shrinkage Cone Method

To address the limitation against exposing samples to variable temperatures, the shrinkage cone method was adapted by the German Cement Works Association (Sören Eppers, 2010) from an apparatus used to measure plastic shrinkage by Kaufmann et al. (2004). Comparative experiments were conducted to address the limitations of the corrugated tube method which are mentioned; the limitation on isothermal conditions and challenges with filling the tubes with sticky mixes. These experiments were carried out using the shrinkage cone method, the standard corrugated tube method and the corrugated tube method using an applicator gun for sticky mixes. This research is valuable because often HPC are mixes with low w/c ratio and may include fibres, which make filling the tubes challenging.

The Schleibinger setup is shown in Figure 2.34. The cone shaped mould is enclosed by a cylindrical jar which allows controlling the of temperature by pumping a coolant of desired temperature between the cylindrical jar and the specimen (Sören Eppers, 2010). This mould shape is also advantageous because it allows the observation of both linear and volumetric volume change. Due to the geometry of the mould, the volume change would be proportional to the power of 3 of the length change (Kaufmann et al., 2004). The geometry is shown in Figure 2.35

The basic setup of the shrinkage cone is a cone-shaped mould filled with concrete and a laser pointing vertically on to the surface of the concrete. The cone used in this experimental study was enclosed by a cylindrical jar, which allows controlling of the surrounding temperature. Once the mould is filled and vibrated, it is sealed with aluminium foil to prevent the effects of evaporation.

Figure 2.36 to Figure 2.41present the test setup and results of the comparative experiments done to validate the shrinkage cone method against the corrugated tube method using an applicator gun and without the applicator.

Figure 2.34: New Design with a double wall metal vessel for easy heating and cooling with an external liquid temperature control unit (Schleibinger, 2000).

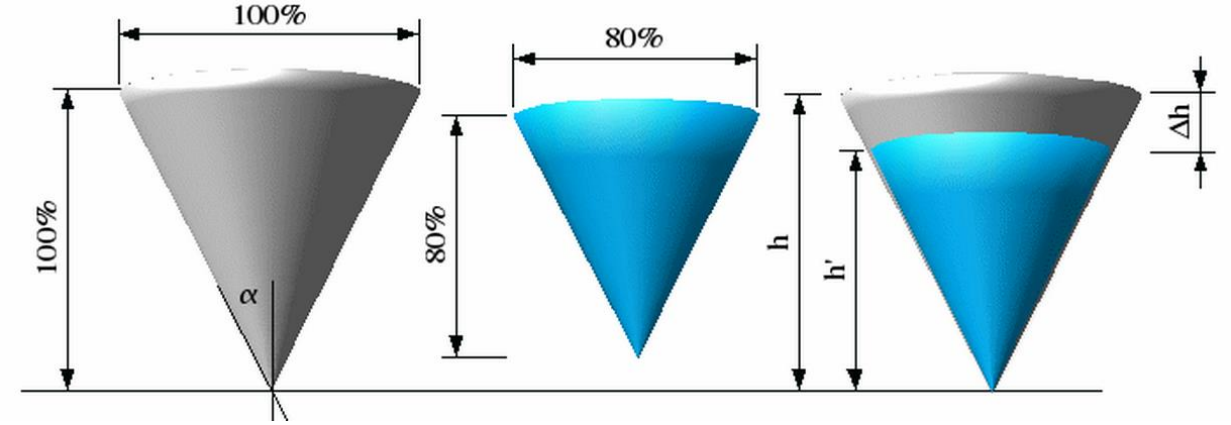

Figure 2.35: Shrinkage cone geometry (Schleibinger, 2000).

Figure 2.36 shows the use of the applicator gun by filling the gun cartridge with mortar and pressing it through a rubber hose, which fills the corrugated tube from the bottom up. The length of the rubber hose is about the height of the corrugated tube and its diameter is just smaller than the diameter of the corrugated tube. The length change measurements were measured using the methods proposed by Tian and Jensen (2008) as mentioned in the previous section, except that the plastic end plugs had an additional metal disc glued to it to ensure a smooth surface and a small magnet to ensure contact between the tube and frame.

Figure 2.36: Filling of the corrugated tube with applicator gun (left), dilatometer benches (top right), probe and metallic cap (mid right), opposite end fixed with a magnet (bottom right) (Sören Eppers, 2010).

In some cases, the autogenous shrinkage results using the shrinkage cone method and corrugated tube method with applicator gun were in agreement, but this is not always the case. An example of where there were pronounced differences in results is shown in . Sören Eppers (2010) suggest that a possibility for this discrepancy could be that the pressure from the applicator gun exerted on the mortar affects the autogenous shrinkage behaviour.

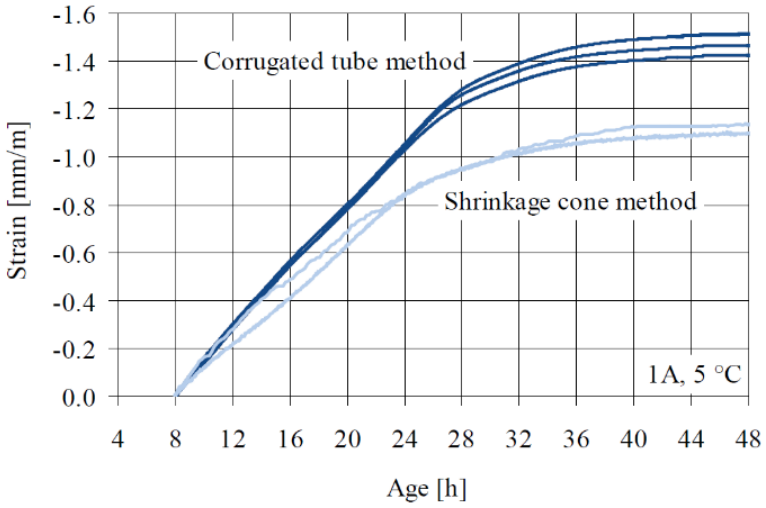

Figure 2.37: Shrinkage strain (sealed conditions) from the age of 8 h, measured with 3 corrugated tubes (filled with applicator gun and 2 shrinkage cones, concrete 1A, T = 5C (Sören Eppers, 2010).

Further experiments were then done to validate this hypothesis. The autogenous shrinkage of two mixes, 1A and 1B with different consistencies, were compared at the same temperature. The results are shown in Figure 2.38. Mix 1A was a fairly fluid mix and was tested using the corrugated tube method with and without the applicator gun and yielded very similar results as can be seen in the figure. However, Mix 1B was a stiffer mix and required more pressure to fill the tubes.

For this mix, autogenous shrinkage measurements from the shrinkage cone method, corrugated tube with applicator gun and without was tested. From Figure 2.38b, it can be seen that the use of the applicator gun had an influence on the results. To further investigate the effect of the applicator gun, porosity tests were carried out on the pressed and not-pressed specimens.

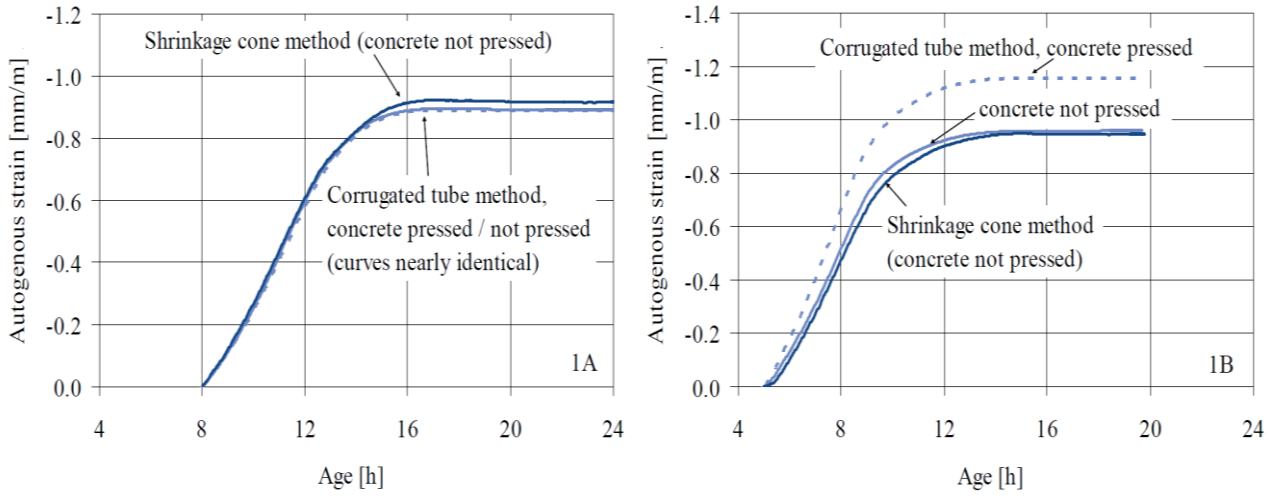

Figure 2.38: Autogenous shrinkage measured with the shrinkage cone method and with the corrugated tubes method with and without use of an applicator gun (pressed / not pressed) a) 1A b) concrete 1B

Mercury intrusion tests were carried out on each mix to observe the porosity. The results of these tests are shown in Figure 2.39 and confirm that the pressure of the applicator gun affects the pore structure which in turn affects the autogenous shrinkage of the mix (Sören Eppers, 2010).

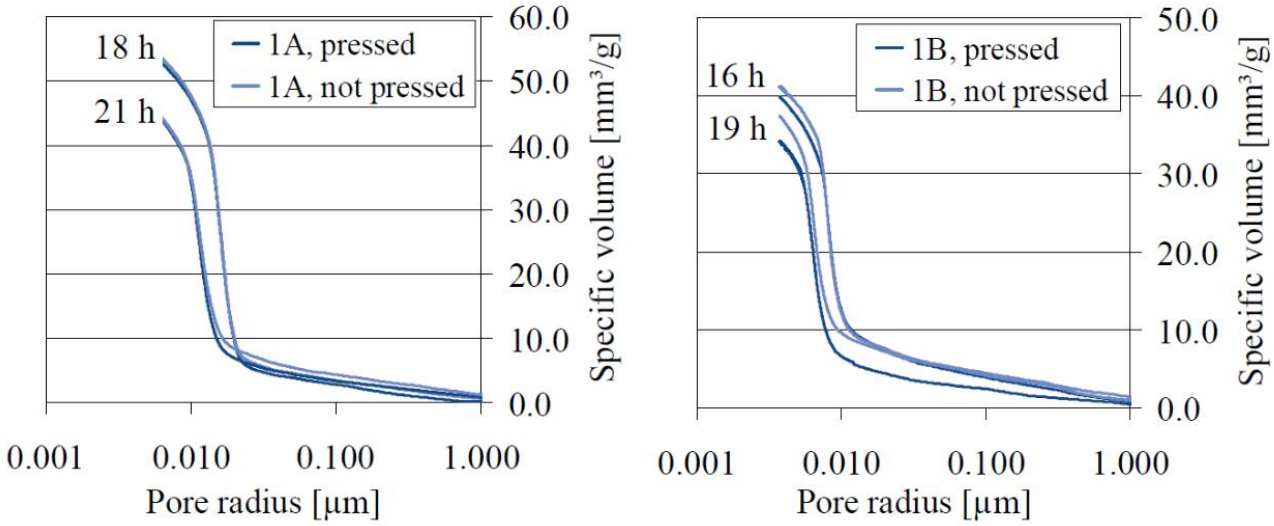

Figure 2.39: Cumulative pore volume tested at early-age, concrete sampled with and without the use of an applicator gun (pressed / not pressed), concrete 1A (left) and 1B (right) (Sören Eppers, 2010).

In conclusion, the shrinkage cone method is a good alternative because it allows the ease of placing all kinds of mixes since the mould can be vibrated. It is also an attractive method because it yields reliable results for autogenous shrinkage under isothermal conditions as well as variable temperatures for ordinary and sticky mixes. However, the cone only allows mortars with a maximum particle size of 2 mm, which is still a limiting factor for the autogenous shrinkage measurement of HPC and UHPC.

Since the corrugated tube method is becoming the reference method for measuring autogenous shrinkage of cement pastes and mortars under isothermal conditions, the identical results obtained by the shrinkage cone confirms it to be a suitable alternative (Sören Eppers, 2010).

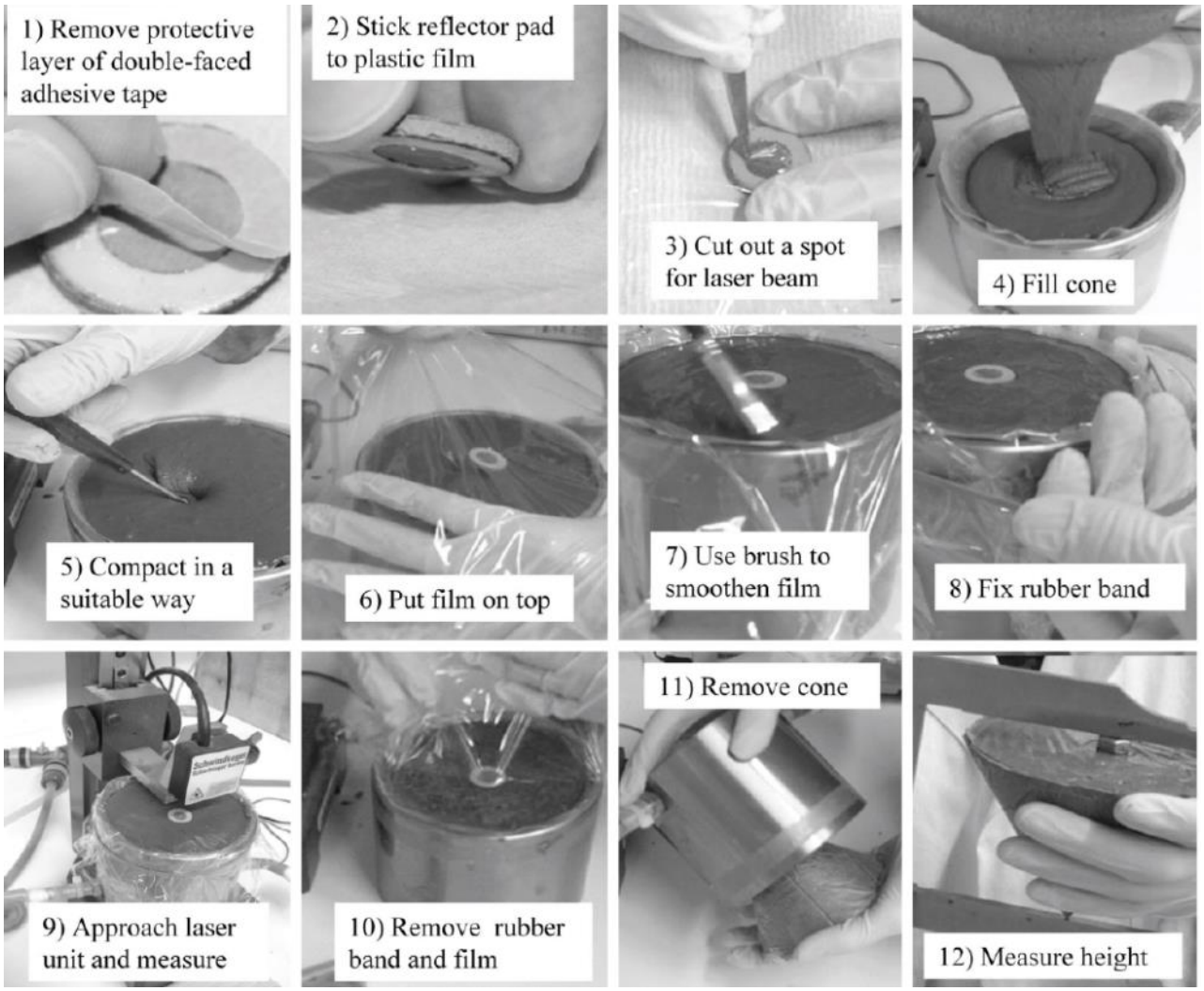

Figure 2.40: Shrinkage cone method for measuring the autogenous shrinkage: measurement procedure (Sören Eppers 2010)

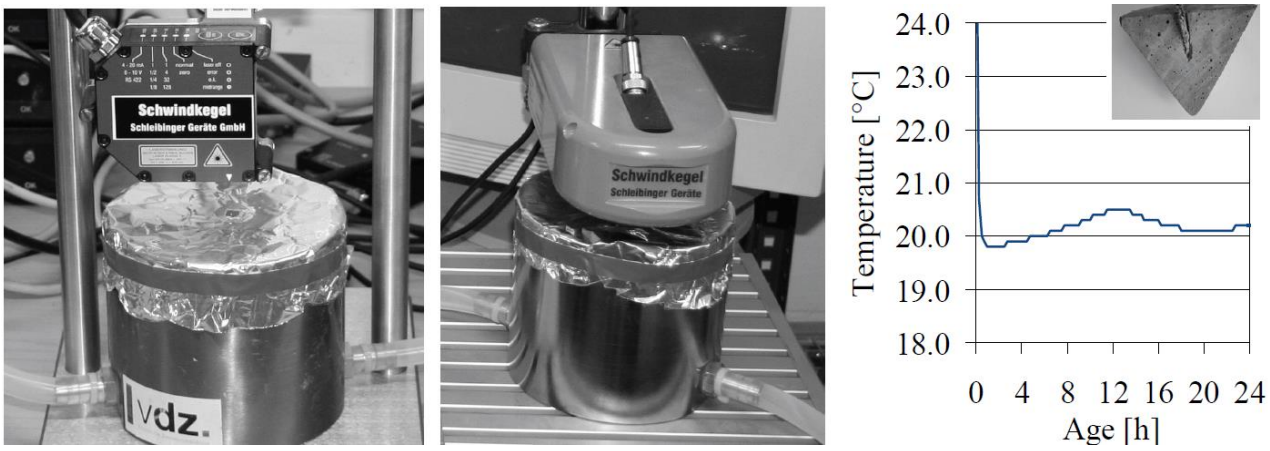

Figure 2.41: Sealing with additional aluminium foil, left: custom-built setup with high-precision laser, centre: standard setup. Right: concrete temperature, set-point: 20 °C (concrete 1A) (Sören Eppers, 2010).

Vessel

All the mentioned methods for measuring autogenous shrinkage are only suitable for mortars and merely gives an indication of the autogenous shrinkage behaviours of HSC and HPC. In 2006, Staquet et al. series conducted some experiments on autogenous shrinkage using a vessel device based on the BTJADE apparatus developed by Boulay. The setup is shown in Figure 2.42 and Figure 2.43.

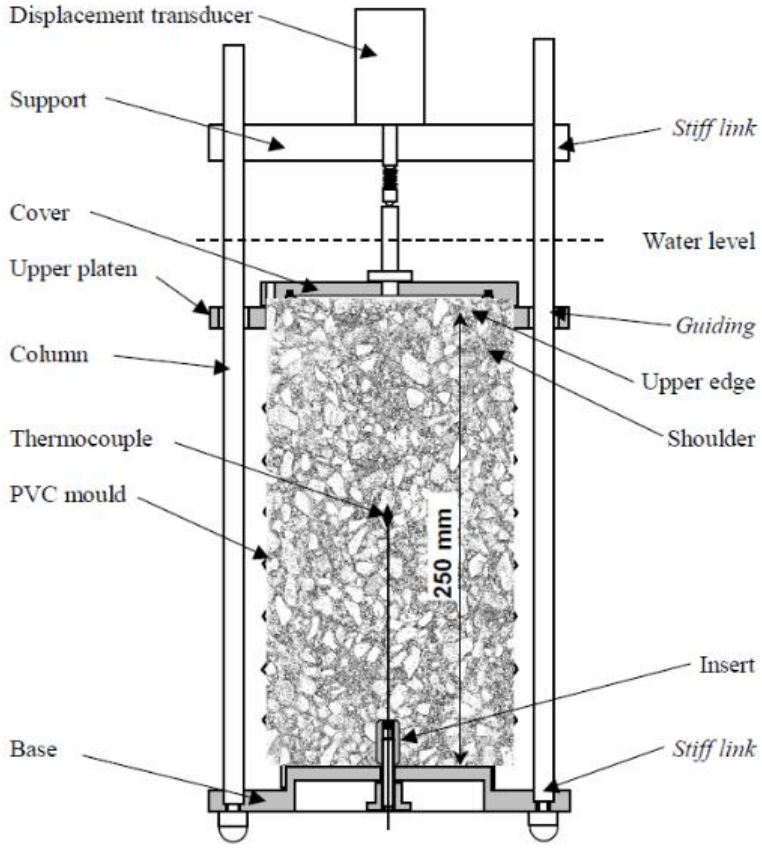

Figure 2.42: Diagram of the test rig. The base length (250 mm) gives the scale (Staquet et al., 2006).

The dimensions of this test setup were adapted from the work of Jensen and Hansen for the use of concrete with larger aggregates while allowing for sufficient heat release within the concrete body. The mould is corrugated PVC with diameter of 125 mm and height of 250 mm which is attached to a stainless steel base plate at the bottom. Three invar alloy columns, attached to the base plate, are spaced at 120° around the test rig and used as a guide for a sliding upper platen which tracks the deformation of the specimen which is measured with a displacement transducer (Staquet et al., 2006). After casting the concrete, an O-ring is bolted to the upper platen to seal the specimen. Once it is completely sealed, it is placed in a thermo-statically controlled water bath.

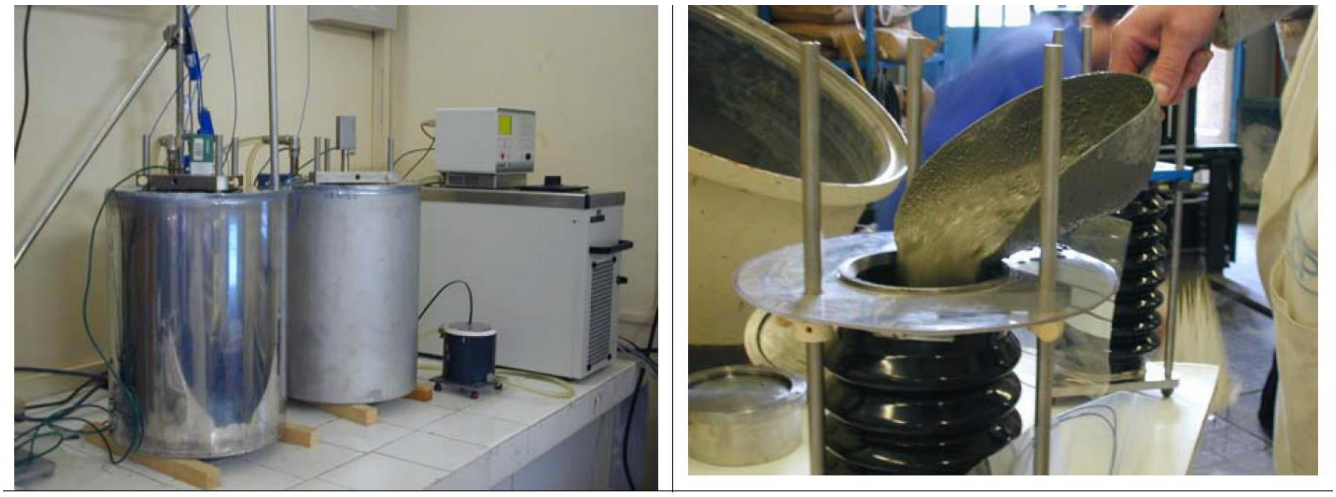

Figure 2.43: The figure on the left shows both rigs immersed in a thermo-statically controlled (Staquet et al., 2006).

Another example is the setup illustrated in Figure 2.44 which was designed at the Universite Libre de Bruxelles to overcome the following issues; measurement inconsistencies due to thermal gradients in the sample, restraint of mould at early-age and friction between the sample and mould (Darquennes et al., 2011)).

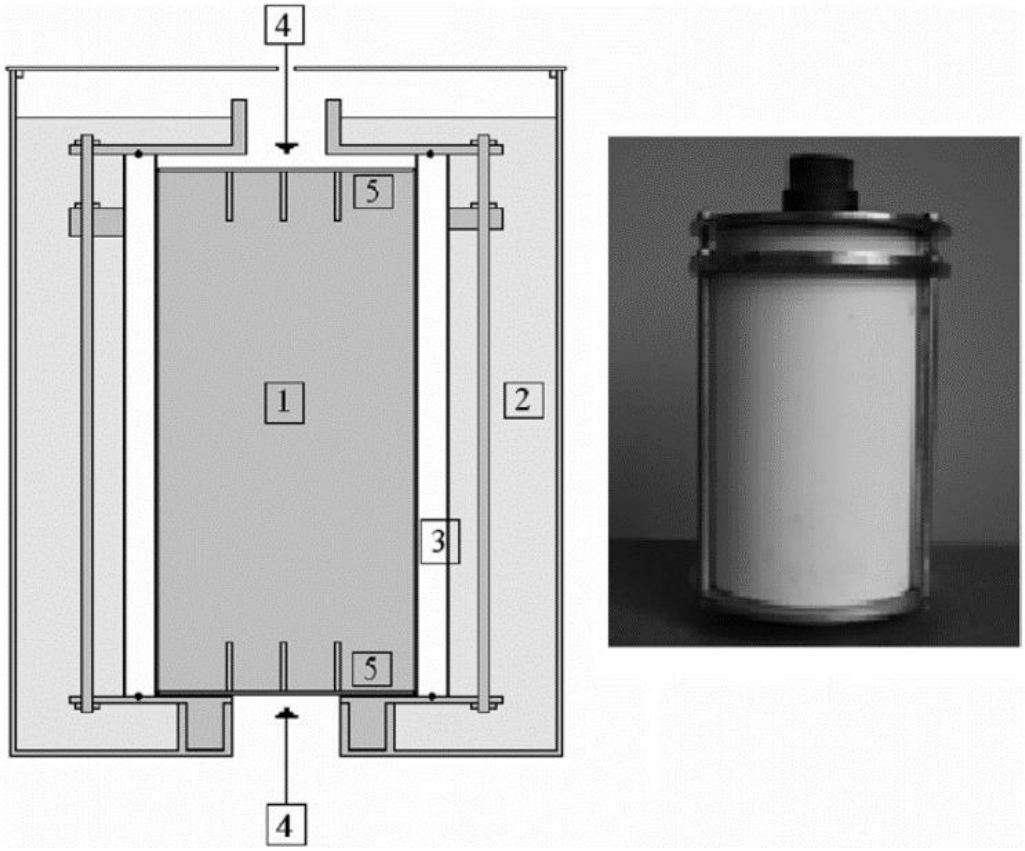

Figure 2.44: The autogenous deformation equipment and its mould (1. concrete sample, 2. vessel, 3. Teflon cylindrical mould, 4. displacement transducers position, 5. steel plates with anchorages) (Darquennes et al., 2011)).

The cylindrical mould shown in the figure is made of Teflon with a diameter of 96 mm and a height of 200 mm. These dimensions minimise the friction between the sample and mould walls (Darquennes et al., 2011)). Two steel plates are anchored to the top and bottom of the specimen and displacement transducers are attached to the plates at both ends. The specimen is mounted on a rigid frame with vertical posts made of Invar, a material with a very low coefficient of thermal expansion. Once the specimen is casted and prepared, it is placed in a temperature-controlled bath.

Some researchers feel that this method should not be used to measure autogenous shrinkage while others feel that it is a suitable method (Darquennes et al., 2011)).

2.2.3 Early-age Cracking

The early-age shrinkages discussed in the preceding sections are unavoidable in HPC. These volume changes become a concern when they develop internal stresses caused by internal or external restraint large enough to lead to micro and macro cracking.

External restraints can be obstacles in the formwork, mainly reinforcing, while internal restraint is exerted by the coarse aggregate, which is notable for autogenous shrinkage.

To date, there is no standard test method for testing plastic or autogenous shrinkage cracking specifically for HPC. The evaluation of this kind of cracking is mostly evaluated by considering the crack risk. The crack risk is evaluated by how much the tensile strength and stiffness of a concrete mix at a particular time exceeds the build-up internal tension stresses at that time. In addition, the available early-age shrinkage cracking tests that are currently available present only comparative results and not enough insight to observe and quantify the effects of the mechanisms that cause the shrinkage, which then lead to the cracking (Bentur, 2003).

The very nature of HPC, high cementitious content, presents both a positive and negative standpoint when considering the crack risk of concrete. High cementitious content causes very high heat of hydration and increased autogenous shrinkage, which cause high tensile forces in the concrete element. The crack risk is increased in the concrete body when it is subjected to internal or external restraint. However, this high cementitious content also means that the concrete body is able to develop a high tensile strength very early on and as such, has a positive effect on reducing the crack risk of HPC. In addition to mechanical strength, the enhancement of viscoelastic properties, such as E-mod and creep/relaxation, also have a positive effect on reducing the early-age crack risk of HPC (Bjøntegaard & Sellevold, 2003).

The mechanisms that generate these internal tension stresses can be well over 50 % of the tensile strength of the concrete at early-ages (Bentur, 2003). Even though the internal stress is less than the tensile strength at this stage, the crack risk is still considerable. Any unexpected load applied to the concrete body such as an accidental imposed load, movement of formwork or a temperature change can easily lead to cracking. This means that even if cracks are not visible on the surface, the concrete body itself is still very vulnerable to cracking due to the confined internal stress build-up.

Furthermore, the use of SCM's increases crack risk in two ways. The first is that its fineness creates a very fine pore structure that amplifies the internal stresses. Secondly, SCM's that have a pozzolanic effect only contribute to strength at later stages, after the vulnerable phase where high tensile strengths are required to counteract the internal stress build-up (Shah & Ahmad, 1994). The latter is mainly of consequence for fly ash and slag, while the former is mainly of consequence for silica fume. The lack of bleeding in HPC also increases the crack risk with decreasing water content. In summary, all the mechanisms that increase the early-age shrinkage of HPC subsequently increase the early-age crack risk. Consequently, all the mechanisms that have the potential to decrease the early-age shrinkage have the potential to decrease the early-age shrinkage cracking.

2.3Super Absorbent Polymers

As discussed in the previous sections, self-desiccation due to a drop in internal relative humidity in the capillary pores, and the autogenous shrinkage that follows, are of most concern in HPC. This is not a concern in NSC as there is sufficient water in the concrete matrix to maintain the internal relative humidity. As free water in the capillary pores of NSC decrease due to hydration, the pores may be replenished by external water applied to the concrete body through various curing methods. Conventional curing methods for NSC are often started after around 24 hours from casting. In the case of HPC, 24 hours after casting is long after the crucial stages of hydration where autogenous shrinkage is already occurring (Aïtcin, 1998). This is the first shortfall with the use of conventional curing methods on HPC.

Adding to this, HPC has a very dense microstructure due to the large amount of fines. With the increased packing density and improved dispersion of fines by the superplasticiser, there is a decrease in pore size and pore volume (Beushausen & Dehn, 2009) which may cut off coalescence of pore networks.

As a result, water that is externally applied to a HPC body cannot penetrate the concrete body equally and entirely in order to supply the additional water that is required in the capillary networks to counter the drop in internal relative humidity. This too is a shortfall with the use of conventional curing methods on HPC.

HPC with high cement and SCM contents are also known to be improbable to bleeding. Overall, the free water in a HPC is much less than in the case of NSC so there is often little or no bleeding taking place. The lack of bleeding also indicates that concrete with high cement and SCM contents are subject to insufficient curing (de Almeida & Goncalves, 1990).

The solution to the inefficient external curing of HPC is providing curing water to the capillary networks through small internal reservoirs of water dispersed in the concrete matrix. To date, superabsorbent polymers (SAPs) are considered to be the most effective additive to provide internal curing to HPC with a dense microstructure. This section considers at how SAPs work by discussing the absorption and desorption kinetics, the influence of the particle size and internal curing water on the fresh and hardened properties. This section also discusses other types of internal curing agents that have been researched as well as previous results on the use of SAP in HPC.

2.3.1 How Superabsorbent Polymers Work

SAPs are chemical polymers made up of cross-linked polyelectrolytes which swell when they come in to contact with water or any aqueous solution (Friedrich, 2012). Figure 2.45 shows the difference between a dry SAP particle (left) and a swollen SAP particle (right), which is formed into a hydrogel after being in contact with water.

From the figure, it can be seen that the swollen SAP particle increases drastically in size and volume when saturated. The amount of water that a single dry SAP particle can absorb is dependent on a number of factors including particle size, chemical make-up and the surrounding conditions.

Craeye et al. (2011) reported that SAP can absorb water up to 500 times its own weight, while Tange et al. (2012) reports that SAP can absorb water up to 1000 times its own weight. It should be noted that not all types of SAP behave the same and are therefore not always suitable for use in concrete and cement-based materials. These extreme absorption capacities are often not reached when the polymers are added to concrete.

Figure 2.45: Dry and swollen SAP particle (Friedrich, 2012)

SAPs are most commonly used in the hygiene industry, specifically baby diapers and explain how television commercials could cut through a soaked diaper without any liquid dripping from it. Only recently has SAPs been used in more technical applications such as concrete technology, cable isolation and soil mechanics.

There has been a number of research studies conducted on the use of SAPs as internal curing agents in HPC over the last few years. The results from these studies are both conclusive; in that SAPs are proven to successfully mitigate autogenous shrinkage in HPC, but also inconclusive in that the results from these studies are specific to the materials used in that particular study itself and cannot always be predicted. The sensitivity of results obtained from studies involving SAPs in HPC is owing to the type of SAP used, the amount of additional internal curing water added and other factors which relate to the composition of the surrounding concrete or cement-based material (Mechtcherine, 2012).

2.3.1.1 Absorption

The SAPs used in concrete are covalently cross-linked polyacrylates and copolymerized polyacrylamides or polyacrylics which have an ionic nature and ionic interconnected structure (Jensen & Hansen, 2001b). This ionic nature allows water to be absorbed into these polymers. The cross-linking of the polymers in its dry and swollen state are schematically represented in Figure 2.46.

The kinetics of the water absorption of SAPs can simply be explained by the process of osmosis. From the dry SAP particle in Figure 2.46, it can be seen that ions in the polymer network are closely packed, resulting in the polymer having a high ionic concentration, or high osmotic pressure inside (Friedrich, 2012). When these polymers are suspended in water, which has a much lower ionic concentration, the water migrates into the polymer to decrease the osmotic pressure inside the initially dry particle. As the polymer swells while it absorbs water from outside, the osmotic pressure inside the particle is reduced. When the SAP is fully saturated, they act as stable, water-filled reservoirs which are able to release this free water back into the capillary pore network when needed (Lura et al., 2012).

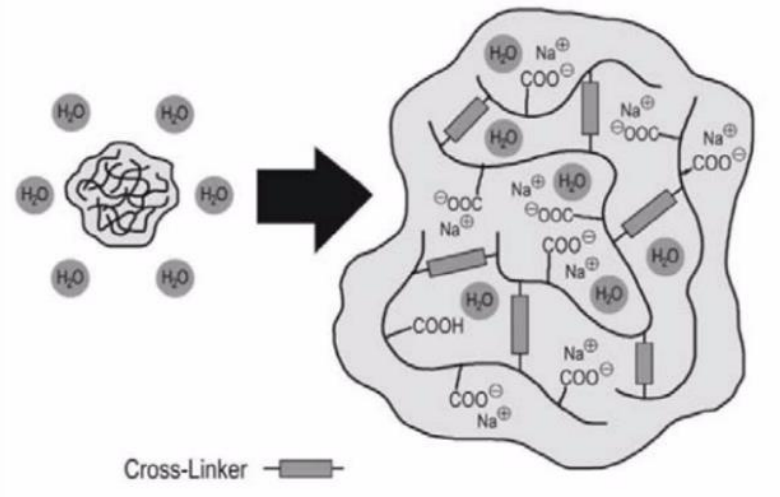

Figure 2.46: Illustration of cross-linking of a dry and swollen SAP particle (Friedrich, 2012)

The rate of water migration from the concrete into the SAP particle is also explained by osmosis. Initially, the absorption of water into a dry SAP particle is rapid due to the high osmotic pressure gradient between the dry particle and the surrounding fluid. However, as the ionic concentration inside the SAP particle decreases with the ingress of water, so does the rate at which the water enters the polymer because of the progressively decreasing osmotic pressure gradient (Jensen & Hansen, 2001b).

2.2.1.2 Desorption

Although more information on the absorption kinetics of SAP is available, the desorption kinetics is perhaps more valuable. Albeit, not much is known about the physical desorption of SAP, as it is hard to observe. Desorption is mostly governed by diffusion and the rate of desorption is dependent on the internal relative humidity in the capillary pores (Mönnig, 2005).

Mönnig observed that for an internal relative humidty of 80%, the desorption rate is 0.032 mℓ/min and when the internal relative humidty dropped to 40%, the desorption rate increased to 0.10 mℓ/min. This is because internal curing water is released from SAPs when the internal relative humidity decreases in the capillary pore system due to hydration (Filho et al., 2012).

In addition to this, is the reverse direction of the osmotic pressure gradient as the pore solution surrounding the swollen SAP particles may have a higher ionic concentration at setting time (Lura et al., 2012). Mönnig (2009) described the absorption and desorption kinetics as a competition for water to relieve the ionic pressure between the inside of the SAP particle and the surrounding cement paste.

Schröfl et al. (2012) found that SAPs that absorbed water quickly also desorbed it quickly. Fast desorption is not particularly desirable. Schröfl et al. (2012) further concluded that autogenous shrinkage was continuously reducing in mixes containing SAP that released internal curing water more slowly. The rapid absorbing and desorbing SAP only reduced autogenous shrinkage over an initial period and then ceased to be effective after a few hours.

2.3.2 Influence of Particle Size Distribution

SAPs can be produced by two distinct processes; gel polymerisation and inverse suspension polymerisation. In both processes, SAPs start off in an aqueous monomer solution. More information on the production process can be found elsewhere (Schröfl et al., 2012). The distinction between the two types of SAP is their shape. Gel polymerisation produces SAP particles that are irregularly shaped, while the inverse suspension polymerisation produces SAP particles that are rounded. This is worthwhile to note as the pores that are left behind by desorbed SAP particles maintain the shape of the swollen particle; irregular or round (Friedrich, 2012). Considering the shape of the voids could give some insight to the expected effect of SAP on compressive strength and capillary pore characteristics.

More influential than the shape of SAP particles, is their size and PSD, which have a significant effect on both the amount of water that is absorbed as well as the rate at which this water is absorbed. This has been observed by Jensen and Hansen (2002), Esteves (2010) and Craeye & De Schutter (2006). Jensen and Hansen (2002) found that bigger particles, a few hundred µm, do not perform optimally in terms of absorption, as they do not have enough time to reach full expansion during mixing. They further advised that very fine SAP particles, a few µm in size, could also be inefficient in absorption as their active surface area that is exposed to the free water is very small.

Fine particles that are smaller than 100 µm may also not be very efficient in absorption. These particles absorb only a small amount of water and when they are only partially swollen, the particles tend to stick together. This is called gel blocking and results in lumps of unswollen SAP particles which do not disperse easily, but this may well be beneficial in employing self-healing properties (Friedrich, 2012).

As long as there is no gel blocking, smaller SAP particles will absorb water faster than bigger particles. The time it takes for a given size range of SAP to absorb water may be as low as 2 minutes and increase up to 20 minutes for a particle size of 118 µm and 300 µm respectively as observed by Esteves (2010). When a smaller range of SAP particles are used in concrete, it would be most effective when mixing them in the dry state along with the other dry ingredients before adding the water (Friedrich, 2012). This will promote a more homogenous distribution without any lumps in the concrete matrix.

The size of the SAP particle also determines how long the diffusion length from the surface of the SAP will stretch out into the concrete matrix (Lura et al., 2012). Smaller particles contain less water and therefore have a shorter diffusion length while larger SAP particles contain more water and may consequently have a longer diffusion length. This is crucial when looking at the effectiveness of a given SAP type to mitigate autogenous shrinkage, however there is not much information available on this (Lura et al., 2012). This can provide more insight into determining how much internal curing water should be added to a concrete mix.

2.3.3 Internal Curing Water

When SAPs along with the internal curing water are added to concrete, it has the potential to either increase or lower the w/b ratio. In the case of the internal curing water being more than what is actually absorbed by the particle, the w/b ratio is effectively increased. While an increased w/b ratio reduces early-age shrinkage, it also compromises the compression strength.

When the internal curing water is less than the amount required to saturate the SAP particles, the w/b ratio is effectively lowered when the SAP absorb water from the free mixing water. This has a direct effect on the yield stress and plastic viscosity, which is now increased and as a result, reduces the flowability and workability (Filho et al., 2012). In addition , Jensen (2008) also stated that the physical swollen SAP particle has an effect on the yield stress and plastic viscosity.

To determine exactly how much internal curing water should accompany a certain dosage of SAP, the kinetics of the absorption needs to be understood. The absorption kinetics of a SAP is governed by the nature of the SAP itself, and also the nature of the fluid that surrounds it (Lura et al., 2012). Currently only the nature of the SAP particle was considered. In the next section the nature of the fluid that should be absorbed by the particle is discussed.

2.3.3.1 Water vs. Pore Solution

After 15 years of research in SAPs, it has been established that the loss of compression strength in HPC containing SAPs is due to an overestimation of the SAPs absorption capabilities (Tange et al., 2012). This overestimation is due to the difference in absorption performance of the SAPs when suspended in water and when dispersed in a concrete matrix. The natures of the two mediums are completely different, particularly in terms of their ionic strength.

The most common test used to determine the absorption capacity of SAPs is the "tea-bag test" and it is traditionally carried out by determining the maximum amount of water that a given type of SAP can absorb. However, the SAP particles do not behave the same in the presence of the pore water found in the concrete matrix to which they are added. The pore water in a concrete mix has high concentrations of ions such as Ca^{+}, K^{+}, Na^{+}, SO_4^{+} and OH^{-} (Lothenbach & Winnefeld, 2006). As soon as water is added to a mix and cement starts to hydrate, the concentration of these ions rapidly increase and then stay relatively constant until setting time (Lura et al., 2012). These ions change the intermolecular and intramolecular interactions along the polymer chains inside the SAPs, especially Ca^{+}, and limits the polymer's absorption abilities (Jensen & Hansen, 2001b and Mönnig, 2009).

A number of studies have been carried out on modelling a synthetic pore solution by adding typical concentrations of the ions mentioned above that would be expected in the concrete mix that is being investigated. (e.g. Jensen & Hansen, 2002, Schröfl et al., 2012, Pieper, 2006 and Lura et al., 2012). All these studies reported a significant reduction in the absorption of SAP in the pore solution compared to water.

It should however be noted that some types of SAPs were affected more in the presence of the ions than others. This emphasises the need to evaluate both the nature of the SAP particle and the medium in which they are suspended.

The behaviour of SAP in a pore solution still leaves room for overestimation of internal curing water, which is to be added to a concrete.

To measure the absorption of SAP in a cement paste or concrete is challenging, but introduces another aspect to the kinetics of water migration in to the SAP particles. SAPs in the presence of other solid particles are in competition for water with these particles, especially the binder materials. Solid particles may also hinder the absorption of water on the surface of the SAP particle, which further reduces the swelling of SAP in a concrete.

Perhaps swelling stops when there is no longer a difference in ionic pressure between the inside of a SAP particle and the surrounding fluid. This requires confirmation and will try to be explored in this investigation.

2.3.3.2 Saturation of SAP

The relationship between cement and water in a concrete mix is relatively simple, but becomes complicated when trying to control certain fresh and hardened properties, especially in the presence of other solid particles and chemical admixtures. Adding SAPs along with internal curing water presents a whole new range of uncertainties when trying to find a balance between autogenous shrinkage, compression strength and workability.

The ideal use of SAPs and its internal curing water would be the case where SAPs are fully saturated when casted in the concrete matrix, and when all the water from the polymer is depleted and completely used for cement hydration (Craeye et al., 2011). The full use of internal curing water maintains the internal relative humidity and is not only efficient in reducing autogenous shrinkage, but also obtaining a higher degree of hydration which leads to a higher compressive strength (Geiker et al., 2004). The voids that are left behind can perform the same as the stable air bubbles in air-entrained concrete, which is advantageous in freeze resistance (Bentz & Jensen, 2004). These are ideal instances, and are not always attained. A calculated guess of the correct amount of internal curing water could be achieved by considering the theoretical amount of water that is needed to cure a HPC for complete hydration.

The degree of hydration of concrete has been a topic of studies for many years from the time of Powers in the late 1940s. Aiming to achieve maximum hydration in low w/b ratio helps to address the concern of compromising compressive strength of HPC using SAPs. Although low w/b ratio concretes contain large amounts of cementitious material, if they are not fully hydrated there will be loss in potential strength gain.

The degree of hydration is not only dependent on the original w/c ratio, but also the space that is available for hydration products to form and the curing conditions (Powers, 1958). Powers' model states that complete hydration for w/c ratio < 0.42 is never reached. This is because the capillary water is used up before all the cement has been hydrated.

In NSC, while there is an external supply of water, capillary water would constantly be replenished until complete hydration is reached. To achieve this in HPC containing SAP, just the right amount of internal curing needs to be added to complete hydration and not an excess of water that will in fact increase the w/c ratio which conversely leads to a decrease in strength.

However, for w/c ratio < 0.36 it is possible that complete hydration still will not be reached even if the right amount of curing water is added. This is because hydration can only take place if there is enough space for the cement gel solids to form as hydration products do not form inside the SAP voids (Tange et al., 2012). Ultimately the strength loss or strength gain of HPC containing SAP is a compromise between the amount of internal curing water that will either increase the degree of hydration leading to a higher compression strength, while there is space for the hydration products to form, or an increase the w/c ratio leading to a lower compression strength.

Using Powers' model of hydration, Tange et al. (2012) and Jensen et al. (2006) formulated the following relationship to estimate the amount of internal curing to be added to a concrete with a given w/c ratio.

$$\left(\frac{w}{c}\right)_{IC} = 0.18 * \left(\frac{w}{c}\right) \qquad \text{for } \left(\frac{w}{c}\right) < 0.36 \qquad \text{Eq. 9}$$

Craeye et al. (2011) found that this formula might in fact underestimate the amount of internal curing water when the internal water cannot traverse through to the pores to reach the unhydrated parts of cement. However, this is dictated by the SAP type, amount, absorbent and desorption kinetics. In the case of the internal curing water being less than the amount required to saturate the SAP particles, the w/b ratio is effectively lowered when the SAP absorb water from the free mixing water. This has a detrimental effect on the fresh properties.

The amount of internal curing water added is thus dependent on the amount of internal curing water needed for complete hydration and also the ability of the SAP in question to absorb and desorb this water. The tea-bag test is helpful in this regard. Observing the absorption of SAP in a pore solution is more valuable than in water but still not a true reflection of its performance in concrete.

In most cases, the optimum amount of internal curing water needed for adequate autogenous mitigation and compression strength in HPC is half of what is observed by the tea-bag test in a pore solution. Olawuyi (2016) observed a 25 g/g absorption of pore fluid via the tea bag test, but in his investigation, he found that 12.5 g/g was the optimum amount of internal curing water for adequate autogenous shrinkage reduction without excessive loss in compression strength.

2.3.4 Previous Results

In 1991, Phileo was the first to recognise the advantageous effects of partially replacing fine aggregate with pre-soaked, porous, lightweight aggregates (LWA). This was the first means of providing internal curing water to HPC to reduce autogenous shrinkage. Weber and Reinhardt (1997) reported improved mechanical properties when using pre-soaked LWA while maintaining an acceptable level of autogenous shrinkage. Other publications reported either a reduction or complete elimination of autogenous shrinkage without considering the effect on compressive strength (Bentur et al., 1999 and Bentur et al., 2001).

The challenge in using pre-soaked LWA is selecting the particle size. A particle size greater than 4 mm is too big and would require a longer diffusion length to deplete all the pre-soaked water (Zhutovsky et al., 2004). This is challenging in a dense microstructure. Particle sizes less than 2 mm too are inefficient as they do not contain a considerable amount of internal curing water. The use of pre-soaked LWA in HPC also presents problems in terms of producing uniform results, such as for the moisture content of aggregate particles, which is difficult to control. Furthermore, the reduction of strength and elastic modulus prevails the reduction of autogenous shrinkage significantly (Jenson & Hansen, 2001).

Following the use of LWA as internal curing agents in HPC, Jensen and Hansen (2001) proposed the use of SAPs instead and presented the needed theoretical background and experimental work. They concluded that the use of SAP and internal curing water is effective in maintaining the internal relative humidity, thus reducing autogenous shrinkage. The SAP used in their study had an absorption capacity of 350 g/g in distilled water and 37 g/g in a synthetic pore solution.

The amount of internal curing water added to the mixes was roughly half of the absorption capacity experienced in the pore solution. A 19 % reduction in compression strength, from 134 MPa to 109 MPa, was found for a concrete containing 0.6 % SAP.

At this dosage of SAP, the internal relative humidity remained constant from setting time until 21 days and likewise the autogenous strain remained constant. The results of their investigation are shown in Figure 2.47 and Figure 2.48

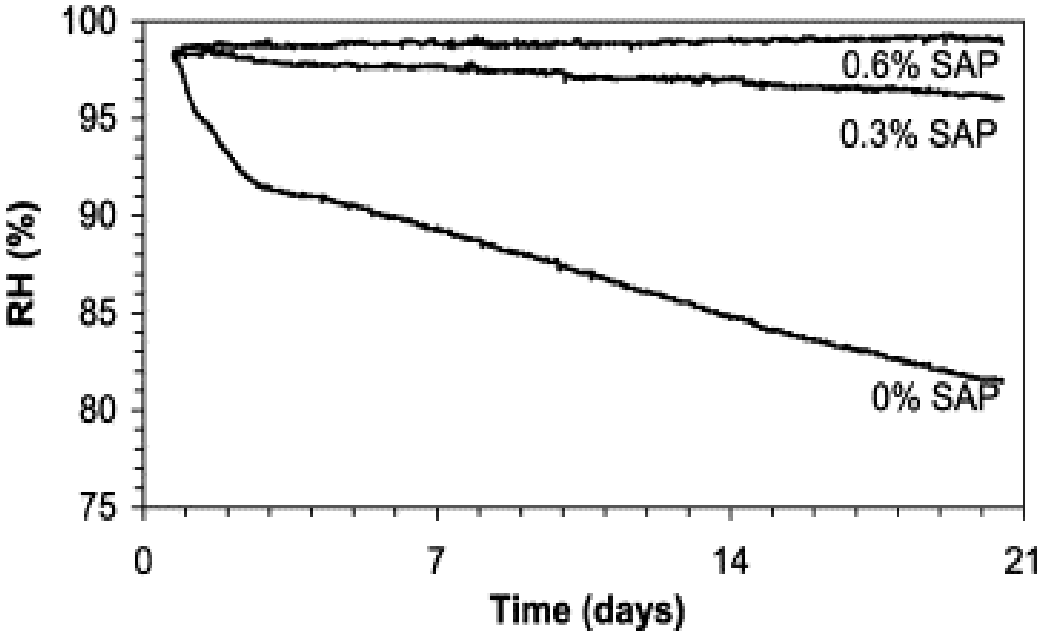

Figure 2.47: Internal relative humidity of a reference mix with w/c ratio 0.3, 0.3 % SAP and 0.6 % SAP (Jensen & Hansen, 2002)

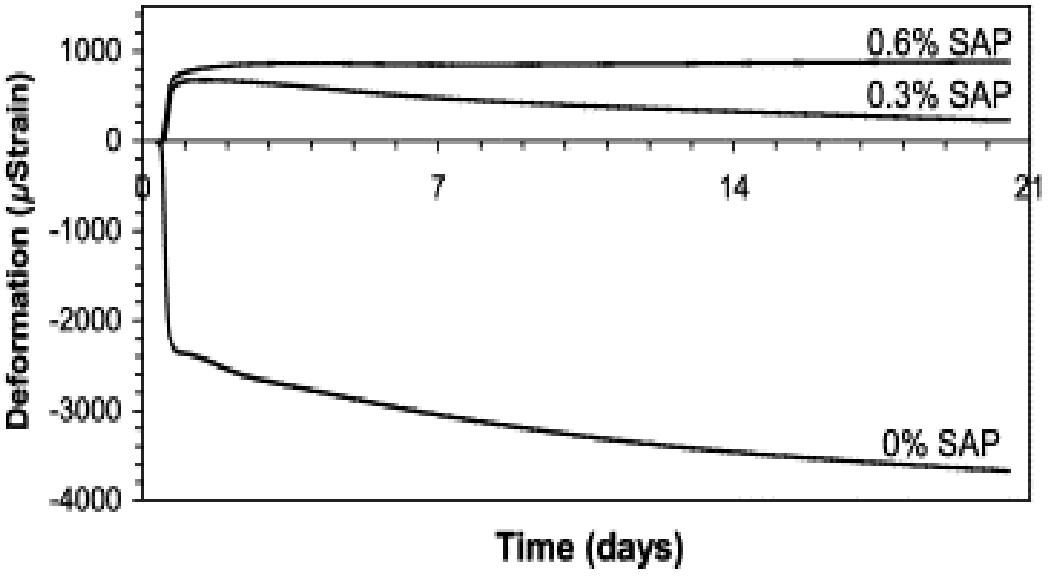

Figure 2.48: Internal relative humidity of a reference mix with w/c ratio 0.3, 0.3 % SAP and 0.6 % SAP (Jensen & Hansen, 2002)

To date, there has been many publications which portray a trend that while the addition of SAP in high strength concrete successfully mitigates the autogenous shrinkage; it is at the cost of its compressive strength (Tange et al., 2012). However, there have also been a number of publications where the addition of SAP either maintained or increased the compressive strength while mitigating autogenous shrinkage.

Lura and Jensen (2006) found almost no reduction in compression strength of mortars with w/c ratio of 0.3 with a SAP dosage of 0.4 % and 5 % internal curing water as a percentage of the cement. However, with the pastes there were a 20 % reduction in compression strength at 7 days and at 28 and 56 days only a 10 % reduction in strength.

Schröfl et al. (2012) investigated the effect of six different SAP types on a mortar with w/c ratio of 0.3, all of which reduced the autogenous shrinkage compared to the reference. The amount of internal curing water needed to maintain the workability of the reference mix was added for each SAP type.

Three of the six types of SAP (SAP D, E and F) which performed the best in mitigating autogenous shrinkage, also had no significant effect on the compression strength. However, SAP C, which had the highest uptake of water, had the lowest compression strength and a stable autogenous shrinkage. The results of their investigation are shown in Figure 2.49 and Figure 2.50.

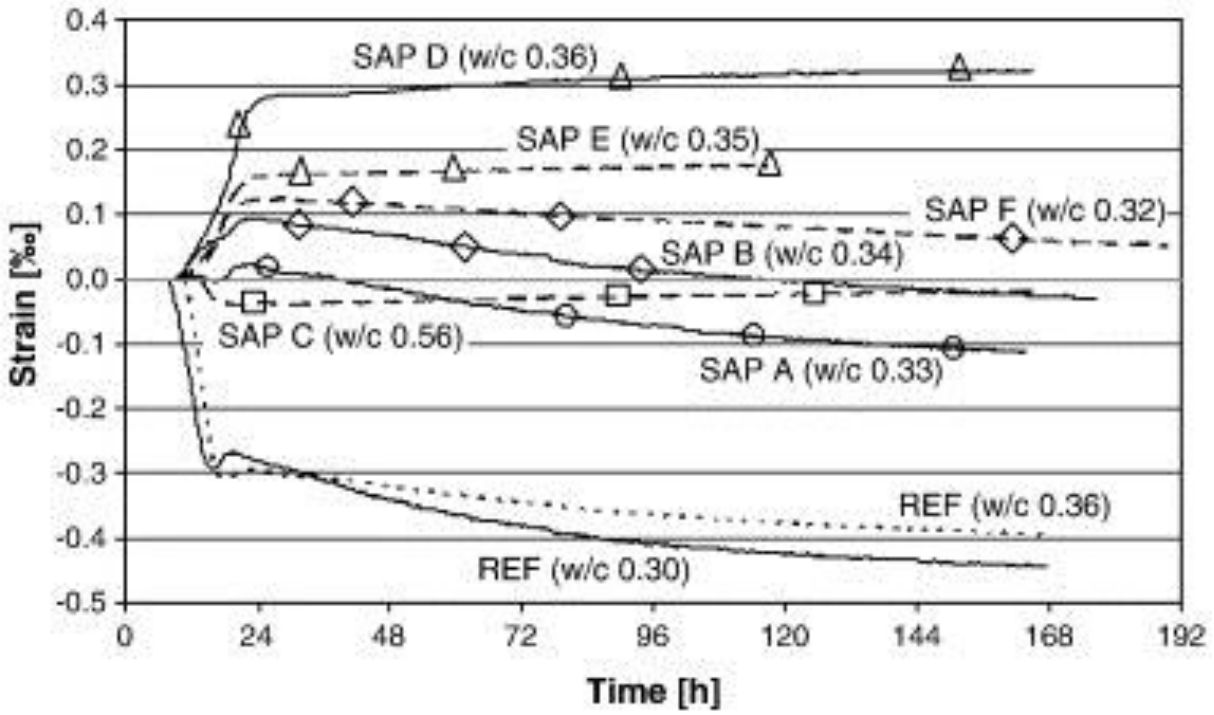

Figure 2.49: Autogenous shrinkage of reference and SAP mixes (Jensen & Hansen, 2002)

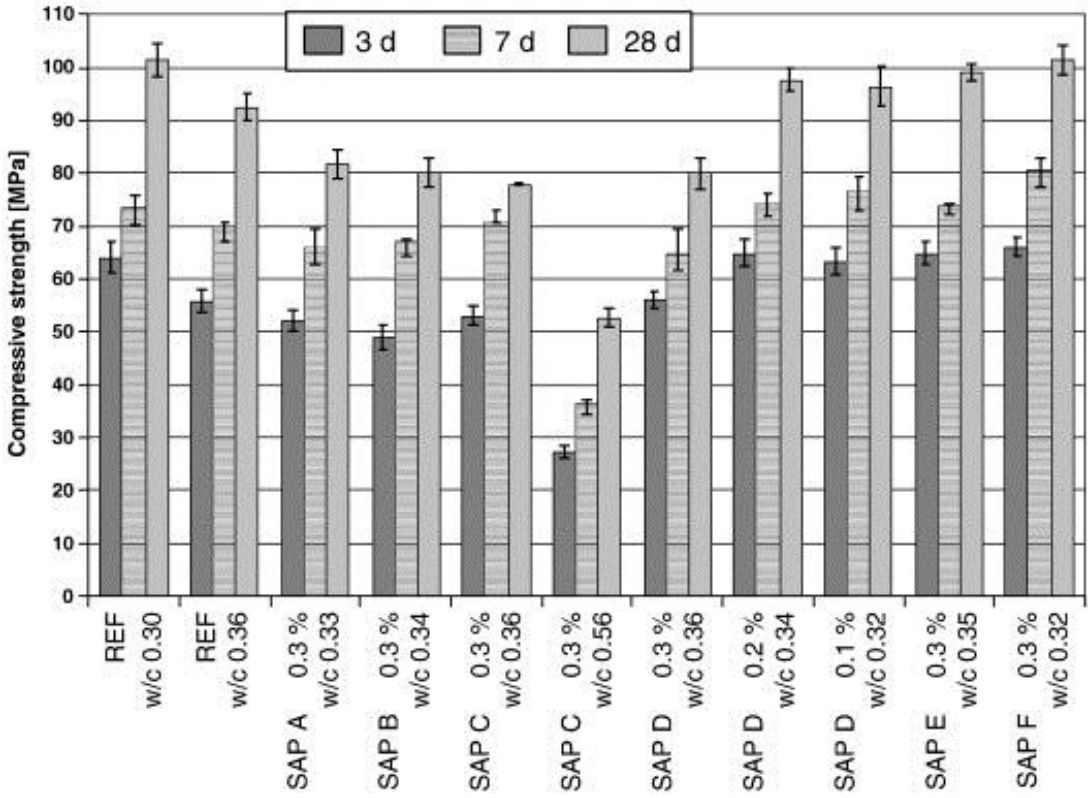

Figure 2.50: 3, 7 and 28 day strength of reference and SAP mixes (Schröfl et al., 2012)

2.4 Concluding Summary

Low w/b ratio concretes are typically sticky mixes that are difficult to work with in the fresh state and also have a short time frame during which they can be successfully placed. Conventional mix design methods are not suitable for HPC. Producing a HPC is more a material selection process as opposed to a mix design process as in the case of NSC. In addition to conventional concrete ingredients, the use of SCM's and superplasticisers are essential to produce a HPC. Although there is no universal mix design method for HPC, the principles used to produce it are well documented and include high quality materials, SCM's, superplasticiser, efficient aggregate proportioning and low w/b ratio.

Low w/b ratio concretes are also known to be prone to early-age shrinkage because of its high fine content. Plastic and autogenous shrinkage are of particular concern for concretes that are subject to high capillary pore pressures because of their very fine pore structure. Furthermore, autogenous shrinkage is of particular concern for concretes with high cement contents because they are subject to self-desiccation.

Special attention needs to be given to the extent of plastic and autogenous shrinkage and the risk of plastic and autogenous shrinkage cracking if HPC is to be a viable solution for specialised construction processes and intricate structures.

Self-desiccation is also a phenomenon that occurs in NSC, but conventional curing methods are sufficient to prevent the detrimental effects thereof. Conventional curing methods however, are not suitable for HPC due to the dense microstructure. The solution to the inefficient external curing of HPC is providing curing water to the capillary networks through small internal reservoirs of water dispersed in the concrete matrix. This is also referred to as internal curing. For efficient use of SAP, the correct type and dosage has to be determined and more importantly, the correct amount of internal curing water. Adding too little internal curing water will reduce the workability and may not be efficient in reducing the autogenous shrinkage, while too much internal curing water may mitigate the autogenous shrinkage, but at the cost of the compressive strength.

The use of SAP in HPC has been researched for about 15 years now and there is still much more that remains unknown. There is still no universal guideline on how to use SAP and internal curing water since, its efficiency is dictated by the particular characteristics of the SAP in use and the paste, mortar or concrete to which it will be added is unique every time

Chapter 3

Mix Design Development

To achieve a high strength concrete (HSC) with good workability is almost contradictory. The low water to binder (w/b) ratio that provides the strength is the precise property that expels the workability. To recover this loss of workability, superplasticisers are used to optimise the dispersion of water and cement particles, which improve flowability. Once more, a higher dosage of superplasticiser, which correspondingly increases the flowability, is at the cost of the retention thereof. The solution required to achieve high strengths together with a good workability and its retention calls for a combination of iterative calculated guesses. The first step in the approach taken in this study is selecting the required w/b ratio followed by optimising the dosage of superplasticiser. Next, the addition of supplementary cementitious materials is considered to both increase the performance of concrete as well as make the mix more economical. The selection of fine and coarse aggregate is also considered by looking at their grading and how they influence the particle size distribution of all the solid particles in a concrete mix by comparing them to ideal grading curves. Lastly, the absorption kinetics of superabsorbent polymers (SAP) are considered followed by the final mix designs based on the discussions in this chapter.

3.1 Approach

Before calculating any mix proportions or conducting trial mixes for this study, each of the locally available mix constitutes at disposal were reviewed to determine if its' quality is good enough for HPC. Thereafter, the interaction of a combination of the pivotal constitutes were examined as well as the variation in behaviour with a variation of the proportions. The concrete mixes were dictated by setting volume fractions for the stone and mortar content of the concrete as well as volume fractions for the sand and paste portions of the mortar.

Furthermore, the cementitious material in the paste was split proportionally as decided through a series of trial mixes. For a selected w/b ratio, only certain amount of water content would satisfy the mix design for a 1000ℓ mix while maintaining the volume proportions as mentioned above.

The solver function in Microsoft Excel was used to determine this amount of water that would satisfy the w/b ratio along with the particular proportions.

Once the proportions of binder, stone, sand and water were chosen, the dosage of superplasticiser was also chosen through an iterative process. This was considered to be the reference mix and then the SAP and internal curing water were added to produce the prescribed variations presented in Sections 4.1.1 and 4.2.1.

Two w/b ratios were prescribed for two reference mixes namely; WB022 and WB027 with a w/b ratio of 0.22 and 0.27 respectively. WB022 and WB027 refer to the complete set of both paste and concrete reference and internally cured mixes which have the respective w/b ratio. WB022_Ref and WB027_Ref refer to the refernece paste or concrete mix containing no SAP and the internally cured mixes with the respective w/b ratio will be further defined in its name refering to the SAP dosage, saturation level of SAP and stone size if applicable.

The term w/b ratio includes a cement replacement of 12 % silica fume as binder. The term w/c ratio will refer to a mix containing only cement as binder in a paste. The selection of this silica fume replacement level used in all mixes in this investigation is discussed in Appendix C.1.

The decision making process of the mix design development is shown in Figure 3.1 and the steps are discussed in further detail in the sections that follow.

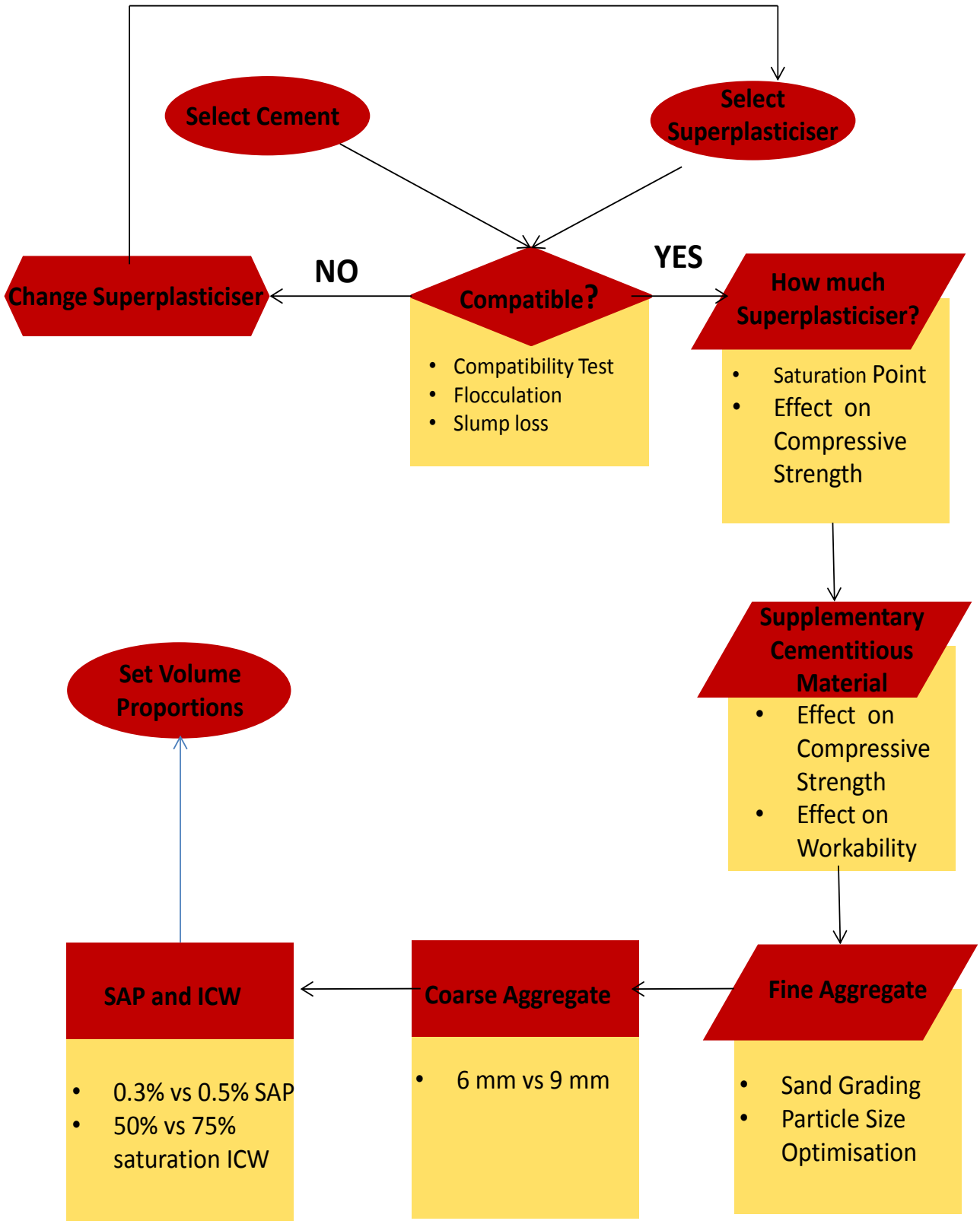

Figure 3.1: Mix design development

3.2 Cement - Superplasticiser Interaction

The cement used in this study was a CEM II 52.5 N cement, supplied by Pretoria Portland Cement PTY Ltd. The chemical composition and grading are respectively shown in

Table 3.1 and Figure 3.2. Cement from the same batch was used as far as possible to reduce the effects of slight variability in chemical composition and particle size distribution (PSD) between different batches of cement.

Table 3.1: Chemical Composition of CEM II 52.5 N cement

Composition	%	Composition	%
Ca0	63.5	TiO_2	0.22
SiO_2	20.7	Na_2O	0.19
Al_2O_3	3.48	Mn_2O_3	0.07
Fe_20_3	3.12	Cl	0.01
SO_3	2.37	P_2O_5	0
MgO	1.12	Cr_2O_3	0
K_2O	0.49	LOI	4.57
		Total	99.8

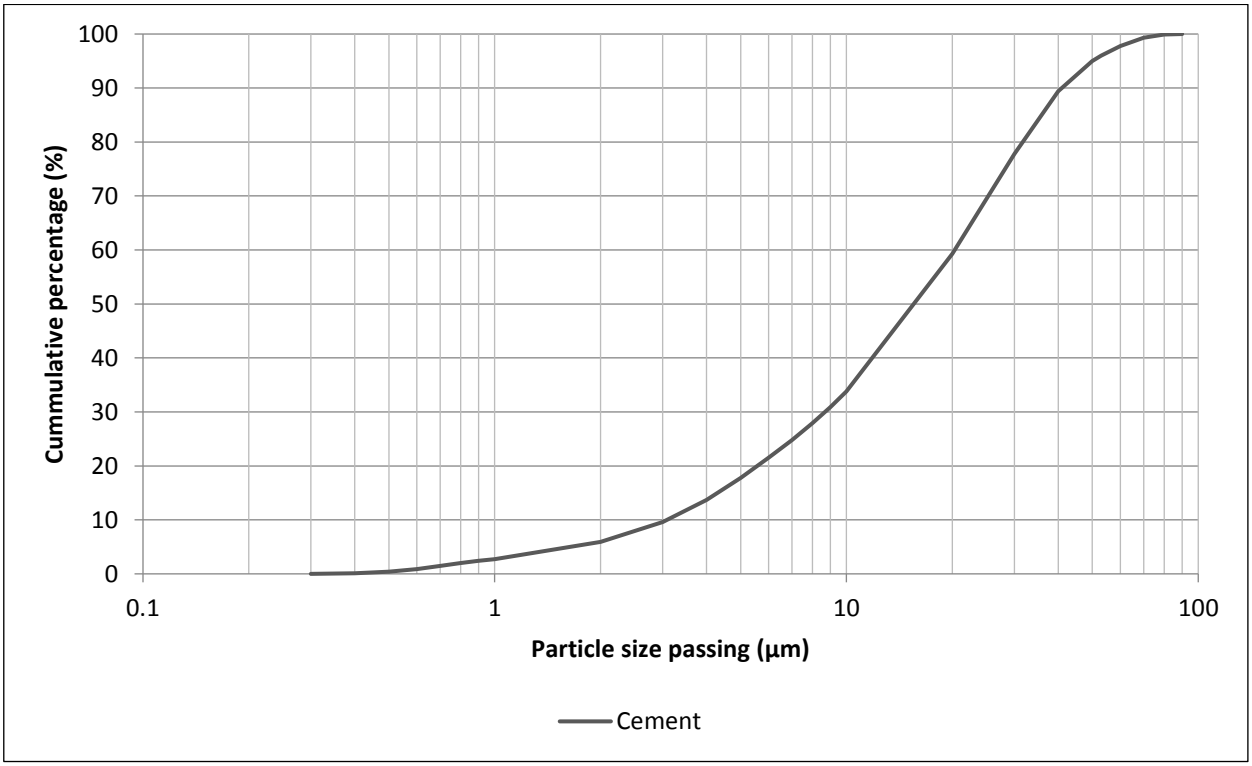

Figure 3.2: Particle size distribution of CEM II 52.5 N cement

The performance of a number of different locally available superplasticisers in combination with the mentioned cement was tested in accordance with the method discussed by Aïtcin (1998), following the marsh flow cone procedure described in ASTM International (2010). The marsh flow cone procedure gives a comparable indication of the performance of different cement-superplasticiser combinations. The superplasticiser used in this investigation was chosen by process of elimination. The flowability of cement pastes with a number of different locally available superplasticisers was observed using the marsh flow cone method. The cement/superplasticiser combinations that performed satisfactorily in the marsh flow cone procedure were then tested to observe the superplasticiser's ability to flocculate cement grains. Before selecting the final superplasticiser with the best flocculating abilities, the slump retention of this combination was also observed to determine if the superplasticiser is suitable to provide flowability, sufficient dispersion of particles as well as an acceptable slump retention. These tests and their results are discussed next.

3.2.1 Compatibility

The marsh flow cone used in this investigation is shown in Figure 3.3a and complies with the specifications in ASTM International (2010) shown in Figure 3.3b. To determine if a given superplasticiser is compatible with the particular cement, 1% of superplasticiser by weight of cement (bwoc) was added to a cement paste with a w/c ratio of 0.35. The paste was mixed in a cake mixer following the procedure shown in Table 3.2.

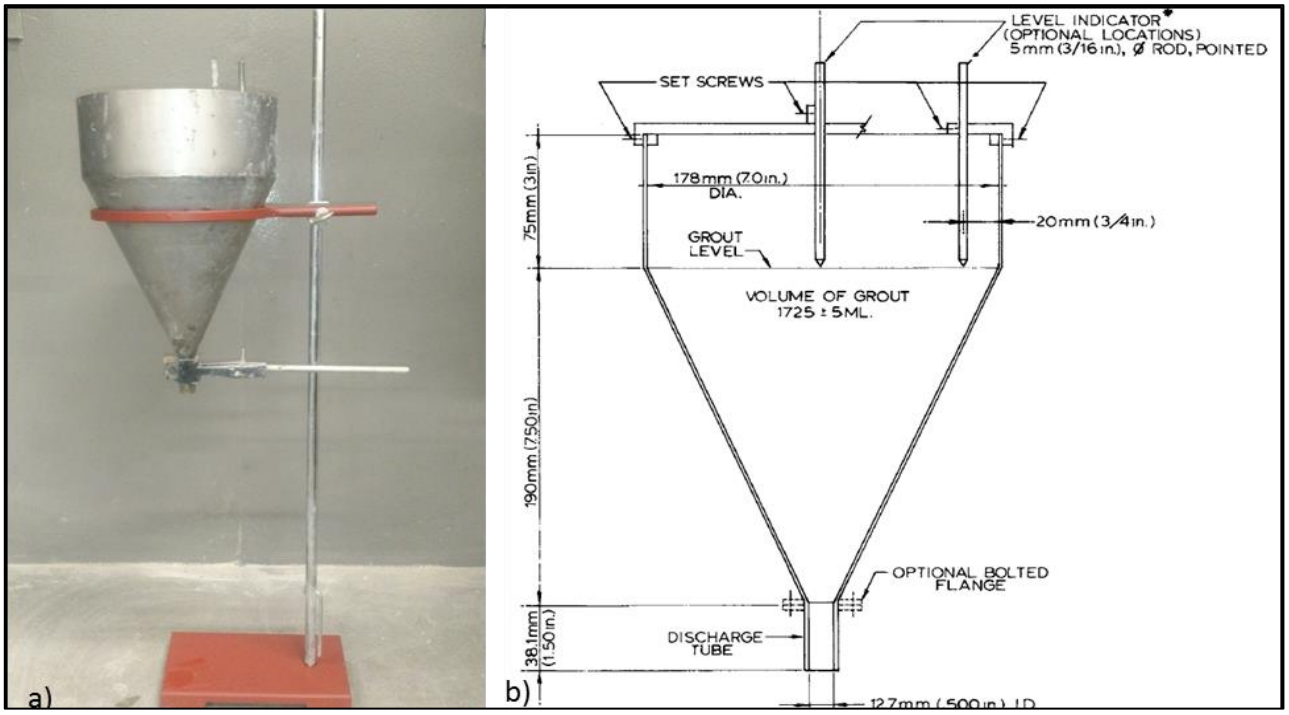

Figure 3.3: Photograph of Marsh Flow Cone and b) schematic representation showing dimensions

Table 3.2: Cement - Superplasticiser mix procedure

Mix Step	Duration
Cement dry mix	30 s
Add water	30 s
Add SP	30 s
Mix on Speed 1	1 min
Mix on Speed 2	5 min
Scrape bottom & sides	30 s
Mix on Speed 2	5 m
Total mixing time	13m

After mixing, approximately 1725 mℓ of cement paste was poured into the marsh flow cone while keeping the discharge tube closed. Once the cone was secured and levelled, the discharge tube was released and the paste was free to flow out of the cone under gravity. The time taken for the paste to empty from the cone was recorded. Table 3.3 summaries the flow times of four brands and eight different types of superplasticisers used with two different types of cement. The table also includes the type of superplasticiser as defined in the product technical data sheets which are each presented in Appendix C.2.

Table 3.3: Cement-Superplasticiser Compatibility

Compatibility		Flow time (sec)	
Name	Type	Sephako	PPC
Chryso Premia 310	Polycarboxylate polymer	-	X
Chryso Fluid Optima	Polycarboxylate polymer	-	X
Viscocrete 10	Polycarboxylate polymer	56 (SEG)	X
Viscocrete 20 HE	Polycarboxylate polymer	49	X
Dynamon SP1	Acrylic polymer (no formaldehyde)	38 (SEG)	SEG
Dynamon SX	Acrylic polymer	50 (SEG)	SEG
Dynamon NRG 1022	Acrylic polymer (no formaldehyde)	-	56
Master Glenium ACE 465	Poly carboxylate ether polymers	-	90

A cement and superplasticiser was said to be compatible if the flow time was between 60 – 90 seconds (Aïtcin, 1998). If a cement paste segregated immediately after mixing, the combination was deemed incompatible. These are marked as "SEG". Some combinations did not appear to segregate immediately after mixing, but once the flow from the cone was completed, the paste showed significant segregation. These are marked with the flow time, followed by "(SEG)" and were also deemed incompatible. Combinations marked with "X" were not flowable at all and combinations marked with "- "were not tested.

3.2.2 Flocculation

A good cement-superplasticiser combination is one that is effective in deflocculating cement grains in the presence of water (Aïtcin, 1998). It is possible that a given compatible cement-superplasticiser combination is more effective in deflocculating cement grains in the presence of water than another compatible combination. From the compatibility experiment carried out, the three superplasticisers that performed the best are Viscocrete 20HE, Dynamon NRG 1022 and Master Glenium ACE 465. These three superplasticisers were then used in the next experiment to observe the effectiveness of each to flocculate the cement grains in the presence of water.

The procedure was adapted from Aïtcin (1998) and is as follows: 12.5g of cement was put in to four 250 mℓ glass cylinders. 2.5 mℓ of each of the three superplasticisers mentioned were then put in to Cylinders 2, 3 and 4. With Cylinder 1 being the reference containing no superplasticiser, it was filled with water to reach the 250 mℓ mark. See Figure 3.4. As soon at the water was added to the cylinder, the cement at the bottom was agitated with a stirrer and flipped upside down until all the particles were uniformly suspended in the water. The cylinder was then put aside and untouched. The same was done for the remaining three cylinders, filling each with water until the 250 mℓ mark and then mixing for about 30 seconds in total until an even suspension was achieved. The cylinders were then left undisturbed for 48 hours. From Figure 3.4a it can be seen that just minutes after agitation, the reference cylinder without any superplasticiser, already shows pronounced settling of cement grains.

From the figure, the proficiency of each of the superplasticisers to hold cement grains in suspension in the presence of water can also be observed. After 48 hours as shown, in Figure 3.4b, the cement grains in the reference cylinder were completely settled, leaving the water above it clear and free of cement grains. The difference in degree of settling in the remaining three cylinders can be observed by looking at the relative heights of the settled cement at the bottom of the cylinder as well as the colour of the water above the settled cement. Cylinder 4, containing the Viscocrete 20HE superplasticiser, appears to be the most effective in deflocculating cement in the presence of water.

The colour of the water in this cylinder is the darkest, indicating that it kept the most cement grains in suspension. The height of the settled cement in this cylinder is also the lowest, meaning that it showed the highest degree of flocculation. The colour of the water in Cylinders 2 and 3 appear similar. Taking a closer look at the settled cement, it can be seen that Cylinder 2 with Master Glenium ACE 456 superplasticiser was slightly higher than Cylinder 3.

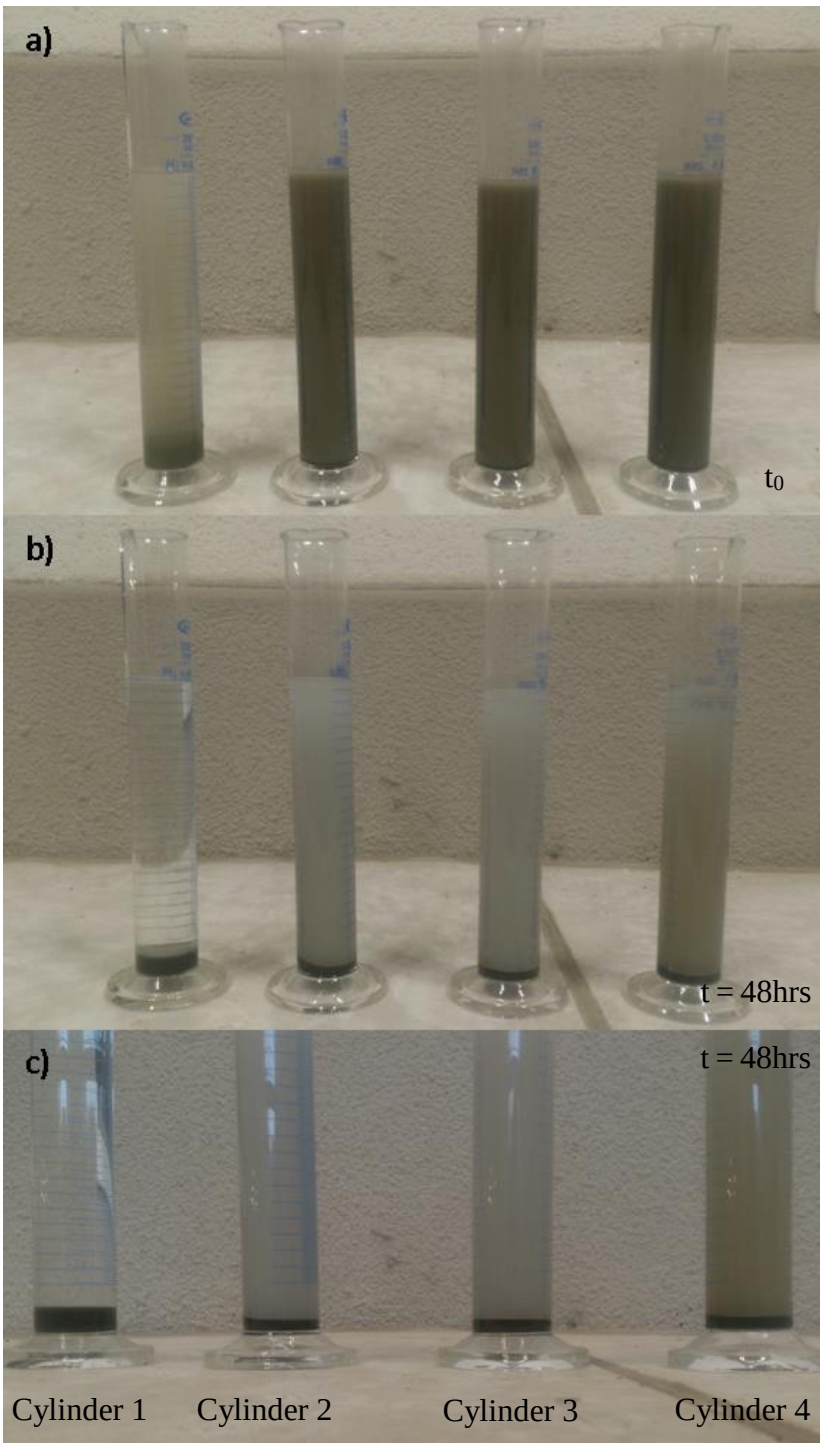

Figure 3.4: Deflocculation efficiency of three different types of superplasticisers a) just after preparation, b) 48 hours later c) close up of b)

From this experiment, it can be concluded that Viscocrete 20 HE superplasticiser was the most effective in deflocculation, followed by Dynamon NRG 1022 and then Master Glenium ACE 456.

Furthermore, when water was added to the cylinder containing Viscocrete 20HE, it started foaming at the top. The foam disappeared a few seconds after stirring. This is an indication of a lignosulphate water-reducing admixture which contain tensoactive components that entrain air (Aïtcin, 1998).

3.2.3 Slump Loss

The two compatibility tests showed that, the Viscocrete 20HE, Dynamon NRG1022 or Master Glenium 456 superplasticiser would be an appropriate choice for further experiments. Although Master Glenium showed the least amount of flocculation in the flocculation test, it was chosen for this investigation since in the compatibility test, Master Glenium showed the longest flow time, within in the compatibility requirement range. This suggests that Master Glenium has the highest segregation resistance, while still providing sufficient plasticising ability. This is important for w/b ratio's less than 0.35, because a lower w/b ratio requires a higher dosage of superplasticiser and the cement should be able to accommodate this. Furthermore, the slump loss of this combination was observed before substantiating its' use for further experiments.

To observe if the combination of cement with Master Glenium ACE 456 has an acceptable slump retention period, the slump loss was observed similar to the procedure described by Aïtcin (1998) and de Almeida & Goncalves (1990). The reference paste mixes used in this investigation were tested for slump loss to determine if its retention is good enough to carry out the autogenous shrinkage test procedure successfully. The mix design for WB022_Ref_Paste and WB027_Ref_Paste are presented in Section 3.7.

The paste was mixed in a cake mixer following the procedure shown in Table 3.2. After taking the first reading, the remaining paste was covered with cling wrap to prevent evaporation and carbonation. After 13 minutes, the paste was remixed in the cake mixer for one minute and then immediately tested for a slump. The results are shown in Figure 3.5.

From these tests, it can be concluded that the PPC-Master Glenium ACE 456 combination can retain an adequate slump period even at a low w/b ratio of 0.22. As expected, the paste with the higher w/b ratio has a higher slump. However, it was expected that the paste with the higher w/b ratio would also have the longest slump retention period, but this was not the case. WB022 showed a slump retention period of 135 min and WB027 showed a slump retention period of 90 minute. The figure also shows that although WB022 had a longer slump retention, its rate of slump loss is higher.

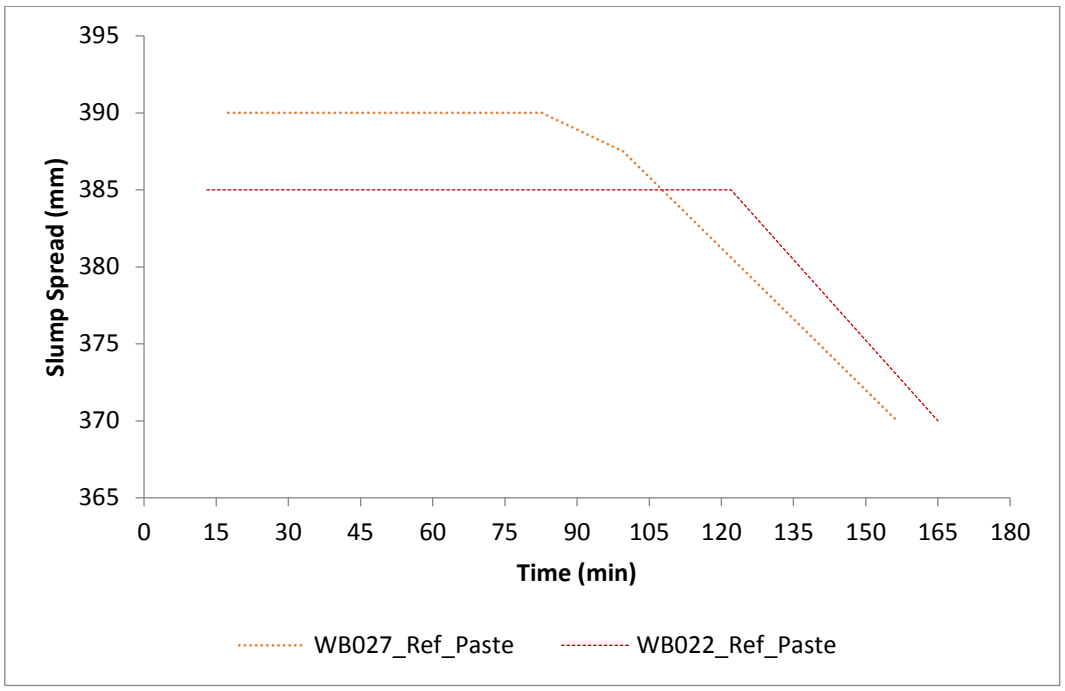

Figure 3.5: Slump loss of CEM II 52.5 N cement with Master Glenium ACE 456

From the three cement-superplasticiser compatibility tests, it was concluded that Master Glenium ACE 456 performed the best and was chosen for the rest of this study. The dosage of this superplasticiser for the prescribed w/c ratio is considered in the next section.

3.3 Superplasticiser Dosage

Prescribing a superplasticiser dosage for a given w/c ratio is a delicate matter to consider. For HPC, the quantity of superplasticiser in a mix is high relative to what is found in NSC because of the high cement content of HPC. This high content of superplasticiser hold many implications for the concrete mix and how it performs during the mix procedure as well as setting.

The relationship between superplasticiser and workability can be looked at in two ways. The most common way to determine a superplasticiser dosage for comparative mixes in an experimental study is to select a dosage that produces a mix with a prescribed slump or slump flow. In this study however, a certain dosage was prescribed for a given w/c ratio and the same dosage as calculated bwoc was used for all variations with the same w/c ratio. This approach was adopted to limit the effects that varying amounts of superplasticiser has on the microscopic interactions in a particular mix.

However, keeping the dosage the same brings about reduction in flowability of mixes that include SAP compared to the reference mix without SAP.

This allows the fresh performance of a mix to be observed with respect to the addition of SAP and internal curing water and conclusions on the effect that SAP and internal curing water has on the mix can be made. This also eliminates the uncertainty that is introduced to a mix at varying superplasticiser dosages because of the added water from the superplasticiser.

The dosage of superplasticiser for all of the mixes was taken to be the saturation point for the particular w/c ratio. The method used to determine the saturation point of superplasticiser for a given w/c ratio was adopted from the method used by Aïtcin (1998).

3.3.1 Saturation Point

This procedure requires the use of the marsh flow cone described in Section 3.2.1. The saturation point was determined for the two prescribed w/c ratio used in this investigation; WC022 and WC027. A cement paste mix was prepared and mixed, for each of these w/c ratio, in accordance with the mix procedure described in Table 3.2. Starting with a superplasticiser dosage of 1 % bwoc, 1725 mℓ of paste was poured into the cone while keeping the discharge tube closed and then released once the cone is secured and level. The time taken for the paste to run out of the cone was recorded. Based on the fluidity of the paste, the dosage was either increased or decreased in 0.1 % increments and then repeated on a new cement paste batch, recording the discharge time every time. The lowest dosage of superplasticiser tested was the dosage that no longer allowed the paste to flow out of the cone. The highest dosage tested was the dosage that resulted in segregation. The flow times were then plotted against their corresponding dosages to observe how the increase in superplasticiser increases the flow characteristics of the paste.

In addition to the flow time, the mini-slump spread of each iteration was also observed and plotted against its corresponding dosage. The curves are presented in Figure 3.6 to Figure 3.8. The saturation point is the dosage at which there is no more significant improvement to the flowability with increasing dosage withstanding segregation. Considering the flow time curves in the figures, it can be seen that from the lowest dosage, the flow time dramatically decreases with a slight increase in superplasticiser dosage and then gradually, the flow time starts to stabilise even with an increasing dosage. This is when the increase in superplasticiser is no longer beneficial to the flowability. Likewise, the mini-slump spread dramatically increases with a slight increase in superplasticiser dosage and then starts to stabilise when the increase in superplasticiser is no longer beneficial.

The curves also show that, there is a critical point that separates the flow improvement from the point of stabilisation in the curves.

However, this is not necessarily the point of saturation. Jayasree and Gettu (2008) defined the saturation point to be at the dosage where the internal angle between two adjacent lines is 140 ±10°. This is an objective value based on experimental results. If a tested point does not fall in the range, the dosage can be found by interpolation. The dotted line on Figure 3.6 to Figure 3.8 indicates the saturation point according to this objective approach. It can be seen that this point is close to the critical point observed from the curves by inspection. Furthermore, the point of stabilisation in the mini-slump spread corresponds with the point of stabilisation in the flow time curves.

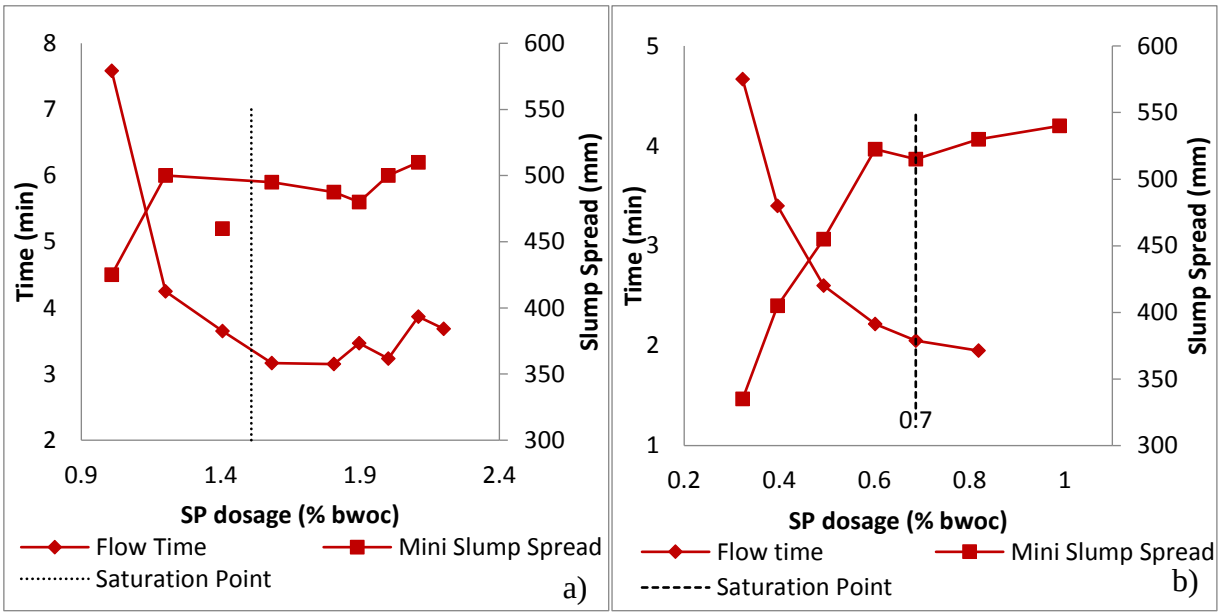

Figure 3.6: Saturation Point of cement paste and NRG1022 for a) w/c ratio 0.22 and b) w/c ratio 0.27

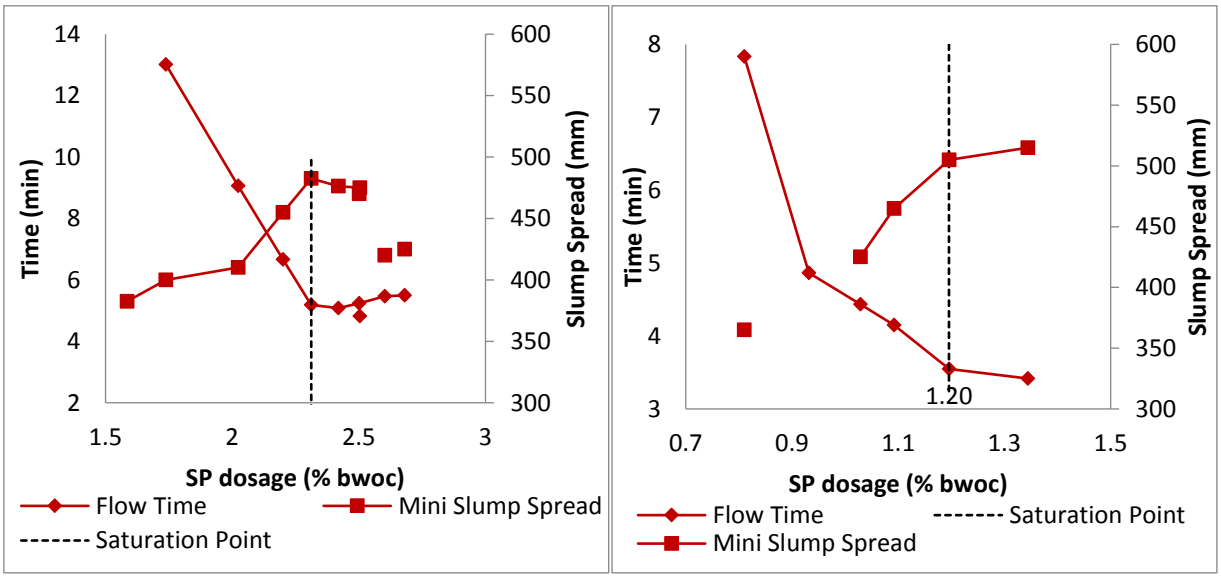

Figure 3.7: Saturation Point of total binder and NRG1022 for a) w/b ratio 0.22 and b) w/b ratio 0.27

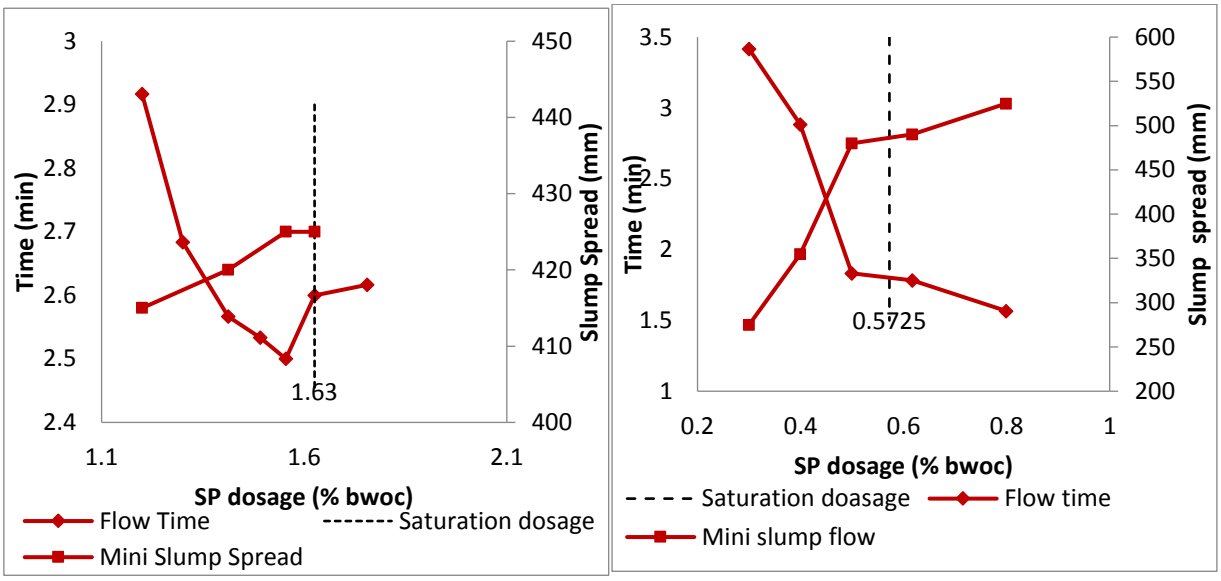

Figure 3.8: Saturation Point of cement paste and Master Glenium 456 for a) w/c ratio 0.22 and b) w/c ratio 0.27

The results also show that the saturation dosage of Master Glenium ACE456 is lower for the corresponding pastes using NRG 1022. The flow times at the saturation dosage is also lower for the pastes that use Master Glenium ACE456. This suggests that Master Glenium is more effective than NRG 1022 and is more compatible with the cement used in this study. Master Glenium ACE 456 was thus selected for the rest of the study because it would require a smaller amount. Large amounts of superplasticiser may introduce complexities to the hydration process and may also result in a higher mix cost.

Although the saturation point of WC027 paste with Master Glenium is indicated as 0.5725 % bwoc, this was not the case for the concrete mix. A dosage of 0.5% in the concrete reference mix with w/b ratio of 0.27 produced no slump, let alone flow. Increasing the dosage to 0.6 % resulted in a 60 mm slump height. The superplasticiser dosage was then increased in increments to obtain the saturation point of the concrete. The increasing flowability of this concrete mix with increase in superplasticiser dosage is shown in Figure 3.9.

Similarly, the saturation dosage indicated by the marsh flow test for WC022 paste resulted in segregation in the corresponding concrete, WB022. The saturation dosage for WB022 was then decreased from 1.63 until the mix no longer segregated. At a dosage of 1.4 %, WB0.22 still segregated. The dosage was then brought down to 1.2 % and was taken as the saturation point as the mix no longer segregated.

In addition to the effect that varying dosages have on the flowability of a given w/c ratio and w/b ratio, the effect thereof was also tested on the compressive strength for WB027.

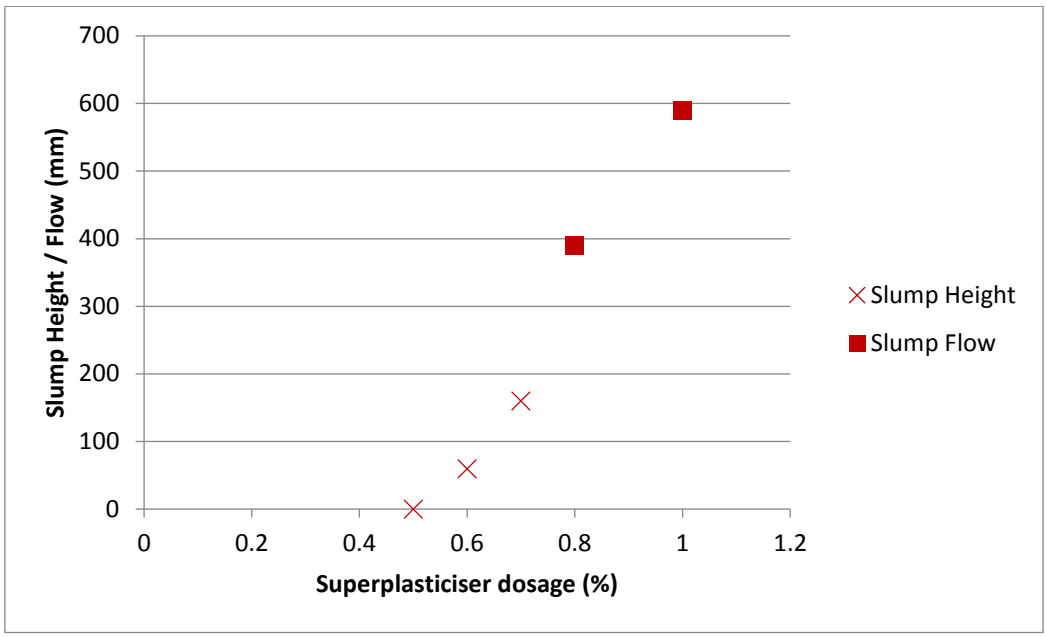

Figure 3.9: Superplasticiser dosage sensitivity

3.3.2 Compressive Strength

While the primary objective of a superplasticiser is to improve workability and flowability, the superplasticiser also influences the strength development. Superplasticiser is a chemical admixture and thus influences the chemical reactions of hydration, which is the basis of strength gain. The effect of an over dosage is more often negative. Increased amounts of superplasticiser effectively increase the w/c ratio, because of the added water in the superplasticiser, decreasing the strength.

The saturation point of a superplasticiser is thus governed by a combination of the flow characteristics as well as strength gain. If an increasing superplasticiser dosage increases the flow of a mix, without segregation, but at the cost of the compressive strength, then it cannot be considered as an optimum dosage.

To observe this, WB027 was tested for compressive strength of concrete along with its flowability at increasing increments from the saturation point of the corresponding paste. These results are presented in Figure 3.10. Starting at 0.5 %, the theoretical saturation point of Master Glenium ACE 456 from Figure 3.8b, the compressive strength for WB027_Ref_9mm was tested. This reference mix is indicated as WB027_0.5 in the figure. The rest of the mixes are similarly indicated with the last number representing the superplasticiser dosage. The results show that the strength increases as the superplasticiser dosage increases, up until 1.4 %, where the 3-day strength decreases.

The increase in strength from 0.5 % to 1.0 % is seemingly either or dually due to the increase in flowability of the mixes, which results in less voids during compaction and better dispersion of particles.

However, slight segregation was observed in the mix containing 1.0 % superplasticiser. Despite the segregation, this mix still resulted in a higher compressive strength. WB027_1.4 exhibited pronounced segregation and is thus the reason for the decrease in strength. 0.8 %, where no segregation was experienced, was consequently chosen as the saturation dosage for WB027.

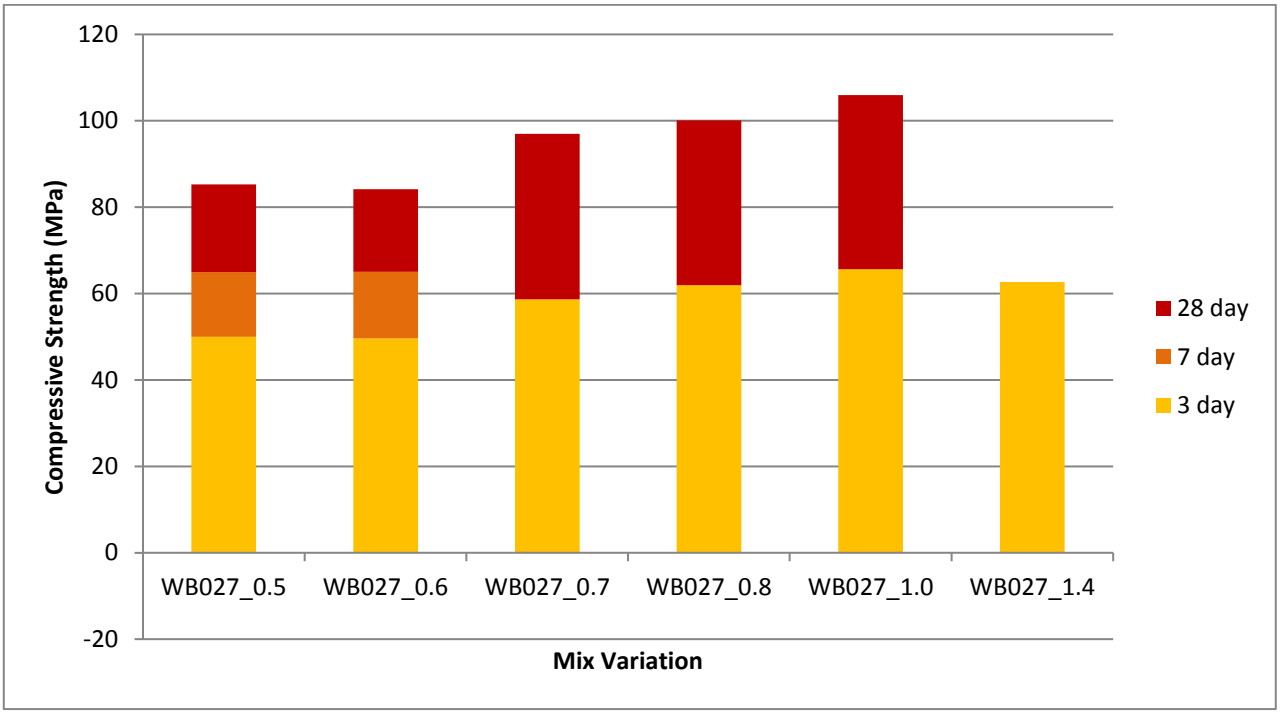

Figure 3.10: Finding the saturation dosage of superplasticiser through compressive strength

The water content in all the mixes were adjusted to take account of the extra water that is added from the superplasticiser. Master Glenium ACE 456 has an average solids content of 44 %, and the rest is water. This 56 % of water from the superplasticiser was reduced from the calculated mix water for all mixes using Master Glenium ACE 456.

3.4 Grading of Particles

The aggregates used in this study are commonly used in practice. Locally available natural quarry sand, known as Malmesbury sand, and Greywacke stone was used as fine and coarse aggregates respectively. The grading of both the sand and stone were carried out to predict their efficiency in particle size optimisation for the concrete mix using the recommendations that were presented in Section 2.1.5. The results and discussion of the aggregates are presented next.

3.4.1 Sand

Two batches of Malmesbury sand were available, a coarse sand blend and a fine sand blend. The grading of fine sand, coarse sand, a blend between the two and fine sand sieved through a 300 µm sieve are shown in Figure 3.11. The sieving was carried out in accordance with SANS 3001-AG1:2014 and SANS 3001-PR10.

The ideal Fuller Parabola for aggregate grading is also shown in the figure. From the curves, it can be seen that the coarse sand is the closest to the ideal parabola with gradation ratio, *q*, of 0.5. This value is more appropriate for NSC as mentioned in Section 2.1.5. None of the sand however, matched the ideal parabola for low w/b ratio SCC with gradation ratio 0.37.

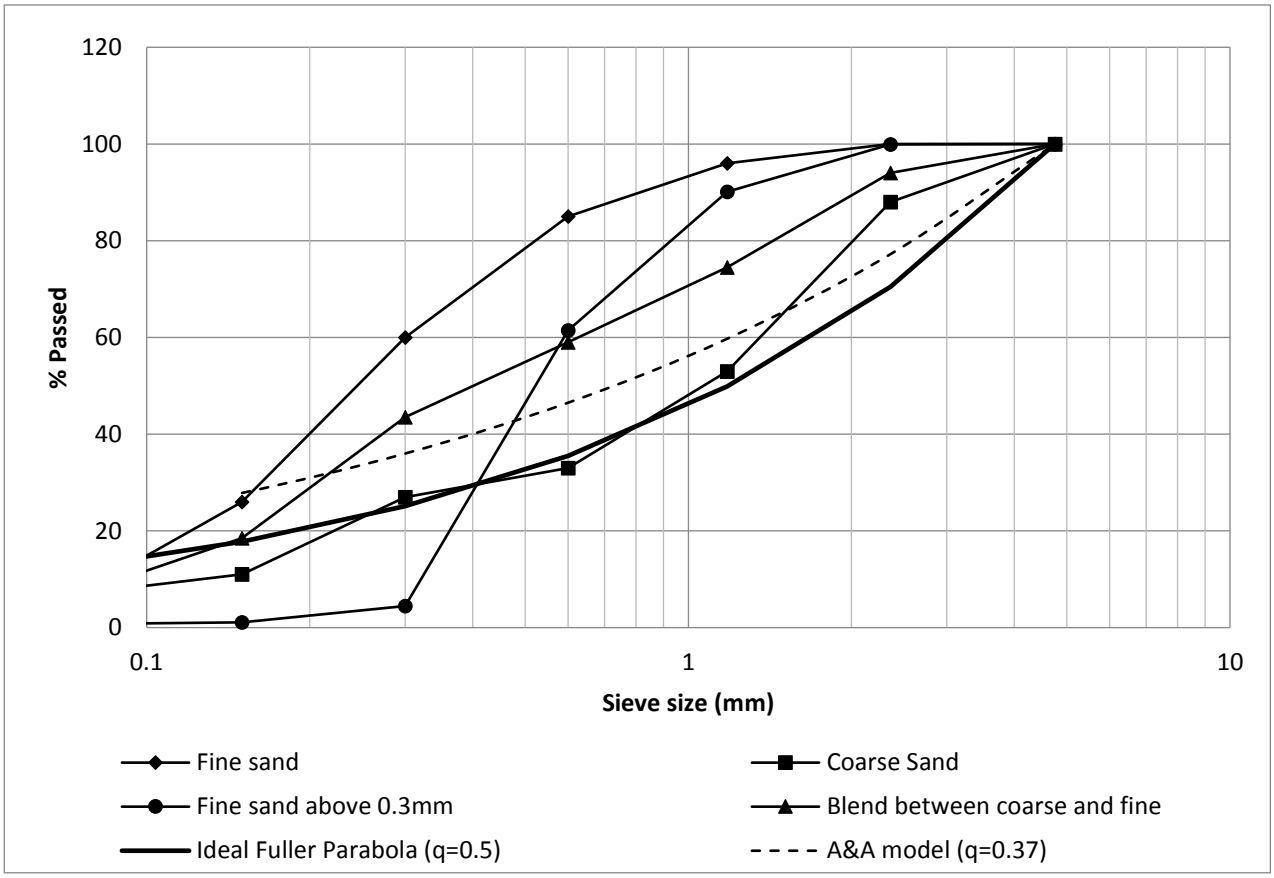

Figure 3.11: Malmesbury Sand Grading

For the production of HPC with a low w/b ratio, a coarser sand with less fines is commonly assumed, to reduce plastic shrinkage and plastic shrinkage cracking. However, in the production of SCC, fine sand may be preferable to reduce the amount of cementitious fines required for optimum particle packing density.

In this study, fine sand was used. The sand was sieved and all particles larger than 300 µm was used. This was done to have a sufficient amount of fines for particle size optimisation, while limiting the fines to avoid an excessive water requirement. Saturated-surface dry sand was used throughout the study to avoid the effects of varying moisture content on the strength and flowability of the concrete mixes.

3.4.2 Stone

The same batch of Greywacke stone was used throughout this study. Nominal sized of 6 and 9 mm stone was chosen since small stone sizes are commonly used in HSC and SCC. The grading of the two stone sizes are shown in Figure 3.12 and were carried out according to SABS SM 852.

The grading of the fine sand sieved through a 300 µm sieve is also shown in the figure along with the proportional combination of fine and coarse aggregate used in the final mix design that is presented in Section 3.6. The same amount of fine and coarse aggregate is used in both WB022 and WB027 and is therefore a representative of both reference mixes. The figure also shows the ideal gradation curves; fullers parabola with q=0.5 and the A&A model with q=0.37. The grading curves show that none of the aggregates or their blends match either of the ideal curves. However, a combination of sand with 6 mm and 9 mm could result in a close relation with the A&A model.

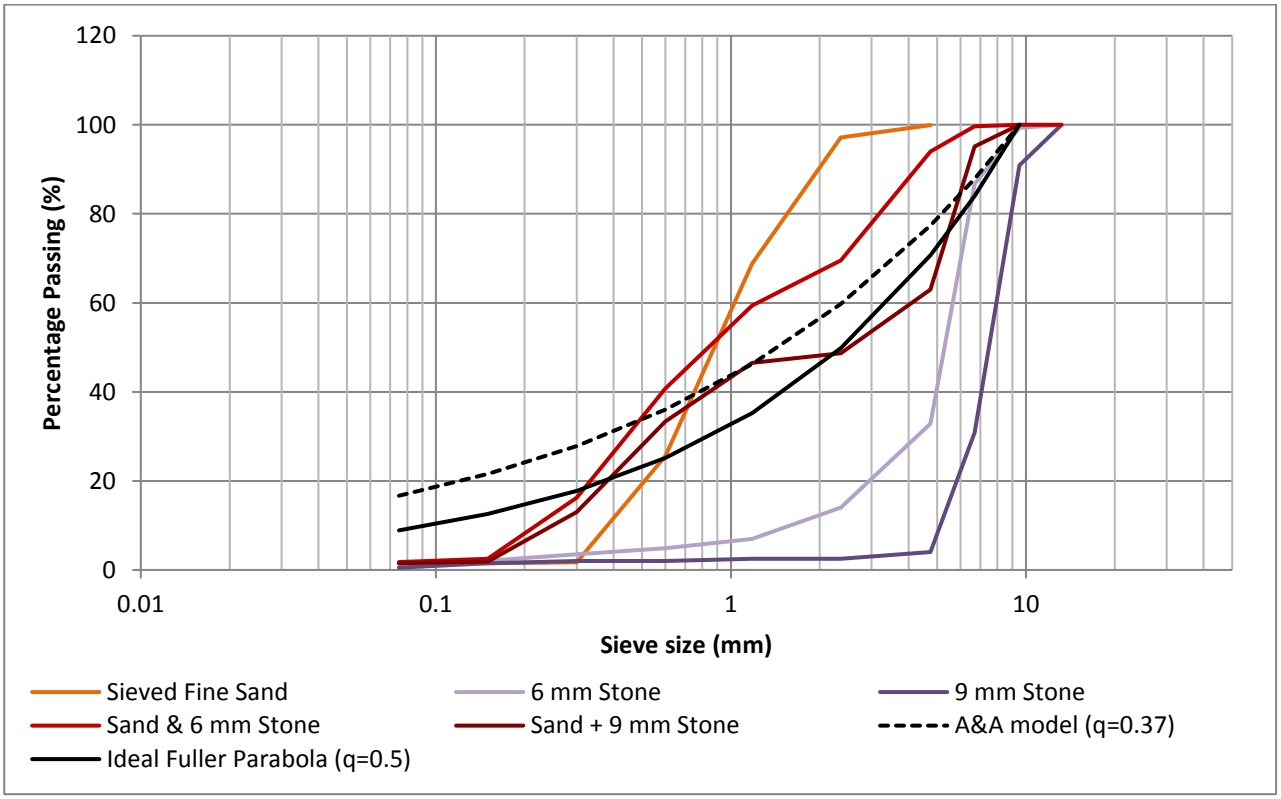

Figure 3.12: Fine and coarse aggregate grading

All the stone used in this study was washed to remove dust which can reduce the workability because of the added fines. The stone was then air dried and used in a saturated surface-dry condition to avoid the effects of varying moisture content on the strength and flowability of the concrete mixes.

3.4.3 All Solid Particles

After selecting the appropriate proportions of all the solid particles that were discussed in the preceding sections, the particle size distribution of all the solid particles in the concrete mix were compared with the ideal gradation curves. The grading of all the individual solid constitutes of the concrete mix is shown in Figure 3.13. WB022_Ref_6mm and WB022_Ref_9mm are presented in Figure 3.14 and WB027_Ref_6mm and WB027_Ref_9mm in Figure 3.15.

To obtain the grading of all solid particles, the grading of cementitious material and aggregates were combined at their relative proportions that make up mix WB022_Ref and WB027_Ref. These final mix designs are presented in Table 3.5 in Section 3.6.

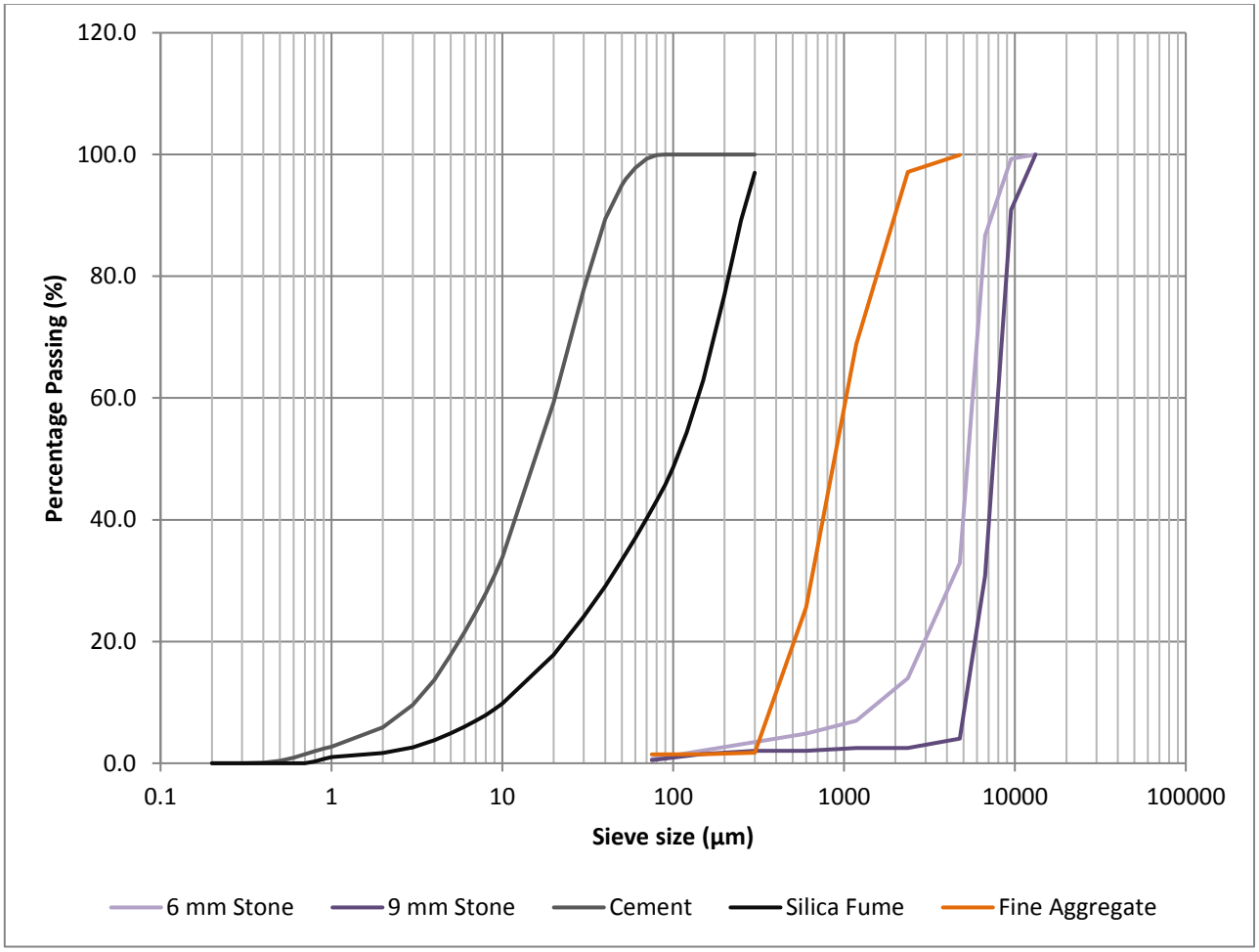

Figure 3.13: Grading of all solid particles

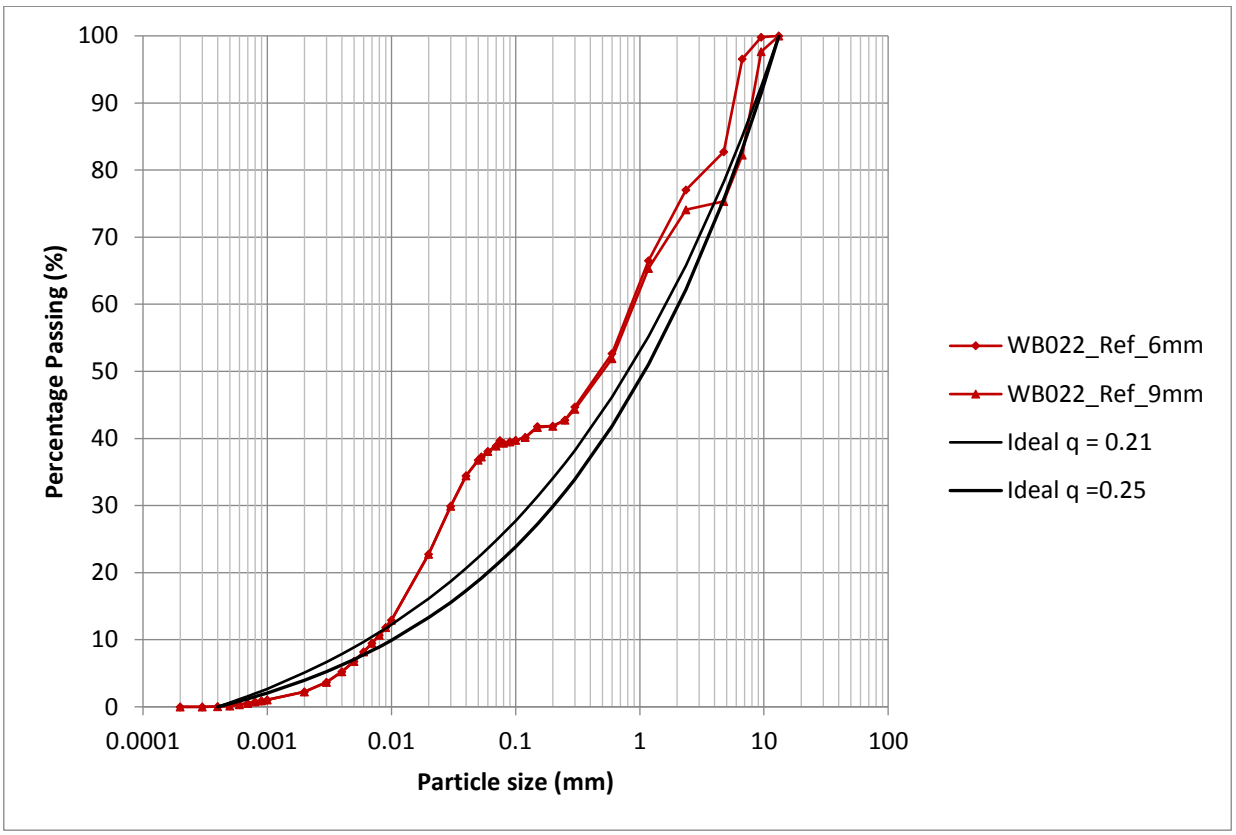

Figure 3.14: Particle size distribution of WB022_Ref

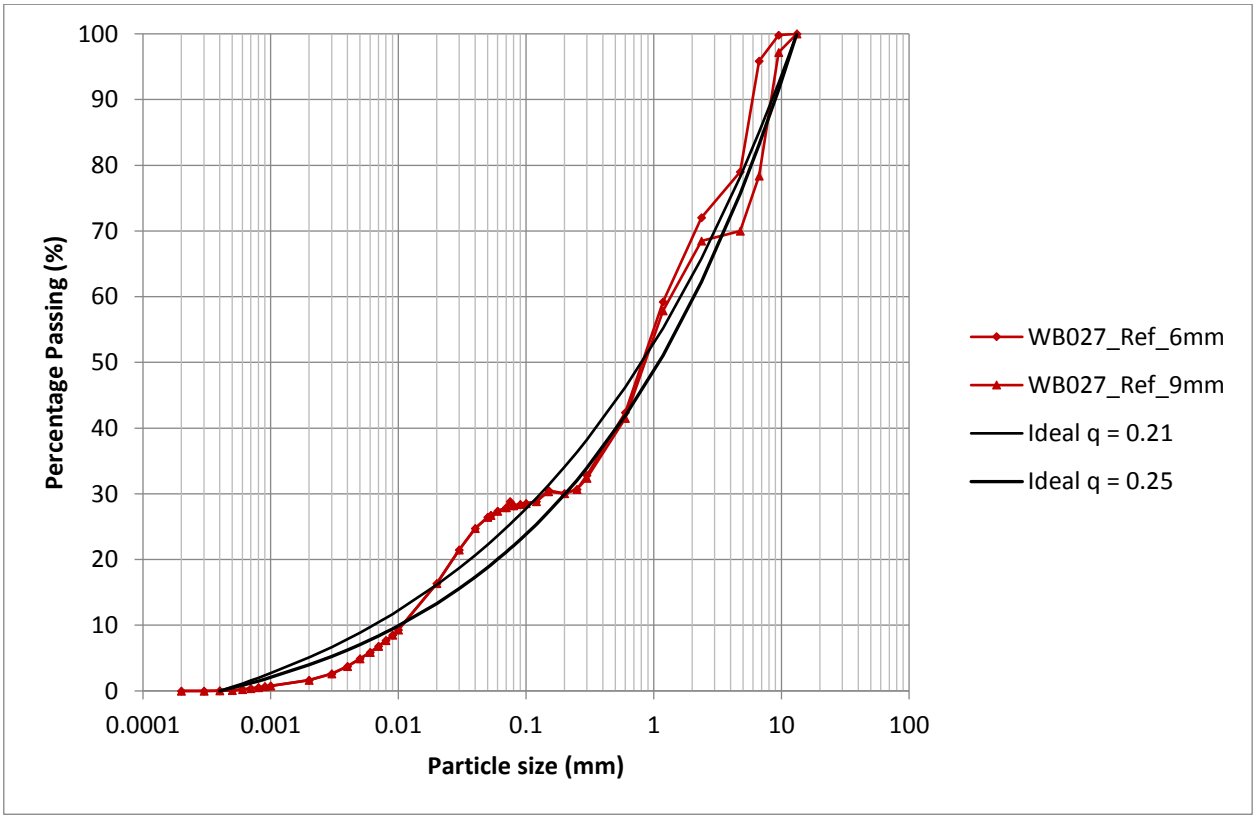

Figure 3.15: Particle size distribution of WB027_Ref

From Figure 3.14 and Figure 3.15, it can be seen that the obtained grading from the mixes used in this study do not exactly follow the ideal curve. There is a jump at 0.075 and 4.75 mm. These jumps are observed at the start and end of particle size intervals of sand and stone, which are much larger than the binders. To overcome this deviance from the ideal curve, more than one range of sand particle sizes could be incorporated in a mix so that the particle sizes overlap one another and produce a smoother curve which follows the ideal curve more closely (Brouwers & Radix 2005).

The figures also show that WB027_Ref is closer to the ideal curves, suggesting that using a w/b ratio as low as 0.22 is perhaps not very efficient in the production of SCC, or the q- values should be adjusted for this increase in fines.

3.5 Superabsorbent Polymers and Internal Curing Water

In this study, one type of super absorbent polymer (SAP) was used in cement paste mixes for autogenous shrinkage measurement and in concrete for plastic shrinkage measurement. The SAP was added at a dosage of 0.3 % bwoc, accompanied by varying dosages of internal curing water. In the pastes, 0.6 % SAP bwoc was additionally observed. The type of SAP used was determined by considering the PSD to predict the efficiency in terms of its absorption and desorption ability. The absorption capacity was observed using the tea bag test in water and four different pore solutions.

3.5.1 SAP Type

The SAP type used in the study is FLOSOFT 27 CC supplied by SNF Floerger. The PSD is shown in Figure 3.16. It was chosen because less than 15 % of the particles are smaller than 100 µm. A SAP type that has a large proportion of particles smaller than 100 µm is prone to gel blocking as mentioned in Section 2.3.2. Furthermore, 95 % of the particles are also smaller than 500 µm. SAP particles that are too big are also expected to be less effective in mitigating autogenous shrinkage as mentioned in Section 2.3.2.

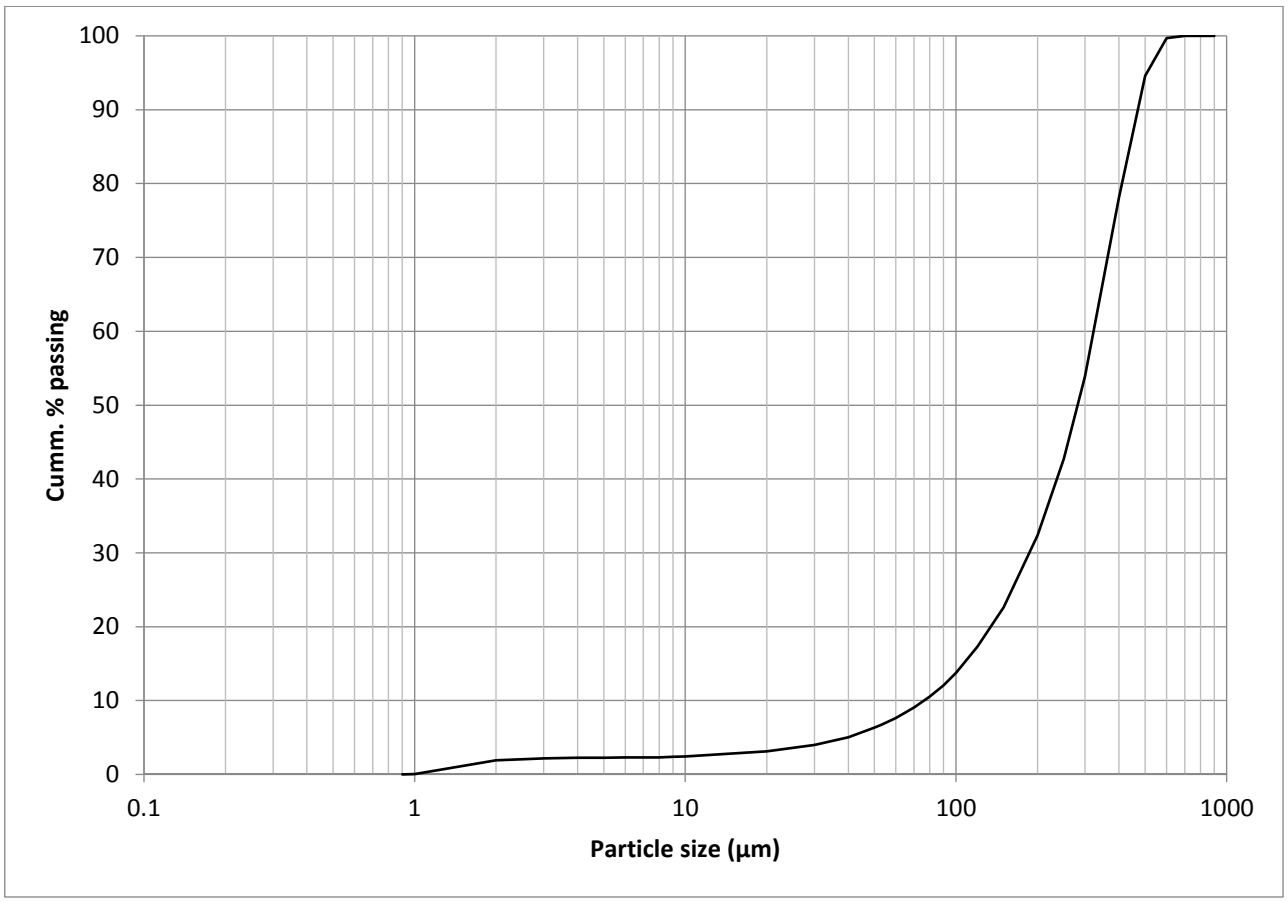

Figure 3.16: Particle size distribution of FLOSOFT 27 CC super absorbent polymer

3.5.2 Absorption Capacity of SAP

The absorption capacity of the chosen SAP in water and different simulated pore solutions were tested using the tea-bag test following the method described by Schröfl et al. (2012). The tea-bag used for this experiment, along with the other materials and apparatus are shown in Figure 3.17. The tea-bags used are disposable paper tea filters with dimensions 180.3 x 83 mm and 135 x 83 mm when sealed with a fold over flap. To observe the amount of water absorbed with respect to the amount of dry SAP, the tea bag was dipped inside the corresponding fluid and the excess water was removed with a paper towel without applying any pressure. A small amount of dry SAP between 0.2 and 0.3 gram, m_1, was then placed in to this pre-wetted tea-bag, which had a weight of m_2. The tea bag was then sealed at the top, completely submerged in to the corresponding fluid, and then removed after 30 seconds. The excess water was removed once again with a paper towel, without applying any pressure to remove loosely bound water and then weighed, m_3. This process was repeated on the same sample for time intervals of 2, 5, 10, 15, 30, 60 and 180 minutes from the start of the experiment. Between readings, the samples were sealed to prevent evaporation and carbonation.

Figure 3.17: Materials and apparatus used for the tea-bag test

The amount of water absorbed by the SAP with respect to the initial dry SAP was calculated using the following equation:

$$m_{abs} = \frac{m_3 - m_2 - m_1}{m_1} \quad \text{g Water /g SAP} \qquad \text{Eq. 10}$$

The same SAP was tested in five different fluids; water and four different simulated pore solutions. To simulate the expected pore fluid of a HPC with a w/c ratio between 0.2 and 0.4, a w/c ratio for the fluid used in the tea bag test was taken as 2.5, 5, and 10 as determined by Olawuyi (2016). A w/c ratio of 2.5 closely represents the ratio of cement to all the other constitutes used in the final mix proportions of the concrete mixes tested in this study. The sample preparation for the three pore fluids mentioned above are summarised in Table 3.4 and illustrated in Figure 3.18. The samples were prepared by adding 750 g of water to the corresponding amount of cement to produce the given w/c ratio. The mixture was stirred continuously while adding the water and then stirred for another 30 seconds. The mix was essentially a paste, but because of the high w/c ratio it represents a very diluted slurry. As observed in the flocculation test carried out in Section 3.2.2, the cement particles tend to settle very quickly in the presence of excessive amounts of water. For this reason, 1 % bwoc of superplasticiser was added to the simulated pore fluid to keep the cement particles in suspension. The appropriate amount of superplasticiser was added to each sample with a syringe, continuing stirring for another 30 seconds.

Table 3.4: Simulated pore fluid

Simulated pore fluid	w/c ratio 10	w/c ratio 5	w/c ratio 2.5
Water (g)	750	750	750
Cement (g)	75	150	300
Superplasticiser (g)	0.75	1.5	3

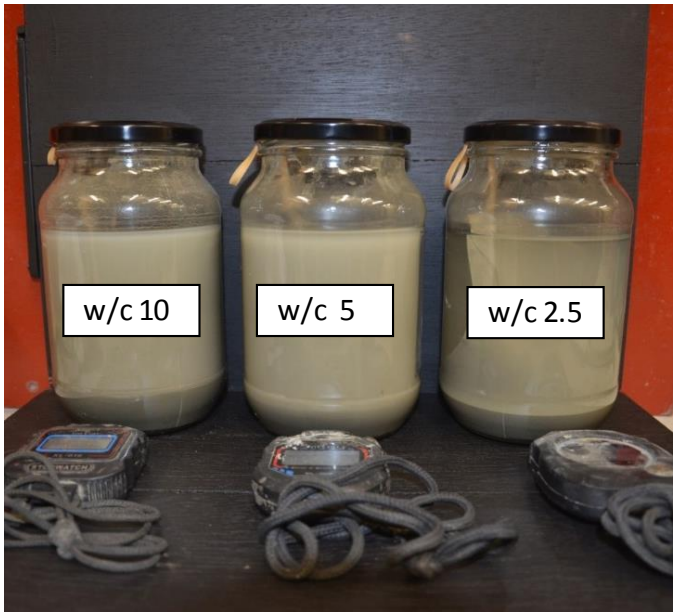

Figure 3.18: Tea-bag test samples in three simulated pore fluids with w/c ratio 10, 5 and 2.5

The SAP absorption was tested in this fluid to observe the reduced absorption capacity of the polymers in the presence of a fluid with a high concentration of ions, as well as in the presence of the physical cement particles. The physical presence of cement particles in the tea-bag test are worthwhile to consider as it represents the competition for water between the SAP particles and the cement particles that is present in a cement paste or concrete mix itself. The reduction in absorption capacity may also be increased by the cement particles, which block the ingress of water in to the SAP particle. It should be noted that the results from this test is merely a representation of the absorption kinetics of SAP in pastes and concrete and is further affected by other factors that are only present in the actual paste or concrete mix.

The cementitious material used in the pastes and concrete mixes of this study included a portion of silica fume, which has different chemical and physical properties to that of cement, which too influence the absorption capacity of the SAP. To observe the effect of silica fume on the absorption capacity of SAP, the fourth simulated pore solution was extracted from the paste mixes used in this study for autogenous shrinkage measurements.

The paste with the lowest w/b ratio of 0.22 was chosen as the most severe case to observe the effect if silica fume. The paste was mixed with the saturation point superplasticiser dosage and 12 % silica fume replacement and as determined in Section 3.3.1 and Appendix C.1 respectively. The paste was mixed in a cake mixer following the same procedure as described in Section 3.2.1 for the compatibility tests. The paste was then placed in a porous fabric bag and hung from a 1 m height. The fluid that dripped from the bag was collected and used in the tea bag test. This approach was followed to get a closer representation of the absorption kinetics of the SAP submerged in the fluid found in the pores of the actual pastes that were tested for autogenous shrinkage in this study. The results of the absorption capacity of the polymer in water and the four different simulated pore solutions are shown in Figure 3.19.

The results of the tea bag tests in pore solution show an unexpected trend. While the graph in Figure 3.19 shows that the absorption capacity is dramatically reduced in all the pore fluids compared to that of water, the absorption capacity decreases with increasing w/c ratio for the three slurries. A decrease in absorption capacity with a decrease in w/c ratio was expected due to the higher cement content and subsequently, higher ion concentration. However, SAP submerged in the slurry with a w/c ratio of 2.5 showed more than double the absorption in w/c ratio of 10. Furthermore, the absorption of SAP in a simulated pore solution containing silica fume is even further reduced. This suggests that the presence of silica fume has a significant effect on the absorption kinetics of SAP. The absorption kinetics of SAP is very intricate and more tests are needed to identify valuable trends.

The rate of absorption of SAP in the simulated pore fluids show a similar trend. A maximum absorption capacity is reached around 30 minutes, where after it starts to stabilise. This trend was not seen for the absorption of water so it must be due to the ions that are present in the pore solution from the cementitious materials. This could perhaps be explained by the ion concentration gradient between the inside of the SAP particle and the surrounding pore solution. At first, water is absorbed by the SAP particle to decrease the ion concentration inside the particle. As the cementitious material react with the water, the ion concentration of the pore fluid surrounding the SAP also increases and then exceeds that of the inside of the SAP particle. Now the concentration gradient is reversed and water moves from the SAP particle back to the surrounding fluid until a state of homeostasis is achieved between the inside of the SAP particle and the surrounding fluid.

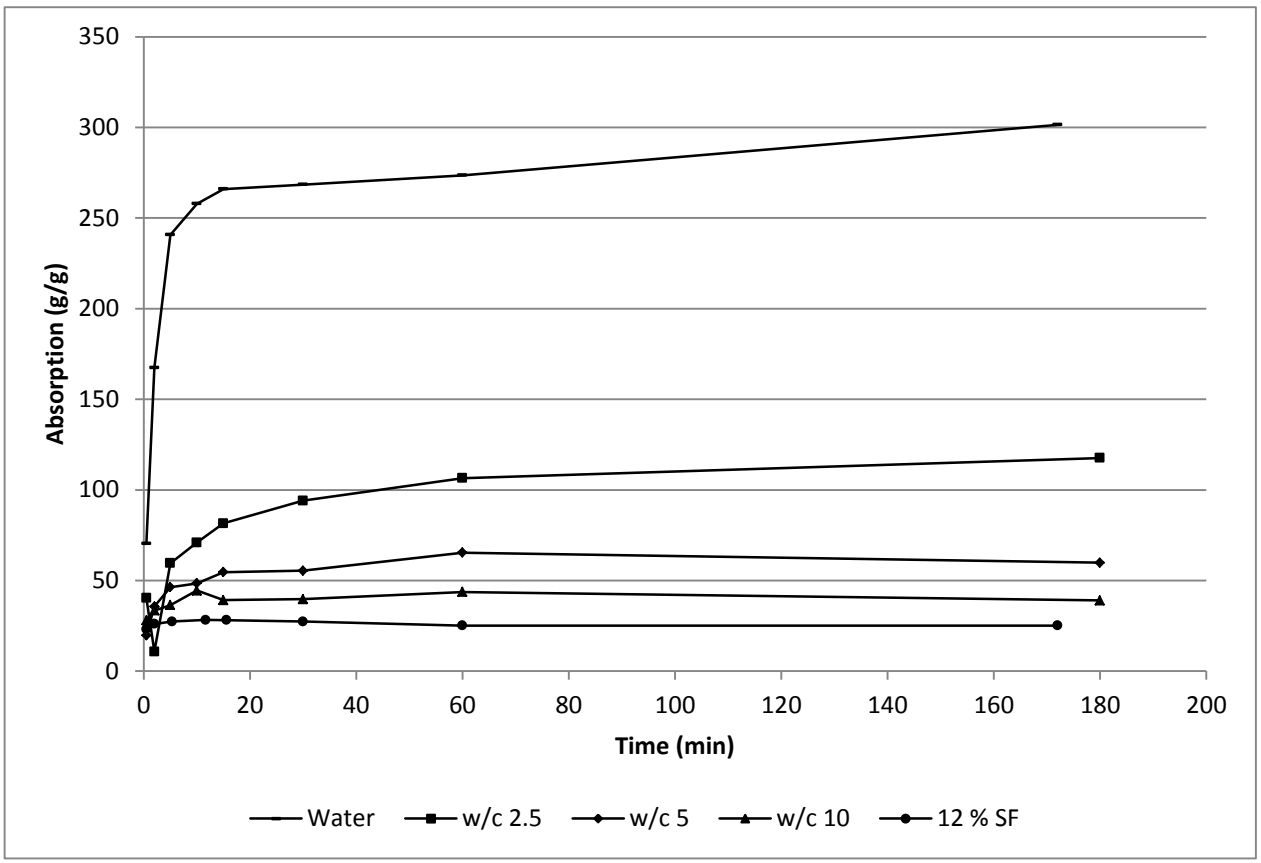

Figure 3.19: Absorption capacity of SAP in water and four different simulated pore solutions

Considering the SAP absorption in a pore fluid containing silica fume, shown in Figure 3.20, a more pronounced desorption of water is observed just after 20 minutes. This can perhaps be explained by the ion concentration of the surrounding fluid being even higher than those containing only cement, that water is released from the SAP particle to reach homeostasis. It should also be noted that the time from the addition of water to the cementitious material for this pore fluid was about 30 minutes, whereas the time of addition of water to the three slurries before the tea-bag containing the SAP was submerged was about 3 minutes. The fluid from the paste containing the silica fume may well have a higher ion concentration at the start time of the tea-bag test.

This could also explain why absorption in this simulated pore solution is the lowest. Furthermore, it may contribute to the deviance in results between the standard tea-bag test method and the real-life situation where mixing time and transportation is not factored into the starting time of the standard tea-bag test.

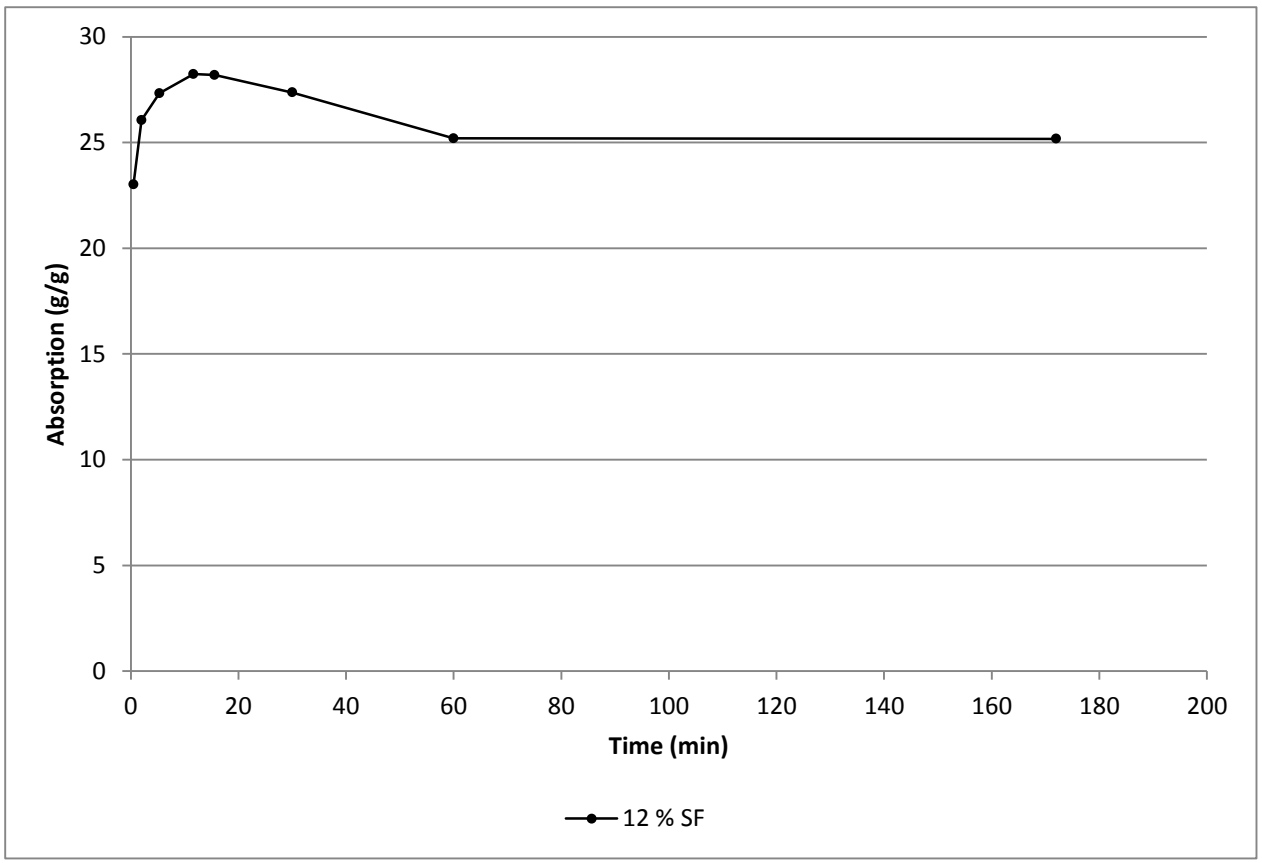

Figure 3.20: Absorption capacity of a paste containing silica fume

3.6 Mix Proportions

After selecting the materials that would be used in the concrete and pastes that were tested in this study, the amount of each was set by volumetric proportion. Figure 3.21 shows a schematic representation of the reference mixes with w/b ratio of 0.22 and 0.27. Both mixes have a 20 % stone content, leaving 80 % mortar. The paste was further reduced to 70 % of the mortar, leaving a sand with 30 % of the mortar by volume. To distinguish the two reference mixes by the two w/b ratio ratios, the amount of water was altered to achieve the desired w/b ratio with a 12 % silica fume replacement.

These concrete mixes were used for the measurement of plastic shrinkage, while the pastes were used for the measurement of autogenous shrinkage. The proportioning of the pastes was the corresponding paste of the concrete, reducing to the amount of water needed to produce the desired w/b ratio with a 12 % silica fume replacement. The mass of each constitute for the reference pastes and concretes WB022 WB027 each are presented in Table 3.5.

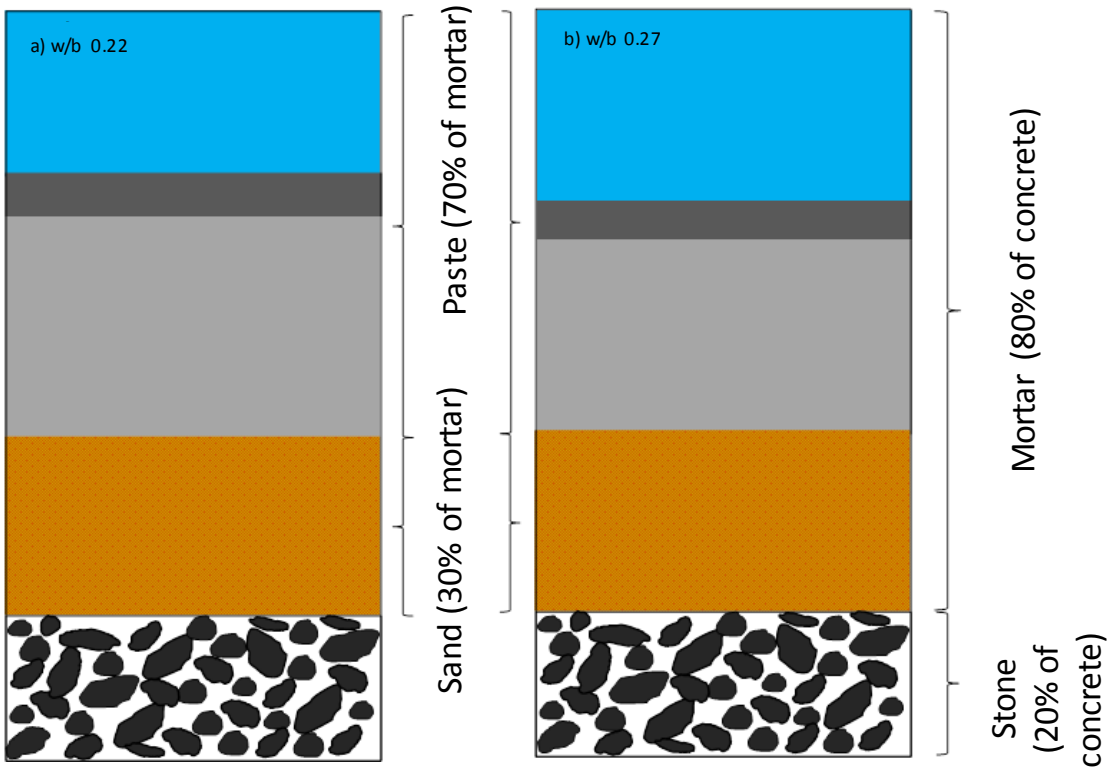

Figure 3.21: Volumetric proportion of the two reference mixes used in this experiment

The amount of superplasticiser used was taken as the optimum saturation point dosage as determined in Section 3.3 for the corresponding w/c ratio. The superplasticiser used contains about 56 % water. To prevent this alteration of the w/b ratio, the amount of additional water provided by the superplasticiser was reduced from the mix water. Furthermore, the concrete mix variations included the use of 6 and 9 mm for each w/b ratio and is indicated in the name as shown in the table below.

Table 3.5: Reference pastes and concrete mix designs

Mix Designs	Mass kg / m³	Mass kg / m³	Mass kg / m³	Mass kg / m³
Constitute	WC022_Ref_Paste	WC027_Ref_Paste	WC022_Ref_6/9mm	WC027_Ref_6/9mm
Water	395	445	221	249
52.5 OPC CEM II	1580	1450	884	812
Silica Fume	215	198	121	111
Malmesbury Sand	-	-	672	672
Stone (6 / 9 mm)	-	-	560	560
Superplasticiser	22	13	12	7
Additional Water	12	7	7	4
Adjusted Water	383	438	214	245

For the observation of the effect of the use of SAP and internal curing water on early-age shrinkage and compressive strength, they were added to each of the reference mixes at varying dosages. For autogenous shrinkage measurements of pastes, 0.3 and 0.6 % of SAP bwoc were tested and only 0.3 % of SAP bwoc was added to concretes for plastic shrinkage measurement. From the tea-bag test described in Section 3.5.2, the absorption capacity of the SAP type used in this experiment is about 25 g/g in the simulated pore solution of the mixes. The internal curing water added to the mix to accompany a given dosage of SAP was taken as the theoretical amount of water needed to saturate the SAP to 50, 75 and 100 %. Table 3.6 summarises the amounts of SAP and internal curing water added to the respective reference paste and concrete mixes to produce the comparative mix variations tested in this study.

Table 3.6: Varying dosages of SAP and accompanying internal curing water

Mass kg / m³		50 % ICW	75 % ICW	100 % ICW	
Paste	0.3 % SAP (4.74 kg)	59.3	88.9	118.5	WC022_Ref_Paste
	0.6 % SAP (9.48 kg)	118.5	177.8	237	
	0.3 % SAP (4.35 kg)	54.4	81.6	108.8	WC027_Ref_Paste
	0.6 % SAP (8.7 kg)	108.8	163.1	217.5	
Concrete	0.3 % SAP (2.65 kg)	33.1	49.7	66.3	WC022_Ref_6/9mm
	0.3 % SAP (2.43 kg)	30.4	45.6	60.8	WC027_Ref_6/9mm

3.7 Concluding Summary

High performance pastes and concretes cannot be designed in the conventional way. To achieve pastes and concretes with high strength together with a good workability, and retain it, calls for a combination of iterative calculated guesses. This chapter presented the preliminary work that was carried out to assist material selection and proportion the final mix based on objective results of various sensitivity tests. Two w/b ratios, 0.22 and 0.27, were prescribed and the superplasticiser was selected based on its compatibility with the locally available cement. The dosage of superplasticiser was taken as the saturation point of the respective w/b ratio using the marsh flow cone method.

The fine and coarse aggregate that was used were also chosen according to what was locally available and their size and proportion was based on an attempt to obtain a particle size distribution that is close to ideal curves that represent an optimum SCC. The dosage of SAP was also prescribed, 0.3 % for concretes and 0.3 and 0.6 % for pastes.

The internal curing water which accompanied the relative SAP dosages was determined by the tea-bag test which indicates the theoretical amount of water required to saturate the SAP. The SAP was tested in four fluid mediums and the absorption capacity of SAP was found to be 25 g/g in a simulated pore fluid. This amount of internal curing water was taken as 100 % saturation level and mixes with 50 and 75 % of this value were also considered.

The different mix variations that make up the test program based on this mix design development are presented in the next chapter.

Stellenbosch University https://scholar.sun.ac.

Chapter 4

Experimental Framework

This chapter presents the different test methods and programs that were followed for the main tests of this study to achieve the aforementioned objectives. To observe early-age shrinkage and crack-risk of high performance concrete (HPC) with superabsorbent polymers (SAP), the plastic shrinkage and plastic shrinkage cracking of concrete was measured and the autogenous shrinkage of the corresponding paste was measured. The compressive strength of both the concrete and pastes were also tested to observe the correlation of compressive strength loss with decreasing shrinkage trend. The test programs for plastic shrinkage, autogenous shrinkage and compressive strength presented here describe the mix variables that were adjusted for the sake of comparison to observe the effect of different w/b ratios, different SAP dosage, varying degrees of saturation and the effect of stone and its size on the desorption of the SAP. The equipment and test setups used to measure the two early-age shrinkages and compressive strength along with their auxiliary tests used for analysis of results are also discussed.

4.1 Plastic Shrinkage

The extent of plastic shrinkage of a concrete body can give an indication of its risk to plastic shrinkage cracking when a restrained concrete body is subject to evaporation. HPC is especially susceptible to early-age cracking. The effect of internal curing water released from SAP to the capillary pore network was observed through plastic shrinkage, plastic settlement, plastic shrinkage cracking and capillary pressure measurements. The test program and setup are further discussed as well as the ambient environmental conditions that these specimens were tested under.

4.1.1 Test Program

The optimum amount of internal curing water to add to a given dosage of SAP is uncertain. In most cases, the theoretical amount of water needed to saturate a SAP particle is overestimated and reduces the strength significantly. For this reason, SAP was tested in HPC at saturation levels of 50 and 75% to observe if lower saturated SAP particles can provide sufficient mitigation of shrinkage while maintaining an acceptable high compressive strength.

Furthermore, 6 and 9 mm stone were tested in mixes with the same proportion to observe if the relative size of the coarse aggregate has an effect on the desorption of SAP. The reference mixes were presented in Table 3.5. Table 4.1 summarises the variations along with its descriptive name. The amount of internal curing water for the different saturation levels were shown in Table 3.6.

Table 4.1: Plastic Shrinkage Test Program

W/B RATIO 0.22	Ref	75 % SAT	50 % SAT
6 mm stone	WB022_Ref_6mm	WB022_0.3SAP_75SAT_6mm	WB022_0.3SAP_50SAT_6mm
9 mm stone	WB022_Ref_9mm	WB022_0.3SAP_75SAT_9mm	WB022_0.3SAP_50SAT_9mm
W/B RATIO 0.27	**Ref**	**75 % SAT**	**50 % SAT**
6 mm stone	WB027_Ref_6mm	WB027_0.3SAP_75SAT_6mm	WB027_0.3SAP_50SAT_6mm
9 mm stone	WB027_Ref_9mm	WB027_0.3SAP_75SAT_9mm	WB027_0.3SAP_50SAT_9mm

4.1.2 Test Setup

The test setup used in this study was adopted from the experimental work of Slowik et al. (2008) and Kronlöf et al. (1995). The moulds that were adopted from Slowik's study, are shown in Figure 4.1 to Figure 4.4. All moulds are square with the dimensions of 30 x 30 x 10 cm (length x width x height). The moulds are made of PVC to ensure that there is no additional loss of water due to absorption of pore water into the moulds. All of the moulds were lined with a thin, even layer of mould oil to create a frictionless surface and to facilitate in the stripping of these moulds.

4.1.2.1 Plastic Shrinkage

Plastic shrinkage and settlement were measured in the same mould. The moulds used to measure plastic shrinkage and settlement have markers and mounts to which these markers are fixed to facilitate the use of linear variable displacement transducers (LVDTs) that track the gradual displacement of the concrete body in both the vertical and horizontal direction as it shrinks. The fixation of these LVDTs are shown in Figure 4.1 and Figure 4.2.

Horizontal displacement, plastic shrinkage, is measured with the use of two markers that are embedded in the concrete on either side of the concrete body as shown in Figure 4.1. These markers are held in place by fixation pins during compaction and transporting of the mould.

Spring tip LVDTs are used for the measurement of plastic shrinkage and rest against the outside end of the shrinkage markers with the outside casing of the LVDT being firmly held in place by a screw on the top to ensure that just the spring tip moves with the markers as the concrete shrinks. This is more clearly shown in Figure 4.2. The fixing pins are removed once the mould is securely placed in the climate chamber, just before testing starts, to allow free linear movement of the LVDT. It is assumed that the same horizontal movement would be observed in both horizontal directions of the mould because of the quadratic base of the concrete body (Slowik et al., 2008).

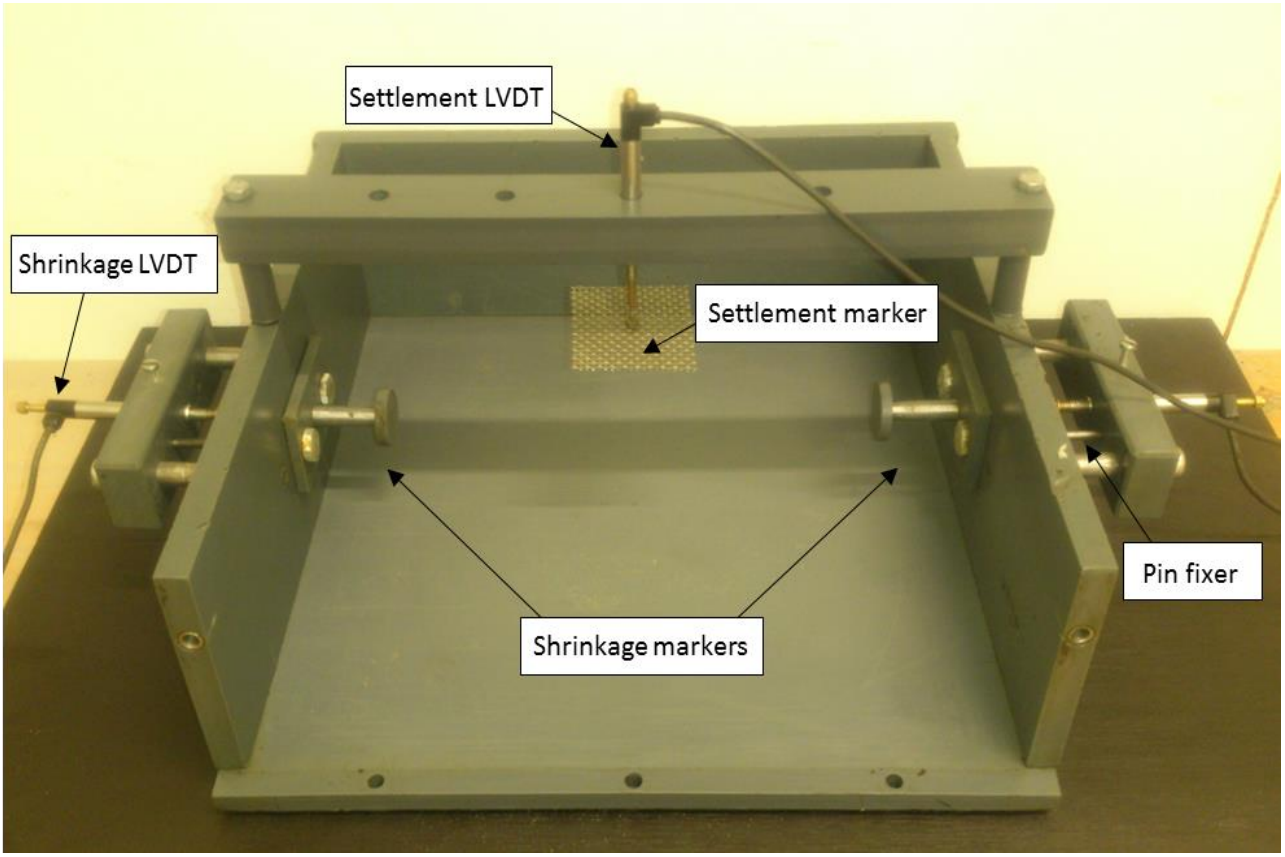

Figure 4.1: Plastic Shrinkage mould with plastic shrinkage and settlement markers and LVDT's

The vertical displacement, plastic settlement, was measured with one screw-tip LVDT placed above the centre of the concrete body with a wire lattice resting on the surface of the concrete body as shown in Figure 4.3. The LVDT is held firmly in place with a screw to ensure that the LVDT casing does not slip, and only the screw tip moves with the wire lattice as the concrete settles. The wire lattice settlement marker prevents flotation of the marker on the concrete surface (Slowik et al., 2008). Since bleeding is not a concern in HPC, an even and secure embedment of the lattice is imperative so that there is uniform movement of the marker with the concrete surface. Without proper embedment from the start of the test, as illustrated in Figure 4.3b resulted in inaccurate measurements.

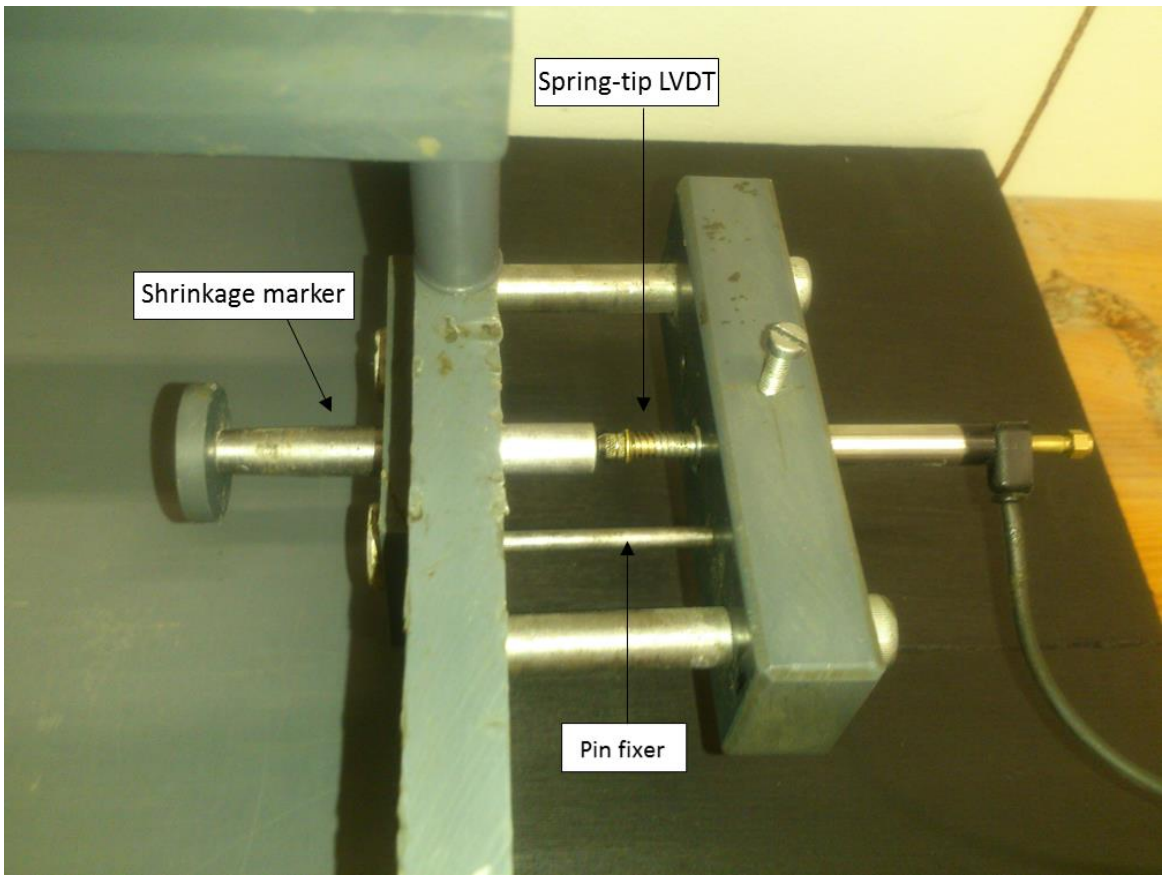

Figure 4.2: Plastic shrinkage LVDT fixation

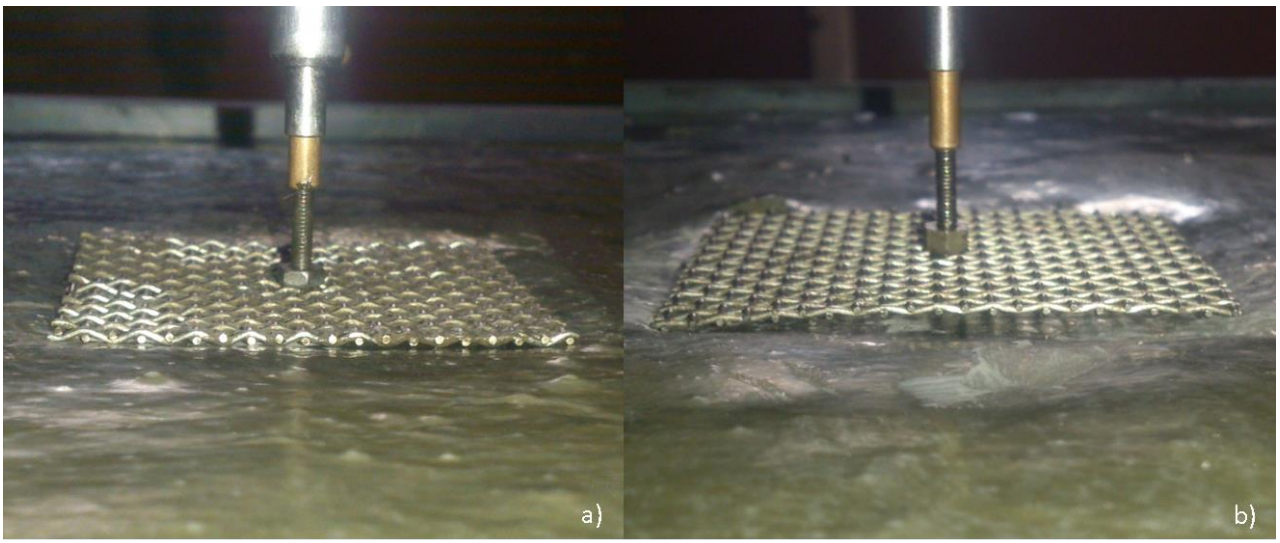

Figure 4.3: a) Proper embedment of settlement marker b) improper embedment

It should also be noted, that in the measurement of vertical displacement, the concrete body may shrink or swell in this direction as nothing would restrain it from swelling, but this is not the case for horizontal displacement.

4.1.2.2 Capillary Pressure

Capillary pressure was measured in a different set of moulds to plastic shrinkage and settlement. The moulds were made of the same material and dimensions. The capillary pressure in the pore system of the concrete was measured with an electric pressure sensor. A metal tube filled with distilled water connects the concrete pore system to the pressure sensor. The pressure sensor is enclosed by a protective casing to prevent damage during placement and transportation of the mould. The metal tube is placed through the centre of one of the faces of the mould and extends 150 mm into the mould so that the tip of the tube, where measurements take place, is central in the concrete body. This is the position in the concrete body that is most unaffected by the faces of the mould and is depicted in Figure 4.4.

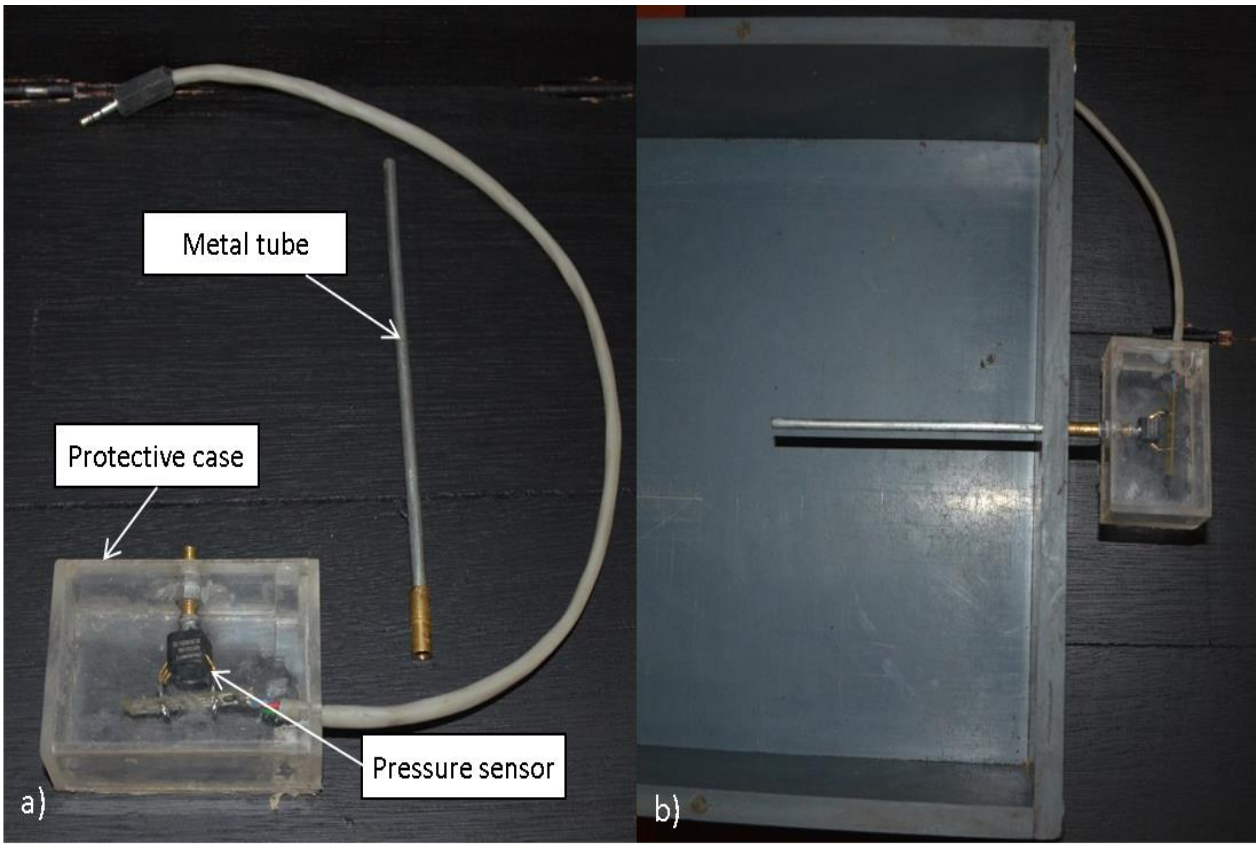

Figure 4.4: Capillary pressure mould and sensor set up

It should be noted that capillary pressure measurement is a local measurement and is merely an indication of what is happening in the rest of the pore system of the concrete body. Capillary pressure was measured in two moulds for comparison.

4.1.2.3 Plastic Shrinkage Cracking

For the observation and measurement of crack growth, the mould shown in Figure 4.5 was used. This mould is designed to provide restraint to the concrete body, which induces a crack across the concrete surface. The restraint layout is specified in ASTM C 1579 (2006) and the mould has dimensions of 600 x 200 x 100 mm (length x width x height) with three triangles spaced at the bottom of the mould. Above the two smaller triangles are steel rods, which provide additional horizontal restraint with the centre triangle, creating a weak spot to induce a single crack on the surface of the concrete body. The dimensions of the restraints are shown in Figure 4.6.

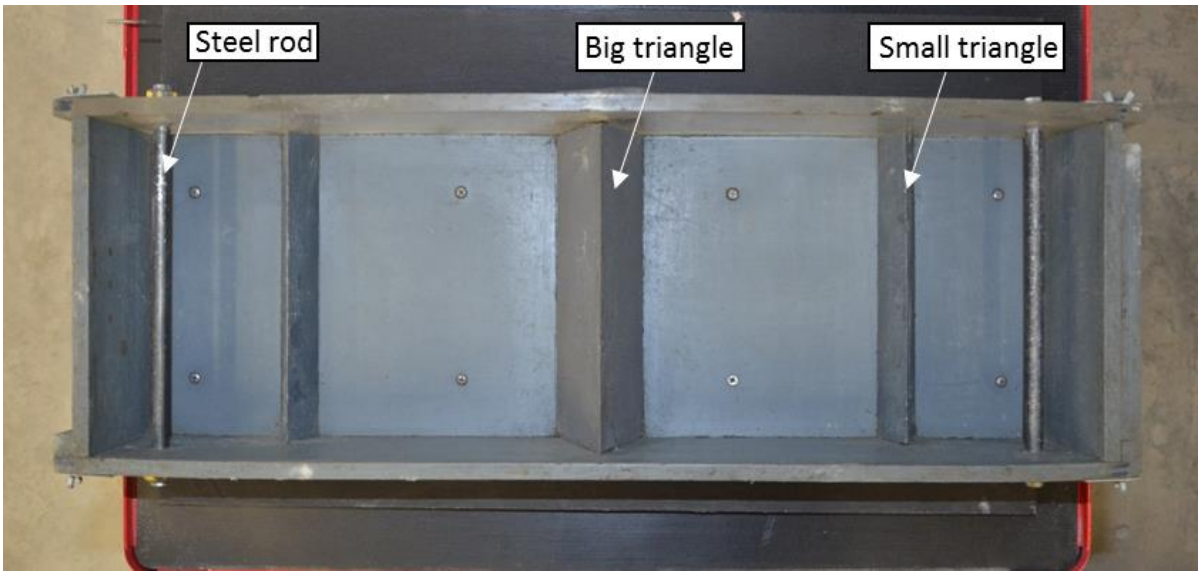

Figure 4.5: Plastic shrinkage crack mould

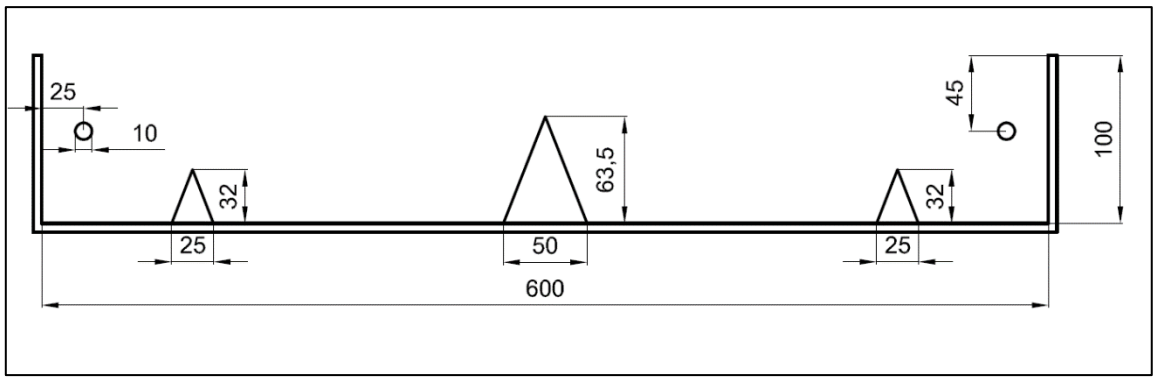

Figure 4.6: Section through plastic shrinkage cracking mould

The crack starts as a hairline crack and as the concrete dries, the crack propagates and widens. Photographs are taken with a high-resolution camera at 20-minute intervals and the crack growth can be measured from the photographs.

4.1.2.4 Climate Chamber

The rate of evaporation of pore water has a direct effect on the rate of plastic shrinkage and plastic shrinkage cracking. To control the rate of evaporation that each specimen experiences, the moulds described in the previous sections were placed inside a climate chamber that regulates defined environmental conditions for testing. Figure 4.7 shows the compartment layout of the climate chamber designed by Combrinck (2011) at the University for Stellenbosch to simulate ideal conditions with a high evaporation rates.

This is achieved by a combination of a low relative humidity, high wind speed and high temperature and is specifically ideal for investigating plastic shrinkage and plastic shrinkage cracking. The climate chamber can generate a temperature of up to 50 °C, a uniform wind speeds up to 70 km/h and a relative humidity as low as 10 %.

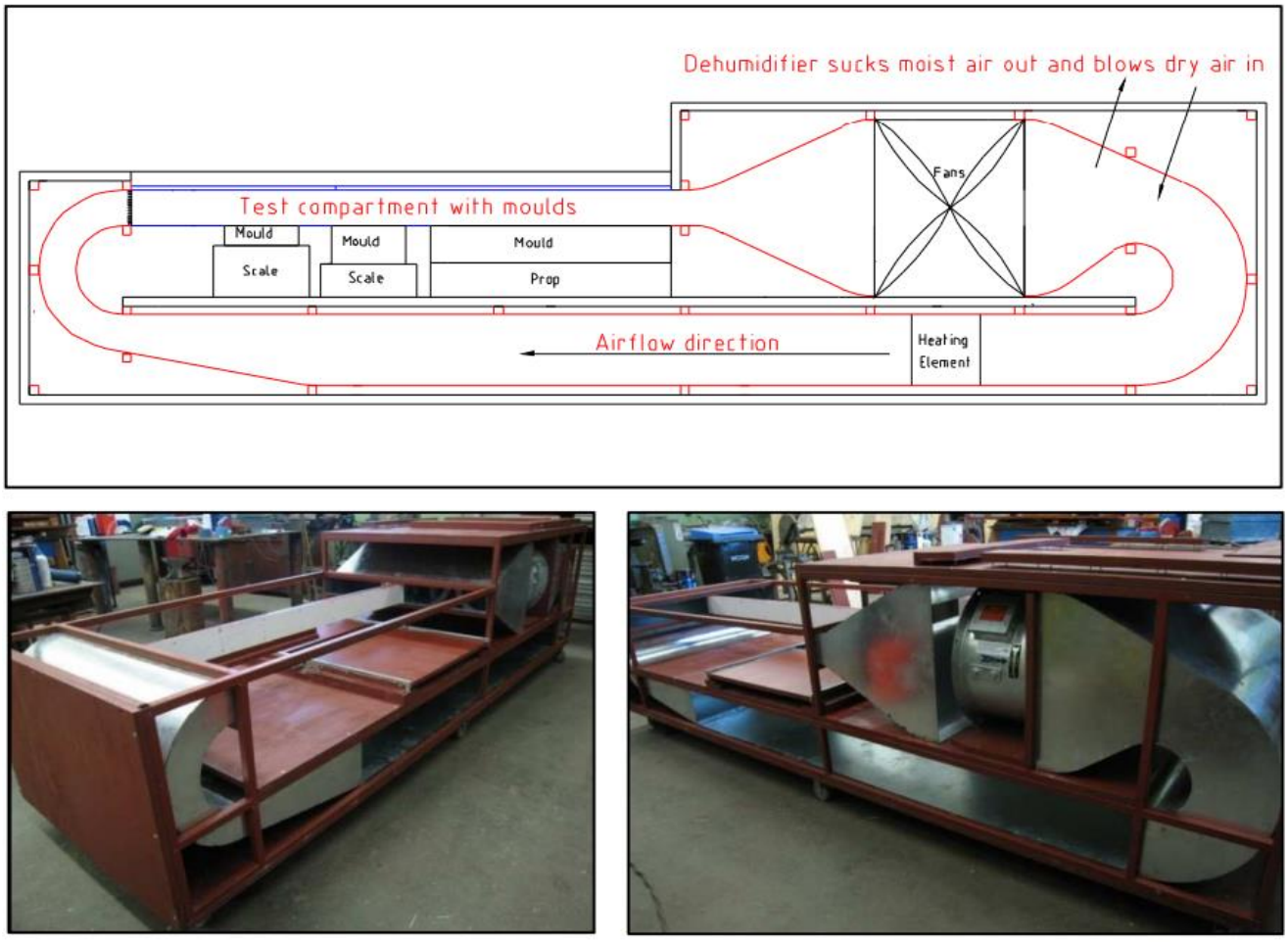

Figure 4.7: Climate chamber compartment layout (Combrinck, 2011)

As mentioned in Section 2.2.1.3, plastic shrinkage is likely to occur in concrete that is exposed to environmental conditions that result in an evaporation rate higher than 1 kg/m^2/h. These conditions are commonly experienced in Cape Town and other parts of South Africa. Table 4.2 presents the air temperature, relative humidity and wind speed that were simulated in the climate chamber to produce an evaporation rate greater than 1 kg/m^2/h.

NSC typically has a temperature of 22°C right after mixing and produces an evaporation rate of 1.03 kg/m^2/h The HPC used in this experiment had an average concrete temperature of 25°C, resulting in an evaporation rate of 1.3 kg/m^2/h.

Table 4.2: Climate chamber environmental conditions

Climate readings					Evaporation Rate (kg/m2/h)	
Tc (°C)	Ta (°C)	r (%/100)	V (km/h)	Frequency (Hz)	Nomograph	Eq. 8
22	40	0.1	23.38	18		1.03
25	40	0.1	23.38	18		1.3

4.2 Autogenous Shrinkage

There are many concurrent mechanisms during the drying and setting of concrete that dictate the rate of early-age shrinkage. To observe early-age shrinkage fundamentally due to hydration, autogenous shrinkage of cement pastes were measured under isothermal conditions. The test program which follows, summaries the cement paste variations that were tested to observe the effect of varying amounts of SAP and internal curing water on autogenous shrinkage. The test setup used to measure autogenous shrinkage is also discussed here along with the procedure used to determine time zero.

4.2.1 Test Program

Besides the uncertainty of the amount of internal curing water needed to accompany SAP in HPC, the amount of SAP itself also lends itself to empirical observation. The reference mixes for pastes with w/b ratio 0.22 and 0.27 were presented in Table 3.5. Table 4.3 summarises the variations along with its descriptive name. The amount of SAP and internal curing water for the different SAP dosages and saturation levels were shown in Table 3.6.

Table 4.3: Autogenous Shrinkage Test Program

W/B RATIO 0.22	Ref	75 % SAT	50 % SAT
0.3 % SAP	WB022_Ref_Paste	WB022_0.3SAP_75SAT_Paste	WB022_03SAP_50SAT_Paste
0.5 % SAP		WB022_0.5SAP_75SAT_Paste	WB022_05SAP_50SAT_Paste
W/B RATIO 0.27	**Ref**	**75 % SAT**	**50 % SAT**
0.3 % SAP	WB027_Ref_Paste	WB027_0.3SAP_75SAT_Paste	WB027_03SAP_50SAT_Paste
0.5 % SAP		WB027_0.5SAP_75SAT_Paste	WB027_05SAP_50SAT_Paste

4.2.2 Test Setup

In recent years, there have been a number of test methods proposed and developed for the measurement of autogenous shrinkage. These test methods can measure the shrinkage either volumetrically, or linearly. Autogenous shrinkage was measured linearly in this experiment following ASTM C1698 – 09, according to which the setup was designed. This method was chosen as it is becoming the standard test method for autogenous shrinkage. The method allows the bulk strain of a cement paste or mortar to be measured in an enclosed vessel in isothermal conditions. For the analysis of autogenous shrinkage, time-zero was determined using the Vicat apparatus to determine the initial and final setting times of the pastes. This section describes the equipment that was used and the test methods that were followed.

4.2.2.1 Autogenous Shrinkage

The uniqueness of the test method used to measure autogenous shrinkage in this study is due to the use of corrugated tube as a mould. The tubes are made of low-density polyethylene (LDPE) plastic with circumferential ridges along the length of the tube as shown in Figure 4.8a. The LDPE exerts low friction and the ridges allow the mould to shrink or expand with the paste as it shrinks or expands over time, without providing much restraint to the volume change of the paste. The tubes have an outside diameter of 22 mm and a length of 400 mm. The diameter is limited to prevent the effects of differential thermal strain caused by heat of hydration (ASTM International, 2009), which is especially noteworthy in pastes with a low w/b ratio. The casting procedure is depicted in Figure 4.8b. The procedure needs to be carried out as quickly as possible, as filling becomes harder as the paste hydrates.

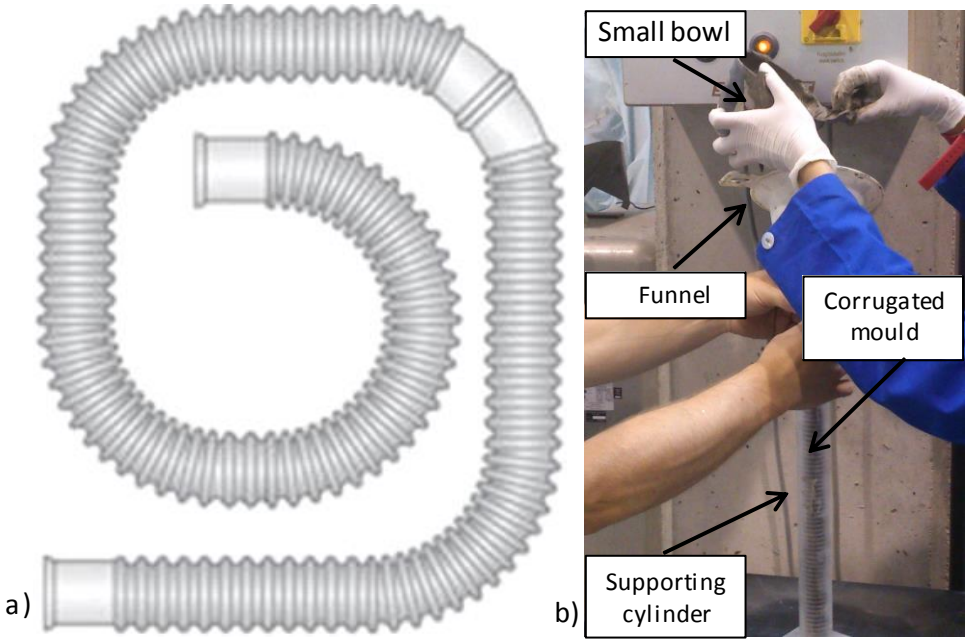

Figure 4.8: a) LDPE corrugated tube and b) casting procedure of corrugated mould (picture taken at the Technical University of Dresden)

To hold the tubes in an upright position during casting, it was placed in a supporting measuring cylinder with a diameter just big enough for the corrugated tube to fit in. With the bottom end of the mould closed with an end plug, the tube was filled by passing the paste through a funnel, from a small bowl, without applying any compression to the corrugated tube. The mixture was passed through steadily, tapping the sides or vibrating on a vibrating table for short intervals as required. The tubes were filled with just enough space left for the top end plug to fit, and then the sides were wiped clean for the end plug to fit tightly and securely. To prevent the paste from getting stuck between the outside ridges of the tube, cling wrap was wrapped around the tube before placing it inside the supporting cylinder. This is vital as any material stuck between the ridges could hinder movement of the tube during testing.

Once the moulds were filled, they were placed in a dilatometer bench made of three stainless steel rods, fixed to two stainless steel plates at either end as seen in Figure 4.9a. The dilatometer bench is placed at a slight angle to ensure that the bottom of the corrugated tube remains in contact with the bottom end of the bench. This ensures that all the displacement is measured at the top. The displacement is measured by means of a dial gauge with a spring tip as shown in Figure 4.9b and c. The dial gauge was supplied by Sylvac and has a range of 20mm and resolution of 0.001mm.

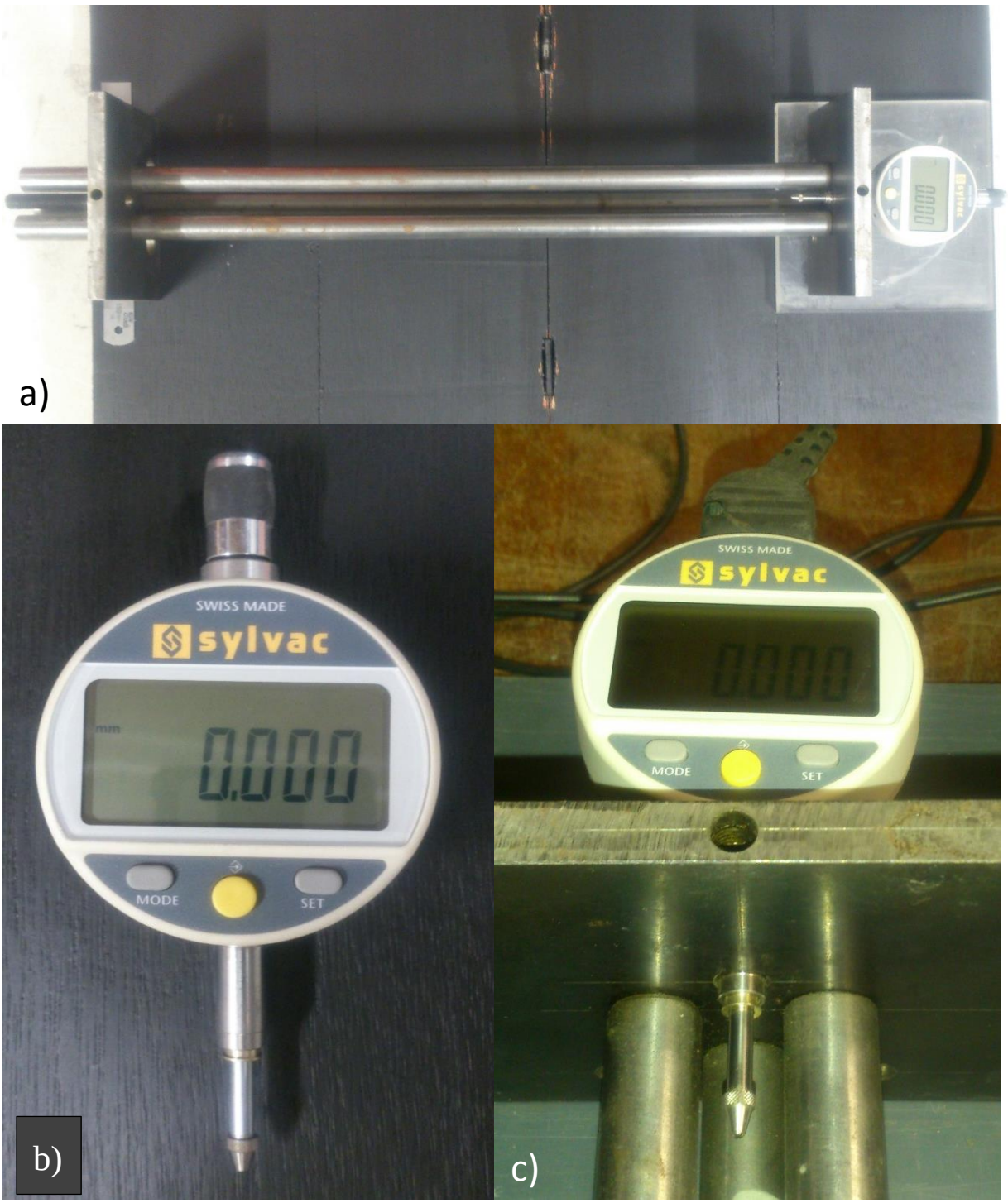

Figure 4.9: Dilatometer bench made of three stainless steel bars, b) dial gauge, c) dial gauge mounted at top of dilatometer bench

The placement of the corrugated tube in the dilatometer bench is shown in Figure 4.10a, c and d. Figure 4.10b shows a close-up of the end plug used to seal the moulds. After filling the moulds, they are transported horizontally with enough support to prevent the tubes from sagging. The data acquisition system was set up before the mixing so that measurements can be taken immediately.

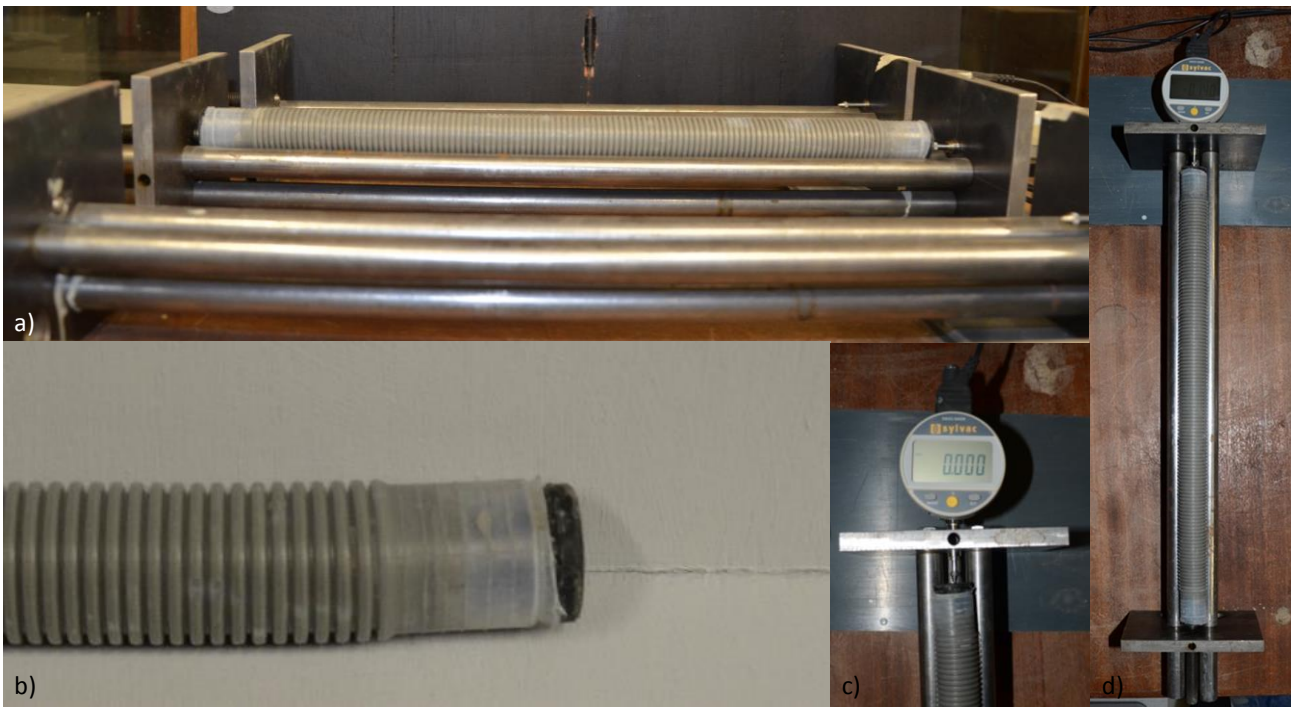

Figure 4.10: Longitudinal view of corrugated mould in dilatometer bench, b) casted corrugated tube with end plug, c) spring tip of dial gauge resting on end plug and d) top view of corrugated tube in dilatometer bench

Four samples for each mix were tested for a period of 3 days, which is the time period over which most of the autogenous shrinkage occurs. The test was conducted in a climate controlled room with a temperature of 24°C, relative humidity of 10% and no wind.

4.2.2.2 Setting Time

To determine the start of autogenous shrinkage readings, t_0, the setting time was determined by means of a penetration test. The initial and final setting time of the pastes was measured using the Vicat apparatus shown in Figure 4.11. The test was carried out in accordance with EN 196-3: 2005. The procedure involves casting a paste into a truncated cone shaped mould as shown in Figure 4.11a, compacting it by hand and then covering it with a PVC plate to prevent evaporation and carbonation. For the initial setting time reading, a needle with a diameter of 1.13 ± 0.05 mm was held just above the surface of the specimen and released, every 20 minutes, two hours after casting, until the needle penetrates the specimen to a depth of 6 ±3 mm from the bottom.

When initial setting time was reached, the specimen was turned around with the larger diameter facing the final setting time needle. The final setting time needle is shown in Figure 4.11b. This needle was dropped on to the specimen, after being brought in to contact with the surface. Final setting time is reach when the outer rim no longer leaves an impression on the concrete surface.

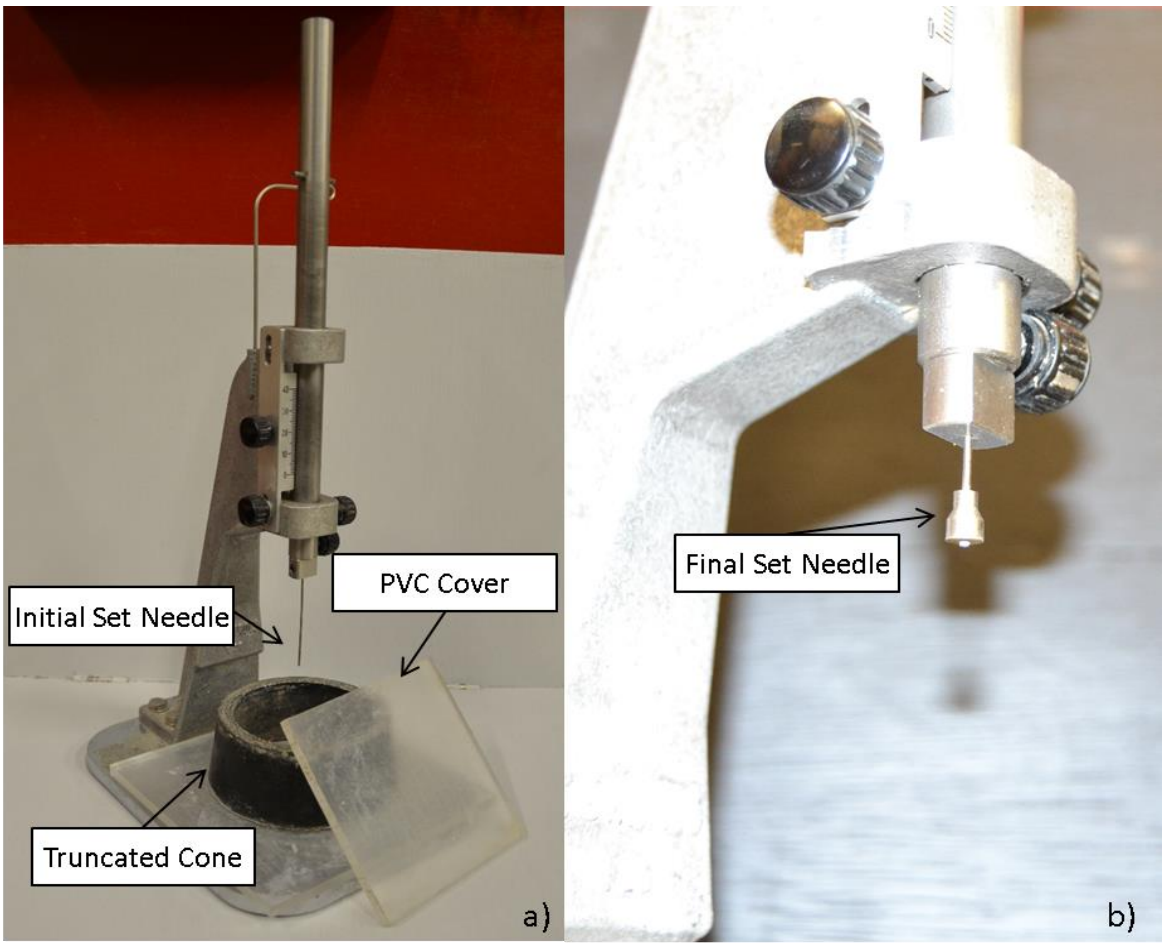

Figure 4.11: Vicat Apparatus a) showing initial set needle with truncated cone mould and PVC cover b) showing final set needle

These readings were also taken at 20 minute intervals, about one hour after initial set. The starting time of both initial and final setting time was taken from the time that water was added to the dry materials.

The paste used in this test was from the same batch of paste used in the autogenous shrinkage tests and the moulds were placed in the same environment to ensure that the setting time is comparable with the autogenous shrinkage measurements. However, it should be noted that this test is still only a representation of the time period over which the pastes reach initial and final set in the autogenous shrinkage moulds.

The setting time was also measured for the concrete mixes used in plastic shrinkage measurements. To obtain the corresponding mortar used in the setting time test, the concrete was sieved through a 4.75 mm sieve held above a bowl, placed on a vibrating table. The mortar that was collected in the bowl was then used to fill the truncated cone and the rest of the procedure follows as described in the previous paragraph.

4.3 Compressive Strength

Each concrete mix tested for plastic shrinkage and each paste mix tested for autogenous shrinkage was also tested for its compressive strength. The concrete cubes had dimensions of 100 x 100 x 100 mm and were tested in accordance with SANS 5863. The mortar cubes had dimensions of 50 x 50 x 50 mm and were tested in accordance with SABS 834. Both the concrete and mortar cubes were cured in a water bath with a temperature of 22°C. The cubes were crushed in a saturated-surface dry condition at 3, 7 and 28 days after casting. Compressive strength of HPC beyond 28 days was seen as irrelevant as the majority of strength of HPC should be reached early to optimise on construction time for the specialised structures that use HPC. The dimensions and weight of each cube was also recorded to give an indication of the density of the cubes. Strength, dimension and weight readings were taken as the average of three cubes at the three specified ages. Where the difference in readings exceeded 15 %, an additional cube was tested to replace the outlier.

The slump flow of the concretes and pastes were also measured immediately after mixing. The slump flow was measured in accordance with SANS 5862-2 and the stiffer mixes, with no flow was measured in accordance with SANS 5862-1. The apparatus used for these tests are shown in Figure 4.12.

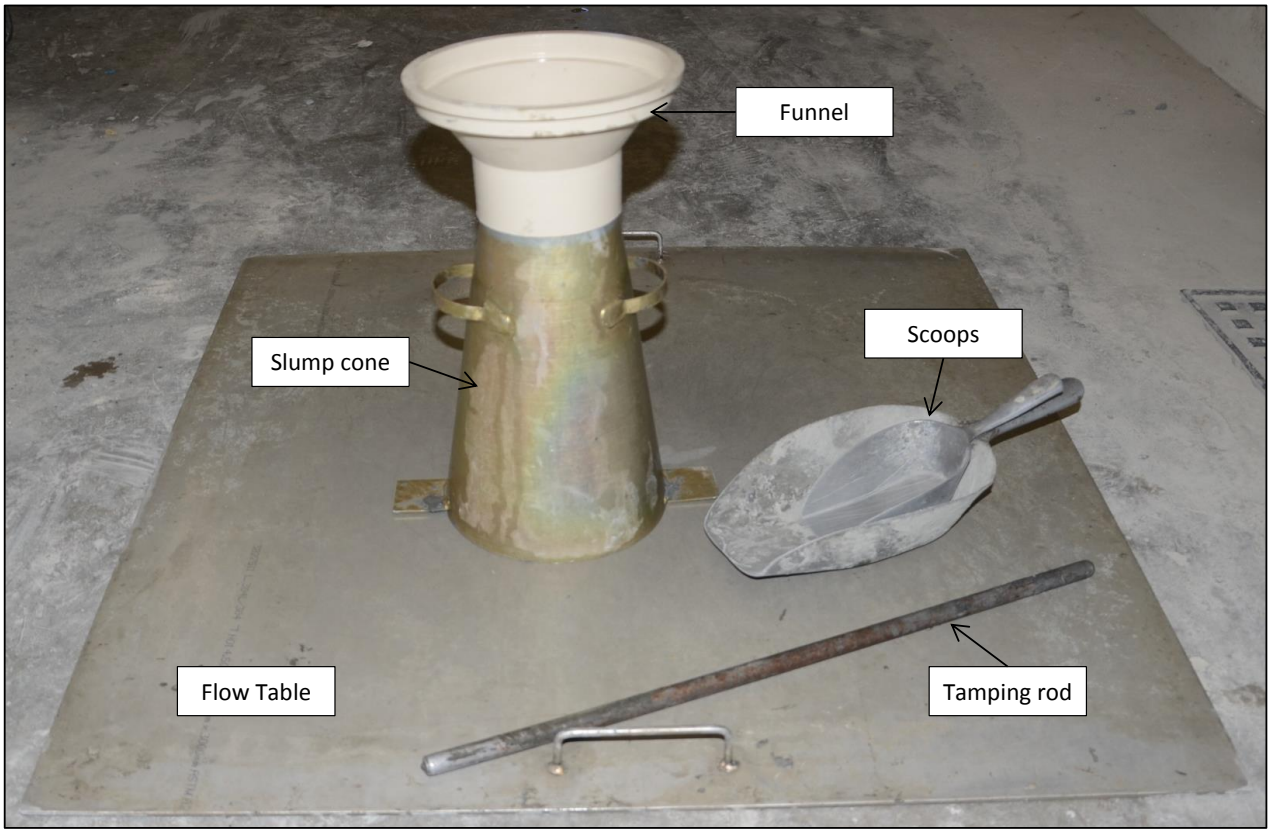

Figure 4.12: Slump flow test

The flow of the mortar mixes were also observed, using the mini-slump flow cone with an outer diameter of 95 mm, inner diameter of 65 mm and a height of 50 mm as seen in Figure 4.13. The flow of the concretes and pastes were also used to give an indication of the repeatability of different batches of the same mix design. If the flow and workability of a particular mix differed from batch to batch, the mix was redone until the flow and workability between batches were comparable.

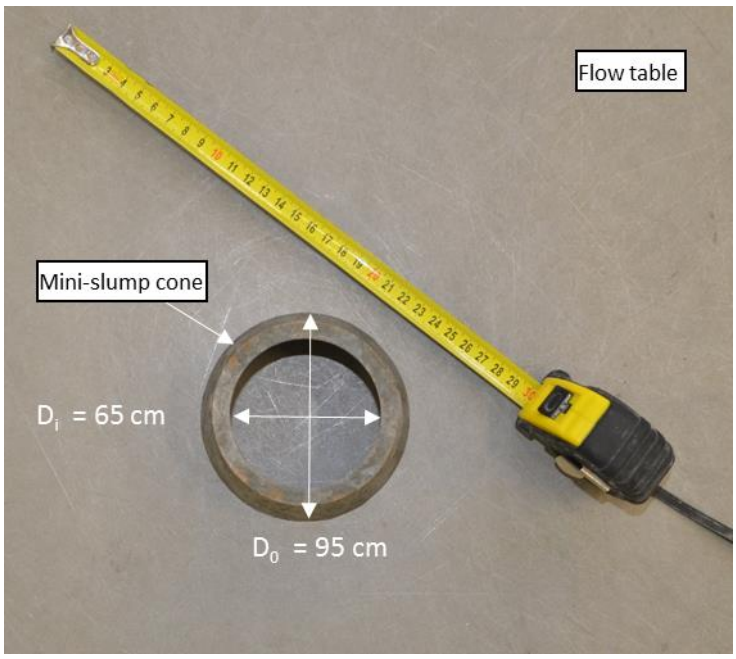

Figure 4.13: Mini-slump flow test

4.4 Concluding Summary

The moulds and test setups used to measure autogenous shrinkage and plastic shrinkage were presented in this chapter. The apparatus and equipment were depicted and a brief description of each test was given along with the references from which they were adapted. Additionally, the test program of the paste and concrete mixes summarising the mix variations were also presented. The next chapter looks at the results obtained from these tests for the respective mixes.

Stellenbosch University https://scholar.sun.ac.

Chapter 5

Results and Discussions

In this chapter, the results of the tests described in the preceding chapter are presented and discussed. The results of each test; autogenous shrinkage, plastic shrinkage, compressive strength and plastic shrinkage cracking, are presented and discussed separately to identify the impending trends that they each portray due to changes in the amount of internal curing water that accompany a given amount of SAP. Later the trends of pastes are compared with that of the concrete to observe the effect of the presence of fine and coarse aggregate on shrinkage and strength development. The discussions in this chapter relate to the objectives for this study as set out in Chapter 1 and lead to further conclusions and recommendations.

5.1 Autogenous Shrinkage

The two paste mixes with w/b ratio of 0.22 and 0.27 tested for autogenous shrinkage are presented in Table 3.5. The reference paste mixes, namely WB022_Ref_Paste and WB027_Ref_Paste, contain only cement, silica fume, water and superplasticiser. 0.3 and 0.5 % SAP by weight of cement (bwoc) were added to the reference mixes together with internal curing water at the theoretical saturation levels of 50 and 75 %. The naming of the respective mixes is summarised in Table 4.1. By definition, autogenous shrinkage is the bulk volume change experienced by a concrete or paste due to self-desiccation that takes place in the hardened skeleton of a paste. Identifying the onset of this hardened skeleton is the first aspect to consider.

5.1.1 Defining Time Zero

Autogenous shrinkage is only considered once a paste or concrete has developed a hardened skeleton in the pore structure. This point is referred to as time zero. Although autogenous shrinkage tests were started about 30 minutes after the addition of water, $t_{w\ add,}$ autogenous shrinkage is only considered at a specified time after the commencement of the test. There is much debate around when the hardened skeleton in a paste is formed. Most researches agree that time zero for autogenous shrinkage is the point of final set, t_f, but there is also the view that time zero should be taken at the point of initial set, t_i.

In this study, the results for all three definitions of time zero are presented and studied to get an indication of the shrinkage development between these periods. Figure 5.1 and Figure 5.2 show the autogenous shrinkage results of the reference pastes, WB022_Ref_Paste and WB027_Ref_Paste respectively. Each are plotted against the initial and final setting time of the respective paste.

The shrinkage results are considered from the time of the addition of water to the paste. In both cases, the shrinkage development is very steep from the time of water addition and then the rate of shrinkage dramatically reduces around the time of initial set. After this, there is another point where the rate of shrinkage suddenly increases again. In both cases this happens about one to two hours after final set and not at the time of final set.

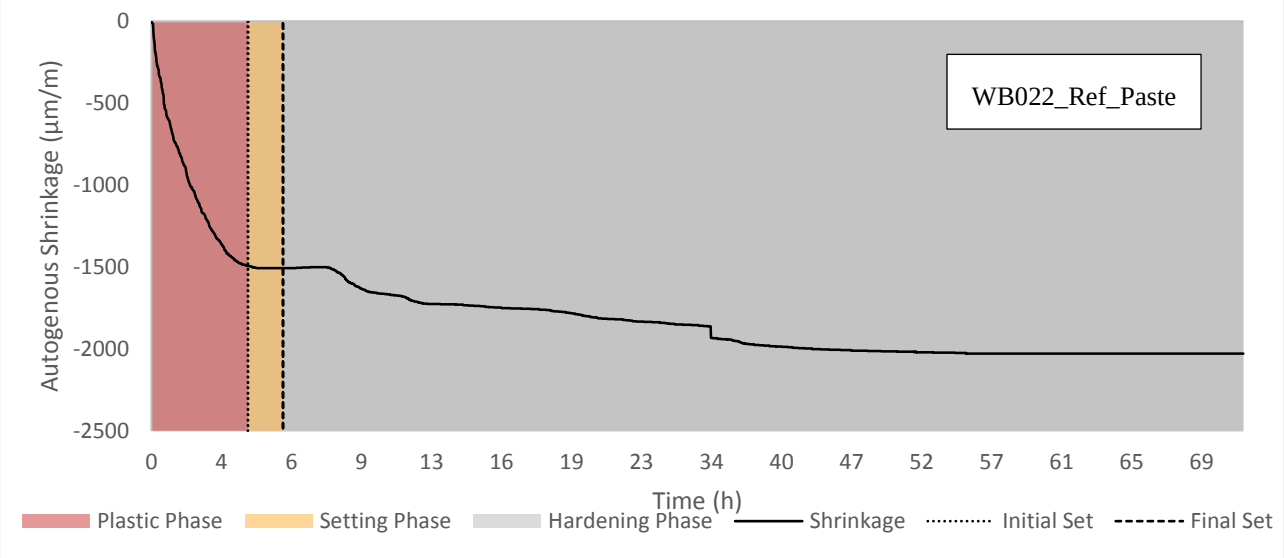

Figure 5.1 Autogenous shrinkage of Mix WB022_Ref_Paste from the time of water addition

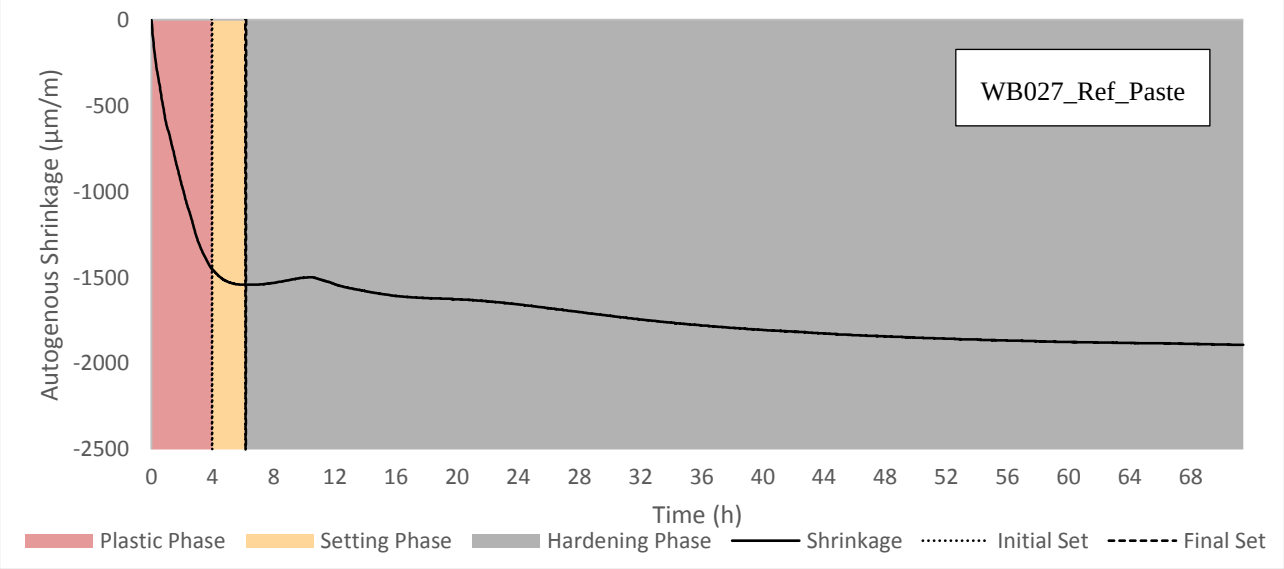

Figure 5.2 Autogenous shrinkage of Mix WB027_Ref_Paste from the time of water addition

5.1.1.1 Plastic Phase

The plastic phase of the pastes is the time period from the addition of water up until initial set. This is the period in which rapid shrinkage is observed. About 75 % of the total shrinkage observed in this 72-hour test is achieved in the first four hours of the test. Strictly speaking, this is termed as chemical shrinkage, and not autogenous shrinkage. The behaviour in this period is however worthwhile to note, as limiting the shrinkage in this phase would ultimately help to limit the overall shrinkage.

Figure 5.3 compares the shrinkage development in the plastic phase of the two reference mixes, WB022_Ref_Paste and WB027_Ref_Paste. As expected, the paste with the lower w/b ratio has the highest shrinkage. Interestingly, the pastes experience the same shrinkage for the first hour, after which they start to deviate. The paste with the lower w/b ratio has a higher rate of shrinkage development, but it also starts to stabilise sooner than the paste with the higher w/b ratio.

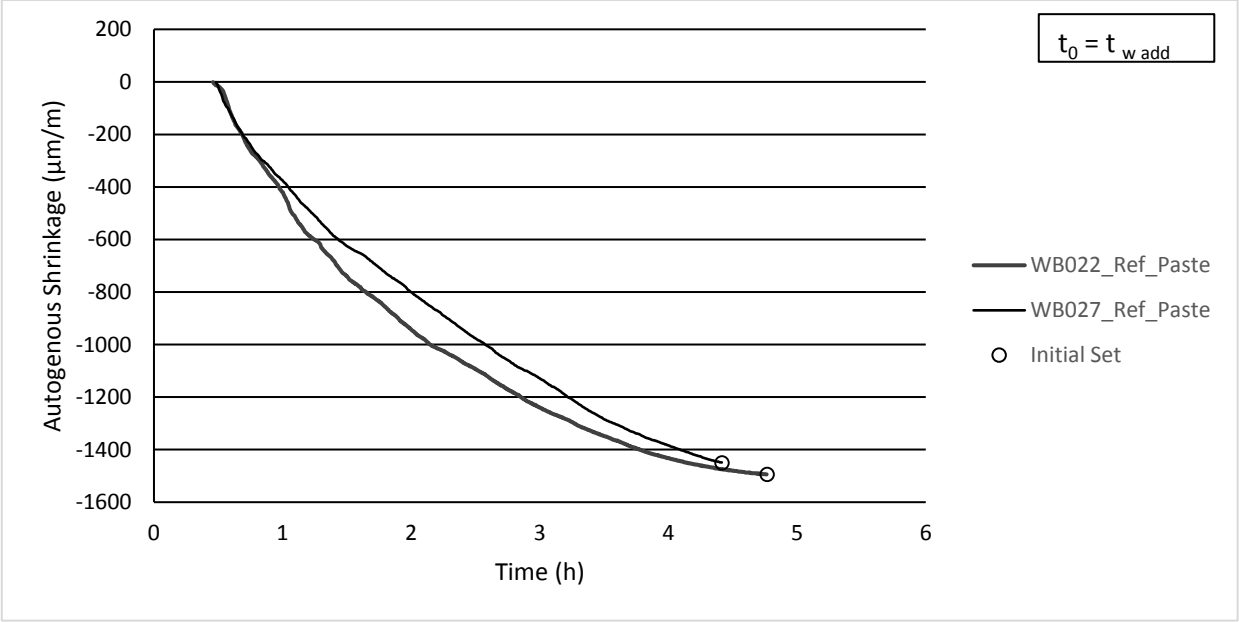

Figure 5.3: Autogenous shrinkage of reference mixes in the plastic phase

5.1.1.2 Setting Phase

The setting phase is the period between initial and final setting time. This is a short period of only one to two hours. Only a small amount of shrinkage is experienced in this phase.

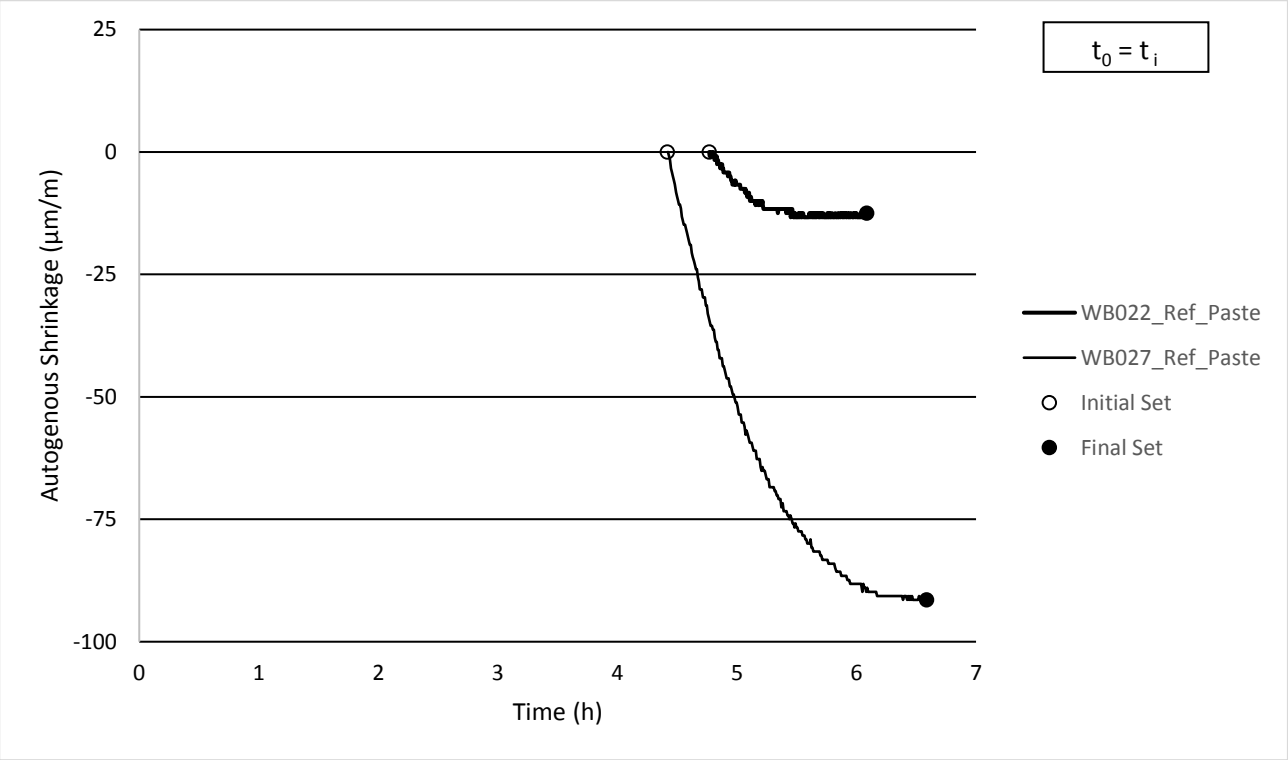

Figure 5.4 shows the shrinkage of the reference pastes in the time between initial and final set. The shrinkage values that are plotted is the absolute shrinkage experienced during this time.

Only about 0.3 % of the total shrinkage of WB022_Ref_Paste and 5 % of WB027_Ref_Paste occurs during this phase. Furthermore, the paste which started to stabilise sooner in the plastic phase, experiences a very low shrinkage in this phase.

The shrinkage in WB027_Ref_Paste continues to develop at a steady rate and starts to stabilise about 30 minutes before final set. This shows that a paste which reaches initial set sooner, can also contribute to developing less total shrinkage.

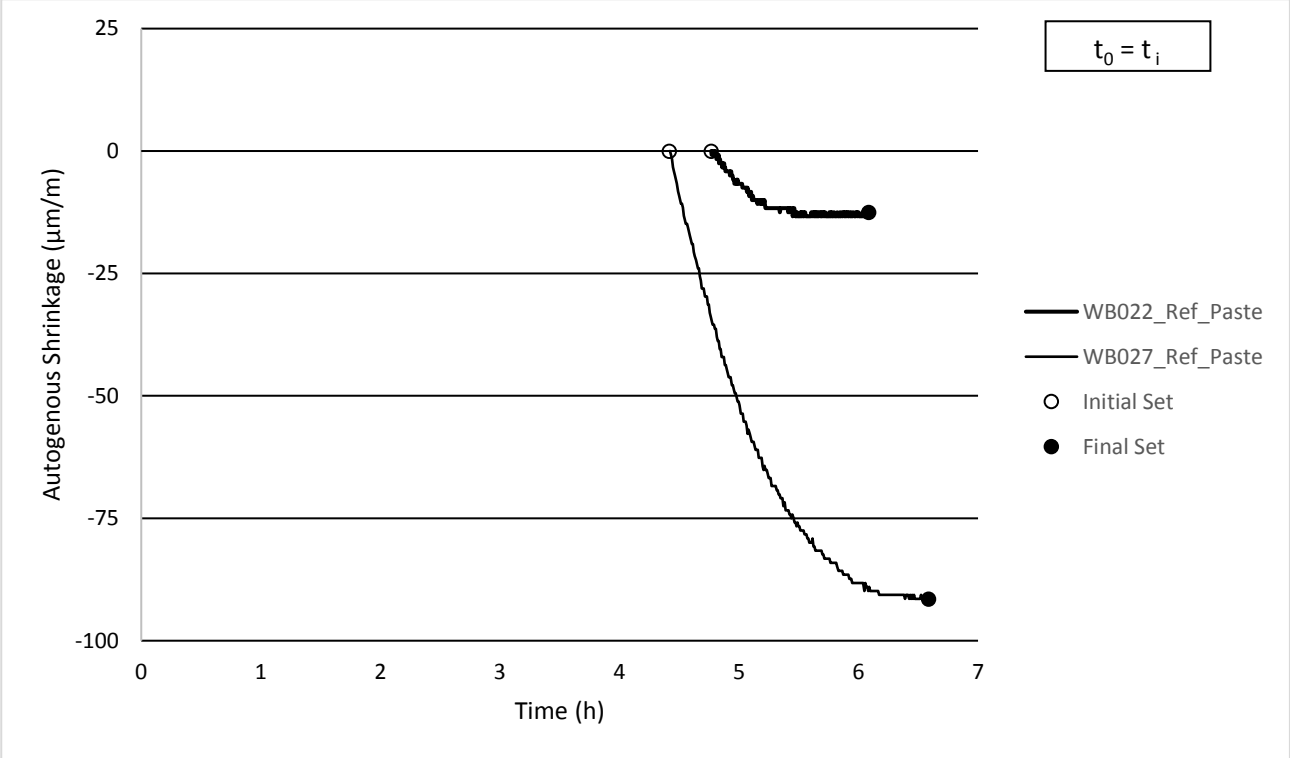

Figure 5.4: Autogenous shrinkage of reference mixes in the setting phase

5.1.1.3 Hardening Phase

The hardening phase is taken from the time of final set for the rest of the test. The shrinkage development in this phase is commonly isolated when studying autogenous shrinkage. The autogenous shrinkage of the two reference pastes in the hardening phase are shown in Figure 5.5. About 18 % of the total shrinkage observed in this three-day test for WB022_Ref_Paste is observed in the hardening period and 25 % for WB027_Ref_Paste. The shrinkage at the time of final set is taken as the starting point for the rest of the shrinkage development for the remainder of the test. WB022_Ref_Paste remains constant for the first 90 minutes, before the shrinkage starts to develop. WB027_Ref_Paste on the other hand shows a sudden expansion, before shrinkage suddenly starts to take place.

Figure 5.5 shows that there are two points where there is a noticeable change in the rate of shrinkage development for WB022_Ref_Paste. As expected, the paste with the lowest w/b ratio showed the highest shrinkage.

This paste also showed a much faster shrinkage development for the first 5 hours after final set and then the rate of shrinkage development decreases at a steady rate till around 36 hours, where the rate of shrinkage changes again. WB027_Ref_Paste also shows its fastest shrinkage growth in the first few hours after final set. About 7 hours from the peak in the graph, the rate of shrinkage development

also slows down. This mix has a smoother development from this point than WB022_Ref_Paste. The shrinkage then starts to stabilise at around 60 hours.

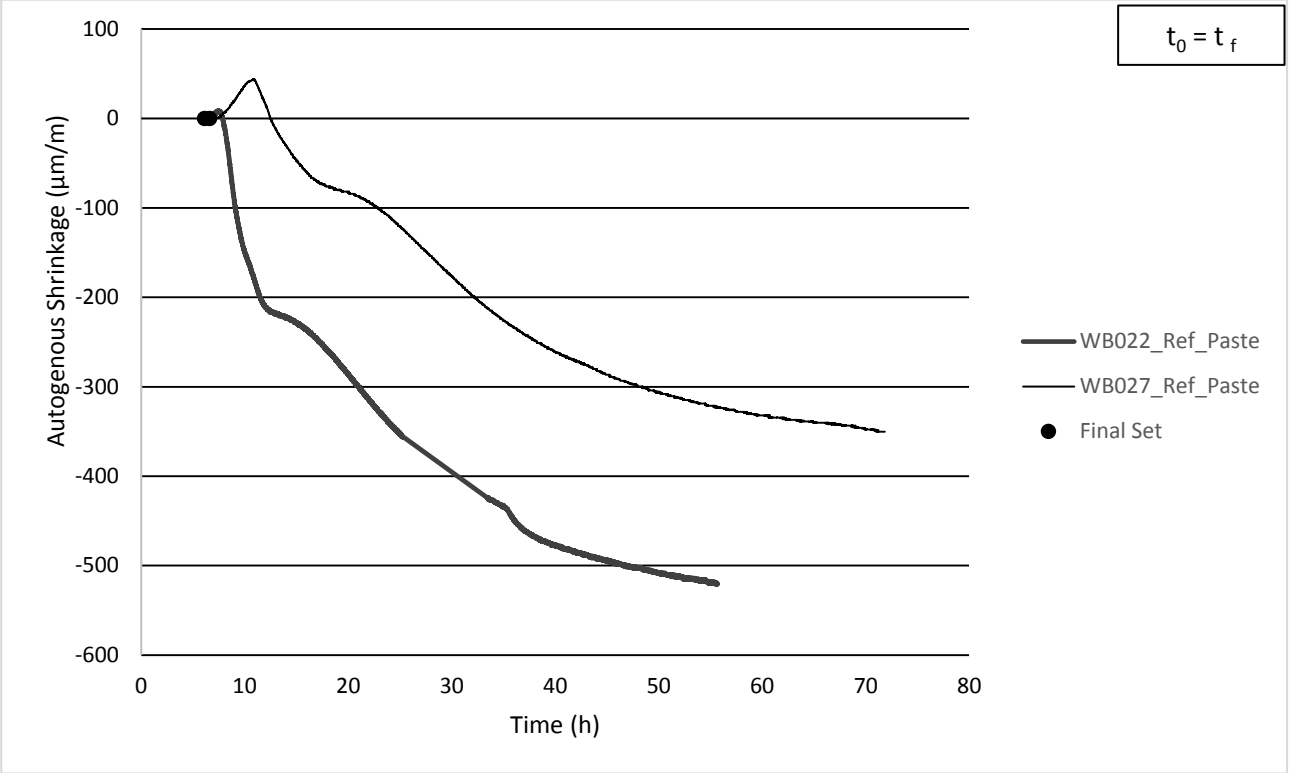

Figure 5.5: Autogenous shrinkage of reference mixes in the hardening phase

5.1.2 Internally Cured Pastes

To observe the effectiveness of SAP to mitigate shrinkage in low w/b ratio pastes, 0.3 % and 0.5 % SAP bwoc were added to each reference mix in Section 5.1. Each dosage of SAP was saturated at 75 % and 50 % and the results of the autogenous shrinkage tests are presented in Figure 5.6 and Figure 5.7. A summary of the mix design can be found in Table 3.5 in conjunction with Table 3.6 showing the amount of SAP and internal curing water for the respective internally cured mixes.

First the WB022 set of test results are discussed. The results are also analysed from the three definitions of time zero as described in Section 5.1.1.

Figure 5.6a shows time zero as the time at which water was added to the mix. The figure shows that the addition of SAP has a significant influence on the shrinkage of a paste.

It was expected that the paste which included SAP at a higher saturation level would be more effective in mitigating shrinkage, due to the higher water content which could potentially reduce the effects of self-desiccation. The mixes that contained SAP saturated at 50 %, mix WB022_03SAP_50SAT_Paste and WB022_05SAP_50SAT_Paste, were in fact more effective in

mitigating shrinkage than its counterpart saturated at 75 % in the plastic phase. In the hardening phase, after final set, the efficiency of the internally cured variations are exactly reversed from the plastic phase.

WB022_05SAP_50SAT_Paste which performed the best in the plastic state, performed the worst in the hardening phase. WB022_03SAT_75SAT_Paste which performed the worst in the plastic phase, performed the best in the hardening phase. The phase between these two, the setting phase, shows the transition between the trends in these two phases.

For the WB027 set of mixes, the paste containing 0.5 % SAP saturated at 50 % performed the best when analysing the results from all three points of time zero. The mix variations showed the same relative performances in each case, with the exception of WB027_03SAP_50SAT and WB027_05SAP_75SAT in the plastic phase. The plastic phase also shows WB027_05SAP_50SAT as developing less than half of the shrinkage of the rest of the mixes, while the difference between this mix and the rest is not significant when analysing the results from initial and final set. This could be due to an inaccuracy in the test sample or starting of the test. This provides a reason for why it is worthwhile to analyse autogenous shrinkage from a time when the paste is more stable and able to withstand minor discrepancies in the test method.

Considering the autogenous shrinkage of the WB027 set from initial and final set, it can be seen that the pastes which performed the best are the ones that contained a higher dosage of SAP. Interestingly, the pastes that contained less water in each case was also the paste that performed the best i.e. 50 % saturated pastes performed better than the corresponding paste saturated at 75 %.

For both sets of tests, the incorporation of SAP has a dramatic effect on autogenous shrinkage. In all cases, the addition of SAP decreased the final autogenous shrinkage. The different amounts of SAP and internal curing water also show that they affect the autogenous shrinkage to different degrees. The graphs in Figure 5.6 and Figure 5.7 show that when considering the shrinkage from each of the three specified time periods, different conclusions can be drawn. Considering the shrinkage from the time of water addition, the shrinkage reduction in mixes containing SAP and internal curing water is noteworthy. However, looking at the shrinkage from the point of final set, the mixes don't only mitigate the shrinkage completely, but swelling is also exhibited.

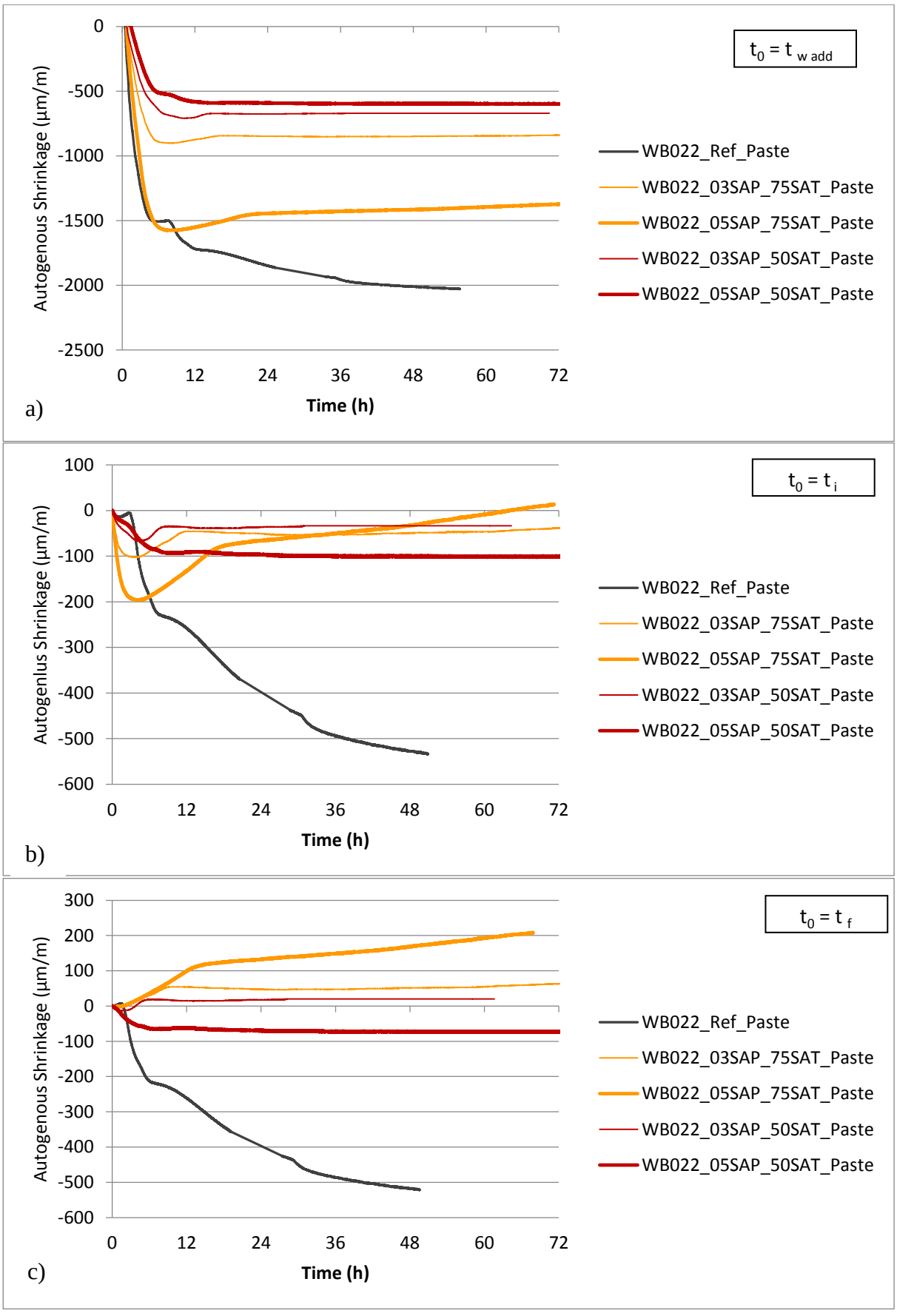

Figure 5.6: Autogenous shrinkage of mix WB022 at the time of a) water addition b) initial set and c) final set

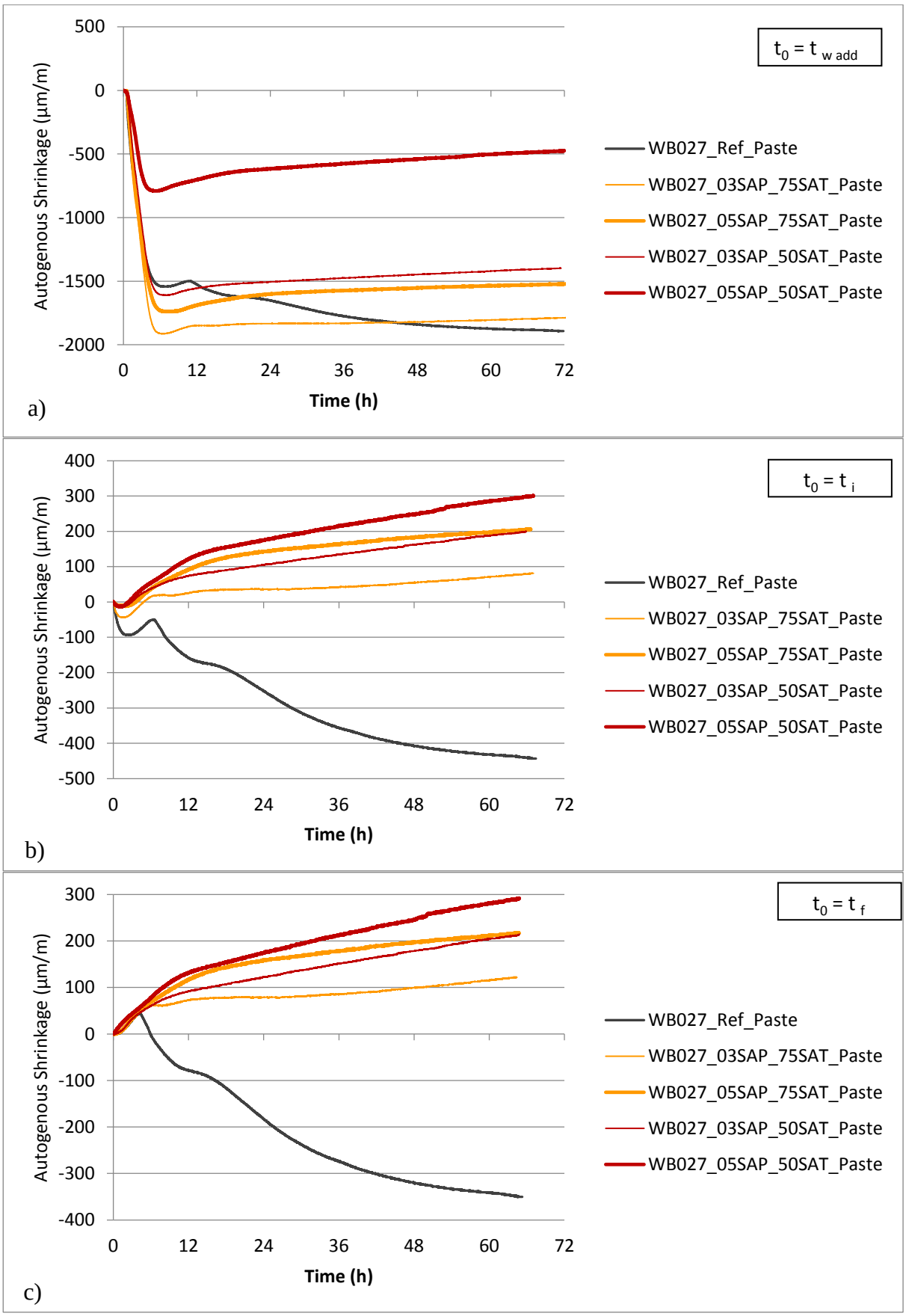

Figure 5.7: Autogenous shrinkage of mix WB027 at a) the time of water addition b) initial set and c) final set

To get a clearer indication of what happens between these time periods, the above results are investigated in isolation between the times of water addition, initial set and final set.

5.1.2.1 Plastic Phase

In the plastic phase of the WB022 set, the addition of SAP is successful in reducing shrinkage. The mixes which contained the SAP saturated at 50 % both performed better than those saturated at 75 %. This is the case for the WB027 set as well, except that the mixes at 75 % saturation level showed an increase in shrinkage relative to the reference mix.

The two dosages of SAP, 0.3 % and 0.5 %, show converse effects with respect to their saturation levels in both WB022 and WB027. For the 50 % saturation level, a higher dosage of SAP reduced shrinkage more than the lower dosage of 0.3 %. For the 75 % saturation level, however, a higher dosage of SAP contained less of an impact on reducing the shrinkage than the lower dosage of 0.3 %. This shows that there is not a linear relationship between the amount of SAP and shrinkage mitigation. Thus increasing the SAP dosage does not necessarily increase the mitigation of shrinkage and there is a compromise between the amount of SAP and the amount of additional water needed which needs to be established.

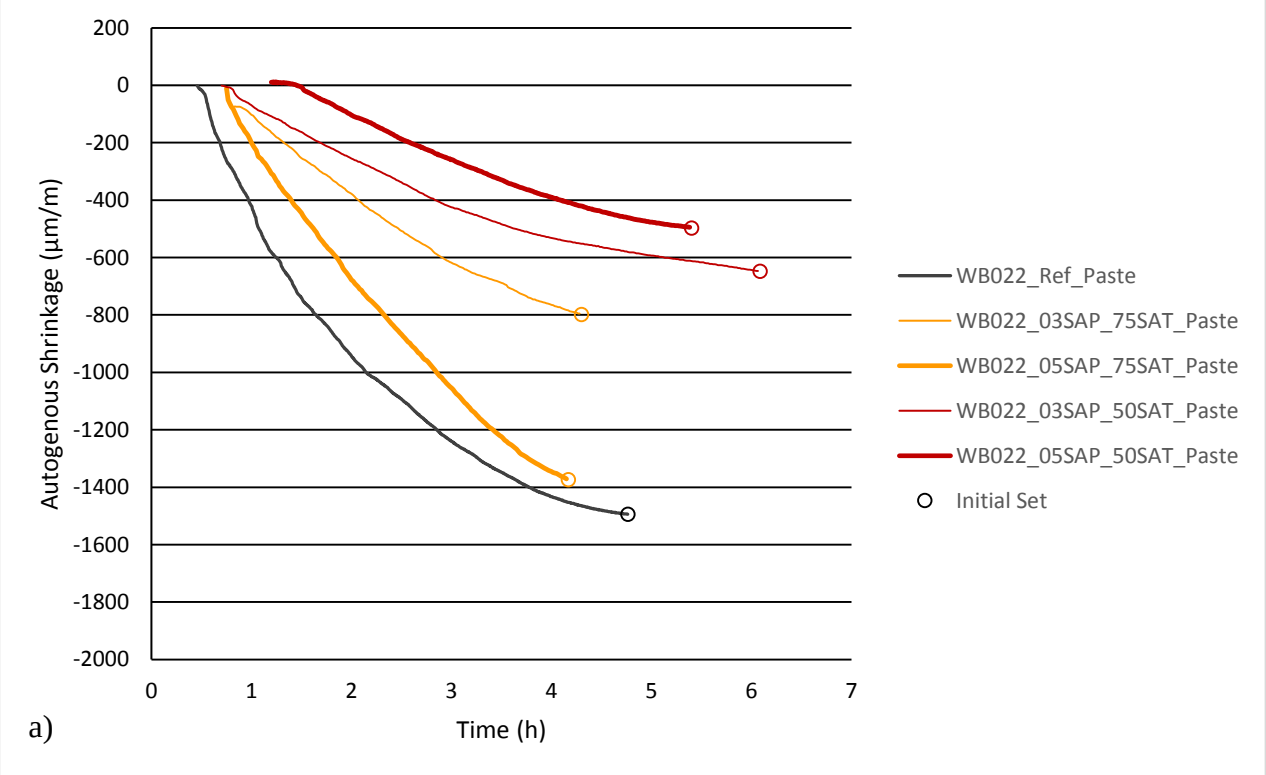

a)

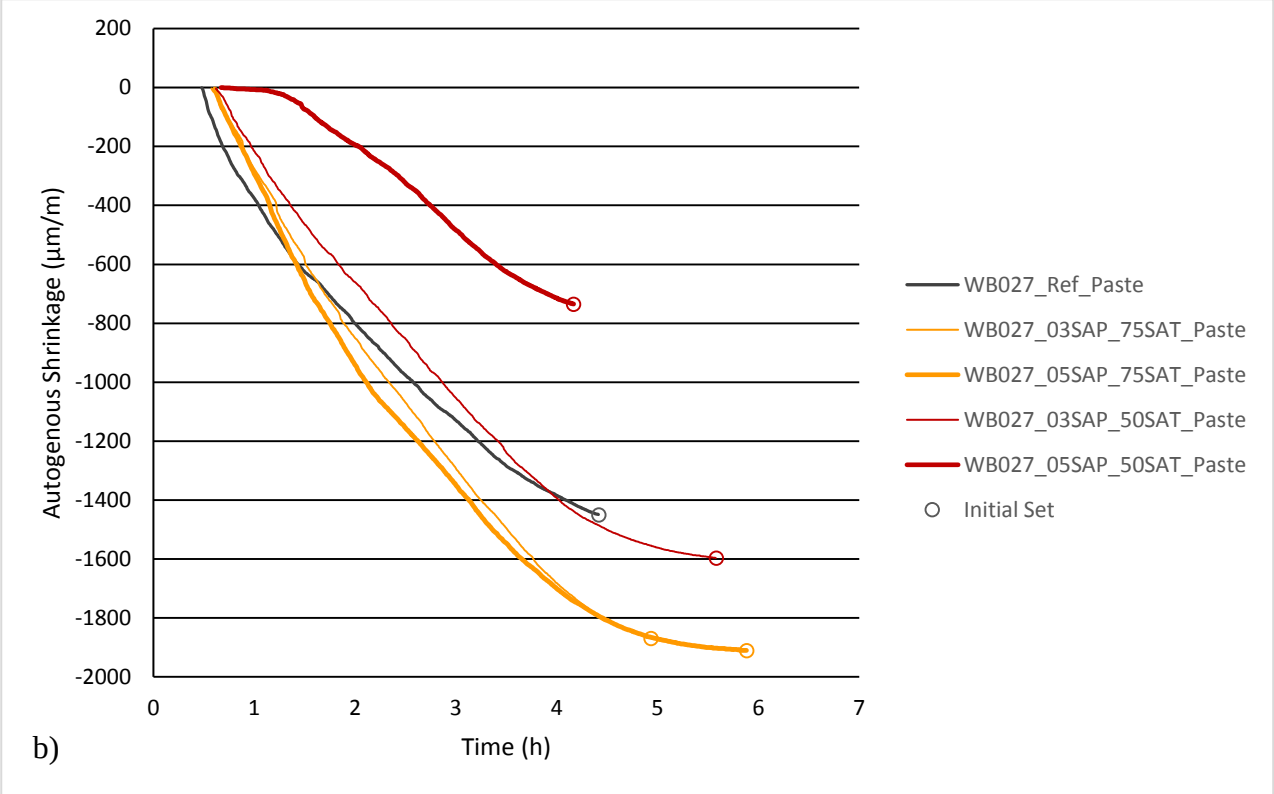

Figure 5.8 Plastic phase of a) WB022 and b) WB027

The reference mix with the higher w/b ratio produced slightly less shrinkage than the paste with the lower w/b ratio. This is expected because an increased amount of water is expected to relieve some of the pore pressure and thus reduce the effects of self-desiccation. This however, was not the case for internally cured pastes. It is interesting to note that in the plastic phase, the internally cured pastes with the higher w/b ratio experienced more shrinkage than the pastes with a lower w/b ratio. This suggests that SAP is more effective in reducing shrinkage in the plastic phase the lower the w/b ratio of the mix.

5.1.2.2 Setting phase

The setting time phase lasts for a short period and the shrinkage that is experienced during this time is not definite. The graphs in Figure 5.9 however show two significant trends. Considering the starting point of the setting phase and the rate of shrinkage development, it can be concluded that the later the initial set, the lesser the rate and magnitude of shrinkage until final set.

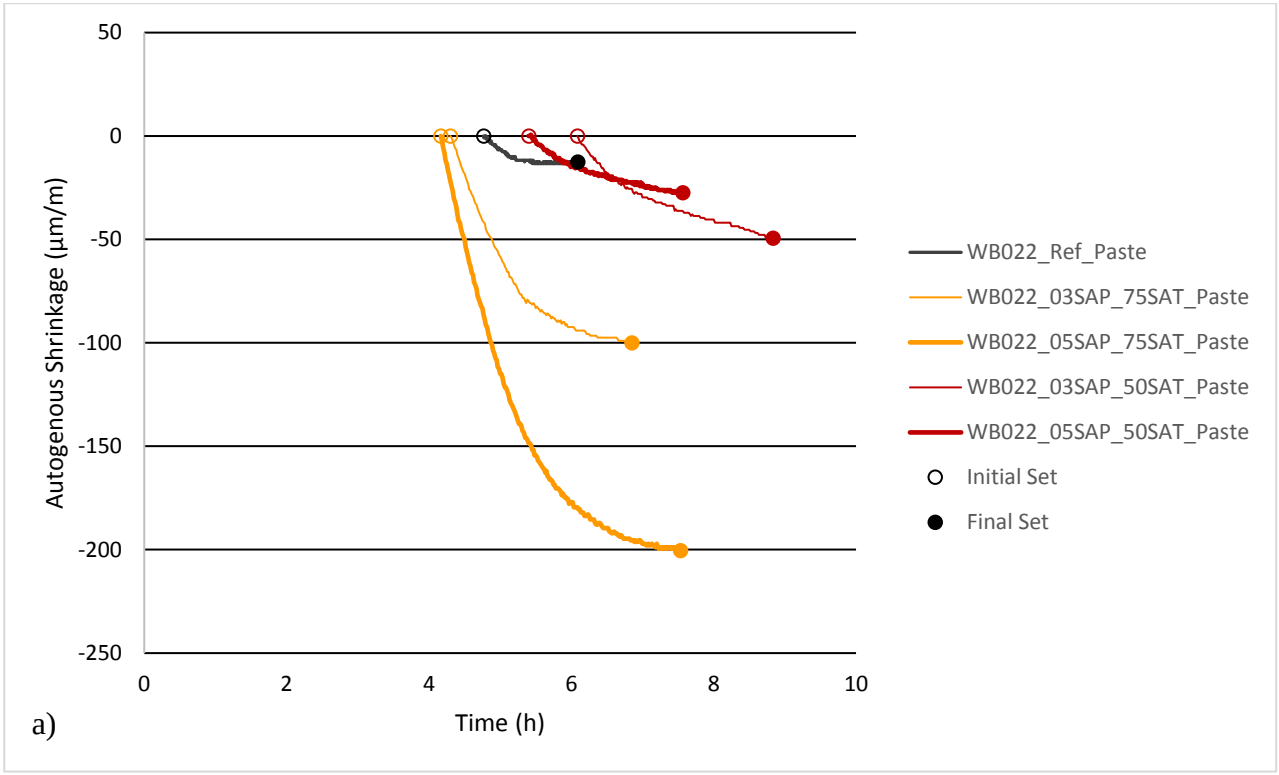

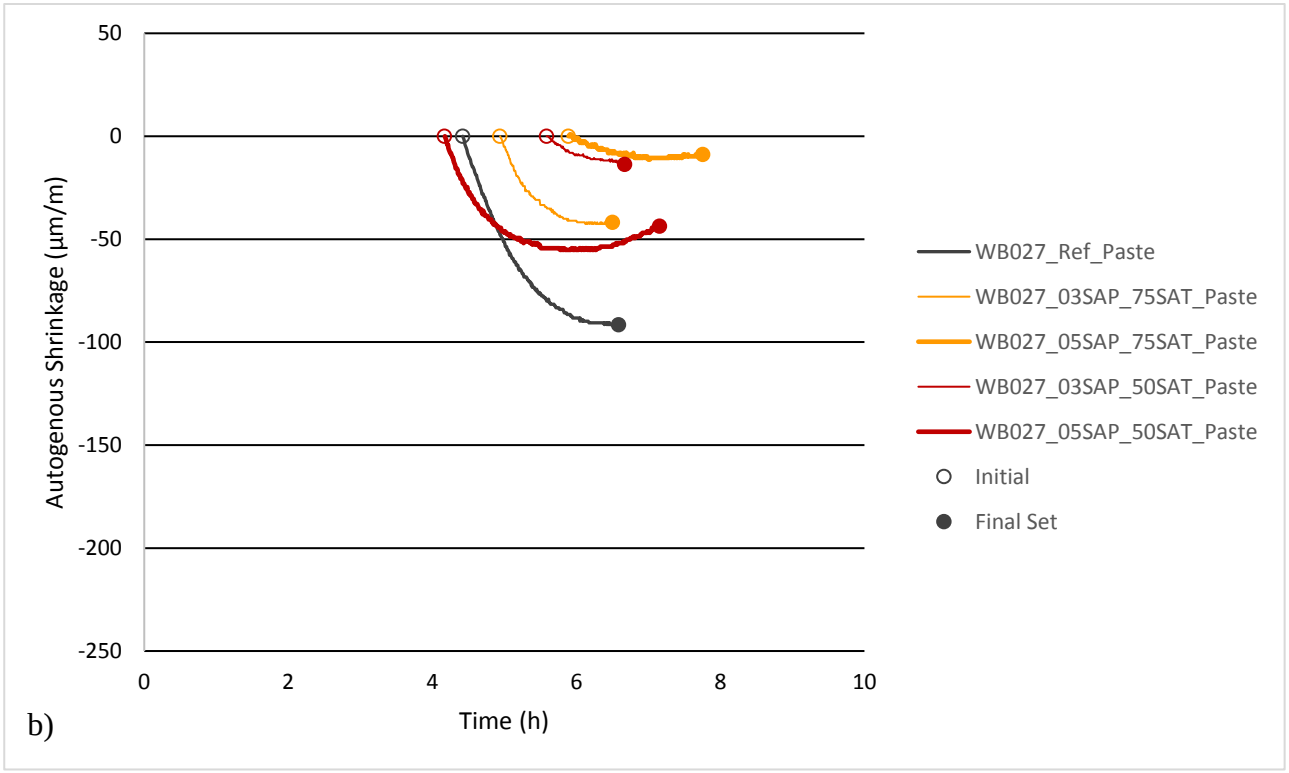

Figure 5.9 Setting phase of a) WB022 and b) WB027

Although this phase is short and there is not much data, the second aspect that can be concluded from this phase is that swelling starts earlier in pastes that contain a higher dosage of SAP. This is seen for both w/b ratios as well as both saturation levels.

5.1.2.3 Hardening Phase

The hardening phase is the longest phase which starts from the point of final set and lasts for the rest of the test which was run for about 72 hours. Both set of tests, WB022 and WB027, show that all the internally cured paste variations that were tested in this test are exceptionally effective in mitigating autogenous shrinkage.

All internally cured mixes, with the exception of WB022_05SAP_50SAT, did not only cancel shrinkage, but resulted in swelling. The relative effect of the different internally cured paste variations differ between the two w/b ratios.

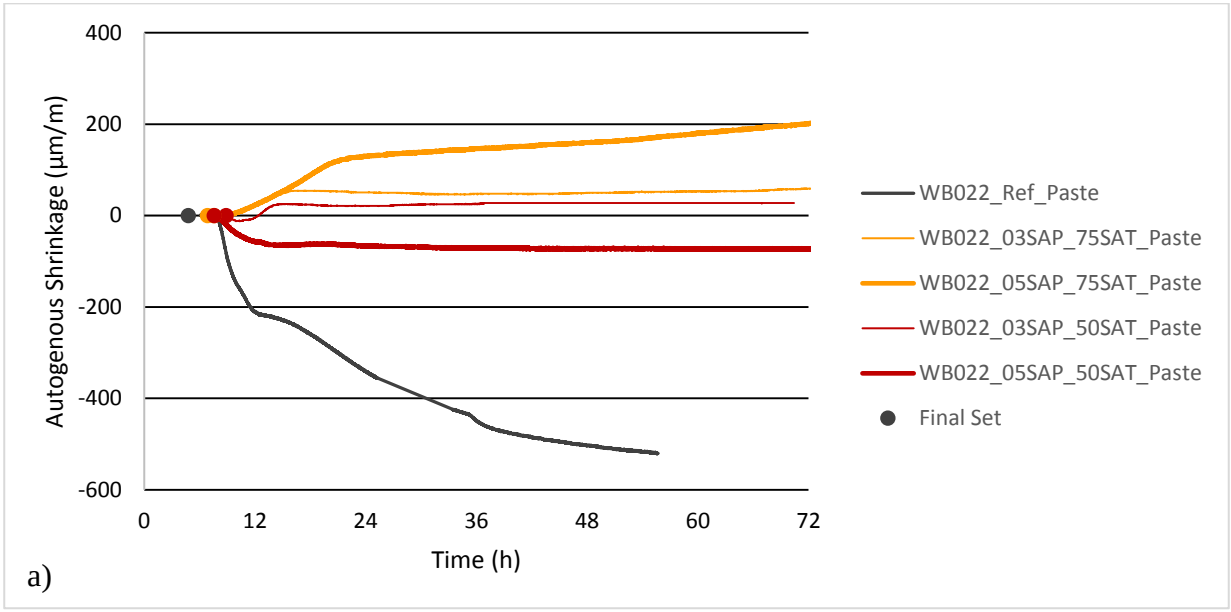

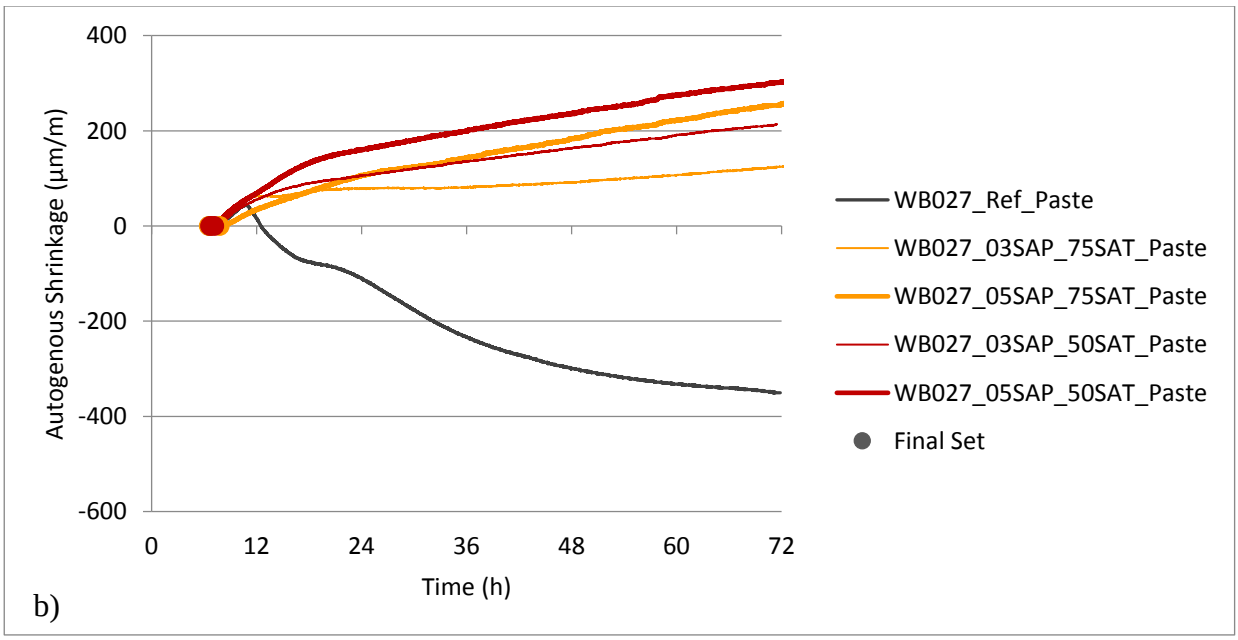

Figure 5.10: Setting phase of a) WB022 and b) WB027

5.1.3 Compressive Strength

Figure 5.11 show the 3, 7 and 28 day compressive strength of the paste mixes tested in this study. The slump test was measured along with the compressive strength to see if the amount of water in a mix is related to the workability and if the workability in turn has a direct effect on the strength. It was expected that a stiff mix, that has difficulty in placing would not only result in a lower slump, but also a lower compressive strength due to inadequate compaction.

The results in the graphs below clearly show which mixes do not contain a sufficient amount of water. WB022_03SAP_50SAT, WB022_05SAP_75SAT, WB022_05SAP_50SAT, WB027_05SAP_75SAT and WB_05SAP_50SAT produced mixes that showed no flow at all. These mixes had slump heights of 80 to 100 mm which were not deemed acceptable since the requirement was mixes which produced slump flows of at least 350 x 350 mm. This is an indication that the SAP is absorbing from the mix water as the added internal curing water is not enough to saturate the SAP particles to a stable degree. However, the absence of flowability did not portray a loss in strength in these mixes with respect to the corresponding mix theoretically fully saturated.

Where a decreased amount of water showed a detrimental effect on the flowability, the compressive strength either stayed the same or increased due to the effective decrease in w/b ratio. All internally cured mixes showed a decrease in both flowability and strength compared to the reference mixes without SAP. Internally cured mixes that were saturated to the theoretical amount of water showed significant decrease in strength for both w/b ratios. This theoretical saturation level is clearly too high, as the strength increases as the saturation level is lowered to 75 and 50 %.

An increase in SAP dosage from 0.3 to 0.5 % bwoc also showed a dramatic drop in both the flowability and strength for both w/b ratios. This could be due to more voids being present in the mixes with 0.5 % SAP bwoc than mixes with 0.3 %.

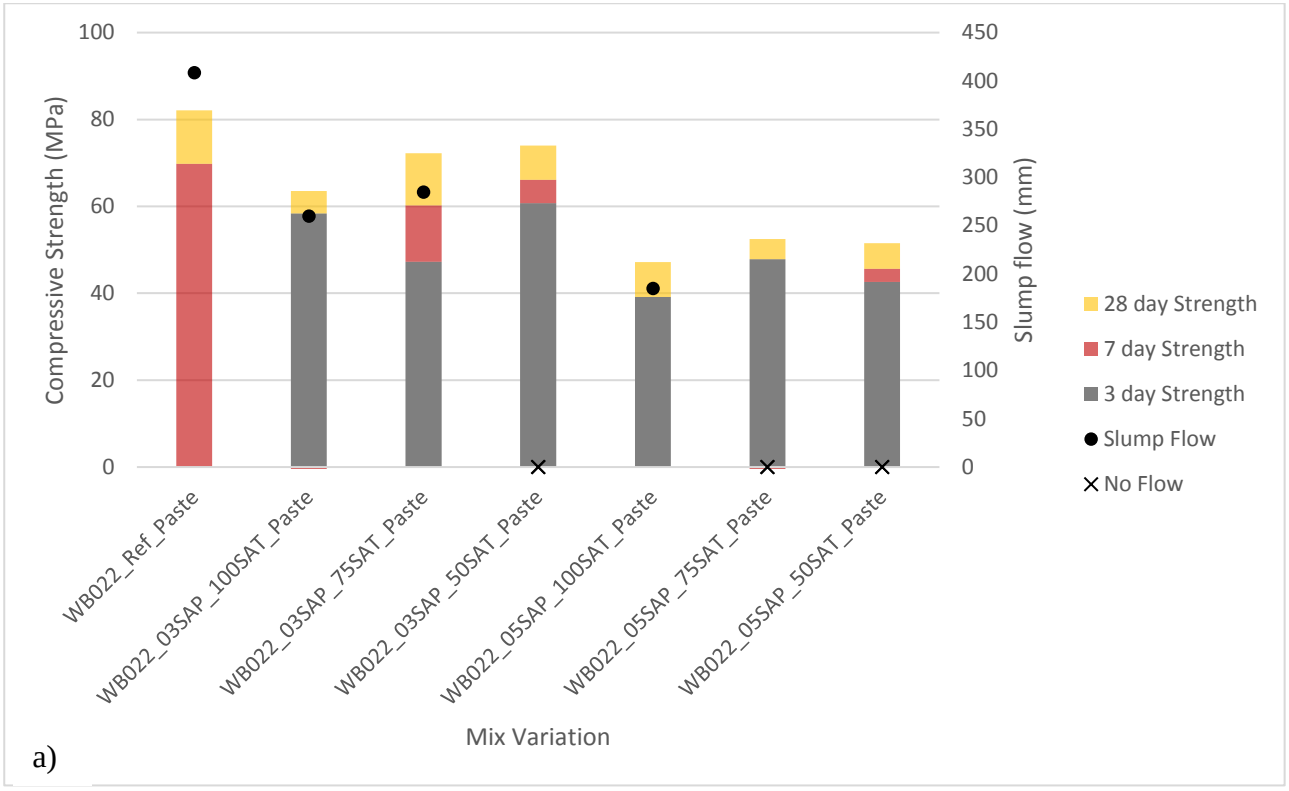

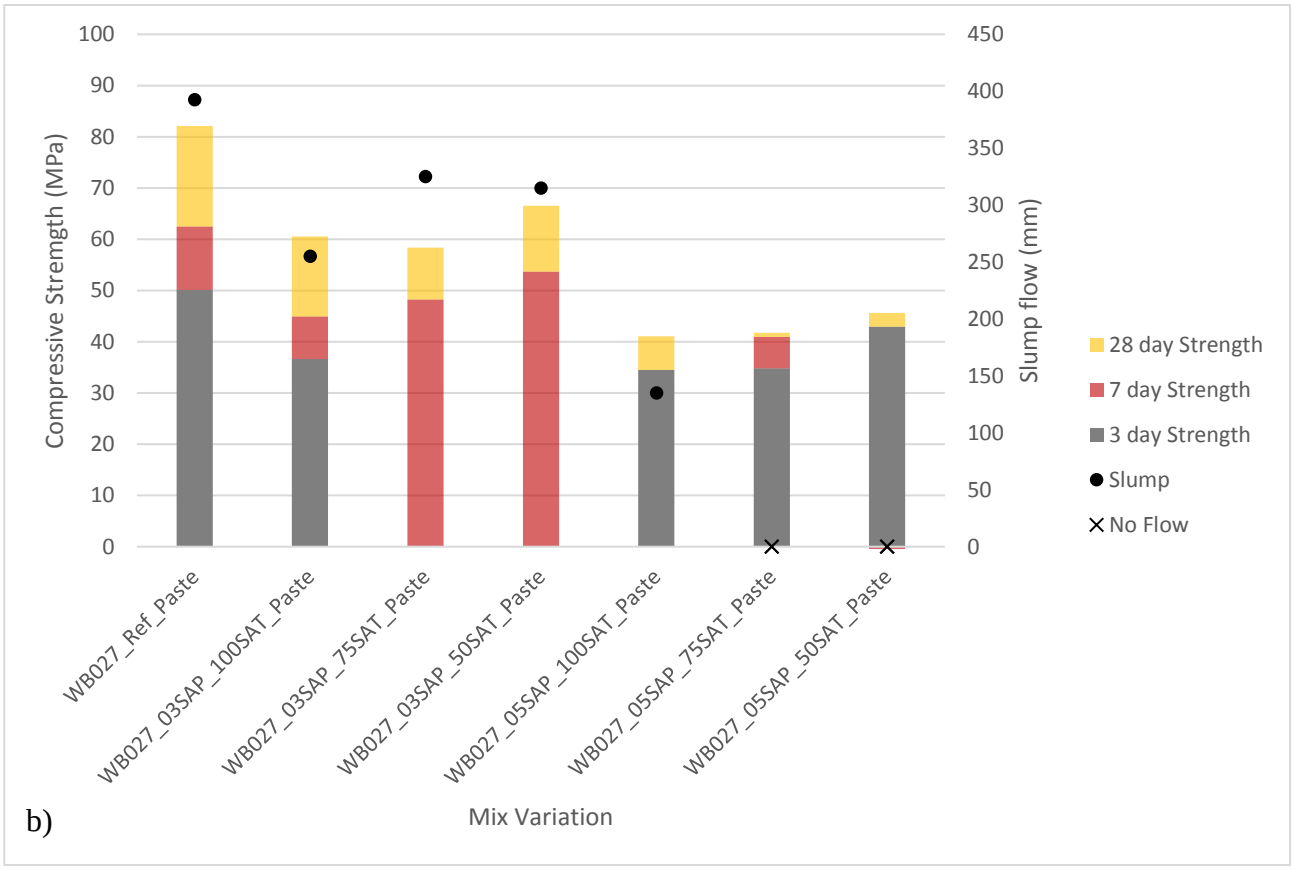

Figure 5.11: Compressive Strength and slump flow of a) WB022_Paste and b) WB027_Paste

5.2 Plastic Shrinkage

For plastic shrinkage, the WB027 set of mixes were tested with 0.3 % of SAP bwoc at saturation levels of 75 % and 50 %. Selective tests from the WB022 set of mixes were then tested for comparison to observe the effect of a change in w/b ratio. The mix variations and proportions are given in Table 3.5. For each mix, plastic shrinkage, plastic settlement, capillary pressure, initial and final set were tested.

5.2.1 Reference Concrete

The reference mix in this set of tests is a concrete mix with a w/b ratio of 0.27, containing no SAP and a stone size of 6 mm. The results of the plastic shrinkage, plastic settlement, capillary pressure, initial and final set for this mix are presented in Figure 5.12. The shrinkage and settlement are shown as strain values based on displacement with respect to the original size of the mould.

Two moulds per mix were tested. Each mould contained two LVDT's measuring the plastic shrinkage and one LVDT measuring plastic settlement. The plastic shrinkage strain is determined by taking the average of the four plastic shrinkage readings and multiplying it by two to get the total horizontal displacement experienced in one mould. This displacement is then divided by 300 mm, the original width of the specimen. The plastic settlement strain is taken as the average of the two settlement readings from each mould, where both readings are within 15 % difference. This average was then divided by 100 mm, the height of the mould. It should be noted that there could be a slight discrepancy between settlement strain values as the exact height of the specimen may vary due to different levels of filling the mould. However, this can be neglected as the difference is very small.

Both the plastic shrinkage and settlement develop rapidly in the first few hours of testing. This region of rapid shrinkage and settlement is before initial set. At the time of initial set, the settlement starts to slow down and by the time of final set, the settlement starts to stabilise at around 6 hours. The shrinkage development is not as rapid in the period before initial set as it is for settlement.

A decrease in plastic shrinkage development is still seen around the time of initial set. After final set there is an increased rate of shrinkage for about an hour before the shrinkage starts to stabilise.

Along with the rapid development of the plastic shrinkage and settlement in the plastic phase, the capillary pressure also increases rapidly. It is expected that the pressure should show a sudden drop to a pressure very close to 0 kPa. However, in this case and a few of the tests that follow, a sudden plateau in the pressure is observed until around final set where the pressure then drops. The reason for this is unclear.

It could be due to the test setup that is not suitable for concrete that contains a large portion of fine materials, causing a blockage in the point of measurement of the capillary tube. This plateau could also imply that there is not a sudden relieve of pressure in the capillary network, as is the case with normal strength concrete (NSC), due to the presence of the fine materials. The pressure drop can thus be considered at the point where the plateau starts, which co-insides with initial set.

A careful look at the capillary pressure development with the plastic shrinkage development shows changes in the rate of plastic shrinkage at the critical points of the capillary pressure. These points are encircled on Figure 5.12 and show that the plastic shrinkage starts to develop rapidly when the rate of capillary decreases a little bit. The plastic shrinkage development then slows down after about two hours around the time of initial set and then stabilises after final set.

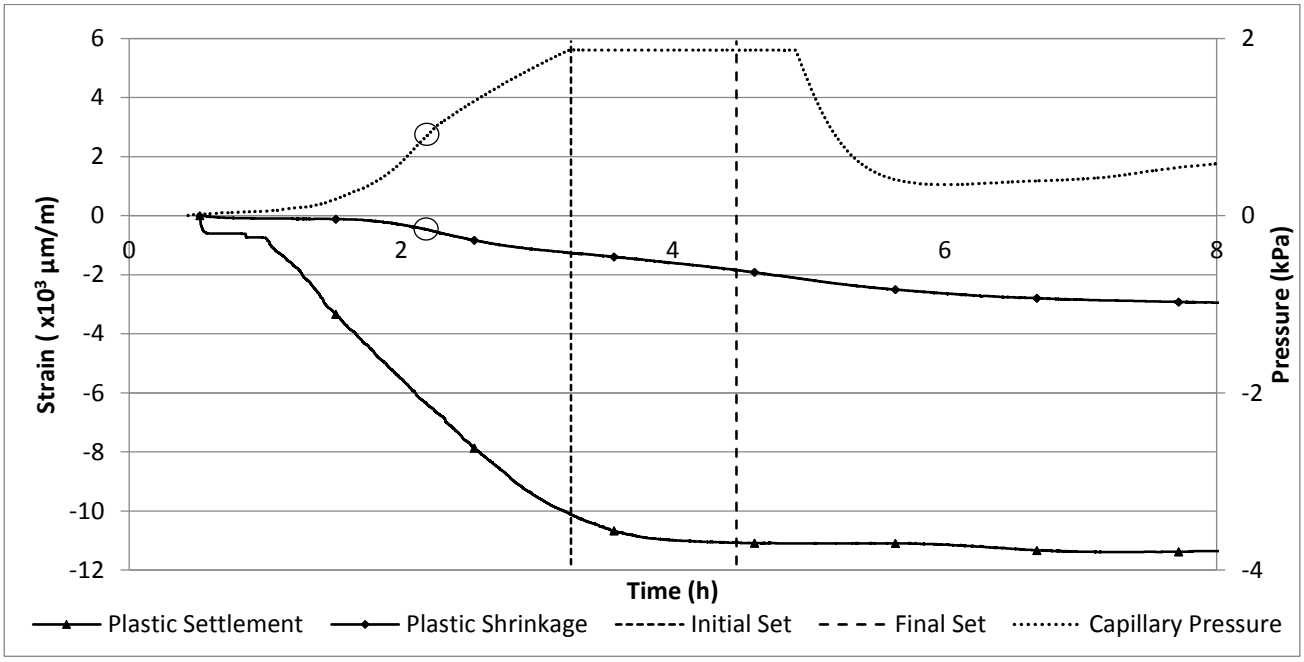

Figure 5.12: WB027_Ref_6mm

5.2.1.1 Influence of w/b

Figure 5.13 shows the results for a reference mix with 6 mm stone and a lower w/b ratio of 0.22. It was expected that a lower w/b ratio would produce a higher plastic shrinkage and settlement due to the higher cement content. However, the results show a decrease in both the shrinkage and settlement. The initial and final setting times of this mix is slightly later than those in the previous mix with a higher w/b ratio. This could be due to the increased dosage of superplasticiser which decreases the surface tension and causes a delay in the setting time.

Neither the initial or final setting time co-inside with the drop in pressure but they do correlate with the rate of plastic shrinkage development as is the case in the previous mix.

The encircled points in Figure 5.13 show that there is an increase in the rate of plastic shrinkage when there is a change in rate in the capillary pressure, similarly to the developments in Figure 5.12. However, in this figure, with the lower w/b, the rate of capillary pressure build-up increases when the plastic shrinkage increases. Comparing the capillary pressure build-up for the two w/b ratios in Figure 5.12 and Figure 5.13, it can be seen that the build-up for the mix with the lower w/b ratio is much slower than the mix with the higher w/b ratio. This slower build-up of pressure results in a slower plastic shrinkage development and may too be attributed to the decrease in surface tension due to the increase in superplasticiser.

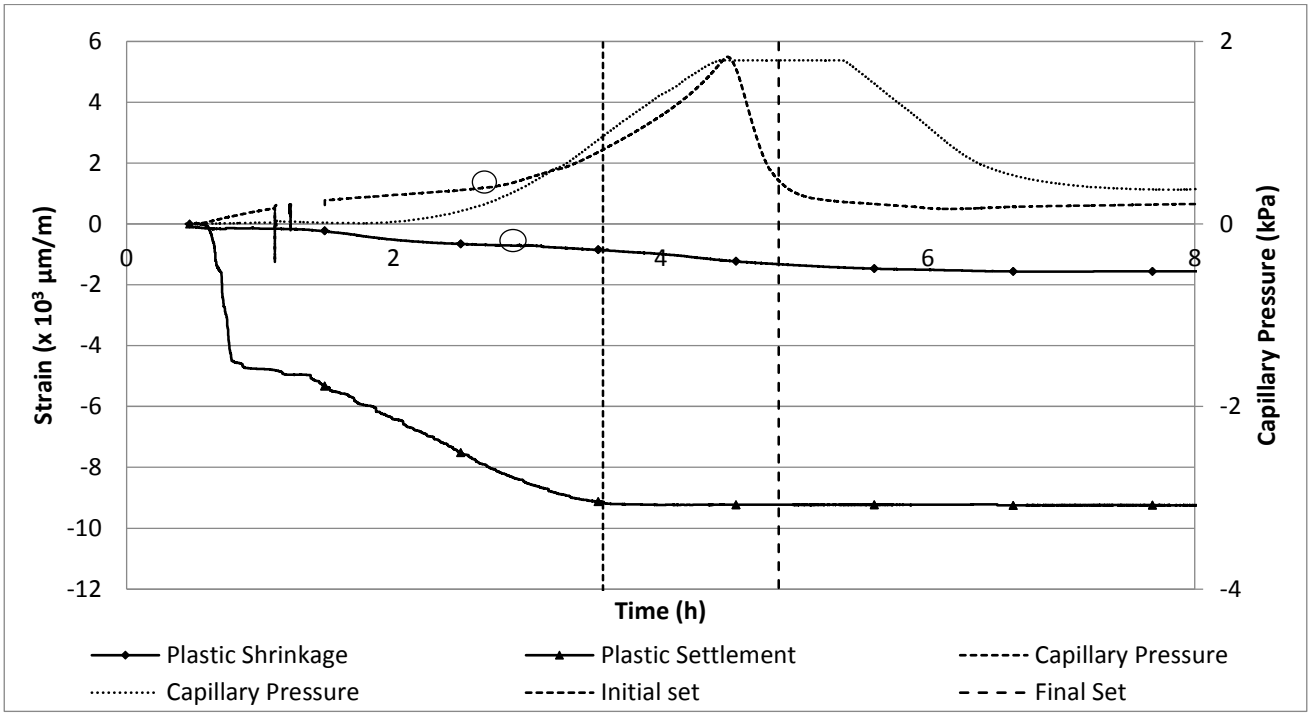

Figure 5.13: WB022_Ref_6mm

5.2.1.2 Influence of Stone Size

The reference w/b ratio of 0.27 was also tested using 9 mm stone to observe the effect of a bigger aggregate. Figure 5.14 shows that the maximum plastic shrinkage and plastic settlement of WB027_Ref_9mm are very similar to WB027_Ref_6mm in Figure 5.12. Differences between the capillary pressure and setting times can also be observed. However, the results of both these tests are localised results and conclusions cannot be drawn without additional tests and variations. The consequence of a larger aggregate is more of a concern for internally cured concrete.

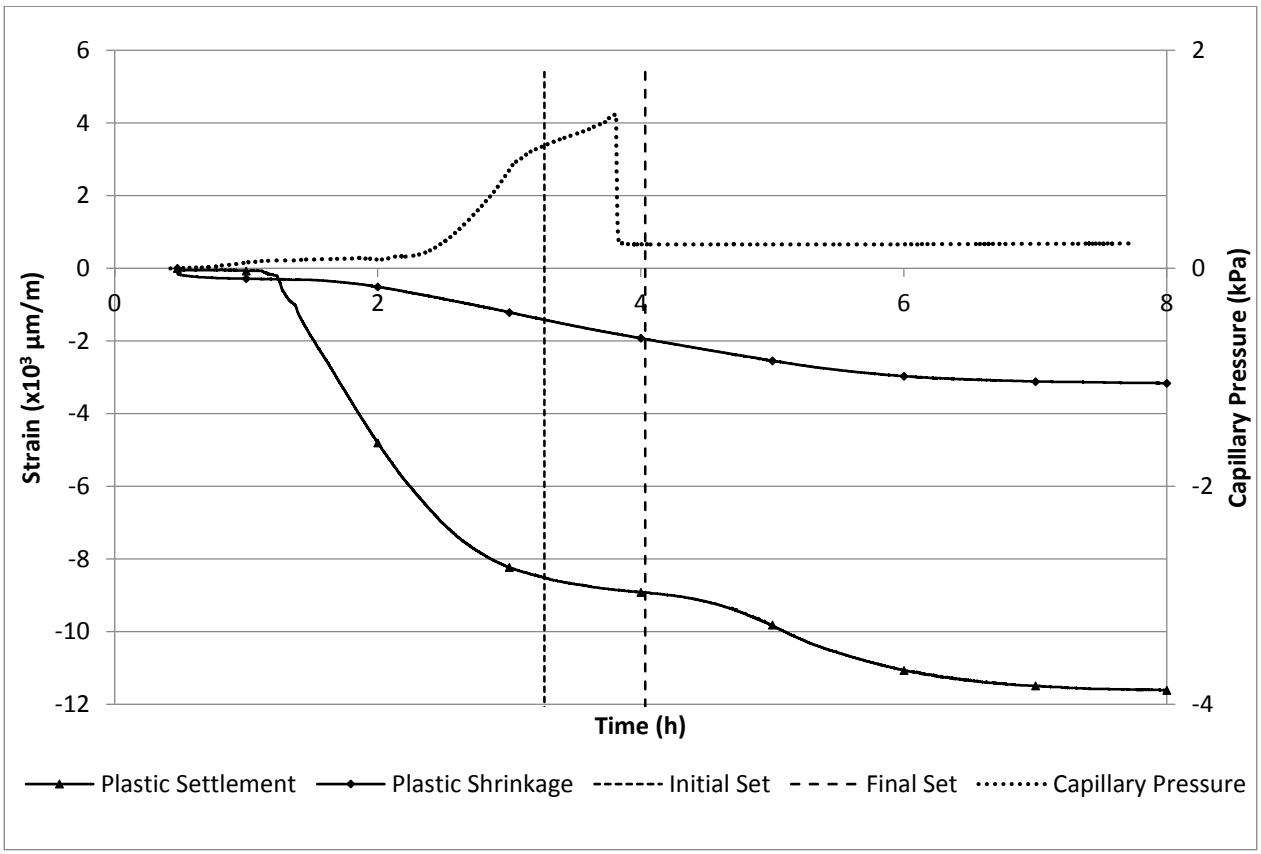

Figure 5.14: WB027_Ref_9mm

5.2.2 Internally Cured Concrete

To examine the influence of SAP with varying amounts of internal curing water, two internally cured mixes were tested at saturation levels of 75 and 50 %. Both of these saturation levels were tested with a 6 and 9 mm stone. A summary of the mix variations is presented in Table 3.5.

5.2.2.1 Saturation Level of 75 %

Figure 5.15 presents the results for a mix containing 0.3 % SAP saturated at 75 % with 6 and 9 mm stone respectively. The results show that the mix containing a bigger stone resulted in a higher plastic settlement. The plastic shrinkage however, is slightly lower. Both mixes show a reduced amount of plastic shrinkage and plastic settlement compared to its respective reference mixes with the same size stone, containing no SAP.

For WB027_03SAP_75SAT_6mm, the initial set is around the time of the pressure drop which is assumed to be at the peak of the one capillary pressure graph and the start of the plateau of the other. This is also the point where the plastic shrinkage and settlement starts to stabilise. The capillary pressure readings for WB027_03SAP_75SAT_9mm is inconclusive.

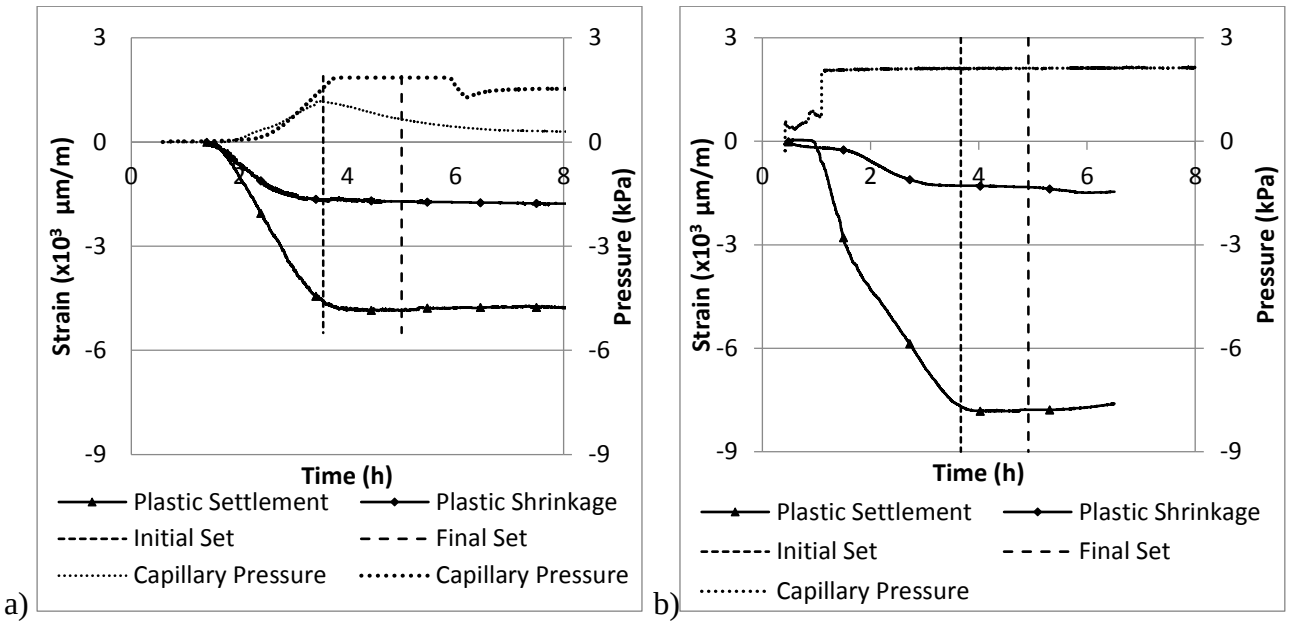

Figure 5.15: a) WB027_03SAP_75SAT_6mm b) WB027_03SAP_75SAT_9mm

5.2.2.2 Saturation Level of 50 %

Below in Figure 5.16 is the results for the internally cured mix saturated at 50 % with a 6 and 9 mm stone respectively. The plastic shrinkage and settlement for both of these mixes are much less than that of the respective reference mix. However, converse to the 75 % saturated mixes, the mix with the bigger stone experienced less settlement and more shrinkage than the mix with smaller stone. The figure also shows that the shrinkage and settlement stabilises around initial set. However, the capillary pressure results for both tests are inconclusive.

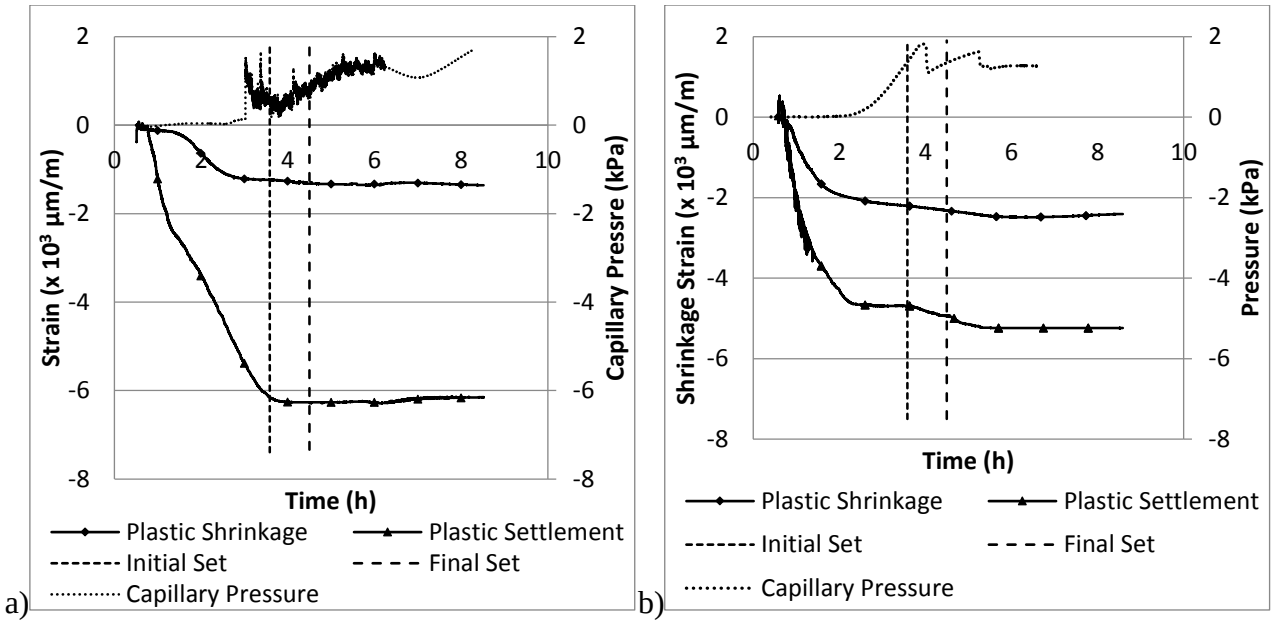

Figure 5.16: a) WB027_03SAP_50SAT_6mm b) WB027_03SAP_50SAT_9mm

5.2.2.3 Saturation Level of 50 % with w/b of 0.22

Internally cured concrete with a 50 % saturation level was also tested with a lower w/b ratio of 0.22. The results are shown in Figure 5.17. Once again, the plastic shrinkage and settlement is significantly lower than the reference mix with w/b of 0.22. The figure also shows that the mix with the bigger stone has less settlement and more shrinkage than the same mix with a smaller stone, as is the case with the 0.27 w/b ratio mix saturated at 50 %. There is one noticeable difference between these mixes and those at a higher w/b; both the initial and final setting time is reached, before the capillary pressure starts to build up. The results also show that the shrinkage and settlement stabilise around the time of the pressure drop, as in the case with all the mixes.

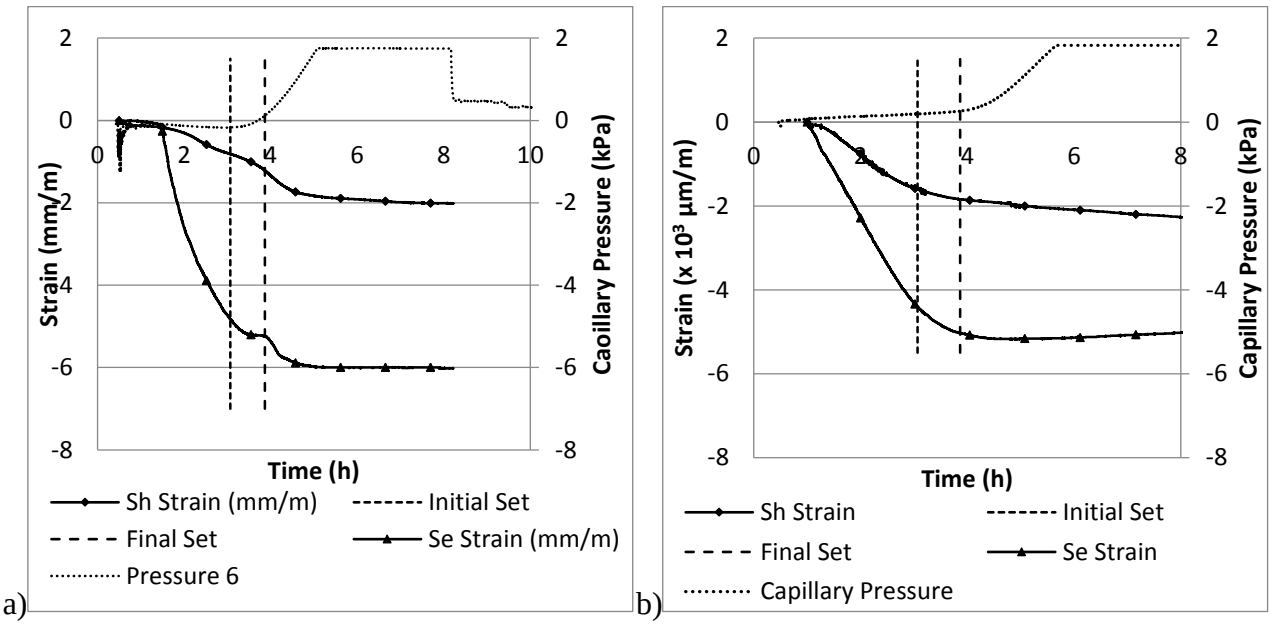

a) b)

Figure 5.17: a) WB022_03SAP_50SAT_6mm b) WB022_03SAP_50SAT_9mm

5.2.2.4 Saturation Level of 75 % with w/b of 0.22

The mix with w/b ratio of 75 % was also tested. This mix was only tested using 9 mm stone. The shrinkage development is steeper than the mixes saturated at 50 % and the settlement is higher. This mix, like those shown in Figure 5.17, show that initial and final set are reached sooner. It also shows that pressure build-up starts around the time of initial set, but the interval between initial and final set is longer and the pressure drop is observed at the time of final set.

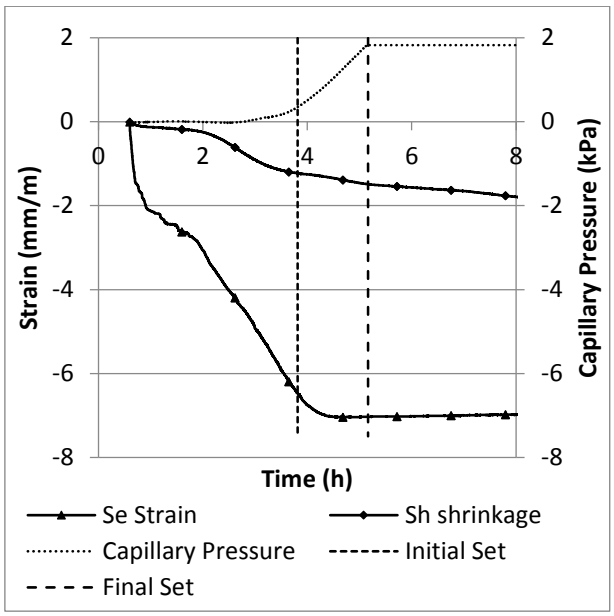

Figure 5.18: WB022_03SAP_75SAT_9mm

5.2.2.5 Summary

Figure 5.19 summaries all the mixes which have a 0.27 w/b with 6 mm stone and include the reference mix and internally cured mixes saturated at 75 and 50 %. Figure 5.20 presents the same mixes with 9 mm stone. These figures show that all internally cured mixes were successful in decreasing the plastic shrinkage and settlement.

It was expected that the internally cured mixes with 9 mm stone would have more settlement and less shrinkage than those with 6 mm stone. This was only observed for the mix saturated at 75 %. The converse was observed for the 50 % saturated mix where the mix with the larger stone exhibited a lower settlement and higher shrinkage than its counterpart containing 6 mm stone. The plastic shrinkage and settlement of the reference mixes with 6 and 9 mm stone were very similar.

One notable trend that can be observed from the plastic shrinkage results is that for internally cured concrete containing 6 or 9 mm stone, the shrinkage development starts sooner than the reference mix containing no SAP. More importantly, the shrinkage of the internally cured mixes also start to stabilise sooner than the reference mix. In fact, the shrinkage of most internally cured mixes stabilise at similar times to the settlement stabilisation. This is much sooner than the stabilisation for the reference mix and could suggest that SAP shows the potential to reduce plastic shrinkage.

Furthermore, these results show that the size of the stone does influence the shrinkage development of internally cured concrete. More tests are however needed to elaborate on how to control and manage this effect.

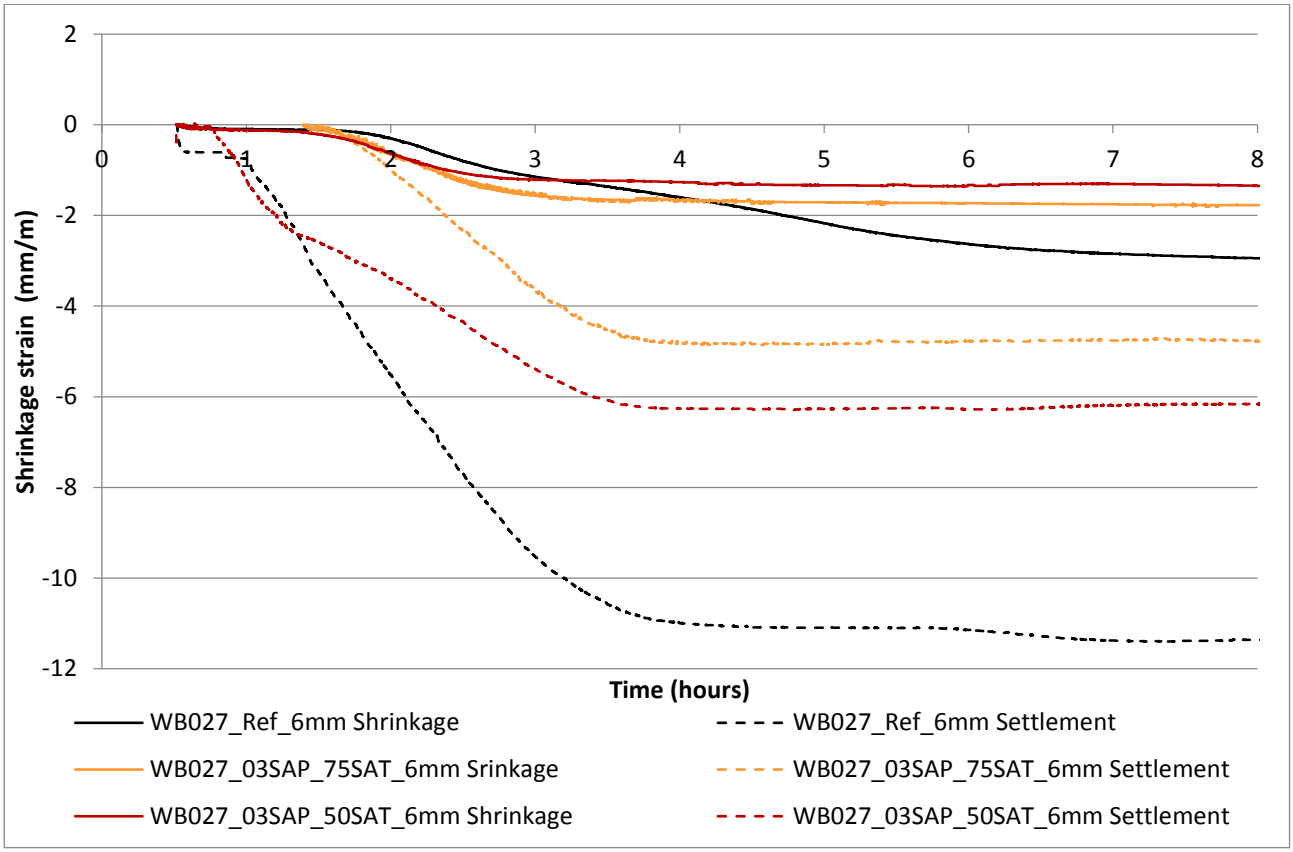

Figure 5.19: WB027_6mm set of tests

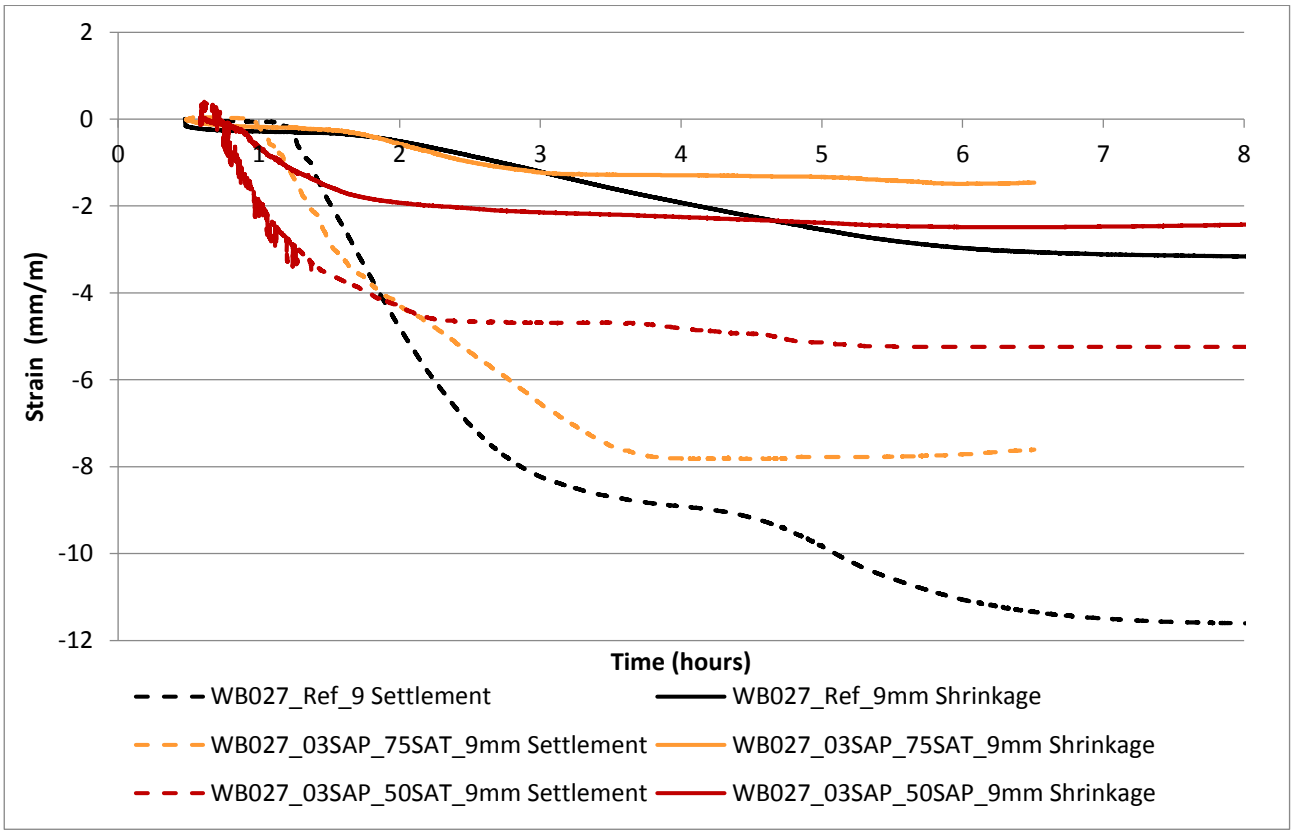

Figure 5.20: WB027_9mm set of tests

5.2.3 Compressive Strength

Figure 5.21 shows the 3, 7 and 28 day compressive strength of the concretes tested in this study. Similar to the paste results in Figure 5.11, the slump flow of each concrete mix was recorded with the compressive strength to determine if the amount of water added to a mix is related to the workability and if the workability in turn influences the strength. Furthermore, the workability and strength of the concretes were tested to observe if the coarse aggregate size caused more water to be available in the mix owing to internal water being squished out of SAP particles by the larger stone.

Different trends are observed for the two w/b ratios. For the WB022 set of mixes, the strength of the mixes with 9 mm stone are consistently lower that the exact same mix containing 6 mm stone. The mixes with 9 mm stone also showed a higher flow than its corresponding mix with 6 mm stone. This could be because a larger size stone has a lower water requirement so there is more mix water available. This small amount of extra water can then cause a higher flow and also results in a higher w/b ratio, causing a decrease in strength. This was observed for both the reference mix and the internally cured mixes, with SAP saturated at 75 %. Both mixes saturated at 50 % with 6 and 9 mm did not produce any flow. This suggests that SAP saturated at 50 % does not contain enough internal curing water. The SAP particles then absorb water from the mix water which effectively decreases the w/b ratio. For both stone sizes, in this set of tests, the presence of SAP increased the compressive strength of the reference mix containing no SAP. Interestingly, the strength gain is improved with a decrease in internal curing water even though the flowability is significantly affected.

In addition to SAP saturated at 75 and 50 %, the theoretical amount of water needed to fully saturate a given dosage of SAP was also tested for the WB027 set of mixes. In this set of mixes, with a higher w/b ratio, the mixes with 9 mm stone showed higher strength than the same mixes which contained 6 mm stone. The slump flows of these mixes does not have a strong correlation with the amount of internal curing water and strength gain. From Figure 5.21 it can be seen that mixes with SAP saturated at 100 % drastically reduces the strength compared to the reference mix. Decreasing the internal curing water to the 75 % saturation level then reduces the strength loss with respect to the reference mix. A further decrease in internal curing water to the 50 % saturation level shows that this amount of water is perhaps too low as the strength then decreases again.

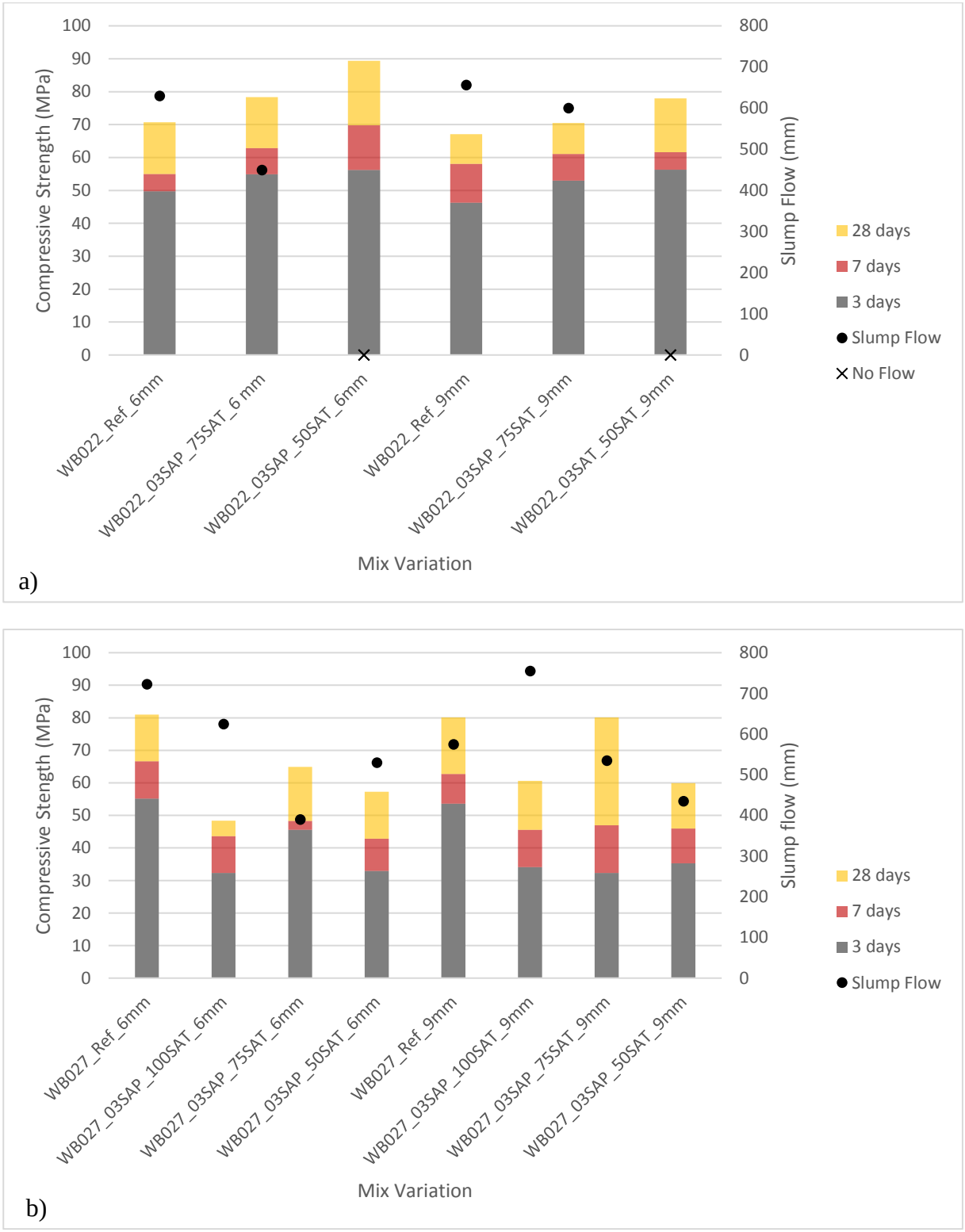

Figure 5.21: Compressive Strength and Slump flow of concretes a) WB022 and b) WB027

Interestingly for the w/b ratio of 0.27, even though the mixes saturated at 50 % had better workability and still produced a flow as opposed to the 50 % saturated mixes in the WB022 set, it did not further increase the strength.

5.3 Plastic Shrinkage Cracking

Only WB022_Ref_6mm was tested for plastic shrinkage cracking. On the first attempt to attain plastic shrinkage cracking results, surprisingly, the mix did not crack. Adjustments were then made to the mould, mix and climate conditions in an effort to get the reference mix to crack so as to implement the use of internal curing agents as a solution to alleviate plastic shrinkage cracking. The crack moulds described in Section 4.1.2.3 were used and were placed in the climate chamber at different evaporation rates as discussed in the following.

5.3.1 Attempt 1

The reference mix WB022_Ref_6mm given in Table 3.5 was used in the first attempt. The layout and dimensions of the crack mould are presented in Section 4.1.2.3. The dimensions of the restraints are the standard dimensions given in ASTM C 1579 (2006). The temperature, wind and relative humidity was set the same as those used for the plastic shrinkage tests which resulted in an evaporation rate of 1.3 kg/m^2/hr and are presented in Table 4.2.

When carrying this test out for NSC, the mixes typically bleed soon after placing and soon after the bleed water is evaporated from the surface of the concrete, a hairline crack forms on the sides of the mould directly above the restraint. The crack would then widen and propagate at an increasing rate until the time of initial set where the crack growth slows down. Typically, crack growth would stop at final set and the test is complete.

These HPC mixes did not bleed and so, it was expected that cracks would form sooner and grow more rapidly than NSC due to the high cement content which lends itself to a bigger crack risk. However, this was not the case. Even after leaving the moulds in the climate chamber for 12 hours, no cracks were visible on the surface of the concrete. After demoulding, a hairline crack could be seen on the sides propagating from the big restraint in the middle of the mould. This can be seen in Figure 5.22. The crack had formed at the point of restraint, but it did not propagate all the way to the surface. The reason for this could be that by the time the crack reaches a certain height, the concrete has already acquired enough strength to resist the shrinkage forces which typically result in surface cracks in the presence of a restraint. Another test was then carried out after adjusting the mould to provide more restraint for the stronger concrete.

Figure 5.22: Plastic shrinkage cracking for the first attempt

5.3.2 Attempt 2

The height of the triangle in the middle of the mould was increased to 75 mm so as to decrease the distance that the crack needs to travel to reach the surface of the concrete. The same mix that was tested in the first attempt was tested in the second, except that the sand was not sieved. This was done to increase the fines content of the mix, consequently increasing its crack risk. Again, no cracks were visible on the surface of the concrete body, even after 12 hours.

After demoulding, a crack was visible propagating from the restraint, but not reaching the surface of the concrete body. Figure 5.23 shows this crack and it can be seen that the distance from the end of the crack to the surface of the concrete is smaller than that in the first attempt. This shows that the restraint provided is still not big enough for the strength that the HPC can develop in the plastic and setting phases.

A third attempt was then carried out using the same mix and mould, but increasing the evaporation rate.

Figure 5.23: Plastic shrinkage cracking for the second attempt

5.3.3 Attempt 3

To simulate extreme conditions in the climate chamber, the wind speed was increased to 35 km/h. This resulted in an evaporation rate of 1.85 kg/m^2/hr, with the temperature and relative humidity the same as for the plastic shrinkage tests. Even with this extreme conditions, cracks were still not visible on the surface of the concrete. Figure 5.24 shows the side of the concrete specimen after the completion of the test. The picture shows that the crack propagated higher than in the previous attempts.

After demoulding, the specimen broke in half, along the breadth where the big restraint is located. This showed that in this attempt, the extreme weather conditions increased the vulnerability to cracking, but the concrete was still able to develop enough strength in the plastic and setting phase to resist the shrinkage forces which result in cracking on the surface in the presence of a restraint.

Figure 5.24: Plastic shrinkage cracking for the third attempt

No further attempts were carried out to observe plastic shrinkage cracking of HPC. It was concluded that the prescribed test method and moulds were not suitable for HPC. From the shrinkage results in Section 5.2, it is evident that HPC has a high plastic shrinkage crack risk because of the high plastic shrinkage and settlement. The plastic shrinkage cracking test carried out in this study does not prove that cracking is not a concern for HPC as the test method was developed for NSC.

5.4 Concluding Summary

This chapter presented the results of autogenous shrinkage and compressive strength of the pastes tested in this study and the plastic shrinkage, plastic settlement, plastic shrinkage cracking and compressive strength results of the concrete mixes. The plastic shrinkage cracking tests were unsuccessful as the mixes did not result in surface cracks. Figure 5.25 and Figure 5.26 summaries the rest of the results of all the paste and concrete mixes for w/b ratio of 0.22 and 0.27 respectively.

The mixes are grouped according to the amount of internal curing water added to a mix as a percentage of the theoretical saturation level of the SAP added per mix. The SAP dosages tested was 0.3 % bwoc for both the pastes and concretes and in addition 0.5 % SAP bwoc were added to the pastes. From these figures it is possible to easily compare the results of concretes which contained the same amount of SAP and internal curing water, but different stone sizes of 6 and 9 mm.

Figure 5.25 for mixes with w/b 0.22 show that the concrete with the bigger stone resulted in a lower compressive strength compared to the 6 mm. Figure 5.26 for mixes with w/b ratio of 0.27 on the other hand consistently showed an increase in compressive strength for mixes with a bigger stone.

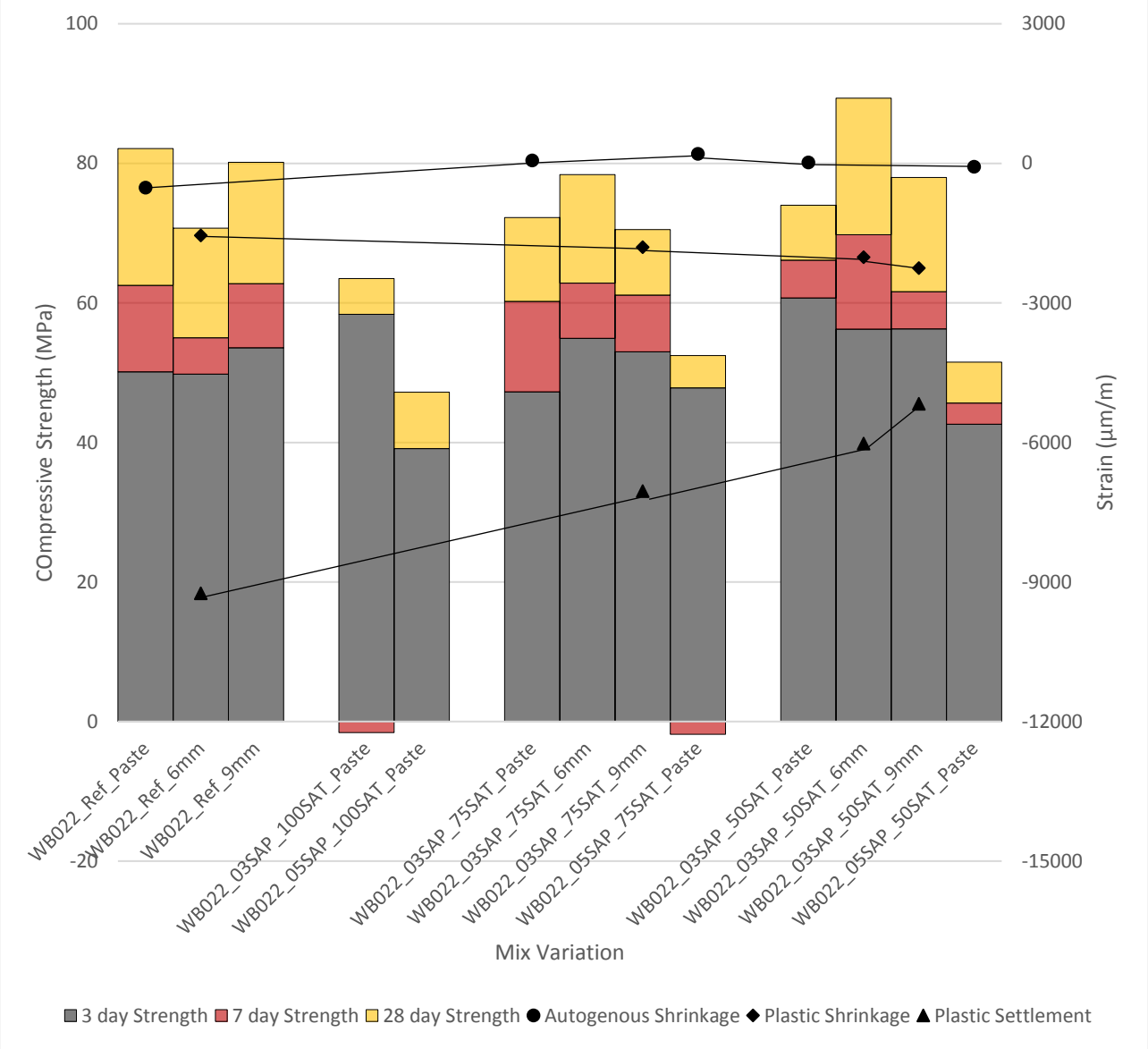

Figure 5.25: Compression Strength, Autogenous Shrinkage, Plastic Shrinkage and Plastic Settlement of WB022 set of mixes

Considering the paste mixes with 0.5 % bwoc, it can be seen that the compressive strength drops considerably from the same mix with less SAP for both w/b ratios. While there is a notable change in compressive strength for a higher dosage of SAP, the change in autogenous shrinkage is not as much. The dots above the zero line on the figure represent autogenous expansion and the markers below represent shrinkage i.e. reduction in volume. The shrinkage data are also shown on these two figures in terms of the maximum shrinkage or expansion experience for that mix.

The plastic shrinkage and settlement show an interesting trend as the amount of internal curing water decreases. As the amount of internal curing water decreases in a mix, the plastic shrinkage seems to increase and the plastic settlement decreases notably.

For the mixes with w/b ratio of 0.22, the plastic shrinkage of the internally cured mixes were all higher than the reference mix while the plastic settlement was mitigated for all internally cured mixes.

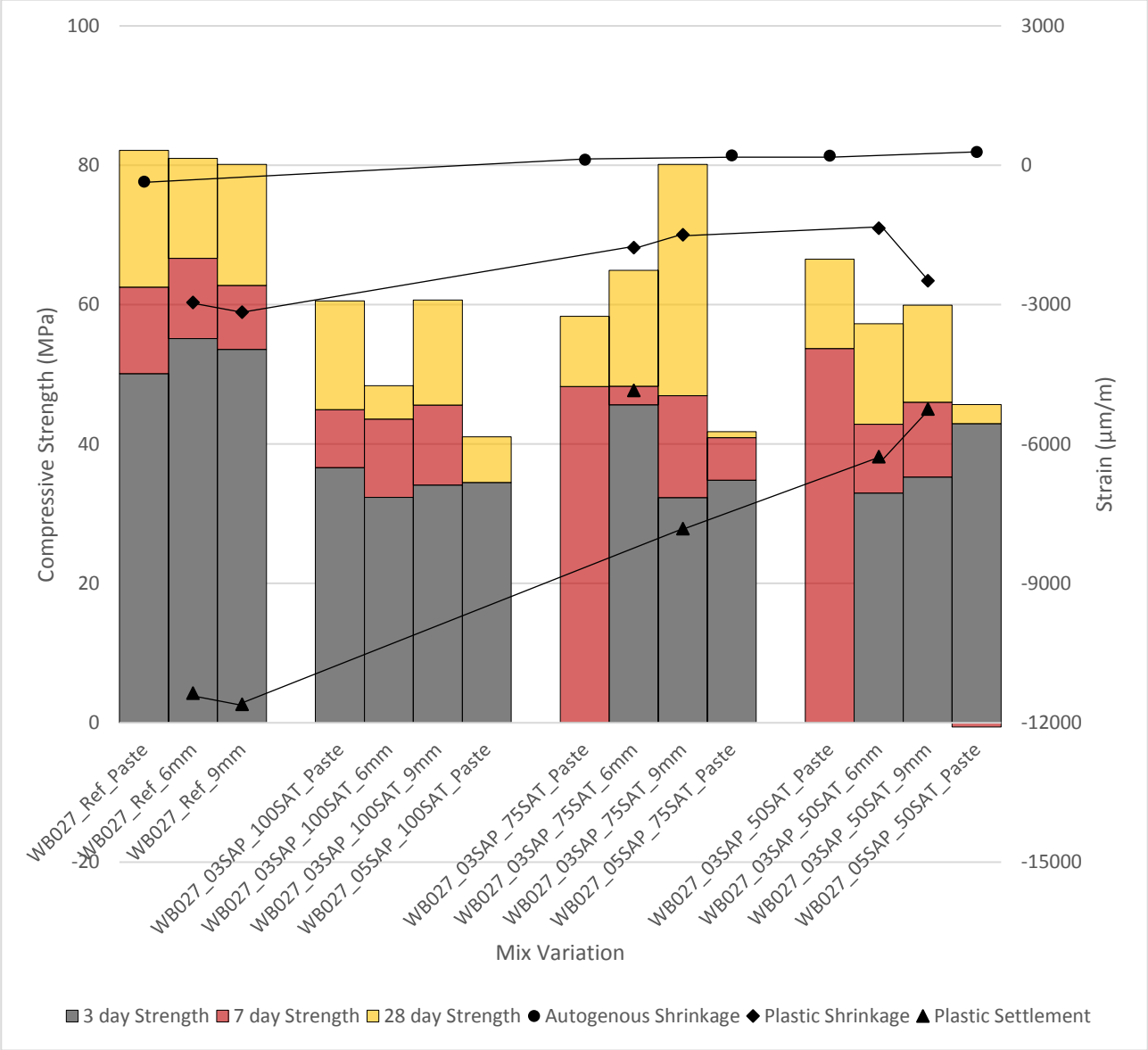

Figure 5.26: Compression Strength, Autogenous Shrinkage, Plastic Shrinkage and Plastic Settlement of WB027 set of mixes

The next chapter summaries all these observations in conjunction with what can be learnt from the literature study and previous tests to draw conclusions and make recommendations for future studies

Chapter 6

Conclusions and Recommendations

The use of high performance concrete (HPC) is becoming more popular and attractive for its excellent durability and prospects of improvement in concrete design and construction. The challenges faced with producing a HPC is sticky mixes and mixes with high early-age shrinkage and cracking due to the low water to binder (w/b) ratio.

This study observed the extent of early-age volume change in HPC with low w/b ratios by observing autogenous shrinkage using the corrugated tube method as well as plastic shrinkage. Super absorbent polymers (SAP), along with extra internal curing water, were introduced to these cement-rich mixes as an internal curing agent to reduce the shrinkage. However, the SAP caused a loss in compressive strength due to the extra water which effectively increased the w/b ratio.

To achieve the objectives of this study to observe the mitigation of autogenous shrinkage of internally cured concrete, the corrugated tube method for autogenous shrinkage of pastes was set up. A careful material selection process was carried out to develop self-compacting mixes that could fill the testing moulds easily without creating too much voids. To provide insight to the use of SAP in HPC in South Africa, the conclusions are summarised as a guideline to the dosage of SAP and internal curing water needed to mitigate early-age shrinkage and cracking without compromising the compressive strength extensively.

6.1 Conclusions

Previous studies have shown that the amount of internal curing water is often over estimated for the absorption capacity of SAP in low w/b concretes. The factors which affect the absorption and desorption kinetics of SAP is w/b, aggregate content and stone size. The theoretical saturation level was determined, using the tea-bag test, for the two w/b ratios tested in this mix, 0.22 and 0.27. This theoretical amount of water was then decreased to 75 % and 50 % to see if it would have a positive effect of the compression strength. The 100 % level of saturation was only tested for compression strength and not for any of the shrinkage tests.

The tea-bag test showed the following:

- The theoretical amount of water needed to saturate a given dosage of SAP is 25 g/g. This is taking into account the presence of cement and silica fume particles in solution.

- The simulated pore solution containing cement and silica fume shows a maximum absorption capacity just before 20 minutes and then a sudden desorption of water from the SAP. This test was carried out 30 min after water was added to the cement and shows that there is an increase in the concentration of the ions after a longer period of time, which reverses the concentration gradient and causes desorption instead of further absorption after only 20 minutes in the pore solution. Not taking this into account adds to the over estimation of the absorption capacity of SAP.

The effect of altering the amount of internal curing water on the compressive strength of paste and concrete mixes is as follows:

- Adding 100 % of the theoretical amount of internal curing, 25 g/g, to the pastes causes a 23 % decrease in the compressive strength of the reference paste with w/b 0.22 and a 26 % decrease for the reference paste with a w/b ratio of 0.27.

- Adding 100 % of the theoretical amount of internal curing, 25 g/g, to the reference concrete with w/b ratio of 0.27 causes a 40 % decrease in the compressive strength of the mix with 6 mm stone and a 25 % decrease for the mix with 9 mm.

- The paste and concrete mixes for w/b ratio of 0.22 show that the compressive strength of the respective mixes increases as the internal curing water is reduced from 100 % to 75 % and 50 %.

- The mixes saturated at 50 % for w/b ratio of 0.22 show no flow. This suggests that the SAP absorbed water from the mix water because the internal curing water added is not sufficient. Although these mixes show no flow, they reach a higher strength due to the decrease in effective w/b, despite the difficulties in placing and compaction.

- The paste and concrete mixes for w/b ratio of 0.27 show that the compressive strength of the respective mixes decrease drastically when saturated at 100 %. Decreasing the internal curing water to 75 % increases the compression strength of the concretes only, and not the pastes. When reducing the internal curing water further to 50 %, the opposite occurs. The compression strength of the concretes now decreases and the compression strength of the paste increase.

- The presence of aggregate has a profound effect on the absorption and desorption kinetics of the SAP. It is also concluded that there is not a linear relationship between the stone size and the compressive strength, but rather that the stone size is a contributing factor to the desorption kinetics in combination with the other physical properties of the mix.

The increase in SAP dosage from 0.3 % to 0.5 % in paste mixes showed the following:

- There is an average of 20 % decrease in compressive strength in pastes that contained 0.5 % SAP bwoc compared to the same paste containing 0.3 % SAP.
- Increasing the SAP dosage, along with the relative increase in internal curing water, increases the effective w/b ratio and also provides more voids which lead to greater strength loss.
- 0.5 % dosage of SAP is too high for pastes and concretes.

The effect of altering the amount of internal curing water on the autogenous shrinkage of paste mixes is as follows:

- Adding SAP and internal curing water successfully mitigates autogenous shrinkage and even results in autogenous expansion for all mixes with the exception of one.
- The same trend is not seen for both w/b ratios. The pastes with a w/b ratio of 0.22 show that the SAP saturated at 75 % for both dosages of SAP are more successful in mitigating autogenous shrinkage than those saturated at 50 %.
- The paste mixes with w/b ratio of 0.27 show more successful mitigation of autogenous shrinkage for mixes which have a higher dosage of SAP. The mixes saturated at 75 % and 50 % with a SAP dosage of 0.5 % perform better than those with a SAP dosage of 0.3 %.
- Analysing the autogenous shrinkage from different points of time zero show completely different results. Comparing the shrinkage from the time water was added to the mix with the shrinkage from the time of initial and final set show that the bulk of the change in volume happens in the plastic and setting phase, but mainly the plastic phase.
- The shrinkage that occurs before final set was not regarded as autogenous shrinkage. Considering the shrinkage development in the three phases between these points of time zero show that the results after final set is more reliable as the specimens are less susceptible to being affected by errors and inconsistencies in the test method. The results after final set are thus more reliable and comparable.

- The shrinkage that happens before final set is often ignored when presenting autogenous shrinkage results. This is misleading and suggests that internal curing mitigates all autogenous shrinkage and that there is no reduction in volume. However, considering the shrinkage from the time water is added shows that there is still a significant shrinkage taking place in internally cured concrete during the plastic and setting phase.

- Although observing autogenous shrinkage from the time of final set is more reliable in terms of ruling out the uncertainties in results introduced by discrepancies in the test set up, it is worthwhile to study the autogenous shrinkage during the plastic phase as well, as most of the shrinkage takes place in this phase.

The effect of two different stone sizes on the plastic shrinkage of concrete mixes was that:

- The larger stone did not increase both the plastic shrinkage and settlement of the same mix containing 6 mm stone as expected.

- The plastic shrinkage and settlement of the reference mix containing no SAP is the same for the mix containing 6 mm and 9 mm stone. This is not the case for the internally cured mixes. In all cases, the bigger stone caused less settlement and more shrinkage than the corresponding mix with the smaller stone.

- The effect of the change in stone size is only seen in the internally cured mixes and not the reference mix which shows that the stone size has a direct effect on the plastic shrinkage and settlement of internally cured mixes.

- It was expected that a bigger stone would provide more resistance to plastic shrinkage and increase plastic settlement due to a larger particle squishing the SAP particles. The reasons for an increase in plastic shrinkage and decrease in plastic settlement is uncertain and more tests are required to reach a conclusion.

The effect of w/b ratio on the plastic shrinkage of concrete mixes is as follows:

- Decreasing the w/b ratio did not increase the shrinkage and settlement for the reference mixes as expected.

- An increase in plastic shrinkage and settlement was seen for the internally cured mixes for the mixes with the lower w/b ratio of 0.22.

- All the mixes with a lower w/b ratio shows that the initial and final set is reached before the capillary-pressure drop. Capillary pressure for these mixes only starts to build up around initial set compared to the mixes with a higher w/b where the pressure drops at initial set.

- A later build up in pressure is related to the later initial and final set and suggests that the plastic shrinkage and plastic settlement should be more. The increase in plastic settlement and plastic shrinkage is because before initial set, the concrete has very little tensile strength capacity to resist the shrinkage forces which cause volume change. This plastic phase is where the bulk of the shrinkage occurs so a longer plastic phase will accumulate more shrinkage.

- This is only observed for the internally cured mixes. It could be that there was a discrepancy in the test results of the reference mixes, but more tests would need to be done to verify this.

The effect of altering the amount of internal curing water on the plastic shrinkage of concrete mixes is as follows:

- The use of SAP and internal curing water was effective in reducing the plastic shrinkage and settlement compared to all reference mixes containing no SAP. The trends shown between saturation level of SAP, w/b ratio and stone size were not linear.

- The only linear trend that is observed was for internally cured concretes which have the highest plastic shrinkage, the settlement is the lowest. And the internally cured mix with the lowest plastic shrinkage, have the highest plastic settlement.

- For all tests, the plastic shrinkage of the internally cured mixes started to develop sooner than that of the reference mix. This may be due to the extra water that is available in the mix that is being evaporated from the mix more readily than the lesser amount of water in the reference mixes.

- On the basis of tensile strength being 10 % of compressive strength, internally cured concrete with a lower compressive strength than the reference mix has a lower tensile strength and consequently cannot resist the shrinkage forces which cause volume change in the plastic phase where the tensile strength for internally cured concrete is lower than the reference mix.

- Although the plastic shrinkage of the internally cured mixes start sooner, they stabilise sooner and result in a lower overall shrinkage.

- For concrete mixes with a w/b ratio of 0.27 and 6 mm stone a 50 % saturation level was most effective in reducing plastic shrinkage and a saturation level of 75 % was most effective in reducing plastic settlement.

- For concrete mixes with a w/b ratio of 0.27 and 9 mm stone, the exact opposite was observed where the saturation level of 75 % was most effective in reducing plastic shrinkage and a saturation level of 50 % was most effective in reducing plastic settlement.

- For concrete mixes with a w/b ratio of 0.22, only the saturation level of 50 % was tested with both 6 and 9 mm and the saturation level was tested with 9 mm stone.

The plastic shrinkage cracking test results were as follows:

- Plastic shrinkage cracking was not observed for WB022_Ref_6mm using the standard method of plastic shrinkage cracking for NSC

- A hairline crack was formed at the restraint, but it did not propagate all the way to the surface.

- Increasing the restraint in the mould caused the crack to propagate higher, but it still not reach the surface.

- Increasing the evaporation rate as well caused the hairline crack to propagate even higher up, but still was not observed on the surface of the concrete.

- This shows that the test method and moulds are not suitable for testing plastic shrinkage cracking of HPC as the strength and shrinkage development of HPC is principally different to that of NSC.

- Furthermore, it can be argued that cracks were not observed at the surface of the concrete as the concrete body is strong enough to resist shrinkage forces, even in the plastic and setting phase.

6.2 Recommendations

After analysing and discussing the results of the tests carried out in this study, the following recommendations can be made for future investigation

- Evaluate the flowability as well as the strength development of pastes with varying dosages of superplasticiser to find the optimum superplasticiser dosage that has high flowability without the reduction in strength.

- Conduct a study on using particle size optimisation for producing a HPC mix.

- Evaluate the use of non-contact electrical resistivity method (ERM) as an alternative to the Vicat apparatus for setting time development in conjunction with strength gain.

- Observe and compare different setting time testing methods that are sensitive to volume change, stress development and structure development.

- Perform the tea bag test at a delayed time after mixing the simulated pore solution to take in to account the mixing and placing time of internally cured pastes and concretes that may have a higher ion concentration.

- Study autogenous shrinkage that occurs in pastes during the plastic and setting phases.

- Observe the autogenous and plastic shrinkage of pastes and concretes at 100 % saturation level as well as saturation levels higher than 100 % for a better insight to the effect of extra internal curing water on compressive strength in relation to early-age volume change.

- Observe tensile strength development of fresh concrete along with shrinkage as it directly affects the ability of the concrete body to resist the shrinkage forces which cause volume change.

- Use tensile strength development in relation to shrinkage development to determine the early-age crack risk of pastes and concretes.

6.3 Closing Statement

The w/b ratio, stone size, SAP dosage and amount of internal curing water are central to the performance of SAP in low w/b ratio pastes and concretes. These factors cannot be isolated and do not affect the compressive strength and early-age shrinkage linearly. An extensive set of tests varying these factors would be worthwhile to provide a guideline for the use of SAP in HPC in South Africa.

References

AbdElrahman, M. & Hillemeier, B., 2014. Combined effect of fine fly ash and packing density on the properties of high performance concrete: An experimental approach. *Construction and Building Materials*, 58, pp.225–233. Available at: http://dx.doi.org/10.1016/j.conbuildmat.2014.02.024.

Addis, B., 1998. *Fundamentals of Concrete*, Cement and Concrete Institute.

Aïtcin, P., 1998. *High-Performance Concrete*,

Aïtcin, P.., 2003. The durability characteristics of high performance concrete: a review. *Cement and Concrete Composites*, 25(4-5), pp.409–420. Available at: http://linkinghub.elsevier.com/retrieve/pii/S0958946502000811 [Accessed May 25, 2016].

De Almeida, I.R. & Goncalves, A.F., 1990. Properties of Freshly Mixed, High Strength Concretes. In H. J. Wierig, ed. *Properties of Fressh Concrete*. Hanover: Chapman and Hall, pp. 227–234.

Andreasen, A. & Andersen, J., 1930. Über die Beziehung zwischen Kornabstufungund Zwischenraum in Produkten aus losen Körnern (mit einigen Experimenten). *Kolloid-Zeitschrift*, (50), pp.217–228.

ASTM C 125, 2000. Terminologly relating to concrete and concrete aggregates. *ASTM International*.

ASTM International, 2009. Standard Test Method for Autogenous Strain of Cement Paste and Mortar. *C1698 – 09*.

ASTM International, 2010. Standard Test Method for Flow of Grout for Preplaced-Aggregate Concrete (Flow Cone Method)1. *C939 – 10*.

Bentur, A., 2003. *Early Age Cracking in Cementitious Systems - Report of RILEM Technical Committee TC 181-EAS: Early age shrinkage induced stresses and cracking in cementitious systems*, Bangneux: RILEM Publications SARL.

Bentur, A., Igarashi, S. & Kovler, K., 1999. Control of autogenous shrinkage stresses and cracking in high strength concretes. In *Proc. 5th Int. Symp. on Utilization of High Strength/Performance Concrete*. Sandefjord, Norway, pp. 1017–1026.

Bentur, A., Igarashi, S. & Kovler, K., 2001. Prevention of autogenous shrinkage in high-strength concrete by internal curing using wet lightweight aggregates. , 31, pp.1587–1591.

Bentz, D. & Jensen, O., 2004. Mitigation strategies for autogenous shrinkage cracking. *American Concrete Institute*, (26), pp.77–85.

Beushausen, H. & Dehn, F., 2009. High-Performance Concrete. In G. Owens, ed. *Fulton's Concrete Technology*. Midrand: Cement and Concrete Institute, pp. 297–303.

Billberg, P., 1999. Fine mortar rheology in mix design of SCC. In *PRO 7: First International Symposium of Self-Compacting Concrete*. pp. 47–57.

Bjøntegaard, Ø. & Sellevold, E., 2003. Very High Strength Concrete. In A. Bentur, ed. *Early Age Cracking in Cementitous Systems - Report of RILEM Technical Committee TC 181-EAS: Early age shrinkage induced stresses and cracking in cementitious systems*. Norweg: RILEM Publications SARL, pp. 285–294.

Bonen, D. & Shah, S.P., 2005. Fresh and hardened properties of self-consolidating concrete. *Prog. Struct. Engng Mater.*, 7, pp.14–26.

Brouwers, H.J.H. & Radix, H.J., 2005. Self-compacting Concrete: The Role of the Particle Size Distribution. In *First International Symposium on Design, Performance and Use of Self-consolidating Concrete*. Changsha, Hunan, pp. 109–118.

Buchholz, F.L. and A.T.G., 1998. Modern superabsorbent polymer technology. In New York: John! Wiley & Sons.

Combrinck, R., 2011. *Plastic shrinkage cracking in conventional and low volume fibre reinforced concrete*. University of Stellenbosch.

Craeye, B., Geirnaert, M. & De Schutter, G., 2011. Super absorbing polymers as an internal curing agent for mitigation of early-age cracking of high-performance concrete bridge decks. *Construction and Building Materials*, (25), pp.1–13.

Craeye, B. & De Schutter, G., 2006. Experimental Evaluation of Mitigation of Autogenous Shrinkage by means of a Vertical Dilatometer for concrete. In O. M. Jensen, P. Lura, & K. Kovler, eds. *Proc. Int. RILEM Concference - Volume Changes of Hardening Concrete: Testing and Mitigation*. pp. 21 – 30.

Darquennes, A. et al., 2011. Effect of autogenous deformation on the cracking risk of slag cement concretes. *Cement and Concrete Composites*, 33(3), pp.368–379. Available at: http://linkinghub.elsevier.com/retrieve/pii/S0958946510001952 [Accessed July 10, 2014].

Domone, P. & Illston, J., 2010. *Construction Materials: Their Nature and Behaviour* Fourth Edi.,

Esteves, P., 2010. ON THE ABSORPTION KINETICS OF SUPERABSORBENT. , (August).

Felekoğlu, B., Türkel, S. & Baradan, B., 2007. Effect of water/cement ratio on the fresh and hardened properties of self-compacting concrete. *Building and Environment*, 42(4), pp.1795–1802. Available at: http://linkinghub.elsevier.com/retrieve/pii/S0360132306000291 [Accessed May 21, 2016].

Filho, R.D.T. et al., 2012. Effect of Superabsorbent Polymers on the Workability of Concrete and Mortar. In V. Mechtcherine & H.-W. Reinhardt, eds. *Application of Superabsorbent Polymers (SAP) in Concrete Construction- State of the Art Report Prepared by Technical Committee 225-SAP*. Springer, pp. 39–50.

Friedrich, S., 2012. Super Absorbent Polymers (SAP). In V. Mechtcherine & H.-W. Reinhardt, eds. *Application of Superabsorbent Polymers (SAP) in Concrete Construction State of the Art Report Prepared by Technical Committee 225-SAP*. Springer, pp. 13 – 19.

Fuller, W.B. & Thompson, S.E., 1907. The Laws of proportioning Concrete. *Transactions of the American Society of Civil Engineers*, LIX(2), pp.67–143.

Fulton, 2009. *Fulton's concrete technology* Ninthe. F. Beushausen, H; Dehn, ed., Midrand: Cement and Concrete Institute.

Funk, J.E. & Dinger, D.R., 1994. *Predictive process control of crowded particulate suspensions*, Massachusets: Kluwer Academic Publishers.

Geiker, M., Bentz, D. & Jensen, O., 2004. Mitigating autogenous shrinkage by internal curing. *American Concrete Institute*, (218), pp.143 – 148.

Goldman, A. & Bentur, A., 1993. Effects of Pozzolanic and non-reactive microfillers on the transition zone in high strength concrete. In J. . Maso, ed. *Interfaces in Cementitious Composites*. Palestine: EN & F Spon.

Hunger, M., 2010. *An integral design concept for ecological self-compacting concrete*. Technische Universiteit Eindhoven.

Jayasree, C. & Gettu, R., 2008. Experimental study of the flow behaviour of superplasticized cement paste. *Materials and Structures*, (41), pp.1581–1593.

Jensen, O., 2008. Use of Superabsorbent Polymers in Construction Materials. In W. et al. Sun, ed. *Proceedings of the first international conference on Microstructure Related Durability of Cementitious Composites*. Nanjing, China, pp. 757 – 764.

Jensen, O. & Hansen, P., 2002. Water-entrained cement-based materials II. Implementation and Experimental Results. *Cement and Concrete Research*, 32(6), pp.973 – 978.

Jensen, O., Lura, P. & Kovler, K., 2006. *Volume Changes of Hardening Concrete: Testing and Mitigation - Proceedings of the international RILEM conference (PRO 52)*,

Jensen, O.M. & Hansen, P.F., 2001a. Autogenous deformation and RH-change in perspective. , m(March), pp.1859–1865.

Jensen, O.M. & Hansen, P.F., 2001b. Water-entrained cement-based materials I. Principles and theoretical background. *Cement and Concrete Research*, (31), pp.647–654.

Jensen, O.M.H.P.., 1995. A dilatometer for measuring autogenous deformation in hardening Portland cement. *Materials and Structures*, 28(7), pp.406–409.

Kaufmann, J., Winnefeld, F. & Hesselbarth, D., 2004. Effect of the addition of ultrafine cement and short fiber reinforcement on shrinkage, rheological and mechanical properties of Portland cement pastes. *Cement and Concrete Composites*, 26(5), pp.541–549. Available at: http://linkinghub.elsevier.com/retrieve/pii/S0958946503000702 [Accessed July 24, 2014].

Khayat, K., 1998. Viscosity-enhancing admixtures for cement-based materials-an overview. *Cement and Concrete Composites*, 20, pp.171–178.

Li, Z., 2011. *Advanced Concrete Technology*, Hoboken, NJ, USA: John Wiley & Sons.

Li, Z. et al., 2007. Determination of Concrete Setting Time Using Electrical Resistivity Measurement. , (May), pp.423–427.

Li, Z. & Li, W., 2003. Contactless, Transformer-based measurement of the Resistivity of Materials. , 2(12), pp.0–5.

Lothenbach, B. & Winnefeld, F., 2006. Thermodynamic modelling of the hydration of Portland cement. *Cement and Concrete Research*, 36(2), pp.209–226. Available at: http://linkinghub.elsevier.com/retrieve/pii/S000888460500075X [Accessed August 7, 2015].

Lura, P. et al., 2012. Kinetics of Water Migration in Cement-Based Systems Containing Superabsorbent Polymers. In *Application of Superabsorbent Polymers (SAP) in Concrete Construction State of the Art Report Prepared by Technical Committee 225-SAP*. Springer, pp. 21 – 37.

Lura, P. & Jensen, O.M., 2006. Measuring techniques for autogenous strain of cement paste. *Materials and Structures*, 40(4), pp.431–440. Available at: http://www.springerlink.com/index/10.1617/s11527-006-9180-2 [Accessed July 12, 2014].

Matsuo, S. et al., 1994. Evaluation of superplasticizers for self compacting concrete with mortar test. *JCA Proc. Cem. Concr*, 48, pp.374–378.

Mechtcherine, V., 2012. Introduction. In *Application of Superabsorbent Polymers (SAP) in Concrete Construction- State of the Art Report Prepared by Technical Committee 225-SAP*. pp. 1 – 6.

Mechtcherine, V. & Dudziak, L., 2012. Effects of Superabsorbent Polymers on Shrinkage of Concrete: Plastic, Autogenous, Drying. In *Application of Super Absorbent Polymers (SAP) in Concrete Construction*. pp. 63–98. Available at: http://www.springerlink.com/index/10.1007/978-94-007-2733-5.

Mehta, K., P & Monteiro, P.J.M., 1993. *Concrete: Microstructure, Properties and Materials* Third., California: McGraw-Hill.

Mohd. Zain, M.F., Islam, M.N. & Basri, I.H., 2005. An expert system for mix design of high performance concrete. *Advances in Engineering Software*, (36), pp.325 – 337.

Mönnig, S., 2009. *Superabsorbing additions in concrete - applications, modelling and comparison of different internal water sources*. University of Stuttgart.

Mönnig, S., 2005. Water saturated super-absorbent polymers used in high strength concrete. *Otto-Graf-Journal*, (16), pp.193 – 202.

Neville, A., 1995. *Properties of Concrete* Fourth Edi., Essex: Longman Group Limited.

Nielsen, L., 1993. Strength development in hardened cement paste: examination of some empirical equations. *Materials and Structures*, (26), pp.255–260.

Okamura, H. & Ouchi, M., 2003. Self-Compacting Concrete. *Advanced Concrete Technology*, 1(1), pp.5–15.

Olawuyi, B.J., 2016. *The Mechanical Behaviour of High-Performance Concrete with Superabsorbent Polymers (SAP)*. University of Stellenbosch.

Owens, G., 2009. *Fulton's Concrete Technology* Nineth. G. Owens, ed., Midrand: Cement and Concrete Institute.

Pieper, M., 2006. *Innere Nachbehandlung von Beton mittels wasserspeichernden Polymeren (Internal curing of Concrete via Superabsorbent Polymers)*. Aachen, Technische Hochschule.

Powers, T., 1958. Structure and Physical Properties of Hardened Portland Cement Paste. *Journal of the American Ceramic Society*, 41(1).

Powers, T., 1969. *The properties of fresh concrete*, New YOrk.

Previte, R.W., 1977. Concrete Slump Loss. *American Concrete Institute*, 74(8), pp.361–367.

Reinhardt, H.-W., Cusson, D. & Mechtcherine, V., 2012. Terminology. In V. Mechtcherine & H.-W. Reinhardt, eds. *Application of Superabsorbent Polymers (SAP) in Concrete Construction- State of the Art Report Prepared by Technical Committee 225-SAP*. Springer, pp. 7–12.

Sant, B.G. et al., 2009. Detecting the Transition in Cement Pastes Comparing experimental and numerical techniques. , (june).

Sant, G. et al., Detecting the Fluid-to-Solid Transition in Cement Pastes: Assessment Techniques. , pp.1–18.

Sant, G., Lafayette, W. & Lura, P., 2005. Measurement of Volume Change in Cementitious Materials at Early Ages: Review of Testing Protocols and Interpretation of Results. , C, pp.1–19. Available at: http://www.aqua-dtu.dk/upload/institutter/byg/nyheder/trb-06-1571-as submitted final.pdf.

De Scchutter, G. et al., 2008. Constituent Materials. In *Self-Compacting Concrete*. Boca Raton, pp. 21–31.

Schröfl, C., Mechtcherine, V. & Gorges, M., 2012. Relation between the molecular structure and the efficiency of superabsorbent polymers (SAP) as concrete admixture to mitigate autogenous shrinkage. *Cement and Concrete Research*, 42(6), pp.865–873. Available at: http://linkinghub.elsevier.com/retrieve/pii/S0008884612000646 [Accessed July 21, 2015].

Shah, S. & Ahmad, S., 1994. *High Performance Concrete: Properties and Application*, McGraaw-Hill.

Skarendahl, A. & Petersson, Ö., 2000. State-of-the-art report of rilem technical committee 174-SCC, self-compacting concrete. In *RILEM Publication*. Paris, pp. 17–22.

Slowik, V. et al., 2009. Simulation of capillary shrinkage cracking in cement-like materials. *Cement and Concrete Composites*, 31(7), pp.461–469. Available at: http://dx.doi.org/10.1016/j.cemconcomp.2009.05.004.

Slowik, V., Schmidt, M. & Fritzsch, R., 2008. Capillary pressure in fresh cement-based materials and identification of the air entry value. *Cement & Concrete Composites*, 30, pp.557–565.

Snoeck, D., Jensen, O.M. & De Belie, N., 2015. The influence of superabsorbent polymers on the autogenous shrinkage properties of cement pastes with supplementary cementitious materials. *Cement and Concrete Research*, 74, pp.59–67. Available at: http://linkinghub.elsevier.com/retrieve/pii/S0008884615001064 [Accessed August 18, 2015].

Sören Eppers, C.M., 2010. THE SHRINKAGE CONE METHOD FOR MEASURING THE AUTOGENOUS SHRINKAGE – AN ALTERNATIVE TO THE. , (August).

Staquet, S. et al., 2006. AUTOGENOUS SHRINKAGE OF A SELF-COMPACTING VHPC IN ISOTHERMAL AND REALISTIC TEMPERATURE CONDITIONS. In M. J. and F. P. J. Marchand, B. Bissonnette, R. Gagné, ed. *2nd International RILEM Symposium on Advances in Concrete through Science and Engineering*. RILEM Publications SARL, pp. 207–224. Available at: http://www.rilem.net/gene/main.php?base=05&id_publication=56&id_papier=2195.

Strategic Highway Research Program, 1991. Materials and Manufacture of High Performance Concrete. In *High Performance Concrete- A State-of-the-Art Report*. Washington, pp. 2.1–2.15.

Su, N., Hsu, K. & Chai, H., 2001. A simple mix design method for self-compacting concrete. , 31, pp.1799–1807.

Su, N. & Miao, B., 2003. A new method for the mix design of medium strength flowing concrete with low cement content. , i, pp.215–222.

Tange, M. et al., 2012. Can superabsorent polymers mitigate autogenous shrinkage of internally cured concrete without compromising the strength? *Construction and Building Materials*, 31, pp.226–230. Available at: http://dx.doi.org/10.1016/j.conbuildmat.2011.12.062.

Tazawa, E.-C., 1998. *Autogenous Shrinkage of Concrete*, Hiroshima: EN & F Spon.

Tian, Q. & Jensen, O.M., 2008. MEASURING AUTOGENOUS STRAIN OF CONCRETE WITH COR- RUGATED MOULDS. , c(October), pp.1501–1511.

Uchikawa, H. et al., 1992. Effect of admixture on hydration of cement, adsorption behaviour of admixture and fluidity and setting of fresh cement paste. *Cement and Concrete Research*, 22(6), pp.1115–1129.

Uno, P., 1998. Plastic Shrinkage Cracking and Evaporation formulas. *ACI Materials Journal*, 95(4), pp.365–75.

Walraven, J., 2003. Structural applications of self compacting concrete. In O. Wallevik & I. Nielsson, eds. *Proceedings of the Third RILEM International Symposium on Selfcompacting Concrete*. pp. 15–22. Available at: https://books.google.co.za/books?hl=en&lr=&id=5k8AD9lRw1gC&oi=fnd&pg=PA15&dq=walraven+self+compacting+concrete&ots=58UDb-B-MX&sig=Hz6U_sqLUhVEsOqrI8ng6L3ZWU4#v=onepage&q=walraven self compacting concrete&f=false.

Wang, X. et al., 2014. Assessing particle packing based self-consolidating concrete mix design method. *Construction and Building Materials*, 70, pp.439–452. Available at: http://linkinghub.elsevier.com/retrieve/pii/S0950061814008927 [Accessed November 3, 2014].

Weber, S. & Reinhardt, H.W., 1997. A New Generation of High Performance Concrete : Concrete with Autogenous Curing. , 7355(97).

Wei, X. & Xiao, L., 2013. Electrical resistivity monitoring and characterisation of early age concrete. *Magazine of Concrete Research*, 65(10), pp.600–607.

West, R.P., 1990. Concrete Retempering Without Strength Loss. In *Properties of Fresh Concrete*. pp. 134–141.

Wittmann, F.H., 1976. CEMENT and CONCRETE RESEARCH. Vol. 6, pp. 49-56, 1976. Pergamon Press, Inc. Printed in the United States. , 6, pp.49–56.

Xiao, L., Li, Z. & Wei, X., 2007. Selection of superplasticizer in concrete mix design by measuring the early electrical resistivities of pastes. *Cement and Concrete Composites*, 29(5), pp.350–356. Available at: http://linkinghub.elsevier.com/retrieve/pii/S0958946507000212 [Accessed June 28, 2016].

Xincheng, P., 2013. *Super-High-Strength High Performance Concrete*,

Zhutovsky, S., Kovler, K. & Bentur, A., 2004. Influence of cement paste matrix properties on the autogenous curing of high-performance concrete. *Cement and Concrete Composites*, 26(5), pp.499–507. Available at: http://linkinghub.elsevier.com/retrieve/pii/S0958946503000829 [Accessed February 24, 2016]

Appendix A.1

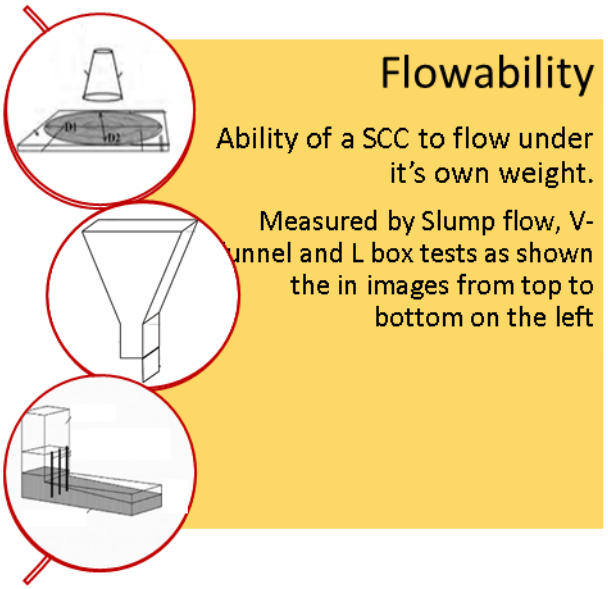

Flowability

Ability of a SCC to flow under it's own weight.

Measured by Slump flow, V-unnel and L box tests as shown the in images from top to bottom on the left

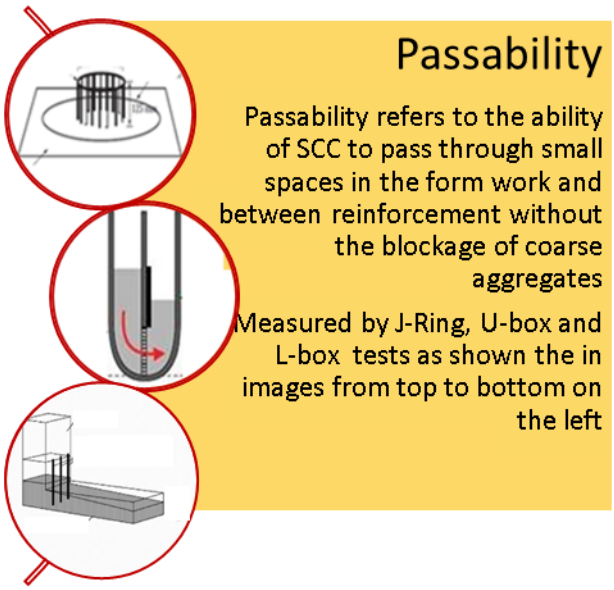

Passability

Passability refers to the ability of SCC to pass through small spaces in the form work and between reinforcement without the blockage of coarse aggregates

Measured by J-Ring, U-box and L-box tests as shown the in images from top to bottom on the left

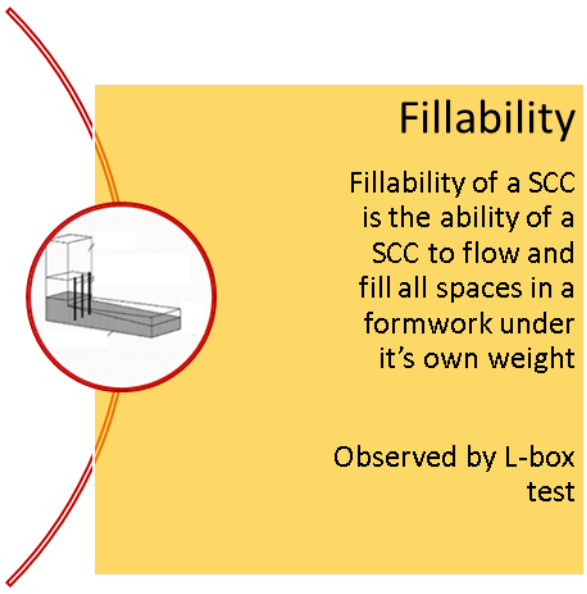

Fillability

Fillability of a SCC is the ability of a SCC to flow and fill all spaces in a formwork under it's own weight

Observed by L-box test

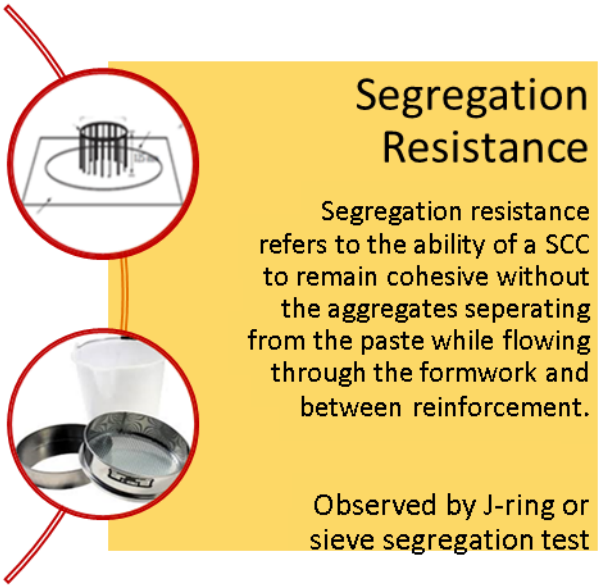

Segregation Resistance

Segregation resistance refers to the ability of a SCC to remain cohesive without the aggregates seperating from the paste while flowing through the formwork and between reinforcement.

Observed by J-ring or sieve segregation test

Appendix A.2

Slump flow classes	
Class	Slump flow in mm
SF1	550 - 650
SF2	660 - 750
SF3	760 - 850

Passing ability classes (L-box)	
Class	Passing ability, H_2/H_1
PA1	≥ 0.80 with 2 rebars
PA2	≥ 0.80 with 3 rebars

Viscosity classes		
Class	T_{500}, s	V-funnel time, s
VS1 / VF1	≤ 2	≤ 8
VS2 / VF2	> 2	9 - 25

Segregation resistance classes, sieve	
Class	Passing ability, %
SR1	≤ 20
SR2	≤ 15

Appendix B.1

Nomogram: ACI 305R-91
Hot Weather Concreting

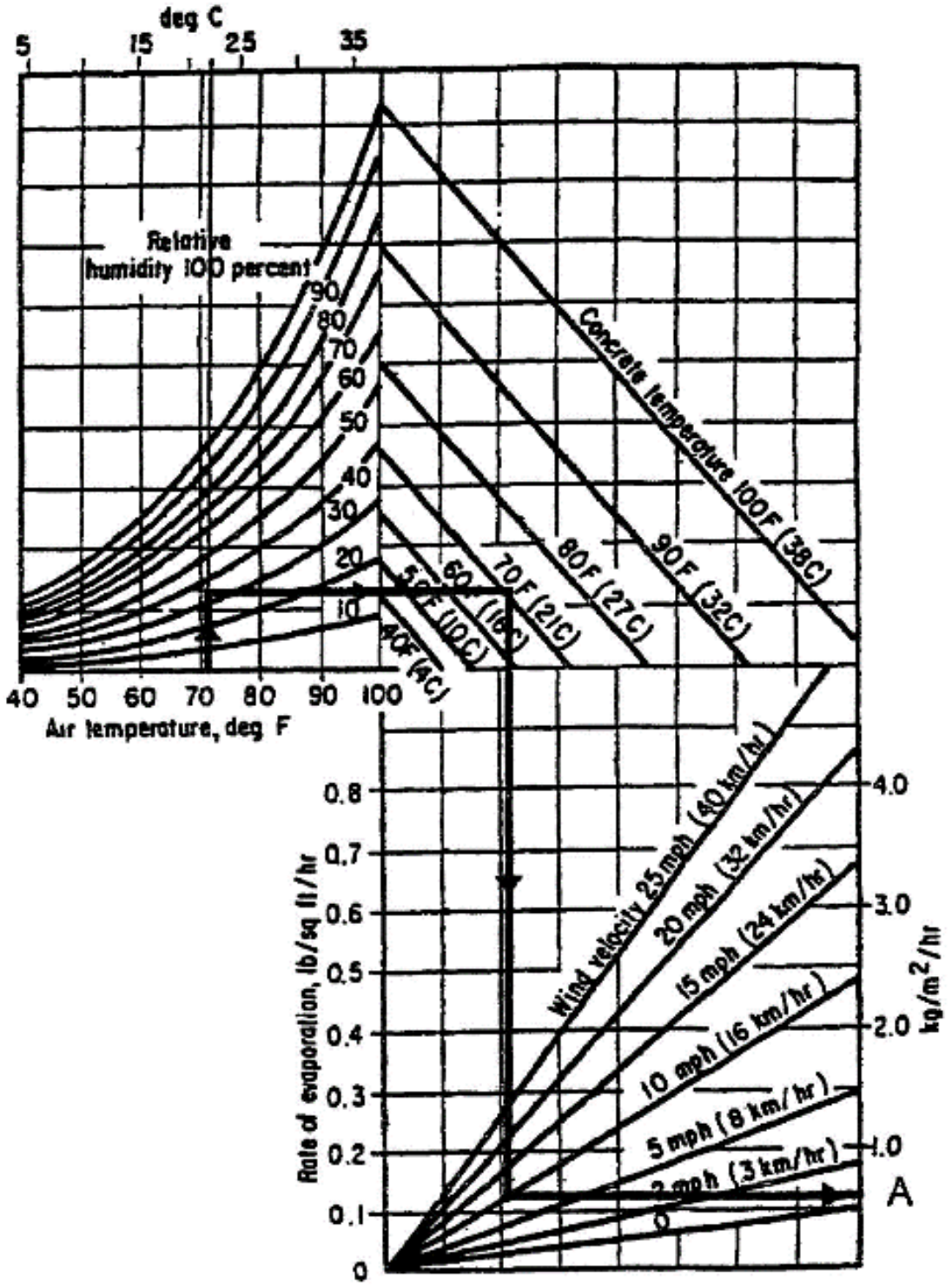

Appendix C.1

Supplementary Cementitious Material

Silica Fume and Fly Ash were considered as SCM in this study. Silica Fume was considered for its influence on strength development and fly ash was considered for its influence on flowability. The graph below shows the particle size distribution of cement, silica fume and fly ash.

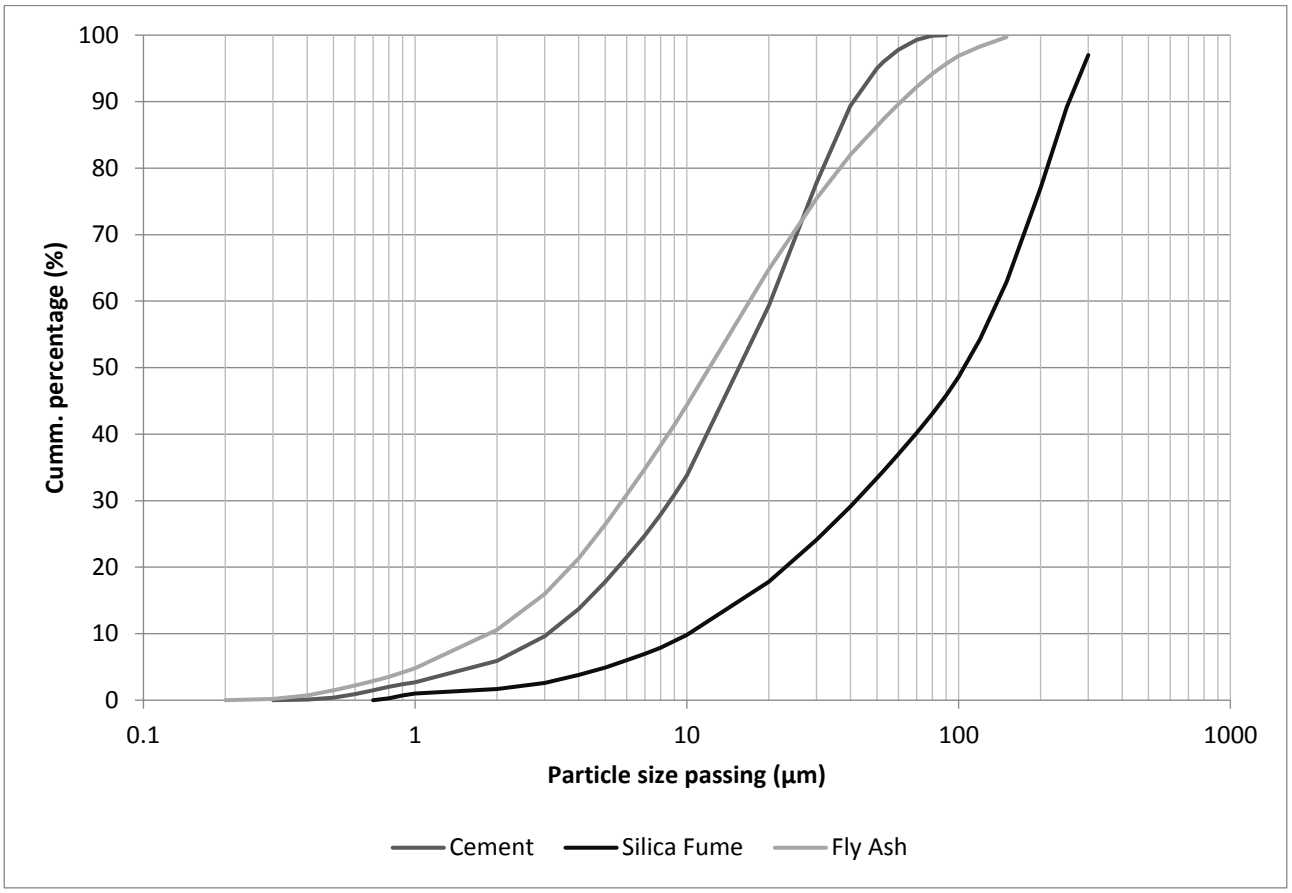

Particle size distribution of Cement, Silica Fume and Fly Ash

The graphs below show the 7 and 28 day strength of pastes with different proportions and combinations of binder made of cement with silica fume and/or fly ash at different w/c ratios. Fine aggregate was added to the paste containing 10 % silica fume to produce the mortar presented in the graphs and 6 mm stone was added to the mortar to produce the concrete. The use of fly ash improved the workability of the mixes dramatically compared to the mixes with only silica fume. However, this was a concern as these mixes were more prone to segregation at high dosages of superplasticiser. For this reason, only silica fume was used as a supplementary cementitious material in the binder as it was more stable in the presence of large dosages of superplasticiser. Looking at the pastes containing silica fume, with a w/c ratio of 0.25, 20 % silica fume replacement is too high and an estimation of 12 %, between 10 and 20 %, was chosen as a medium.

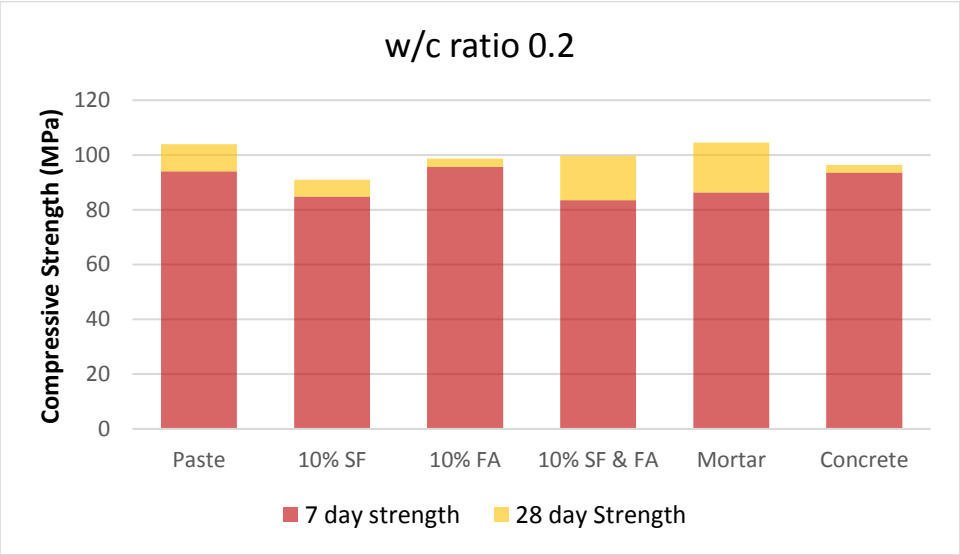

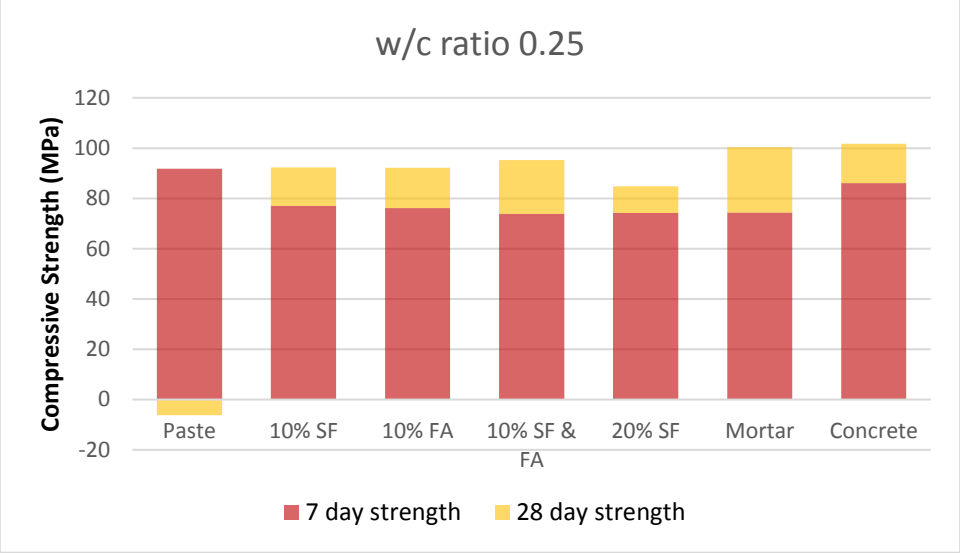

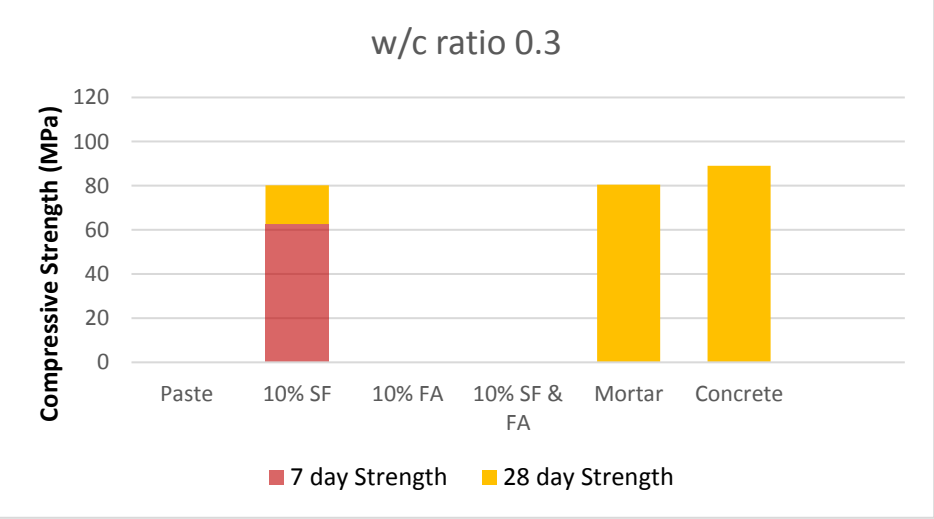

Appendix C.2

Superplasticiser Technical Datasheets

CHRYSO
LA CHIMIE AU SERVICE DES MATERIAUX DE CONSTRUCTION

CHRYSO®Fluid Premia 310

Superplasticizer – High range water reducer

CE NF NBN EN 934-2 | BENOR | 04/21

Description

CHRYSO®Fluid Premia 310 is a new generation superplasticizer based on a modified polycarboxylate polymer.

CHRYSO®Fluid Premia 310 is particularly recommended for concrete requiring high short and long term strength.

CHRYSO®Fluid Premia 310 allows the realisation of concrete with very low water / cement ratio.

CHRYSO®Fluid Premia 310 allows the realisation of self-compacting concrete, with an important filling capacity.

Thanks to its water reducing and workability maintaining performances, **CHRYSO®Fluid Premia 310** is particularly adapted for the realisation of self-compacting concrete for the realisation of reinforced concrete elements.

Characteristics

- Nature: liquid
- Colour: opalescent greenish grey
- Density (20° C): 1.050 ± 0.010
- pH: 6.7 ± 2.0
- Cl ions content: ≤ 0.10%
- Na_2O equivalent: ≤ 1.5%
- Dry extract (halogen): 24.0% ± 1.2%
- Dry extract (EN 480-8): 24.3 % ± 1.2%

Packaging

- Bulk
- Drums of 60 L
- Varitainers of 1000 L

Conformity

CHRYSO®Fluid Premia 310 is a superplasticizer – high range water reducer which conforms to CE marking.
The appropriate declaration can be found on our internet site.
CHRYSO®Fluid Premia 310 also conforms to NF 085 certification, which technical specifications are those applied in the non harmonized part of the NF EN 934-2.
CHRYSO®Fluid Premia 310 also conforms to the belgium standard **NBN EN 934-2**.

AFNOR – 11 avenue F. de Pressensé – 93571 Saint Denis La Plaine cedex - France

Application

Domains of application

- All types of cement
- All concrete which must be easy to lay and / or where initial strength must be high
- Reinforced concrete; pre-stressed concrete
- Plastic to fluid concrete
- Self-compacting concrete

Method of use

Dosage: between 0.3 and 3.0 kg per 100 kg of cement.
A 1% dosage of the product of the weight of cement is commonly used.

CHRYSO®Fluid Premia 310 may be added to the mixing water or afterwards.

Precautions

- Store **CHRYSO®Fluid Premia 310** away from frost, at a temperature above 0° C.
- Should the product freeze, it will recover its properties after thawing and agitating until the product is completely homogeneous.
- Shelf life: 12 months.

CHRYSO : 19, place de la Résistance - 92446 Issy les Moulineaux cedex France - Tél. : 01 41 17 18 19 - Fax : 01 41 17 18 80

CHRYSO®Fluid Premia 310

Superplasticizer – High range water reducer

NBN EN 934-2 | BENOR | 04/21

Safety

CHRYSO®Fluid Premia 310 is a product classified as « harmless ». It is recommended to wear the normal protective equipment.

For further information, please refer to the safety data sheet on our internet site www.chryso.com.

CHRYSO : 19, place de la Résistance - 92446 Issy les Moulineaux cedex France - Tél. : 01 41 17 18 19 - Fax : 01 41 17 18 80

1.1-26

CHRYSO®Fluid Optima 350

Superplastifiant – Haut réducteur d'eau

Descriptif

CHRYSO®Fluid Optima 350 est un superplastifiant de dernière génération, particulièrement recommandé pour le béton prêt à l'emploi et les chantiers de génie civil.

CHRYSO®Fluid Optima 350 est destiné à créer une forte réduction d'eau et/ou une augmentation de l'ouvrabilité du béton. Ainsi **CHRYSO®Fluid Optima 350** peut être utilisé dans une gamme étendue de bétons.

CHRYSO®Fluid Optima 350 est particulièrement adapté pour les ciments ayant une forte demande en adjuvant et permet l'obtention d'un long maintien d'ouvrabilité.

CHRYSO®Fluid Optima 350 est particulièrement adapté à la formulation de bétons auto-plaçants.

Caractéristiques

- Nature : liquide
- Couleur : ambrée
- Densité (20° C) : 1,04 ± 0,02
- pH : 6,5 ± 1,0
- Teneur en ions Cl^- : ≤ 0,10 %
- Na_2O équivalent : < 1,0 %
- Extrait sec (halogène) : 20,0 % ± 0,9 %
- Extrait sec (EN 480-8) : 19,5 % ± 0,9 %

Conditionnement

- Vrac
- Tonnelets de 60 L
- Fûts plastiques de 215 L
- Cubitainers de 1000 L

Conformité

CHRYSO®Fluid Optima 350 est un superplastifiant – haut réducteur d'eau qui satisfait aux exigences réglementaires du marquage CE. La déclaration correspondante est disponible sur notre site internet.
CHRYSO®Fluid Optima 350 est conforme au référentiel de certification NF 085, dont les spécifications techniques sont celles de la partie non harmonisée de la norme **NF EN 934-2**.
AFNOR – 11 avenue F. de Pressensé – 93571 Saint Denis La Plaine cedex - France

Application

Domaines d'application

- BPE
- Ouvrages d'art
- BHP - BTHP
- Bétons plastiques à très fluides
- Bétons auto-plaçants

Mode d'emploi

Plage de dosage : 0,3 à 3,0 kg pour 100 kg de ciment.

CHRYSO®Fluid Optima 350 doit être ajouté de préférence dans l'eau de gâchage.

Dans le cas d'un ajout différé sur le béton frais et dans un camion malaxeur, il est nécessaire de malaxer à grande vitesse 1 minute par m³ de béton (avec un minimum total de 6 minutes).

L'efficacité maximale de **CHRYSO®Fluid Optima 350** doit être déterminée après des essais de convenance prenant en compte les caractéristiques rhéologiques et les performances mécaniques souhaitées pour le béton.

Selon les applications prévues, il est possible d'utiliser **CHRYSO®Fluid Optima 350** en synergie avec d'autres adjuvants **CHRYSO®**.

Précautions

- Stocker à l'abri du gel.
- En cas de gel, le produit conserve ses propriétés une fois dégelé et homogénéisé par agitation.
- Durée de vie : 12 mois.

CHRYSO : 19, place de la Résistance - 92446 Issy les Moulineaux cedex France - Tél. : 01 41 17 18 19 - Fax : 01 41 17 18 80

1.1-26

CHRYSO®Fluid Optima 350

Superplastifiant – Haut réducteur d'eau

Sécurité

CHRYSO®Fluid Optima 350 est un produit "sans danger ". Le port d'équipements de protection individuelle est recommandé.

Pour plus d'informations, consulter la fiche de données de sécurité sur le site internet www.chryso.com.

" Se renseigner sur la dernière mise à jour "

Dernière modification : 04/08

CHRYSO : 19, place de la Résistance - 92446 Issy les Moulineaux cedex France - Tél. : 01 41 17 18 19 - Fax : 01 41 17 18 80

Product Data Sheet
Edition 21/02/2012
Identification no:
02 01 01 01 200 0 000097
Sika® ViscoCrete®-10

Construction

Sika® ViscoCrete®-10

High performance superplasticiser

Product Description

Sika® ViscoCrete®-10 is a third generation superplasticiser for concrete and mortar. It meets the requirements for set retarding / high range water reducing superplasticisers according to EN 934 - 2.

Uses

Sika® ViscoCrete®-10 is especially suitable for concrete mixes with extended transportation times and extended workability requirements, ultra high water reduction and excellent flow characteristics.

Sika® ViscoCrete®-10 is mainly used for the following applications:

- Concrete with ultra high water reduction (up to 30%)
- High performance concrete
- Concrete in hot weather and with extended transportation and workability requirements

Characteristics / Advantages

Sika® ViscoCrete®-10 is a powerful superplasticiser which acts through several mechanisms.

Though surface adsorption and sterical effects separating the cementitious binder particles the following properties are achieved:

- High water reduction, resulting in high density, high strength and reduced permeability
- Excellent plasticising effect, resulting in improved flow, placing and compaction characteristics
- Reduced shrinkage during curing and reduced creep when hardened

Sika® ViscoCrete®-10 does not contain chlorides or any other ingredients which promote the corrosion of steel. It is therefore suitable for use in reinforced and pre-stressed concrete structures.

Tests

Approval / Standards	Conforms to the requirements of EN 934 – 2, Table 11.1 / 11.2.

Product Data

Form

Appearance / Colour	Liquid	Light brownish
Packaging	25, 200 and 1000 Litre containers	

Storage

Storage Conditions / Shelf -Life	12 months from date of production if stored properly in undamaged unopened, original sealed packaging, in dry conditions at temperatures between +5°C and +30°C. Protect from direct sunlight and frost.

Technical Data

Chemical Base	Modified polycarboxylate in water.
Density	Specific density: 1.06 kg/l (at +20°C)
pH Value	4.25 ± 0.5

System Information

Application Details

Consumption / Dosage	Recommended dosage for concrete: 0.4 - 1.5% by weight of cement.

Application Conditions / Limitations

Compatibility	Sika® ViscoCrete®-10 may be combined with many other Sika products and particularly: - Sika® Stabilizer-229 ZA - Sika Retarder® - Fro-V5-A / -V30 Note: Always conduct trials before combining products in specific mixes.

Application Instructions

Dispensing	Sika® ViscoCrete®-10 is added to the gauging water or added with it into the concrete mixer. To take advantage of the high water reduction, a wet mixing time of at least 60 seconds is recommended. To avoid excess water in the concrete, the final dosage must begin only after 2/3 of the wet mixing time.
Application Method / Tools	The standard rules of good concreting practice, concerning production and placing, are to be followed. Fresh concrete must be cured properly and as early as possible.
Cleaning of Tools	Clean all tools and application equipment with water immediately after use. Hardened / cured material can only be mechanically removed.
Notes on Application / Limitations	Frost: If frozen and / or if precipitation has occurred, Sika® ViscoCrete®-10 may be used after thawing slowly at room temperature and after intensive mixing.
Notes	All technical data stated in this Product Data Sheet are based on laboratory tests. Actual measured data may vary due to circumstances beyond our control.
Local Restrictions	Please note that as a result of specific local regulations the performance of this product may vary from country to country. Please consult the local Product Data Sheet for the exact description of the application fields.

Construction

Health and Safety Information

Protective Measures	Upon contact with skin, wash off with soap and water. In case of contact with eyes or mucous membranes, rinse immediately with clean water and seek medical attention without delay.
Ecology	
Transportation Class	
Important Notes	Residues of material must be removed according to local regulations. Fully cured material can be disposed of as household waste under agreement with the responsible local authorities. Detailed health and safety information as well as detailed precautionary measures e.g. physical, toxicological and ecological data can be obtained from the Material Safety Data Sheet.
Toxicity	

Legal Notes

The information, and, in particular, the recommendations relating to the application and end-use of Sika products, are given in good faith based on Sika's current knowledge and experience of the products when properly stored, handled and applied under normal conditions in accordance with Sika's recommendations. In practice, the differences in materials, substrates and actual site conditions are such that no warranty in respect of merchantability or of fitness for a particular purpose, nor any liability arising out of any legal relationship whatsoever, can be inferred either from this information, or from any written recommendations, or from any other advice offered. The user of the product must test the product's suitability for the intended application and purpose. Sika reserves the right to change the properties of its products. The proprietary rights of third parties must be observed. All orders are accepted subject to our current terms of sale and delivery. Users must always refer to the most recent issue of the local Product Data Sheet for the product concerned, copies of which will be supplied on request or access on the Internet under www.sika.co.za.

Sika South Africa (Pty) Ltd
9 Hocking Place,
Westmead, 3608
South Africa

E-mail: headoffice@za.sika.com
Phone +27 31 792 6500
Telefax +27 31 700 1760
www.sika.co.za

Responsible Care

Certified Quality System ISO 9001/EN 29001 since 1986

Construction

Sika® ViscoCrete®-20 HE

High Performance Superplasticizer

Product Description

Sika® ViscoCrete®-20 HE is a third generation superplasticizer for concrete and mortar. The product is suitable for tropical and hot climatic conditions

Uses

Sika® ViscoCrete®-20 HE is especially suitable for the production of concrete mixes which require high early strength development, powerful water reduction and excellent flowability.

Sika® ViscoCrete®-20 HE is mainly used for the following applications:

- Pre-cast concrete
- Fast track concrete
- In situ concrete requiring fast stripping time
- Self-Compacting Concrete (SCC)

Advantages

Sika® ViscoCrete®-20 HE as a powerful superplasticizer acts by different mechanisms. Through surface adsorption and sterical effects separating the binder particles the following properties are achieved:

- Pronounced increase in the early strength development, resulting in very economic stripping times for pre-cast and in situ concrete
- Extremely powerful water reduction, resulting in high density, high strengths and reduced water permeability etc.
- Excellent plasticizing effect, resulting in improved flowability, placing and compacting behavior
- Reduced energy cost for steam cured pre-cast elements
- Especially suitable for the production of Self-Compacting Concrete (SCC)
- Improved shrinkage and creep behavior
- Reduced closure times for repairs of roads and runways

Sika® ViscoCrete®-20 HE does not contain chlorides or other ingredients which promote the corrosion of steel reinforcement. It is therefore suitable for reinforced and pre-stressed steel.

Tests

Approval / Standards

Sika® ViscoCrete®-20 HE complies with the requirements for superplasticisers according to ASTM C494-86; SIA 262 (2003) and EN 934-2.

Product Data

Form	Liquid
Appearance / Colour	Light brownish, clear to slightly cloudy
Packaging	1000 lt. flow bins

Innovation & Consistency | since 1910

Storage

Storage Conditions	Store in a dry area between 5ºC and 35ºC. Protect from direct sunlight and frost.
Shelf Life	12 months minimum from date of production if stored properly in original unopened packaging.

Technical Data

Chemical Base	Aqueous solution of modified polycarboxylates
Density (at 25°C)	Approximately 1.08 kg/lt
pH value	Approximately 4.3
Chloride content	Nil (EN 934-2)
Effect on setting	Non-retarding
Effect of overdosing	Bleeding may occur

Application Details

Dosage

Recommended dosage:

- For medium workability: 0.2-0.8% by weight of cement
- For concrete of high workability, very low water/cement ratio and for Self Compacting Concrete: 1.0 – 2.0% by weight of cement.

It is advisable to carry out trial mixes to establish the correct dosage.

Compatibility

Sika® ViscoCrete®-20 HE may by combined with the following Sika Products among others:

- SikaPump®
- Sika® Ferrogard®-901
- Sika® Fume
- SikaRapid®
- Sika Retarder® and Sika® Retardol 25

Pre-trials are always recommended before combining products. Please consult our Technical Services Department for further advice and information.

Dispensing

Sika® ViscoCrete®-20 HE is added to the gauging water or added with it into the concrete mixer. For optimum utilization of the high water reduction property we recommend thorough mixing at a minimal wet mixing time of 60 seconds.

Concrete Placing

The standard rules of good concreting practice, concerning production as well as placing, are to be followed. Refer to relevant standards.

Curing

Fresh concrete must be cured properly, especially at high temperatures in order to prevent plastic and drying shrinkage. Use Sika Antisol® products as a curing agent or apply wet hessian.

Cleaning

Clean all equipment and tools with water immediately after use.

Notes on Application/Limitations

When accidental overdosing occurs (within reason), apart from retardation of the initial set and increased bleeding, no detrimental effect will take place.

When using **Sika® ViscoCrete®-20 HE** to produce Self-Compacting Concrete, a suitable mix design must be selected and local material sources should be trialled.

Before pouring, suitability tests on the fresh concrete must be carried out.

Construction

Value Base	All technical data stated in this Product Data Sheet are based on laboratory tests. Actual measured data may vary due to circumstances beyond our control.
Local Restrictions	Please note that as a result of specific local regulations the performance of this product may vary from country to country. Please consult the local Product Data Sheet for the exact description of the product uses.
Health and Safety Information	For information and advice on the safe handling, storage and disposal of chemical products, users shall refer to the most recent Material Safety Data Sheet containing physical, ecological, toxicological and other safety related data.
Legal Notes	The information, and, in particular, the recommendations relating to the application and end-use of Sika products, are given in good faith based on Sika's current knowledge and experience of the products when properly stored, handled and applied under normal conditions in accordance with Sika's recommendations. In practice, the differences in materials, substrates and actual site conditions are such that no warranty in respect of merchantability or of fitness for a particular purpose, nor any liability arising out of any legal relationship whatsoever, can be inferred either from this information, or from any written recommendations, or from any other advice offered. The user of the product must test the product's suitability for the intended application and purpose. Sika reserves the right to change the properties of its products. The proprietary rights of third parties must be observed. All orders are accepted subject to our current terms of sale and delivery. Users must always refer to the most recent issue of the local Product Data Sheet for the product concerned, copies of which will be supplied on request.

All products are manufactured under a management system certified to conform to the requirements of the quality, environmental and occupational health & safety standards ISO 9001, ISO 14001 and OHSAS 18001.

Sika UAE LLC
P.O. Box 126212
Dubai
United Arab Emirates
Phone: +971 4 4398200
Fax: +971 4 4393606
info@ae.sika.com
www.sika.ae

Sika Gulf B.S.C
Building 925, Road 115
Sitra Area 601
Adliya, Kingdom of Bahrain
Phone: +973 17738 188
Fax: +973 17732 476
sika.gulf@bh.sika.com
www.sika.com.bh

Sika Saudi Arabia Co. Ltd
Obaikan Building
Al-Zahra
Jeddah 23522-4522
Saudi Arabia
Phone: +966 2 692 7079
Fax: +966 2 692 1272
www.sika.com.sa

Innovation & Consistency since 1910

BASF
The Chemical Company

GLENIUM® ACE 456

Essential component of ZERO ENERGY SYSTEM – A new generation of high-performance polycarboxylate ether (PCE) superplasticizers for the Precast industry.

Description and field of application

GLENIUM ACE (Admixture Controlled Energy) 456 consists of a range of innovative superplasticizers based on newly developed polycarboxylate ether polymers. The particular molecular configuration of GLENIUM ACE 456 accelerates the cement hydration by exposing increased surface of the cement grains to react with water. As a result, it is possible to obtain earlier development of the heat of hydration, rapid development of the hydration products and, as a consequence, higher strengths at very early age. The polymer structure of GLENIUM ACE 456 is specially designed to improve the rheology of precast concrete, making it very flowable and low viscous even at very low water/cement ratios, without increasing stickiness. Robustness is a distinctive feature of the precast concrete produced with GLENIUM ACE 456.

ZERO ENERGY SYSTEM:

Zero Energy System is based on a combination of the latest GLENIUM ACE superplasticizers and advanced self-compacting concrete technology. The Zero Energy System has been developed to help the precast concrete producer to rationalize his production process and save on energy costs combined with improved quality of the product and the working conditions.

Fields of Application

GLENIUM ACE 456 is suitable for making precast concrete elements with highly-fluid concrete without segregation but low water cement ratio and, consequently, high early and final strengths. GLENIUM ACE 456 may be used in combination with RheoMATRIX for producing advanced self-compacting concrete like Smart Dynamic Concrete (SDC, latest V-type SCC), without the aid of vibration, for economic, ecological and ergonomic precast production.

Features & Benefits

GLENIUM ACE 456 offer the following benefits for the precast concrete industry:

- Production of highly flowable, robust self-compacting concrete having a low water cement ratio along with an optimal rheology.
- Enhanced robustness and consistency in concrete quality with low stickiness.
- Environmentally friendly, CO_2 reduced mix-design optimization.
- Elimination of heat curing.
- Improved surface appearance.
- Durable precast concrete elements as per EN 206-1.
- Elimination of the energy required for placing, compaction and curing (ZERO ENERGY).
- Optimization of the curing cycles by reducing curing time or curing temperature.
- Increased productivity.

Packaging

GLENIUM ACE 456 is available in bulk, containers, drums or cans.

Standards

GLENIUM ACE 456 meets the requirements of EN EN934-2 and ASTM C494 Type A, E & F.

BASF
The Chemical Company

GLENIUM® ACE 456

***Technical Data/Typical Properties**

Appearance and Form	Whitish to light Brownish liquid
Specific gravity @ 25°C	1.060 typical
pH-value @ 25°C	4-7
Chloride ion content ≤	≤0.01%
Alkali content (Na2O equivalent %)	< 3%

Directions for use

GLENIUM ACE 456 is a liquid admixture to be added to the concrete during the mixing process. The best results are obtained when the admixture is added to the mixing water that is used for the concrete mix after all the other components are already in the mixer and after the addition of at least 80% of the total water. The water content is adjusted to obtain the desired consistence or workability.

Optimal water reduction is obtained if the GLENIUM ACE 456 is poured into the concrete mix right after the addition of the initial 80-90% of mixing water. Avoid adding the admixture to the dry aggregates. After adding GLENIUM ACE 456 admixture provide enough mixing time to secure a homogenous dispersion. Continue mixing and adjust the water content to obtain the required workability.

Dosage rate

The recommended dosage rate is 0.3 to 2.0 liters per 100 kg of the binder.

Other dosages may be used in special cases according to specific production conditions. In this case please consult our Technical Services Department.

Compatibility

GLENIUM ACE 456 is compatible and recommended for use with:

- RheoMATRIX to modify the viscosity of SCC.
- MICRO-AIR, air entraining admixture, to improve freeze-thaw resistance (exposure class XF1 to XF4, EN 206-1)
- RHEOFINISH, demoulding agent for easy formwork removal and improved finish.
- MASTERKURE, curing compound for highly efficient water retention and friendly use.

GLENIUM ACE 456 is **not compatible** with all admixtures of RHEOBUILD series.

Storage

GLENIUM ACE 456 must be stored in a place where the temperature does not drop below 5°C. In case of freezing, warm up and homogenise the admixture solution before using. If stored in unopened containers according to manufacturer's instructions, the shelf life is 12 months.

Handling & Storage

No special requirements must be observed while the product is used. Protection gloves and glasses are recommended. Do not eat, drink or smoke during the application. GLENIUM ACE 456 is not-flammable, non-toxic or irritant and are not subject to special transport requirements.

BASF
The Chemical Company

GLENIUM® ACE 456

Note

Field service, where provided, does not constitute supervisory responsibility. For additional information contact your local BASF representative.

BASF reserves the right to have the true cause of any difficulty determined by accepted test methods.

Quality and care

All products originating from BASF's Dubai, UAE facility are manufactured under a management system independently certified to conform to the requirements of the quality, environmental and occupational health & safety standards ISO 9001, ISO 14001 and OHSAS 18001.

11/2008 BASF_CC-UAE revised 06/2009

* Properties listed are based on laboratory controlled tests.

BASF Construction Chemicals UAE LLC
P.O. Box 37127, Dubai, UAE
Tel: +971 4 8090800 Fax: +971 4 8851002
www.basf-cc.ae e-mail: marketingcc.mideast@basf.com

Certificate No. 963680
Certificate No. 945787
Certificate No. 772556